International
Progress Report

IPR-08-18

Äspö Hard Rock Laboratory

The TASS-tunnel – project ”Sealing of tunnel at great depth”

Geology and hydrogeology – Results from the pre-investigations based on the boreholes KI0010B01, KI0014B01 and KI0016B01

Carljohan Hardenby, Vattenfall Power Consultant AB
Oskar Sigurdsson, HAskGeokonsult AB
Lisa Hernqvist, Chalmers
Niclas Bockgård, Golder Associates AB

October 2008

Svensk Kärnbränslehantering AB
Swedish Nuclear Fuel
and Waste Management Co

Box 250, SE-101 24 Stockholm
Phone +46 8 459 84 00

Äspö Hard Rock
Laboratory

Report no.
IPR-08-18
No.
SU 3.25.16
Author
Carljohan Hardenby
Oskar Sigurdsson
Lisa Hernqvist
Niclas Bockgård
Date
October 2008
Checked by
Mansueto Morosini
Date
2008-11-13
Johan Berglund
2008-11-24
Approved
Anders Sjöland
Date
2009-06-25

Äspö Hard Rock Laboratory

The TASS-tunnel – project ”Sealing of tunnel at great depth”

Geology and hydrogeology – Results from the pre-investigations based on the boreholes KI0010B01, KI0014B01 and KI0016B01

Carljohan Hardenby, Vattenfall Power Consultant AB
Oskar Sigurdsson, HAskGeokonsult AB
Lisa Hernqvist, Chalmers
Niclas Bockgård, Golder Associates AB

October 2008

Keywords: Sealing of tunnel at great depth, TASS-tunnel, Pre-investigation, Core drilling, Core logging, Boremap, Hydrogeology, Hydro gelogical tests, Water bearing structures, Aperture, Inflow, KI0010B01, KI0014B01, KI0016B01

This report concerns a study which was conducted for SKB. The conclusions and viewpoints presented in the report are those of the author(s) and do not necessarily coincide with those of the client.

Abstract

SKB decided in 2006 to execute the project “Fintätning av tunnel på stort djup” (Sealing of tunnel at great depth) at Äspö HRL. The grouting material silica sol was going to be tested at depths (450 m below sea level) that are going to be used for the final repository for spent nuclear fuel in the future. At the same time tests on different types of explosives, drilling techniques and layouts for blasting boreholes etc were going to be performed. The purpose for this is to achieve as good tunnel contour as possible and to keep the damage of the tunnel walls, roof and floor as small as possible.

A new tunnel (called the TASS-tunnel) was needed for the tests. Its starting point was from TASI-tunnel at the -450 m level. The chosen location for the new tunnel was near the site for the True Block Scale Experiment. This experiment involved injection of minor amounts of radioactive trace elements into the rock volume. To be certain that the site of the TASS-tunnel was free from radioactivity a number of tests had to be performed. The results from these tests showed that the TASS site was free from radioactive substances.

Three core boreholes (each about 100 m long) called KI0010B01, KI0014B01 and KI0016B01 respectively were drilled to give information on the rock quality and to ensure that no major deformation/crush zones were going to be encountered during the excavation of the TASS-tunnel. The major rock type in the cores is Äspö diorite with minor amounts of pegmatite, fine grained granite and mafic rock. The fracture intensity and quality of the rock is of “normal” Äspö HRL standard. The dominating fracture orientation has a strike of about NW and a steep dip towards NE or SW which corresponds to the common fracture pattern at Äspö HRL. The planned tunnel direction is at a rather large angle to this dominating fracture orientation.

Along with the drilling, pressure build up tests were performed in the boreholes. The full-hole pressure in KI0010B01 was about 3 MPa. It was soon found out, however, that the holes were connected with each other by intersecting water bearing structures. The Prototype repository was affected by the drilling which caused changes in the inflow of water as well the pressure in the repository. After completed drilling of the boreholes PFL-logging (only in KI0010B01) and double packer tests were performed in them.

The inflow of water into the boreholes (full length) varied between 40 l/min in KI0010B01 and almost 100 l/min in borehole KI0016B01. When the inflow is calculated in sections of the boreholes it is evident that the water inflow is concentrated to certain sections of the holes. The transmissivity and the hydraulic aperture have been calculated for the inflows found along the boreholes.

With the help of the hydraulic tests interpretations have been made on where TRUE Block Scale structures might intersect the new boreholes. The structures #5, #7, #8, #20 and #22 are believed to be identified in the holes. Some open fractures and minor crush zones in the drill cores from KI0010B01, KI0014B01 and KI0016B01 have been interpreted to represent the same five TRUE Block Scale structures. Some of the structures in the boreholes appeared in the BIPS-images to be water bearing.

The results from the pre-investigations indicate that the choice of location for the TASS-tunnel is suitable not only for the excavation of the tunnel but also for the tests that are planned.

Sammanfattning

SKB bestämde sig 2006 att genomföra projektet "Fintätning av tunnel på stort djup" i Äspölaboratoriets underjordsdel. Injekteringsmedlet silica sol skulle testas på stort djup (-450 m), d.v.s. på samma djup som det planerade slutförvaret för utbränt kärnbränsle är tänkt att anläggas på. Inom samma projekt skall även tester av spängämnen, borrteknik, borrhålslayouter mm utföras för att se hur den bästa tunnelkonturen och de minsta skadorna på tunnelns väggar, tak och sula skall kunna uppnås.

För att kunna utföra de olika testerna behövdes en ny tunnel, som så småningom kom att kallas TASS-tunneln. Den nya tunneln tänktes utgå från TASI-tunneln. Ett problem med lägesvalet var att det låg i anslutning till det område som utnyttjades av TRUE Block Scale Experimentet i vilket det injicerades mindre mängder radioaktiva isotoper i berget. För att vara säkra på att området för den nya tunneln inte var kontaminerat utfördes ett antal radiologiska tester. Det visade sig dock att området kunde friklassas från radioaktiva ämnen.

Tre ca 100 m långa kärnborrhål (KI0010B01, KI0014B01 och KI0016B01) borrades för att få information om bergkvalitén och försäkra sig om att inga större deformations-/krosszoner korsade den planerade tunneln. Den vanligaste bergarten i borrkärnorna var äspödiorit med mindre inslag av pegmatit, finkornig granit och mafiska bergarter. Sprickfrevensen och bergkvalitén har bedömts som normal för Äspölaboratoriets underjordsdel. Den dominerande sprickorienteringen har en NW strykning och en brant stupning mot NE eller SW vilket följer det normala sprickmönstret i Äspölaboratoriet tunnlar. Den planerade tunnelriktningen skulle således ha en ganska stor vinkel mot den förhärskande sprickorienteringen.

I samband med att borrningen utfördes gjordes tryckuppbyggnadstester i det aktuella hålet. I borrhål KI0010B01 var trycket för hela hålet omkring 3 MPa (30 bar). Det kunde dock ganska snart konstateras att hålen stod i kontakt med varandra genom vattenförande strukturer. Även det ganska närliggande Prototypförvaret påverkades av att de tre nya hålen borrades vilket gav sig till känna genom förändringar i inflöde och tryck i förvaret. Efter det att borrningarna hade avslutats utfördes PFL-loggning (bara i KI0010B01) och dubbelmanschettmätningar i hålen.

Infödet, mätt över hela hålen, varierar mellan 40 l/min i KI0010B01 och närmare 100 l/min i KI0016B01. Om vatteninflödet beräknas i borrhålssektioner framgår det att inflödet sker endast i vissa av dem. Transmissivitet och hydraulisk sprickvidd har beräknats för inflödena längs borrhålen.

Med hjälp av de hydrauliska testerna har tolkningar gjorts på var strukturer identifierade i TRUE Block Scale projektet kan tänkas skära de nya borrhålen. I borrhålen har troligen strukturerna #5, #7, #8, #20 and #22 kunnat identifieras. Några öppna sprickor och mindre krosszoner i borrkärnorna från KI0010B01, KI0014B01 och KI0016B01 har ansetts motsvara samma fem TRUE Block Scale strukturer. Några av strukturerna tycks i BIPS-bilderna vara vattenförande.

Resultaten från förundersökningen tyder på att valet av TASS-tunnelns placering är passande inte bara för tunnelindriften utan även för de tester som är tänkta att utföras.

Contents

1 Introduction **9**
1.1 Background 9
1.2 Location of the test-tunnel 9
1.2.1 The Pre-investigation – purpose and requirements 9
1.3 The aim of the report 11

2 Core drilling **15**
2.1 Controlling documents 15
2.2 Contractors involved 16
2.3 Drill rigs 16
2.4 Location and other borehole data 18
2.5 Some arrangements around the drill site 21
2.5.1 Scaffolds 21
2.5.2 Casing 21
2.5.3 Flush and return water – flow-chart 22
2.5.4 Radioactivity 24

3 Borehole mapping/core logging **27**
3.1 Introduction 27
3.2 Objective and scope 28
3.3 Description of equipment/interpretation tools 29
3.3.1 Borehole Image Processing System – BIPS 29
3.3.2 Core logging with Boremap 30
3.4 Execution of the core logging 33
3.4.1 General 33
3.4.2 Preparations 33
3.4.3 Execution of field work 34
3.4.4 Data handling 35
3.5 Results 36
3.6 Summary and discussions concerning the core logging 49

4 Hydrogeological investigations **53**
4.1 Pressure measurements 53
4.1.1 The effect on surrounding boreholes and rock mass 54
4.2 Double packer flow logging 57
4.3 PFL difference flow logging 58

5 Hydrogeological evaluation **63**
5.1 Introduction 63
5.2 Methods 63
5.2.1 Equivalent hydraulic aperture b_{eq} 64
5.3 Evaluation of tests performed during drilling 65
5.3.1 Interpretation of pressure measured in a long section of a borehole 65
5.4 Evaluation of double packer tests 68
5.5 Evaluation of Posiva Flow Log 69

5.6 Comparison of the results based on the different test methods for each of the boreholes 69
5.7 Results and discussion concerning the hydrogeological evaluations 69
5.7.1 Tests during drilling 69
5.7.2 Double packer tests 78
5.7.3 PFL-logging 79
5.7.4 Comparison of the results based on the different test methods 80
5.7.5 Open fracture positions 81

6 Predictions and outcome in relation to the TRUE Block Scale model 85
6.1 Predictions and outcome based on core logging 85
6.2 Predictions and outcome based on hydro-geological responses 100

7 Concluding remarks 103
7.1 Conclusion 104

Acknowledgements 105

References 107

Appendices 109

1 Introduction

1.1 Background

Svensk Kärnbränslehantering AB (SKB, Swedish Nuclear Fuel and Waste Management Co) decided in 2006 to execute tests on Silica sol as an alternative and/or complement to cement-based compounds to seal fractures. One advantage with Silica sol is its capability to seal very narrow fractures (about 0.01 mm width). The compound has not, however, been tested at great depths such as those for the planned storage of nuclear waste (400-700 m below ground level). The project performing the Silica sol tests has been called "Fintätning av tunnel på stort djup" ("Sealing of tunnel at great depth") or shortly "Fintätningsprojektet".

SKB decided also to test different types of explosives, drilling techniques and borehole layouts to achieve as good tunnel contours as possible and to keep the damage of the tunnel walls, roof and floor as small as possible. These tests were going to be performed within the same tunnel and project as the silica sol.

1.2 Location of the test-tunnel

To carry out both these tests a new tunnel was needed. A suitable location was found at the -450 m level of the Äspö Hard Rock Laboratory (Äspö HRL, Figure 1-1). The locality was chosen since it appeared to fulfil a number of conditions such as tunnel orientation in relation to water-bearing structures, location outside the main draw down of the ground water surface (Figure 1-2), not interfering too much with other activities and location good for transportation. The prospective tunnel was given the name TASS (T=tunnel, AS=Äspö site, S=letter ID for the tunnel in question).

1.2.1 The Pre-investigation – purpose and requirements

The investigation, that preceded the excavation of the new tunnel commenced in 2007. It included three core-drilled boreholes (KI0010B01, KI0014B01 and KI0016B01), core logging and a number of borehole tests such as pressure measurements, PFL-logging (PFL=Posiva Flow Log), double packer flow logging and BIPS-logging (BIPS=Borehole Image Processing System). Table 1-1 summaizes the activities that took place during the pre-investigation.

Table 1-1. Summary of activities.

Borehole	Activity	Date	Comments
KI0010B01	Casing drilling	2007-03-12	
KI0014B01	Casing drilling	2007-03-19 - 20	
KI0016B01	Casing drilling	2007-03-13 - 14	
KI0010B01	Preliminary core logging (core from casing drilling)	2007-03-27	Including core photography Core log and photos are not shown in the report
KI0014B01	Preliminary core logging (core from casing drilling)	2007-03-27	Including core photography Core log and photos are not shown in the report
KI0016B01	Preliminary core logging (core from casing drilling)	2007-03-27	Including core photography Core log and photos are not shown in the report
KI0010B01	Core drilling	2007-04-11 - 21	
KI0014B01	Core drilling	2007-06-14 - 18	
KI0016B01	Core drilling	2007-06-01 - 08	
KI0010B01	Drilling reports: flush water, return water drill rate and up-takes	2007-03-12 2007-04-11 - 21	Only in the Sicada archive
KI0014B01	Drilling reports: flush water, return water drill rate and up-takes	2007-03-19 – 20 2007-06-14 - 18	
KI0016B01	Drilling reports: flush water, return water drill rate and up-takes	2007-03-13 – 14 2007-06-01 - 08	
KI0010B01	Bips logging in borehole	2007-04-26	
KI0014B01	Bips logging in borehole	2007-07-04	
KI0016B01	Bips logging in borehole	2007-07-04	
KI0010B01	Preliminary core logging	2007-06-20 - 22	Including core photography Core log and photos are not shown in the report
KI0014B01	Preliminary core logging	2007-06-27 - 29	Including core photography Core log and photos are not shown in the report
KI0016B01	Preliminary core logging	2007-06-25 - 27	Including core photography Core log and photos are not shown in the report
KI0010B01	Core logging with Boremap	2007-05-22 – 06-20	
KI0014B01	Core logging with Boremap	2007-07-26 – 09-06	
KI0016B01	Core logging with Boremap	2007-09-24 – 10-11	
KI0010B01	Double packer flow logging	2007-07-16 - 17	
KI0014B01	Double packer flow logging	2007 -07-18 - 19	
KI0016B01	Double packer flow logging	2007-07-10 - 12	

Borehole	Activity	Date	Comments
KI0010B01	PFL Difference flow logging	2007-05-21 - 22	
KI0010B01	Pressure measurements	2007-04-11 - 21	Measured during drilling
KI0014B01	Pressure measurements	2007-06-14 - 18	Attempt was made to measure while drilling - No data
KI0016B01	Pressure measurements	2007-06-01 - 08	Measured during drilling Data difficult to interpret
KI0010B01	Full-hole inflow	2007-04-11 - 21	Measured during drilling
KI0014B01	Full-hole inflow	2007-06-14 - 18	Measured during drilling
KI0016B01	Full-hole inflow	2007-06-01 - 08	Measured during drilling
Site area	Measurements of radioactivity	2007	Before, while and after drilling
KI0010B01	Measurements of radioactivity	2007	While and after drilling
KI0014B01	Measurements of radioactivity	2007	While and after drilling
KI0016B01	Measurements of radioactivity	2007	While and after drilling

A number of geological and hydro-geological requirements had to be fulfilled before the suggested location of the test-tunnel could be accepted (see "Krav på plats för TASS tunnel och metodik för platsval", Johan Funehag 2007, internal SKB document 1081795):

1. No major deformation zones closer than 100-150 m to the tunnel mouth
2. The length of the test site must must be at least 100 m
3. The drill cores must have 1-2 fractures/metre
4. The main orientation of the fractures must be close to perpendicular (about 70-90°) to the prospective tunnel
5. The fractures must have a hydraulic aperture of 10-300 μm
6. The ground water pressure must be > 3.5 MPa at a borehole depth/length of 25 m or >3 MPa measured over the full length of the borehole.

1.3 The aim of the report

The intention with the report is to describe how the pre-investigation was performed, to describe the rock volume in terms of rock types and fractures etc and the hydraulic conditions of the site area.

Therefore the major part of the report concerns the core logging and the hydrogeological evaluation that has been written by Oskar Sigurdsson and Lisa Hernqvist respectively.

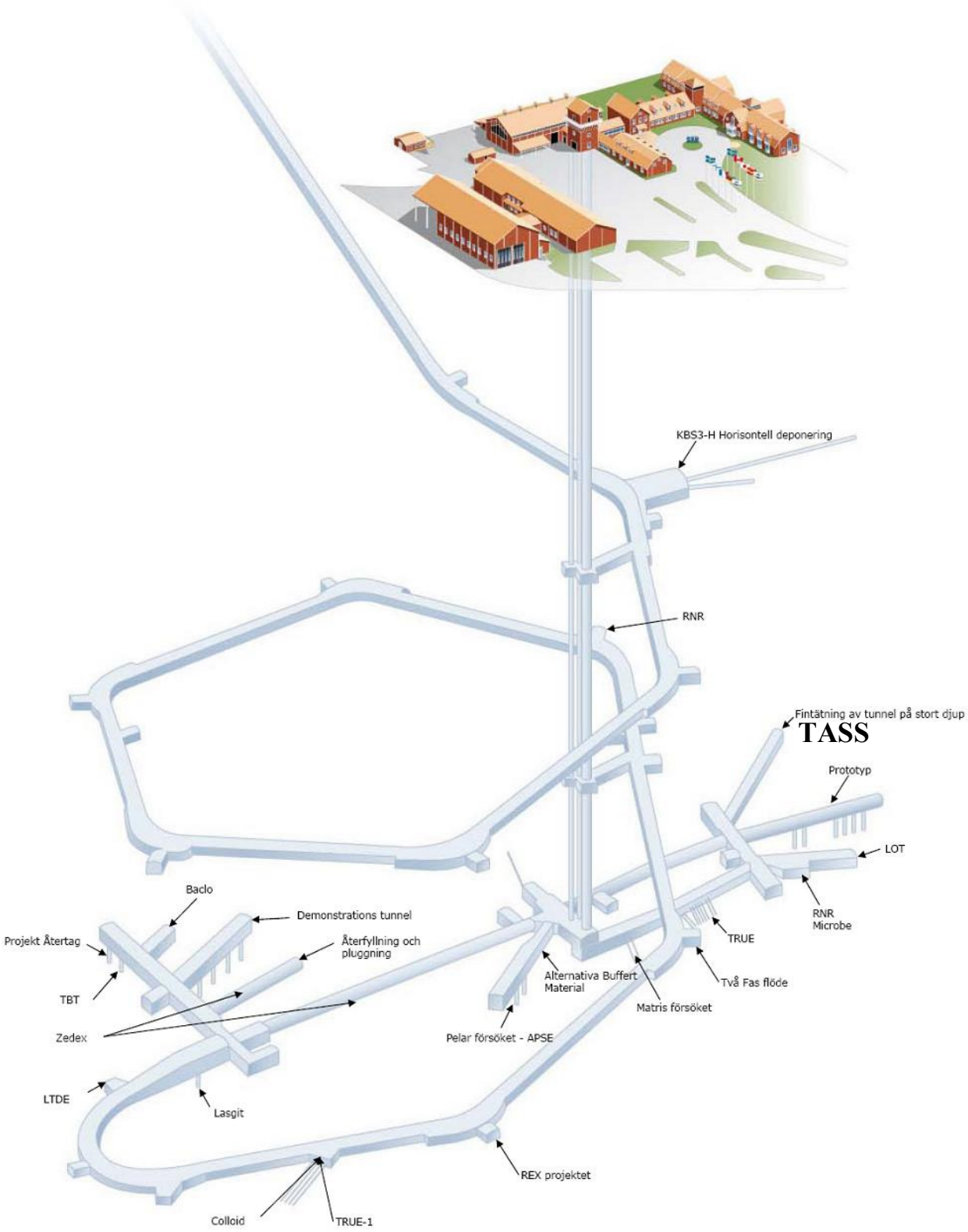

Figure 1-1. *Layout of the Äspö HRL showing for example the location of the TASS-tunnel.*

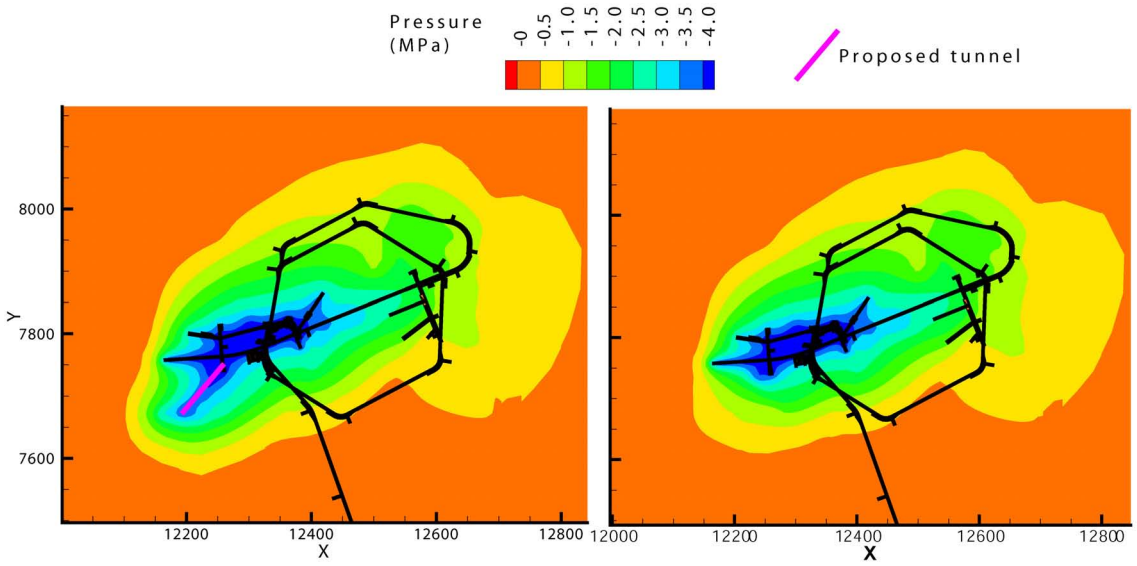

a) ***b)***

Figure 1-2. a) *Location and orientation of the planned new tunnel TASS. The figure shows also the simulated effect of the new tunnel on the groundwater pressure.* ***b)*** *The present groundwater model without the new tunnel. The 0 MPa value (red) in the legend above represents undisturbed groundwater pressure at -450 m depth. The -4 MPa value (blue) in the same legend represents pressure reduction to atmospheric pressure (modified after Ch. Andersson 2006, Platsval Injekteringstunnel "Location of injection tunnel", internal SKB document).*

2 Core drilling

2.1 Controlling documents

All activities that take place in the Äspö HRL are governed by certain documents; so called Activity Plans. Thus, the drilling and all related on-site operations were performed according to a specific Activity Plan (AP TD SU32516-07-015). Reference is given in the activity plan to procedures in the SKB Method Description for Core Drilling (SKB MD 321.002, Version 3.0) and relevant method instructions for handling and sampling of drill core see Table 2-1.

Table 2-1. Controlling documents for the performance of the activity.

Activity plan	**Number**	**Version**
Installation av foderrör i kärnborrhål KI0010B01, KI0014B01 och KI0016B01. Fintätning av tunnel på stort djup (Installation of casing in the core boreholes KI0010B01, KI0014B01 and KI0016B01. Sealing of narrow fractures in tunnels at great depths)	AP TD SU32516-07-015	1.0
Kärnborrning av KI0010B01, KI0014B01 och KI0016B01 (Core drilling of KI0010B01, KI0014B01 and KI0016B01)	AP TD SU32516-07-018	1.0
Bips i KI0010B01, KI0014B01 och KI0016B01 (Bips measurements in KI0010B01, KI0014B01 and KI0016B01)	AP TD SU 32516-07-027	0.1
Method descriptions	**Number**	**Version**
Metodbeskrivning för kärnborrning (Method description for core drilling)	SKB MD 321.002	3.0
Instruktion för hantering och provtagning av borrkärna (Instruction to handle and sample drill cores)	SKB MD 143.007	2.0

The activity plans and method descriptions are SKB internal documents. All data concerning the drilling were stored in the SICADA database for Oskarshamn.

2.2 Contractors involved

A number of contractors were involved in the drilling of the new holes:

- The contractor “Smålands Betonghåltagning AB” performed the casing drilling.
- SKB supplied the casing.
- The contractor ”BorrBoLaget, entreprenad väst AB” contributed with information about how to perform epoxy injection to seal the casing against the borehole wall.
- The contractor Drillcon Core AB executed the core drilling as well as the epoxy-injections.

2.3 Drill rigs

Three different drillrigs were used to accomplish the boreholes KI0010B01, KI0014B01 and KI0016B01 (Figure 2-1):

- A Husqvarna 406 HL drill rig was used to perform the casing drilling (Figure 2-1)
- An Onram 2000 CCD (Computer Controlled Drilling) drill rig supplied with accessories was used for the core drilling of borehole KI0010B01 (Figure 2-2a, b and c).
- An Atlas Copco Diamec 282E drill rig supplied with accessories was used for the core drilling of the holes KI0014B01 and KI0016B01 (Figure 2-3).

Figure 2-1. *Husqvarna 406HL drill rig used for the casing drilling, driller is Mikael Gustafsson, Smålands Betonghåltagning AB. The power package is situated outside the picture (photo: Oskar Sigurdsson).*

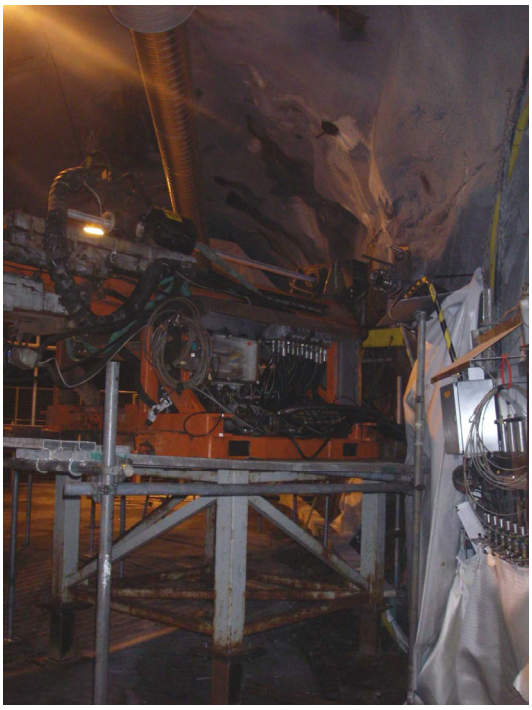

a) ***b)***

Figure 2-2 a&b. *The Onram 2000 CCD computer controlled drill rig used for the core drilling of KI0010B01 (photos: Elinor Örtendahl).* ***a)*** *the rig in position.* ***b)*** *the computer aided control unit.*

c)

Figure 2-2 c. *The Onram 2000 CCD computer controlled drill rig used for the core drilling of KI0010B01. The rig is in position for drilling KI0010B01 (photo: Elinor Örtendahl).*

Figure 2-3. *The Atlas Copco Diamec 282E drill rig at KI0016B01, it was used for the core drilling of both KI0014B01 and KI0016B01. Drillcon driller Anders Asp at the mechanical/hydraulic control unit to the left (photo: Oskar Sigurdsson).*

2.4 Location and other borehole data

All three core boreholes were drilled from the right wall of the tunnel TASI located at the -450 m level in the Äspö tunnel system and parallell to the planned new tunnel. As can be seen in Figure 2-4 two of the boreholes (KI0014B01 and KI0016B01) were drilled within the tunnel contour and one (KI0010B01) outside. For some additional borehole data see Table 2-2 below.

Originally all three boreholes were intended to be drilled within the tunnel contour to get as much information as possible about the rock volume to be excavated. To place them in the corners of an imaginary triangle would make it possible to orient a planar structure, such as a fracture, if it could be identified in all three holes. The first set up of the holes was an equilateral triangle with two holes on a horizontal line at the top and the third one in a triangle corner underneath. Unfortunately this set-up interfered with some of the initial test for the sealing project. The triangle was then moved sideways but then one of the holes came too close to the planned tunnel contour. Eventually the borehole set-up got its present shape.

The borehole placed outside the tunnel contour was initially intended to be kept open as an observation hole during the excavation of the TASS-tunnel. Later it was, however, considered that the hole might disturb the blasting work and/or that the casing and valve at the opening of the hole (see chapter 2.5.2) might be thrown out from its position by blasts. Due to these risks the hole was grouted together with the other two holes as described in the internal SKB document “AP TD SU32516-07-056 Fyllning av tre kärnborrhål” (AP TD SU32516-07-056 Grouting of three core boreholes).

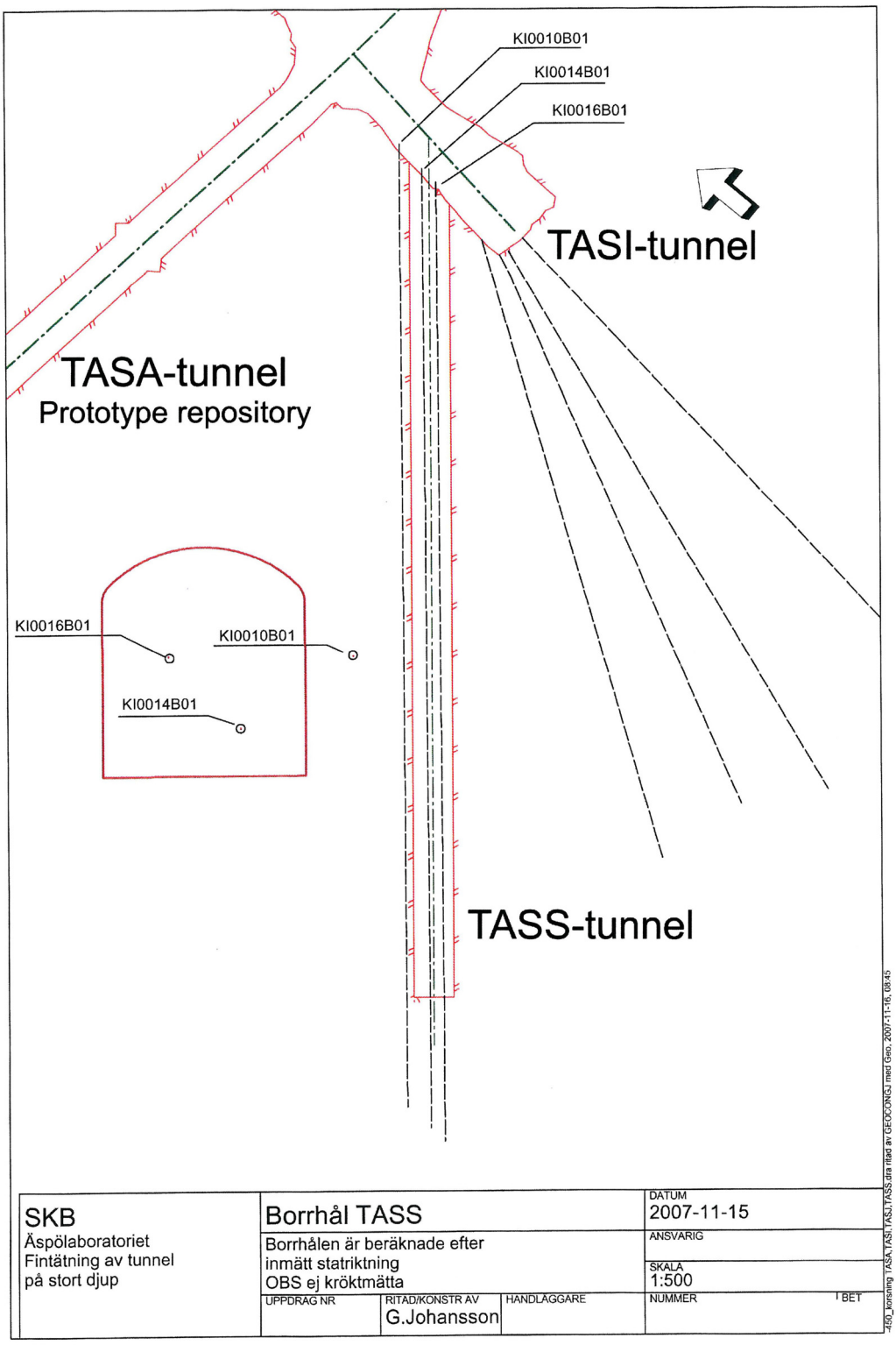

Figure 2-4. *Drawing of the Äspötunnel at -450 m level with boreholes KI0010B01, KI0014B01 and KI0016B01 marked, they are 100.64, 100.27 and 100.24 m long respectively. The arrow points to north in the Äspö96 coordinate system. The direction of the boreholes is measured at the starting point and then the layout of the boreholes is calculated from that. Present tunnel outlines are marked in red as well as the planned outline of the TASS tunnel (parallel to the three boreholes). To the left a cross section of the planned TASS tunnel is drawn in red with the positions of the three boreholes marked (The slightly modified drawing by courtesy of Gerry Johansson, Geocon AB).*

Table 2-2. Geometric and technical data for boreholes KI0010B01, KI0014B01 and KI0016B01.

Parameter	KI0010B01	KI0014B01	KI0016B01
Drilling period, Casing	From 2007-03-12 to 2007-03-12	From 2007-03-19 to 2007-03-20	From 2007-03-13 to 2007-03-14
Casing borehole length, referring to rock surface/wall	0.00 - 2.30 m	0.00 - 2.30 m	0.00 - 2.30 m
Casing outside rock surface/wall [*(0.61etc)* refers to top of casing]	0.60 *(0.61)* m	0.70 *(0.64)* m	0.60 *(0.61)* m
Drilling period, ordinary borehole below casing	From 2007-04-11 to 2007-04-21	From 2007-06-14 to 2007-06-18	From 2007-06-01 to 2007-06-08
Ordinary borehole length, referring to top of casing	2.91 - 100.64 m	2.94 - 100.27 m	2.91 - 100.24 m
Starting point coordinates (coordination system: Äspö96)	Northing: 7254.30 m Easting: 1954.09 m Elevation: -446.01 m.a.s.l.	Northing: 7250.84 m Easting: 1953.61 m Elevation: -447.56 m.a.s.l.	Northing: 7248.80 m Easting: 1953.49 m Elevation: -446.06 m.a.s.l.
Borehole azimuth (0 - 360º)	229.84º	229.75º	229.79º
Borehole inclination at starting point (0 - 90º, negative values = downward plunge)	-0.55º	-0.65º	-0.53º
Borehole diameter Section / diameter (m), [Section refers to top of casing except *(0.0-2.30)* that refers to rock surface/wall]	0.0 - 2.91 *(0.0-2.30)* / 0.120 2.91 - 100.64 / 0.076	0.0 - 2.94 *(0.0-2.30)* / 0.120 2.94 – 100.27 / 0.076	0.0 - 2.91 *(0.0-2.30)* / 0.120 2.91 - 100.24 / 0.076
Core diameter Section / diameter (m), [Section refers to top of casing except *(0.0-2.30)* that refers to rock surface/wall]	0.0 - 2.91 *(0.0-2.30)* / 0.110 2.91 - 100.64 / 0.050	0.0 - 2.94 *(0.0-2.30)* / 0.110 2.94 – 100.27 / 0.050	0.0 - 2.91 *(0.0-2.30)* / 0.110 2.91 - 100.24 / 0.050
Casing diameter Section / diameter (m), (Section refers to top of casing & $Ø_i$ = Inner diameter, $Ø_o$ = Outer diameter)	0.0 - 2.77 / $Ø_i$ = 0.080 $Ø_o$ = 0.100	0.0 - 2.81 / $Ø_i$ = 0.080 $Ø_o$ = 0.100	0.0 - 2.79 / $Ø_i$ = 0.080 $Ø_o$ = 0.100

2.5 Some arrangements around the drill site

2.5.1 Scaffolds

A number of arrangements had to be made before the drilling could commence. Scaffolds were built to reach two of the boreholes since they were situated about 2.5 m above the floor of the TASI-tunnel. First a weaker constructed scaffold was built for the casing drilling. The core drill rigs were, however, much heavier and a more sturdy construction was needed (Figure 2-2a, 2-5a and b).

a) ***b)***

Figure 2-5*. Scaffolds with platforms built in the TASI-tunnel on which the drill rigs could be placed.* ***a)*** *In front of the scaffold a container used for sedimentation of drill mud and cuttings while the casing drilling took place (photo: Oskar Sigurdsson).* ***b)*** *The scaffold used for the core drilling. The weaker part of construction is for staff and the sturdy one is for the drill rigs (photo: Elinor Örtendahl).*

2.5.2 Casing

The casing that was used was specially made to withstand the high water pressures that were expected (see the principle sketches in Appendix 1A-C and Figure 2-6a and b). The casing was supplied with a number of valves and a pressure gauge. When the core drilling took place the drill pipes had to go through the valves (see Figures 2-6a and b). The inner part of the casing was glued to the borehole wall and outside the hole it was anchored to the tunnel wall by bolts.

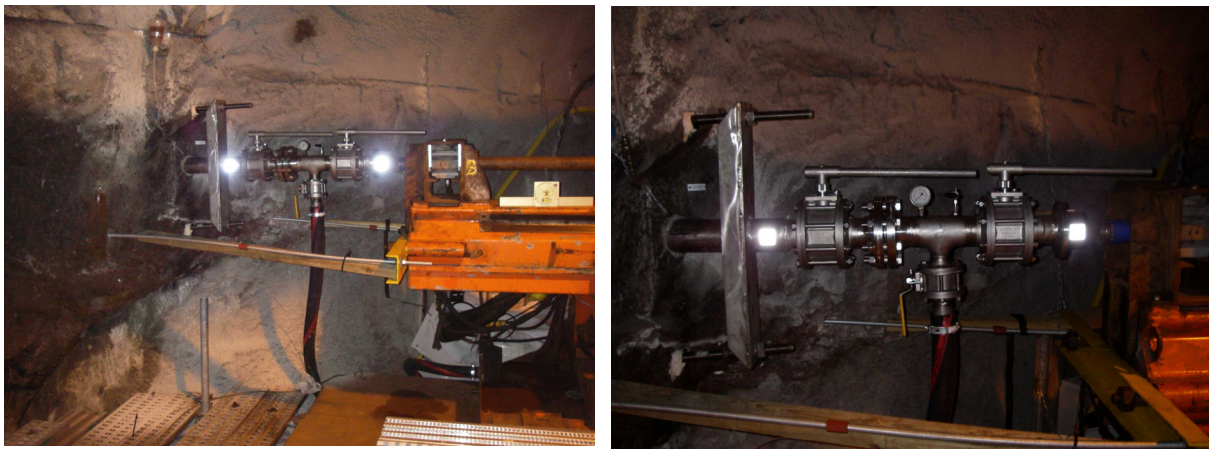

a) ***b)***

Figure 2-6*. The arrangement of the casing and the core drill rig.* ***a)*** *The drill rig is fastened to the tunnel wall by bolts and the drill pipe is in place in the casing (photo: Elinor Örtendahl).* ***b)*** *A close-up of the valve taps and the water pressure gauge (photo: Oskar Sigurdsson).*

2.5.3 Flush and return water – flow-chart

The drilling water had to be handled in accordance with a specific flow chart (Figure 2-7). One reason for this was to avoid that drill mud and cuttings got into the drainage system of the Äspö HRL. Another reason to follow the flow chart was to avoid possible radioactivity (see section 2.5.4 below) to leak out when the water was discharged. The return water was discharged via the draining-well in the intersection of the tunnels TASA-TASI down to the weir MA3411G in the TASA-tunnel and further via a drain to the pumping station PG5 in the TASF-tunnel.

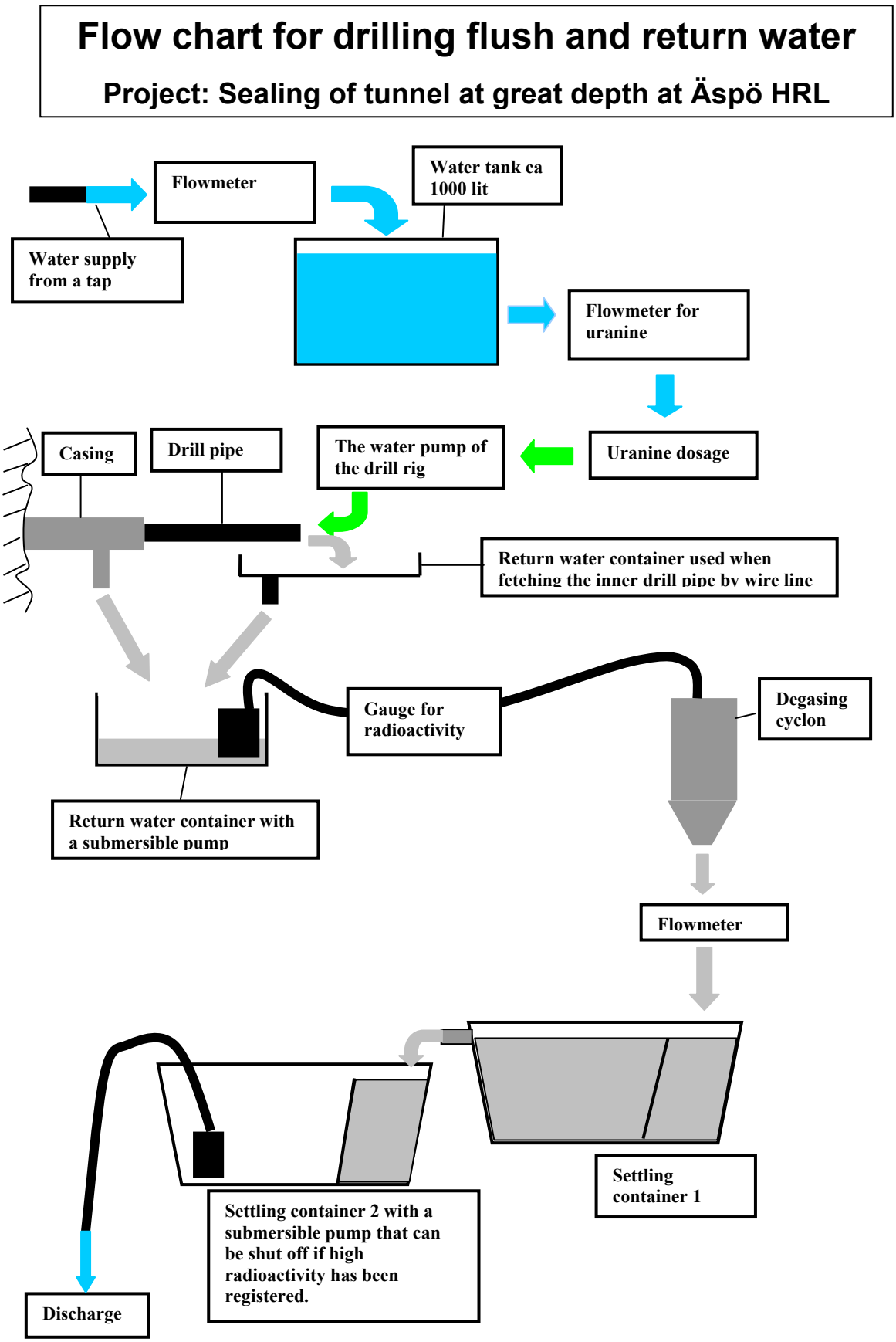

Figure 2-7. *The flowchart regulating how the drill water should be handled (Modified from Nils Håkanson 2007, Håkanson Coring Consultants, for SKB, internal document).*

2.5.4 Radioactivity

The TASI-tunnel had earlier been used for experiments within the True Block Scale project (TRUE= Tracer Retention Understanding Experiment) that involved the use of minor amounts of radionuclides (Andersson, Byegård and Winberg 2002b). The possibility to encounter radioactive trace elements while drilling the three new boreholes was discussed in the internal SKB document "PM rörande en radiologisk riskanalys av kärnborrning inför och bygge av tunnel utgående från TASI, Äspölaboratoriet" (PM concerning a radiolgic risk analysis for core drilling due to the planned excavation of a tunnel emanating from TASI, Äspö Hard Rock Laboratory, J. Byegård, C. Hjerne and P. Andersson 2007, Geosigma AB for SKB). Figure 2-8 shows the preliminary location of the new tunnel TASS in relation to some major structures that were identified and used within the True Block Scale experiment.

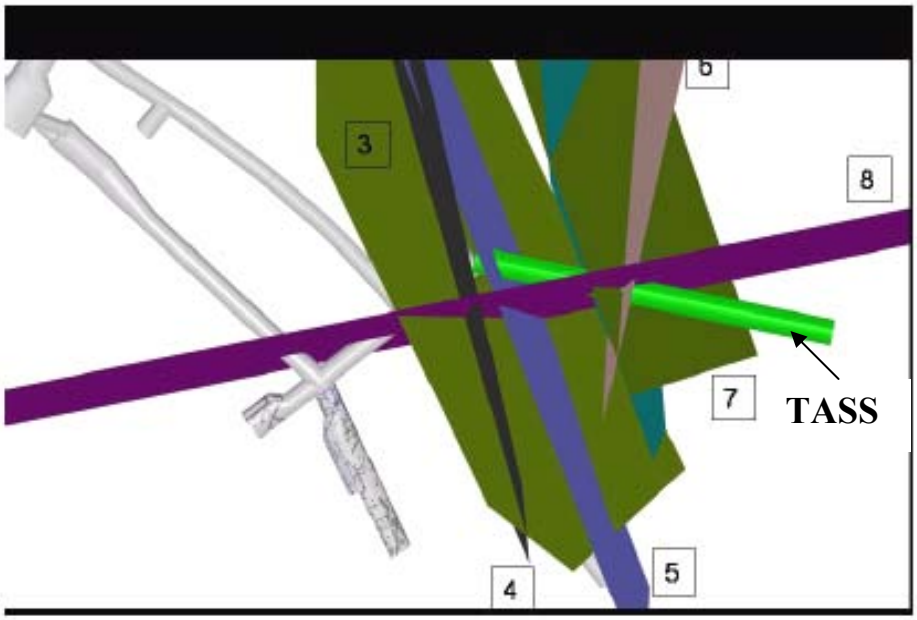

Figure 2-8. *Location of structures (3-8) modelled in the True Block Scale that may intersect the prospective TASS-tunnel (green). Existing tunnels are shown in grey colour (slightly modified from "PM rörande en radiologisk riskanalys av kärnborrning inför och bygge av tunnel utgående från TASI, Äspölaboratoriet", J. Byegård, C. Hjerne and P. Andersson 2007, Geosigma AB for SKB, internal document).*

Although no radioactive trace elements were expected measurements were made on the return water during the drilling according to a procedure described in the activity plan AP TD SU32516-07-018 (internal SKB document). For example, a RNI 10/SR-instrument, measuring the effective dose rate, was placed on the return water pipe to ensure that the radioactivity of the returning drill water stayed below allowed limits. Before the drill rigs and other equipment were allowed to leave the drill site after having completed their mission they were tested for radioactivity. Also the site itself was checked (Figure 2-9). Besides the measurements performed directly on site a number of "wipe samples" were taken to be analysed. The "wipe samples" were collected by wiping equipment and various other items at the site with pieces of cloth that were sent to a laboratory for analyses. All these analyses were below the detection limits or in a few cases just above (0.021-0.077 Bq/cm^2). Bjarne Karlsson from CLAB (Central interim storage facility for spent nuclear fuel) performed all the tests.

a) ***b)***

Figure 2-9. a) *Equipment used for measurements of radio activity.* ***b)*** *The tunnel wall of TASI is tested by Bjarne Karlsson from CLAB using a scintillation detector (photos: Oskar Sigurdsson).*

Table 2-3 shows the results from some of the measurements that took place. It is only the analyses of Mn-54 and Cs-137 that are relevant since the rest of them (Co-54, Zn-65 and Ag-110) refer to substances that never were injected into the rock mass during the True Block Scale experiment. All the analyses shown in Table 2-3 and measurements around the drill site showed that the radioactivity was non-existent or below detection limits and below approved limits. As far as water is concerned the allowed limit is 500 Bq/litre (”PM rörande en radiologisk riskanalys av kärnborrning inför och bygge av tunnel utgående från TASI, Äspölaboratoriet”. J. Byegård, C. Hjerne and P. Andersson 2007, Geosigma AB for SKB, internal document). Besides the tests on water Table 2-3 includes five core samples that were taken from the core of borehole KI0010B01 to be analysed on radioactive isotopes. Since the radioactivity in all the core samples was below the detection limit the result of the test is summarized in just one row in Table 2-3.

Also the personnel that were involved in the pre-investigations had to be tested for possible influence of radioactivity. This involved a medical examination at the beginning of the project. While the investigations were going on the staff had to carry a dosimeter which was handed in every month for analyses. The old dosimeter was replaced with a new one. The dosimeters indicated none or at least no harmful radioactivity (well below the upper accepted limit of 20 mSV/year, see ”PM rörande en radiologisk riskanalys av kärnborrning inför och bygge av tunnel utgående från TASI, Äspölaboratoriet”. J. Byegård, C. Hjerne and P. Andersson 2007, Geosigma AB for SKB, internal document).

Table 2-3. Results from analyses of radioactive isotopes during the pre-investigations of the prospective TASS-tunnel (modified after compilation by M. Kronberg, 2007 SKB internal document).

Date year-month-day	Type of sample	Mn-54 (kBq/kg)	Co-60 (kBq/kg)	Zn-65 (kBq/kg)	Ag-110m (kBq/kg)	Cs-137 (kBq/kg)	Comments
2007-03-14	Water, stainless container	<1,2E-3	<2,4E-3	<3,0E-3	<1,5E-3	<1,0E-3	Sample taken at the end of casing drilling of KI0016B01
2007-03-14	Water, plastic container	<1,1E-2	<1,9E-2	<3,4E-2	<1,6E-2	<1,1E-2	Sample taken at the end of casing drilling of KI0016B01
2007-03-20	Drill water	<1,4E-2	<2,5E-2	<3,0E-2	<1,8E-2	<1,2E-2	Sample taken after casing drilling of KI0014B01
2007-04-16	Drill water	<1,0E-2	<2,6E-2	<3,6E-2	<2,0E-2	<1,4E-2	During drilling of KI0010B01 at approx. 56 m length
2007-04-19	Drill water	<5,0E-4	<1,0E-3	<1,3E-3	<8,3E-4	<5,5E-4	During drilling of KI0010B01 at approx. 83 m length
2007-06-05	Water, sedimentation-tank	<1,3E-3	<4,1E-3	<4,7E-3	<2,8E-3	<2,2E-3	During drilling of KI0016B01 at approx. 49 m length
2007-06-14	Water, sedimentation-tank		1,9E-03				During drilling of KI0014B01 at approx. 10 m length
2007-06-19	Water, sedimentation-tank	<6,5E-3	<1,8E-2	<2,5E-2	<1,5E-2	<9,5E-3	After completion of the drilling of KI0014B01
2007-06-26	Water, KI0010B01	<9,8E-3	<2,1E-2	<3,3E-2	<1,8E-2	<1,3E-2	Borehole completed 2007-04-21
2007-06-26	Water, KI0014B01	<1,5E-2	<2,5E-2	<4,4E-2	<2,3E-2	<1,5E-2	Borehole completed 2007-06-18
2007-06-26	Water, KI0016B01	<9,5E-3	<2,0E-2	<3,2E-2	<1,8E-2	<1,3E-2	Borehole completed 2007-06-08
2007-06-20	Rock material/drill cores from KI0010B01	<2,0E-3	<3,6E-3	<9,5E-3	<5,3E-3	<4,3E-3	For sections see below

Sample (No) & Sections: (1) 18.249 - 18.291, (2) 20.645 - 20.696, (3) 36.105 - 36.146, (4) 40.625 - 40.664 and (5) 75.495 - 75.544 adjusted lengths, see section 3.4.2

3 Borehole mapping/core logging

3.1 Introduction

The three cored boreholes KI0010B01, KI0014B01 and KI0016B01 (Figure 2-4) were BIPS logged (see section 3.3.1) and mapped according to the Boremap method (see section 3.3.2).

The work was carried out in accordance with activity plan AP TD SU32516-07-017. The core logging according to the Boremap method is described in the method description SKB MD 143.006. Table 3-1 lists the controlling documents for performing this activity. Both activity plan and method description are SKB internal controlling documents.

The Boremap mapping method is based on combined information from detailed drill core logging and BIPS-image to determine both petrographical (rock types, rock occurrences and alteration) and structural (fractures, crush zones and ductile deformation) information. In addition the Boremap mapping software calculates the orientation (strike and dip) of each marked planar feature in the borehole using information from the BIPS-image and borehole surveying (see Table 2-2 for some surveying and borehole data).

The outer parts of the boreholes were not BIPS-logged but were, however, logged with the Boremap system. Due to the lack of BIPS-images no orientations could be obtained for planar structures and no core logs have been made for this part of the boreholes.

All data were stored in the primary SKB database Sicada for Oskarshamn and are traceable by the activity plan number.

Table 3-1. Controlling documents for the performance of the activity.

Activity plan	**Number**	**Version**
Boremapkartering av KI0010B01, KI0014B01 och KI0016B01 *(Boremap logging of KI0010B01, KI0014B01 and KI0016B01)*	AP TD SU32516-07-017	1.0
Method descriptions	**Number**	**Version**
Metodbeskrivning för Boremap – kartering *(Method desription for Boremap logging)*	SKB MD 143.006	2.0
Mätsystembeskrivning (MSB) för Boremap kartering. Boremap version 3.0 *(Desription of the messuring system, MSB, for Boremap logging. Boremap version 3.0)*	SKB MD 146.005	1.0
Nomenklatur vid Boremap-kartering *(Boremap logging Nomenclature)*	SKB MD 143.008	1.0
Regler för bergarters benämningar vid platsundersökningen i Oskarshamn *(Rules for rock type names to be used at the site investigations at Oskarhamn)*	SKB MD 132.004	2.0

3.2 Objective and scope

The purpose of this survey is to map all lithological and structural parameters of boreholes KI0010B01, KI0014B01 and KI0016B01 by using the Boremap mapping method.

- The mapped parameters of the Boremap mapping are:
- Rock types (>1 m wide)
- Rock occurrences (<1 m wide)
- Rock contacts
- Fractures (open and closed as well as sealed networks, cataclastic structures, breccia and crush zones)
- Fracture fillings
- Ductile structures (e.g. foliation, shear zones etc.)
- Alterations

The rock type nomenclature used in this survey is from the site investigation at Oskarshamn and is shown in Table 3-2 [internal SKB document "Instuktion: Regler för bergarters benämningar vid platsundersökningen i Oskarshamn", SKB MD 132.004. (Instruction: Rules for rock type names to be used at the site inverstigations at Oskarshamn)].

Table 3-2. The rock nomenclature (rock types and rock occurrences) used in the Boremap mapping.

Rock type	Rock code	Rock description
Dolerite	501027	Dolerite
Fine-grained Götemar granite	531058	Granite, fine- to medium-grained, ("Götemar granite")
Coarse-grained Götemar granite	521058	Granite, coarse-grained, ("Götemar granite")
Fine-grained granite	511058	Granite, fine- to medium-grained
Pegmatite	501061	Pegmatite
Granite	501058	Granite, medium- to coarse-grained
Ävrö granite	501044	Granite to quartz monzodiorite, generally porphyritic
Ävrö granodiorite	501056	Granite to granodiorite, generally porphyritic
Ävrö quartz monzodiorite	501046	Quartz monzonite to quartz monzodiorite, generally porphyritic
Quartz monzodiorite	501036	Quartz monzonite to monzodiorite, equigranular to weakly porphyritic
Äspö diorite	501037	Quartz monzodiorite to granodiorite, porphyritic

Rock type	Rock code	Rock description
Diorite/gabbro	501033	Diorite to gabbro
Fine-grained dioritoid	501030	Intermediate magmatic rock
Fine-grained diorite-gabbro	505102	Mafic rock, fine-grained
Greenstone	508107	Mafic rock, undifferentiated
Mylonite	508004	Mylonite
Sulphide mineralization	509010	Sulphide mineralization
Sandstone	506007	Sandstone

3.3 Description of equipment/interpretation tools

3.3.1 Borehole Image Processing System – BIPS

The BIPS 1500 system used is owned by SKB and described in the SKB internal controlling documents MD 222.006 "Metodbeskrivning för TV-loggning med BIPS" ("Method description concerning TV-logging with BIPS", A. Stråhle and L. Stenberg 2002) and MD 222.005 "Mätsystembeskrivning (MSB) – Allmän del. Mätning med BIPS-1500" ("Measuring system description (MSB) – general part. Measuring with BIPS-1500", Ch. Gustafsson 2003). The BIPS method for borehole logging produces a digital scan of the borehole wall. In principle, a standard CCD video camera is installed in the probe in front of a conical mirror (see Figure 3-1). An acrylic window covers the mirror part and the borehole image is reflected through the window and displayed on the cone, from where it is recorded. During the measuring operation, pixel circles are grabbed with a resolution of 360 pixels/circle.

The system orientates the BIPS images according to two alternative methods, either using a compass (vertical boreholes) or with a gravity sensor (inclined boreholes). The BIPS probe is via a cable connected to the instrument and control box (Figure 3-2). The text and figure 3-1 of this section (3.3.1) has been copied and slightly modified from J. Gustafsson and Ch. Gustafsson (p. 12, 2005)

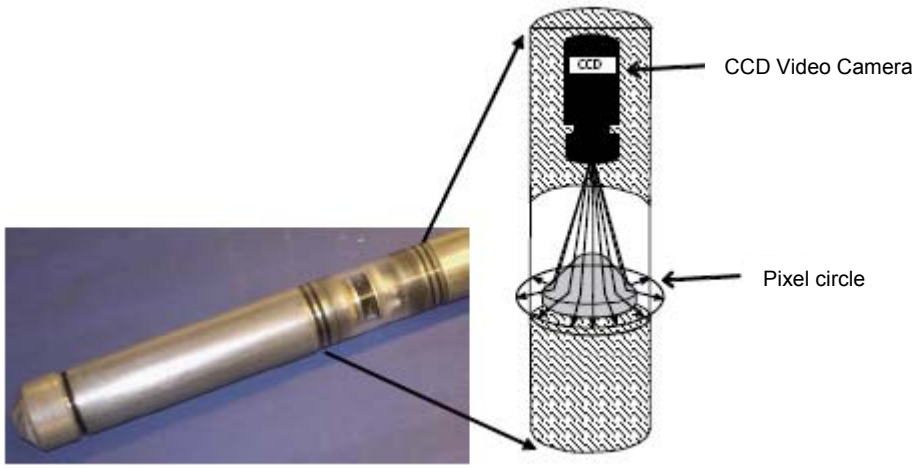

Figure 3-1. *The BIPS-system, Illustration of the conical mirror scanning.*

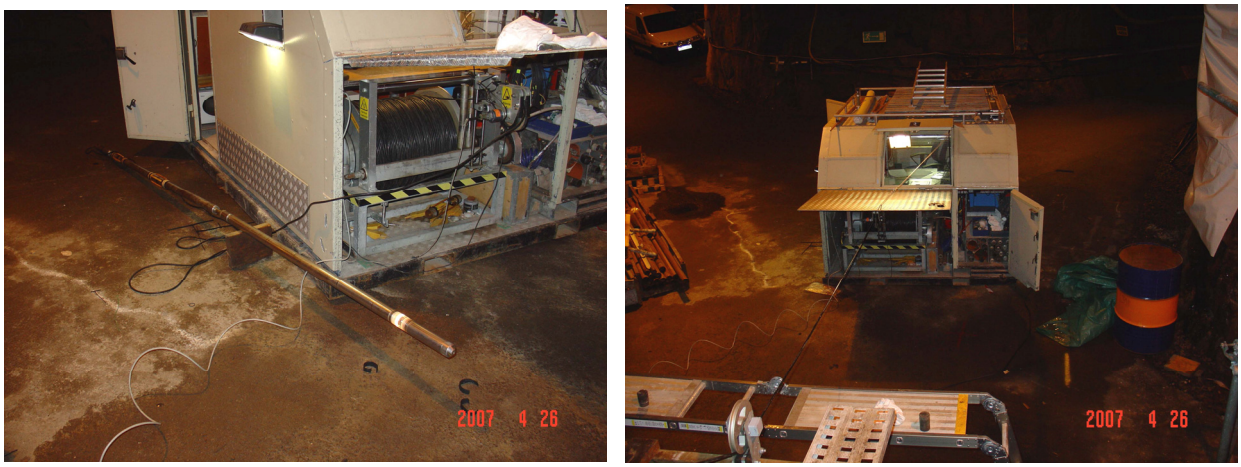

a) ***b)***

Figure 3-2. a) *The BIPS probe and the instrument & control box.* ***b)*** *The instrument & control box. The BIPS probe is inserted in a borehole and connected to the box with a cable (photos: Ch. Gustafsson).*

3.3.2 Core logging with Boremap

Mapping of BIPS-images and drill cores according to the Boremap method is done on a desktop computer using the software Boremap (version 3.9.21), which shows the BIPS-image (Figure 3-3). The Boremap software is loaded with the SKB rock and mineral standard. The software Boremap facilitates the extraction of the geometrical parameters length, width, strike and dip from the BIPS image.

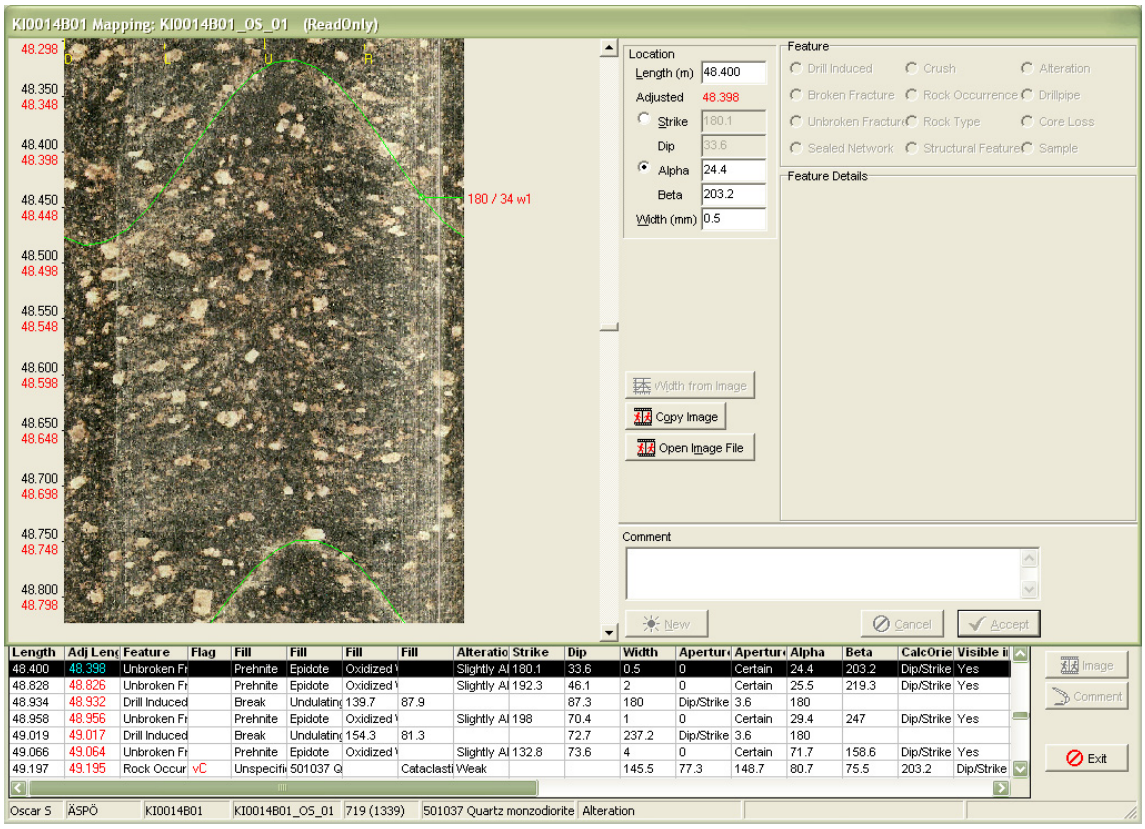

Figure 3-3. *A good quality BIPS-image as it is seen in the Boremap software. Borehole KI0014B01, length 48.3 – 48.8 m adjusted length (see section 3.4.2), showing grey, and medium to coarse grained, massive, porphyritic Äspö diorite. The thin lines on each side of the figure are air bubbles or small pieces of mud on the cover glass of the BIPS camera. Green lines mark unbroken fractures logged by the geologist, showing slight alteration.*

The possibility of the Boremap mapping method to accurately map the geological parameters that the borehole traverses depends mainly on the following parameters:

- The quality of the drill core (e.g. the amount of drill induced fractures, core loss, grinding of core pieces etc.)
- The accuracy of the measurements of the boreholes length, diameter and orientation, i.e. the azimuth and dip
- The BIPS-image, which in turn is dependent on
    - The technical limitations of the BIPS-image (i.e. resolution and contrast)
    - The clarity of the borehole water (i.e. the amount of material in suspension)
    - The condition of the borehole walls (e.g. the amount of sedimentation on the borehole wall)

The BIPS-image quality of borehole KI0010B01 is good down to a crush zone at approximately 54.5 m (adjusted length), where the number of stripes/lines in the image increases. These are air bubbles or small mud fragments on the cover glass of the BIPS camera. The stripes/lines increase in number with borehole length, impairing visibility somewhat.

In borehole KI0014B01 the BIPS image quality is good down to 51.1 m. There an approximately 3 cm wide crush zone occurs. According to the BIPS image it seems to be water yielding. The result is a BIPS image with some mud in suspension and stripes/lines on the image. Visibility is not impaired seriously until about the last meter of image.

The BIPS image of borehole KI0016B01 is of good quality until approximately 48.8 m length. There an open fracture, possibly water yielding, occurs and some increase of stripes/lines in the image takes place. At ca 70.8 m length some minor amounts of mud comes into suspension below an approximately 1.5 cm wide crush zone (water yielding), resulting in somewhat decreased visibility (see Figure 3-4). Finally below approximately 84 m length until the end of the borehole the visibility of the BIPS image is poor because of the amount of mud in suspension.

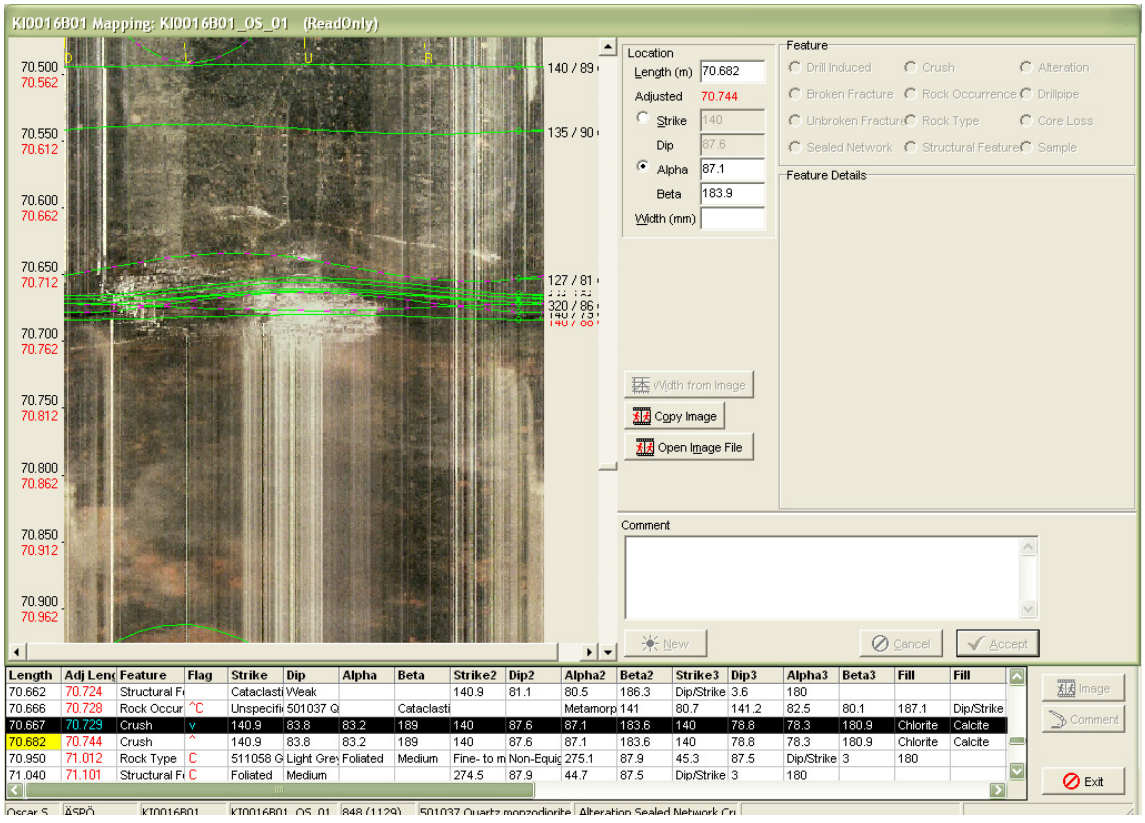

Figure 3-4. *Medium quality BIPS-image as seen in Boremap from borehole KI0016B01, length 70.6 –71 m adjusted length; showing a crush zone. The thin bands on both sides of the figure are impurities on lower side of the camera cover glass, they show a marked increase below the crush zone and also the image becomes diffuse because of mud in suspension. The interpretation is that the crush zone is most probably water yielding.*

The equipments used for examining the drill cores are; a hand held lens, streak plate (a piece of white, unglazed porcelain), small magnet, hydrochloric acid (HCl 10% solution) and a knife. Length measurements of the cores were done by folding rule and water spray gun (atomizer filled with tap water) was used to wet the core for clearer view of rock and mineral colours. Susceptibility meter SM20 from GF instruments was used for measurements of the magnetic susceptibility of the drill cores, as well as a stereomicroscope Zeiss Stemi DV 4 (magnification 8X-32X) when necessary.

3.4 Execution of the core logging

3.4.1 General

The cores are lying in open core boxes on horizontal roller tables in the core logging facilities at Äspö while they are being mapped with the Boremap system. A computer is placed at the roller table where the BIPS-image is opened in the Boremap program and the observed appropriate parameters are marked and described.

The mapping is done in accordance with the activity plan “Boremapkartering av KI0010B01, KI0014B01 och KI0016B01” (AP TD SU32516-07-017, SKB internal document). The method description for Boremap mapping “Metodbeskrivning för Boremap kartering” (SKB MD 143.006, v2.0, SKB internal document) is used. Chapter 3.2.3 in that document was, however, excluded since no geophysical logging was conducted in the hole nor any reference slots cut in the borehole wall. The measuring system description for Boremap mapping “Mätsystembeskrivning (MSB) för Boremapkartering. Boremap version 3.0” (SKB MD 146.005, SKB internal document) was also used as well as the instruction ”Nomenklatur vid Boremap-kartering” (SKB MD 143.008, SKB internal document) and ”Regler för bergarters benämning vid platsundersökningen i Oskarshamn” (SKB MD 132.004, SKB internal document) The latter document dictates the rules for rock names at the Oskarshamn site investigation, with the exceptions for rock names according to the Äspö nomenclature (see Table 3-1 and 3-2).

3.4.2 Preparations

Boremap mapping uses data from the SKB database Sicada, e.g. borehole direction and inclination as well as borehole diameter, borehole length and length of casing. The measured length registered in the BIPS-image deviates from the true length by a factor of approximately 0.5 m per 100 m. The adjusted length of the BIPS-image is thus calculated from the known end of the casing (Figure 3-5) to bottom of image according to a constant (ca 0.5 m/100 m).

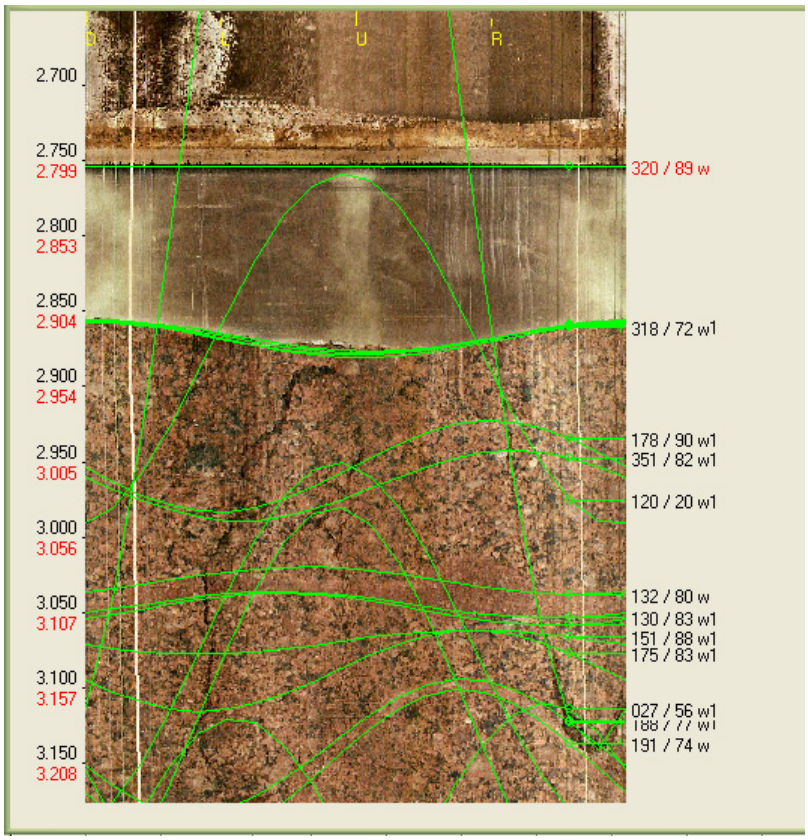

Figure 3-5. *Good quality BIPS-image as seen in Boremap, borehole KI0014B01, length 2.8 - 3.2 m, showing the lowest part of casing pipe and ca 10 cm of Epoxy from the bottom plug and borehole wall. Rock type is Äspö diorite showing red staining (alteration) of medium intensity, cut by two thin (2 and 1.5 cm wide) fine-grained granite veins. Green lines mark the top of rock type, rock occurrences, fractures (both broken and unbroken) and top of red staining. Vertical streaks are impurities on the protective glass of the BIPS-camera. Bottom of casing pipe is at 2.8 m.*

The basis for calculating the strike and dip of the mapped planar structures are borehole diameter and the orientation of the borehole i.e. the azimuth and dip. Data from deviation measurements with Flexit were used to correct for changes in direction of the boreholes with length.

3.4.3 Execution of field work

BIPS-images make it possible to obtain reliable orientation of mapped planar structures in the borehole core. Such structures are fractures, rock contacts and deformational structures.

Fractures that are visible in both core and BIPS-image are compared and marked. Aperture is usually measured in the BIPS-image. All apertures less than 1 mm are given the designated aperture of 0.5 mm (the uncertainty of measurement in the BIPS-image, +/- 0.5 mm). Fractures found in the core but not visible in the BIPS-image are marked and oriented in the BIPS-image by comparing them with nearby similar fractures from the core visible in the image. The “non-visible fractures” are marked as ‘not visible in BIPS’ in the Boremap software. Drilling-induced fractures are marked on the core

boxes by the drillers (the letter F). The core is handled with care to minimize further breaking. However, there exist fractures with perfect fit between the two fracture surfaces that are not visible in the BIPS-image. Normally these fractures are interpreted as being drill-induced or have at least a note in the comment field in the Boremap mapping that they are possibly drill-induced. Fractures that do not cross the centre of the core are not orientated in the BIPS-image and are marked as "not centrum covered" in the Boremap mapping.

Fracture fillings are noted in the order of decreasing abundance; if there are more than four minerals identified they are noted in the comment field. The abundance of each mineral is subjective and is decided by ocular observations with the help of magnifying lens and hydrochloric acid. This may result in possible misrepresentation of certain minerals depending on their visibility, distribution in the fracture or reaction to hydrochloric acid as well as whether the fracture is open or closed. For example calcite could be overrepresented because of its strong reaction to hydrochloric acid and pyrite underrepresented in closed fractures since it often appears in small (< 1mm) grains on fracture surfaces.

Cataclastic structures are here mapped as structural parameters within the Boremap parameter rock occurrence. This has an upper and lower contact which is used to define the width of the rock occurrence. Usually these rock occurrences are dominated by green Epidote and/or Prehnite matrix with various amounts of clasts, normally consisting of Äspö diorite. In this case the rock occurrence is defined as Äspö diorite (501037). Strike and dip of the cataclastic structure is obtained by setting it as a structural parameter within the rock occurrence, see Figures 3-6 and 3-9. This makes it possible to plot it on stereograms, rose diagrams and present it in a separate WellCad column (structure orientation).

In this mapping the term crush zone is used when both the core and BIPS image show a prominent increase in open fractures (see Figure 3-4). Crush zones have upper and lower contacts, which are parallel to dominating fracture directions within the zone. In addition two dominating fracture orientations are marked within each zone when possible. The piece length is defined as the average size of broken rock bits within the zone in mm.

The term sealed network is used here when the core shows marked increase in mainly thin (less than 1 mm wide) and mostly Epidote and/or Prehnite sealed fractures. Sealed networks also have designated upper and lower contacts. When possible they follow existing fractures, but at other times a line is drawn at the upper and lower borders of a significant increase in the number of sealed fractures, see Figure 3-9.

3.4.4 Data handling

The Boremap mapping is performed on a desktop computer connected to the SKB network at the core storage facility on Äspö. It has a daily back up at a separate location on the SKB internal network. The mapping is checked by the geologist that is performing the mapping and with the help of a computer routine in Boremap before the daily back-ups as well as when the mapping is finished. The data is then submitted to SKB for quality assessment and exportation to the Sicada database.

3.5 Results

The results from the Boremap mapping for boreholes KI0010B01, KI0014B01 and KI0016B01 are given below. Some screen dumps, illustrating BIPS images, are shown as examples from the core logging with the Boremap software (Figures 3-6 through 3-9). The percentages of different lithologies are given in Tables 3-3 through 3-5.

Various portions of the rock show red staining (oxidation) as well as green staining (epidotization). Table 3-6 shows the distribution as well as the intensity of the staining. In this Boremap mapping the alteration intensity was defined as weak when red- and/or green- staining could be observed in the core. The alteration was defined as medium when the red- and/or green- staining dominated over the original rock colour.

Table 3-7 shows the number of fractures in the mapped boreholes (open, sealed and partly open fractures) and the average fracture frequency per meter. Crush zones mapped from the cores and BIPS-image are in Table 3-8. There length to the upper contact, width of each zone, the average piece length and the strike and dip of the upper contact are listed.

Table 3-9 lists the number and direction of the cataclastic structures mapped in the three boreholes. Also the average width of the rock occurrence that contains the cataclastic structure parameter is given. These cataclastic bands/structures are usually light green and dominated by secondary minerals, mainly Epidote and Prehnite. Fragments of Äspö diorite can sometimes be seen in the matrix.

Table 3-10 shows the number of sealed networks mapped in the boreholes, along with the average width and direction of upper contact.

The orientations of all fractures, all open fractures, all closed fractures, sealed networks, cataclastic structures and crush zones are illustrated in the diagrams in the Figures 3-10 through 3-15. For the separate boreholes see Appendices 2C, 3C and 4C.

Figure 3-16 shows the relationship between the various geographical systems used at Äspö HRL. Beside the tables, figures and appendices that are included in this report, original data can be found in SKB's Sicada data base.

KI0010B01

See Appendix 2A for a WellCAD graphic presentation of mapping results. The BIPS image of the borehole is shown in Appendix 2B and the orientations of all the logged fractures, all open fractures, all closed fractures, sealed network and cataclastic structures are illustrated in Appendix 2C.

Lithology: The dominant rock type is Äspö diorite with small fragments of fine-grained diorite-gabbro (at Äspö HRL often called "greenstone"), cut by minor dykes and veins of pegmatite and fine-grained granite (Figure 3-6 and Table 3-3).

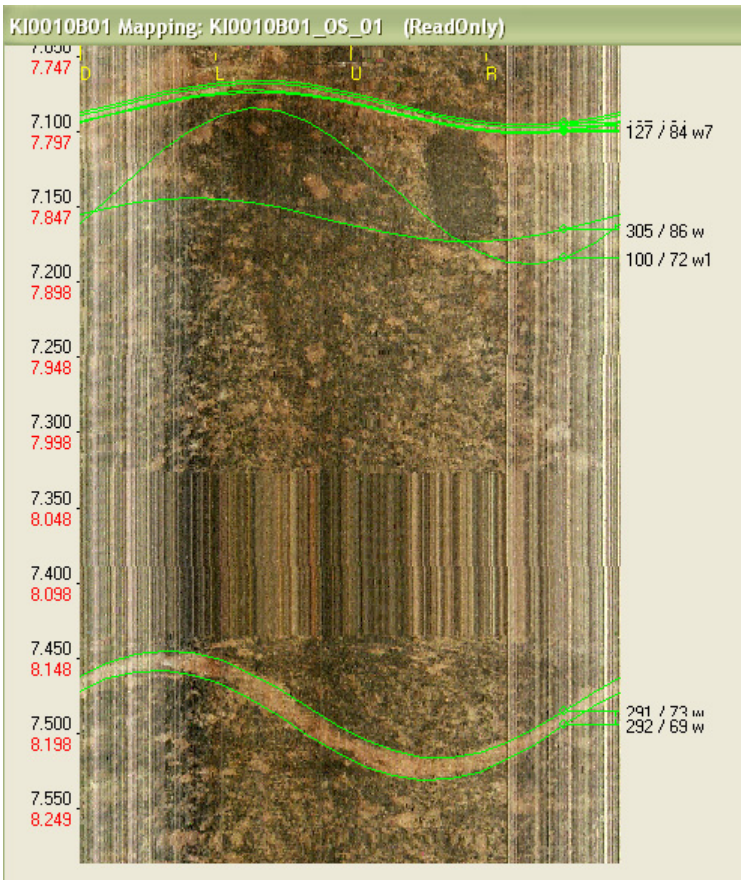

Figure 3-6. *BIPS-image as seen in Boremap from borehole KI0010B01, length 7.7 – 8.2 m adjusted length. The rock type is Äspö diorite with a minor fragment of fine-grained diorite/gabbro ("greenstone"). In the lower part of the image a thin dyke/vein of fine-grained granite cuts the rock, just below an example of vertical enlargements of pixels due to stick-slip movement of the camera probe. Alteration is weak oxidation and epidotization. In upper part of the image a thin cataclastic band with epidote-dominated matrix cuts the Äspö diorite. This band is logged as a rock occurrence of Äspö diorite with a cataclastic structure marked in the middle (with strike/dip: 127/84 degrees).*

Table 3-3. Lithology of KI0010B01. Percents calculated from adjusted length of BIPS-image.

Rock name	SKB rock code	%
Äspö diorite	501037	95.4
Pegmatite	501061	4.3
Fine-grained granite	511058	0.3

Alteration: Alteration in the form of red staining (oxidation) occurs in ca 90% of the core and in the form of epidotization ca 91% (see Table 3-6 and Appendix 2A). The alteration is mainly weak (see Appendix 2A).

Fractures: The number of mapped open fractures are 215, resulting in an average of 2.2 per meter, sealed fractures are 565 (5.7 per/meter) and partly open fractures 48 (ca 0.5 per meter) see Table 3-7. Two thin crush zones were observed at 35.1 and 54.5 m length respectively, in total approximately 0.4 m wide (see Table 3-8). At 54.5 m a possible inflow of water is noted. The number of mapped cataclastic structures is 43 with an average width of 3.5 cm (see Table 3-9), while the number of sealed networks are 59 with average width of 39.5 cm (see Table 3-10).

KI0014B01

See Appendix 3A for a WellCAD graphic presentation of mapping results. The BIPS image of the borehole is shown in Appendix 3B and the orientations of all the logged fractures, all open fractures, all closed fractures, sealed network and cataclastic structures are illustrated in Appendix 3C.

Lithology: The dominant rock type is Äspö diorite (see Figure 3-3) containing minor amounts of fine-grained diorite-gabbro, all cut by subordinate dykes and veins of pegmatite and fine-grained granite, see Figure 3-7 and Table 3-4.

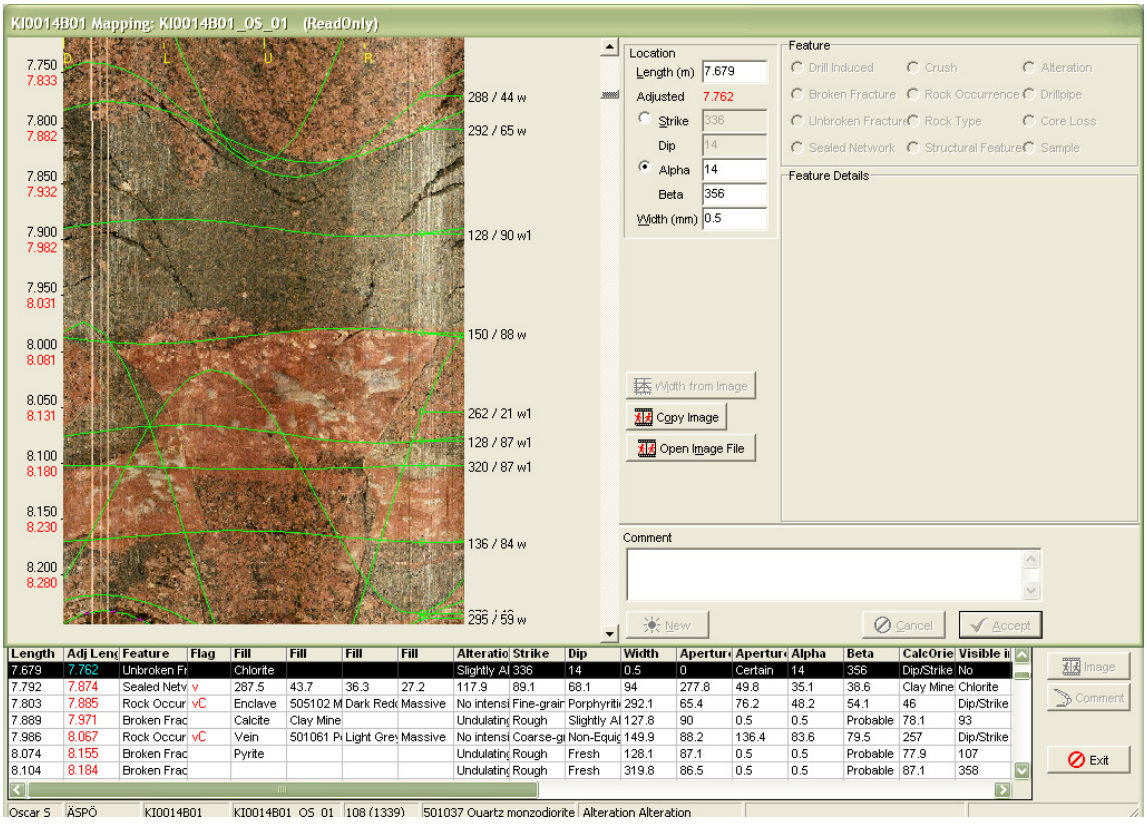

Figure 3-7. *Good quality BIPS-image as seen in Boremap from borehole KI0014B01, length 7.8 –8.3 m adjusted length; Red coloured (oxidized) Äspö diorite containing a xenolith of fine-grained, dark grey diorite-gabbro. Both are cut by a red pegmatite vein/dyke in the central part of the image. All rocks have then been faulted at a later geological event. Broken and unbroken fractures are marked with green lines.*

Table 3-4. Lithology of KI0014B01. Percents calculated from adjusted length of BIPS-image.

Rock name	SKB rock code	%
Äspö diorite	501037	94.0
Pegmatite	501061	2.9
Fine-grained granite	511058	2.1
Fine-grained diorite/gabbro	505102	1.0

Alteration: Alteration in the form of red staining (oxidation) occurs in ca 33% of the core (see Figure 3-5). About 10% of the red staining is of medium intensity (reddish colour dominates over the original colour of the fresh rock). Weak alteration in the form of epidotization makes up ca 84% of the core; see Table 3-6 and Appendix 3A. The epidotization often occurs in connection with and within sealed networks dominated by thin irregular epidote filled fractures and/or veins of Epidote.

Fractures: Mapped open fractures are 340, resulting in an average of 3.5 per meter, sealed fractures 407 (4.2 per/meter) and partly open fractures 24 (ca 0.2 per/m); see Table 3-7. Eight thin crush zones were observed at core length 3.9, 8.5, 13.6, 14.8, 33.2, 40.4, 50.5 and 51.1 m. In total they are approximately 0.6 m wide, where the crush zones at 14.8 and 40.4 m make up ca 54% of the total width; see Table 3-8. Cataclastic structures are 52 with an average width of 1.5 cm (see Table 3-9), while sealed networks are 61 with average width of 63.2 cm (see Table 3-10).

KI0016B01

See Appendix 4A for a WellCAD graphic presentation of mapping results. The BIPS image of the borehole is shown in Appendix 4B and the orientations of all the logged fractures, all open fractures, all closed fractures, sealed network and cataclastic structures are illustrated in Appendix 4C.

Lithology: The dominant rock type is Äspö diorite with minor occurrence of Ävrö granite and occasional small fragments of fine-grained diorite/gabbro, all cut by minor dykes and veins of pegmatite and fine-grained granite; see Table 3-5 and Figures 3-4, 3-8 and 3-9).

Table 3-5. Lithology of KI0016B01. Percents calculated from adjusted length of BIPS-image.

Rock name	SKB rock code	%
Äspö diorite	501037	92.2
Fine-grained granite	511058	3.3
Ävrö granite	501044	2.9
Pegmatite	501061	1.4
Fine-grained diorite/gabbro	505102	0.2

Alteration: Alteration in the form of red staining (oxidation) occurs in ca 44% of the core (approximately 42% is weak and 3% is of medium intensity). Weak alteration in the form of epidotization (commonly as sealed network, see Figure 3-9) makes up ca 69% of the core; see Table 3-6 and Appendix 4A.

Fractures: The number of mapped open fractures are 230, resulting in an average of 2.4 per meter, sealed fractures 216 (2.2 per/meter) and partly open fractures 23 (ca 0.2 per/m); see Table 3-7 and Figure 3-8. Four thin crush zones were observed at core length 12.8, 13.3, 31.0 and 70.7 m, see Figure 3-4. In total they are approximately 0.9 m wide, where the crush zone at 31.0 m makes up ca 94% of the total width; see Table 3-8. The number of cataclastic structures are 51 with an average width of 1.1 cm (see Table 3-9 and Figure 3-9), while the number of sealed networks are 62 with average width of 57.8 cm (see Table 3-10 and Figure 3-9)

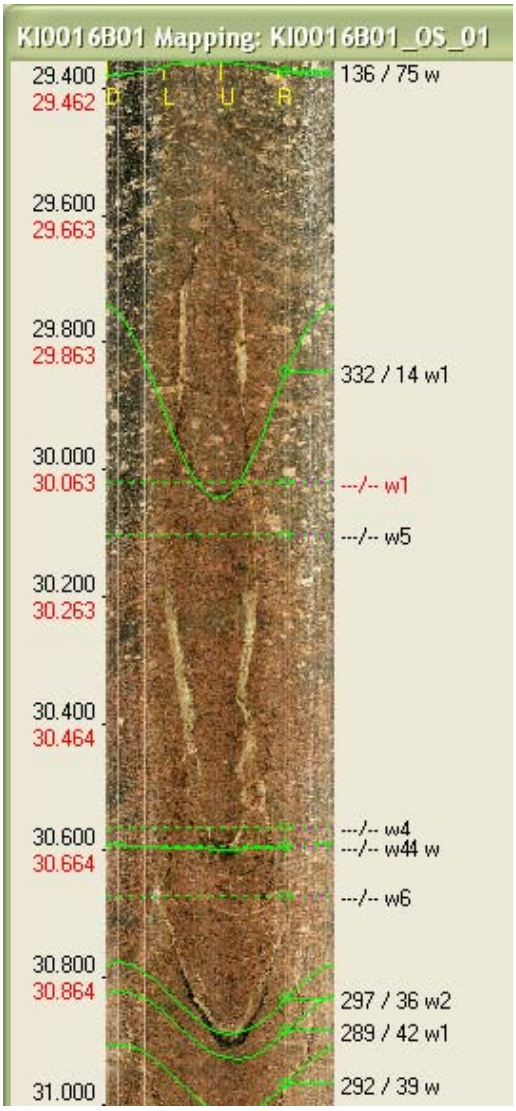

Figure 3-8. *Good quality BIPS-image as seen in Boremap from borehole KI0016B01, length 29.5 –30.9 m adjusted length; showing fractures both broken and unbroken with some red staining that do not cut through the centre of the core (dashed lines mark the approximate centre of these fractures in this screen image from the Boremap software).*

Table 3-6. Total amount of alteration in boreholes KI0010B01, KI0014B01 and KI0016B01.

Alteration	Intensity	KI0010B01 (%)	KI0014B01 (%)	KI0016B01 (%)
Oxidation	Weak	88.6	23.3	41.7
	Medium	1.8	10.1	2.6
Epidotization	Weak	88.6	83.9	68.9
	Medium	2.3	-	-

Table 3-7. Total number of fractures in boreholes KI0010B01, KI0014B01 and KI0016B01.

Borehole ID	Tot nr of open fractures	Fractures / meter	Tot nr of sealed fractures	Fractures / meter	Tot nr of partly open fractures	Fractures / meter
KI0010B01	215	2.2	565	5.7	48	0.5
KI0014B01	340	3.5	407	4.2	24	0.2
KI0016B01	230	2.4	216	2.2	23	0.2

Table 3-8. Mapped crush zones in boreholes KI0010B01, KI0014B01 and KI0016B01. Adjusted length and strike/dip are from upper contact of each crush zone.

Borehole ID	Adjusted length (m)	Total width of zone (m)	Piece length (m)	Strike/dip (degrees)
KI0010B01	35.1	0,20	0.20	151/18
KI0010B01	53.7	0,16	0.05	304/84
KI0014B01	3.9	0.04	0.07	332/11
KI0014B01	8.5	0.04	0.10	359/11
KI0014B01	13.6	0.08	0.10	090/01
KI0014B01	14.8	0.19	0.10	062/30
KI0014B01	33.2	0.05	0.15	207/42
KI0014B01	40.4	0.13	0.10	135/29
KI0014B01	50.5	0.03	0.05	347/12
KI0014B01	51.1	0.03	0.10	019/18
KI0016B01	12.8	0.02	0.07	130/83
KI0016B01	13.3	0.01	0.02	310/89
KI0016B01	31.0	0.80	0.70	292/39
KI0016B01	70.7	0.02	0.05	141/84

Table 3-9. Mapped cataclastic structures in boreholes KI0010B01, KI0014B01 and KI0016B01. Average width is the difference between upper and lower contact of the rock occurrences containing the cataclastic structures in each borehole. Average strike/dip of contacts is the mapped orientation from both upper and lower contacts of the rock occurrences containing the cataclastic structures. Lastly the average strike/dip of structure is the mapped orientation of the designated cataclastic structures within each rock occurrence.

Borehole ID	KI0010B01	KI0014B01	KI0016B01
Total number	43	52	51
Average width (m)	0.035	0.014	0.011
Average strike/dip of contacts (degrees)	167/81	132/78	153/76
Average, strike/dip of structures (degrees)	133/81	137/78	134/76

Table 3-10. Mapped Sealed Networks in boreholes KI0010B01, KI0014B01 and KI0016B01. Strike/Dip averaged from two estimated main fracture directions within each network.

Borehole ID	KI0010B01	KI0014B01	KI0016B01
Total number	59	61	62
Average width (m)	0.395	0.632	0.578
Average direction, strike/dip (degrees)	185/78	173/69	186/75

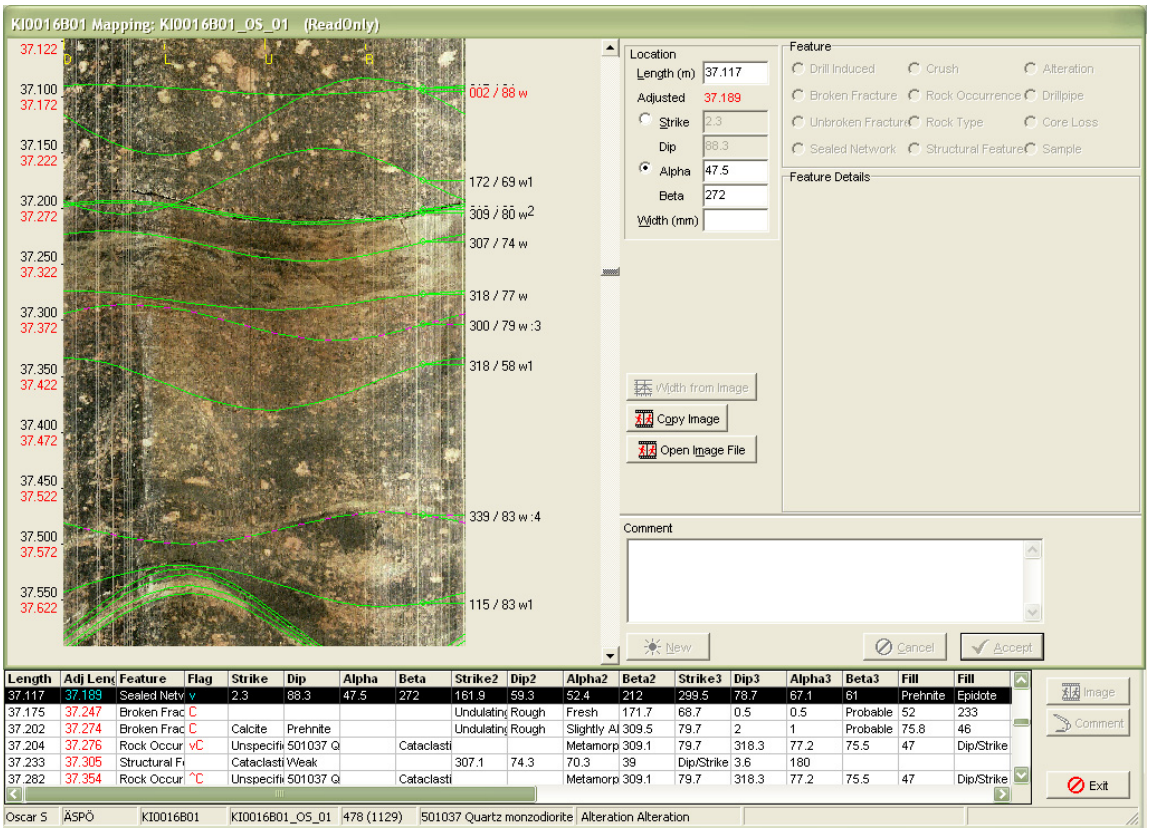

Figure 3-9. *Good quality BIPS-image as seen in Boremap from borehole KI0016B01, length 37.1 –37.6 m adjusted length; showing unaltered Äspö diorite containing cataclastic bands, sealed network and fractures.*

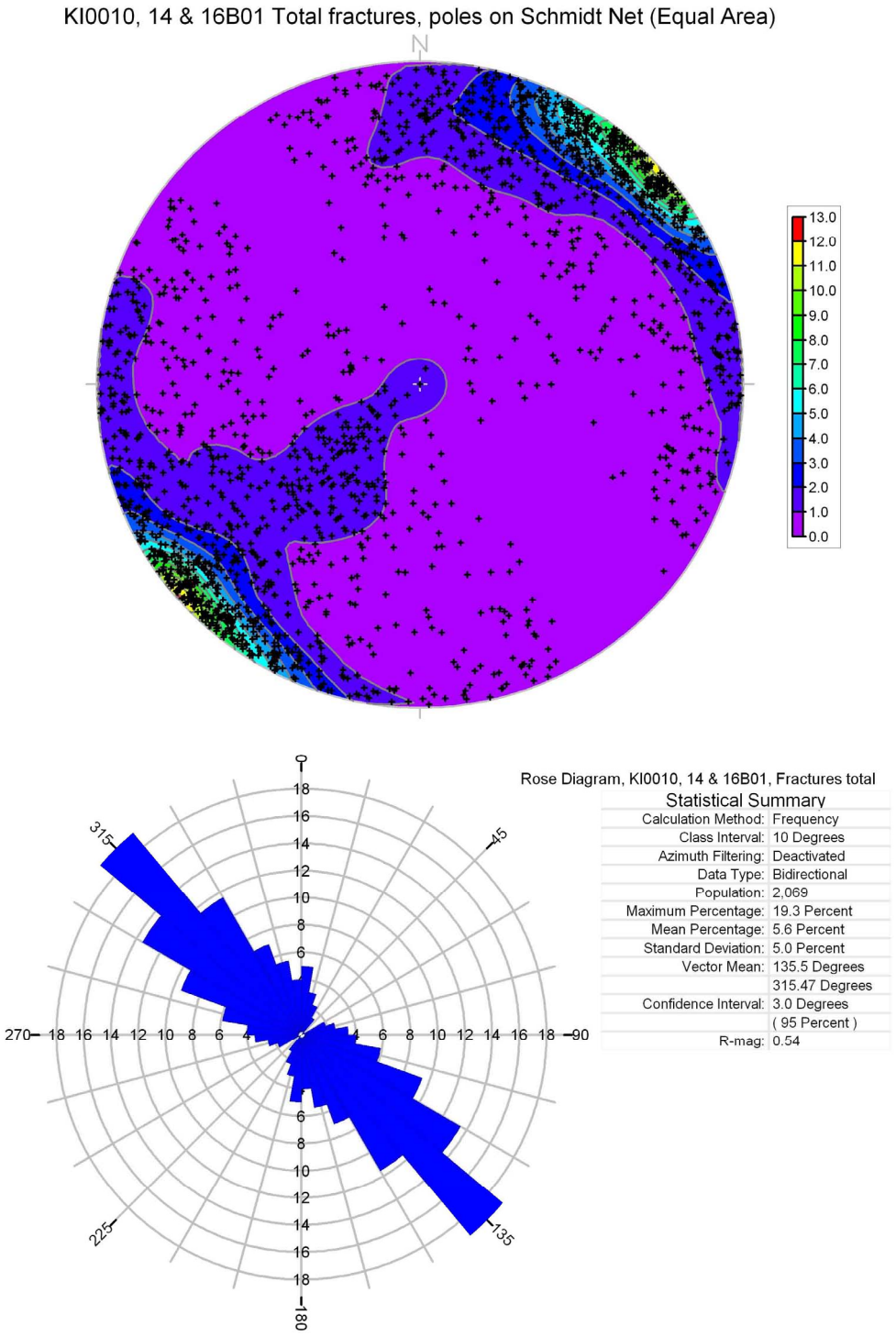

Figure 3-10. *Data from structural measurements in Boremap of all fractures in the boreholes KI0010B01, KI0014B01 and KI0016B01. The coordinate system is Äspö96. Top: Schmidt net stereogram (poles to fracture planes, strike/dip), contouring indicates concentration in % of total number per 1 % area, colour bar on right side in %. Bottom: Rose diagram (strike), including all fractures independent of dip.*

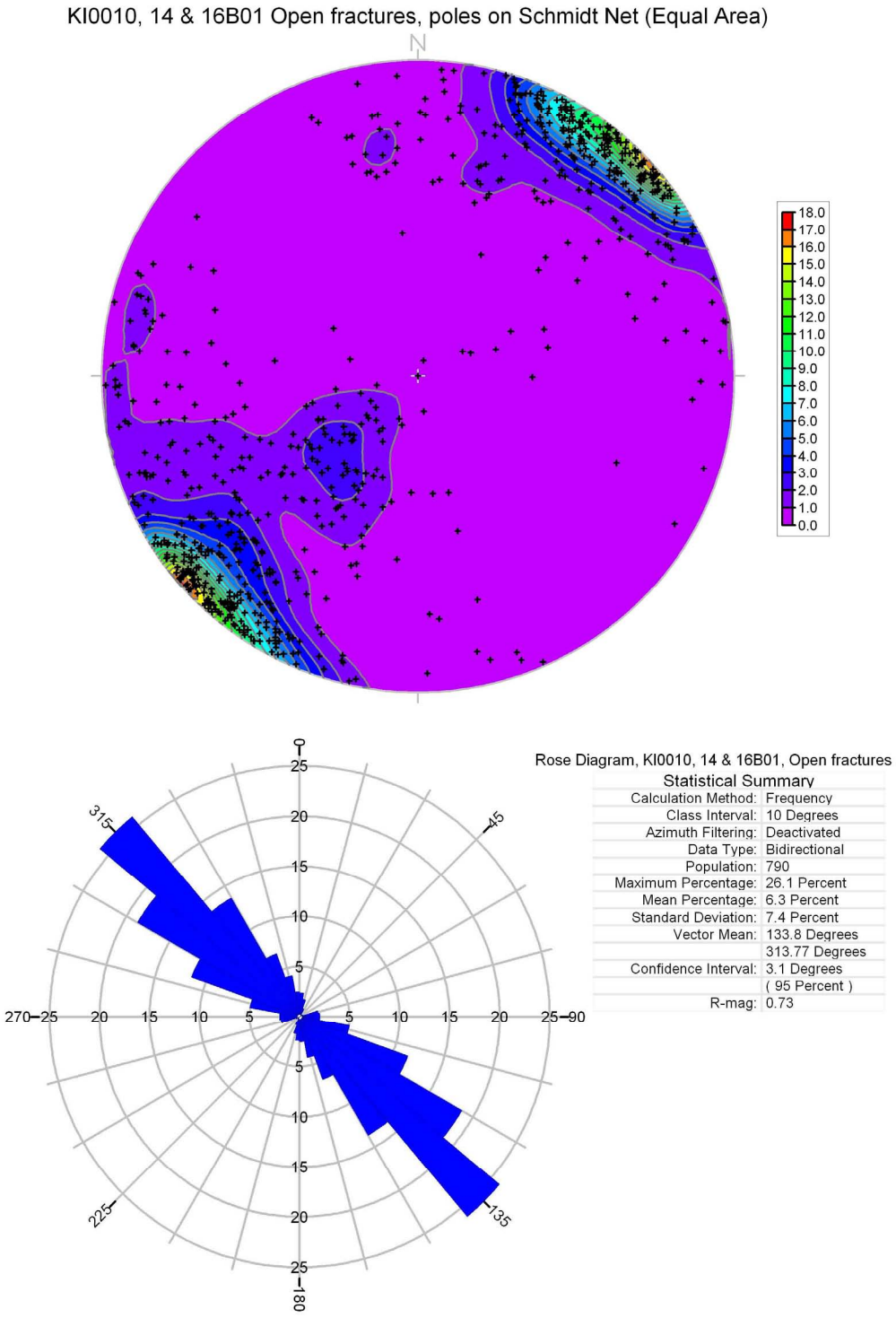

Figure 3-11. *Data from structural measurements in Boremap of all open fractures in the boreholes KI0010B01, KI0014B01 and KI0016B01. The coordinate system is Äspö96. Top: Schmidt net stereogram (poles to fracture planes, strike/dip), contouring indicates concentration in % of total number per 1 % area, colour bar on right side in %. Bottom: Rose diagram (strike), including all fractures independent of dip.*

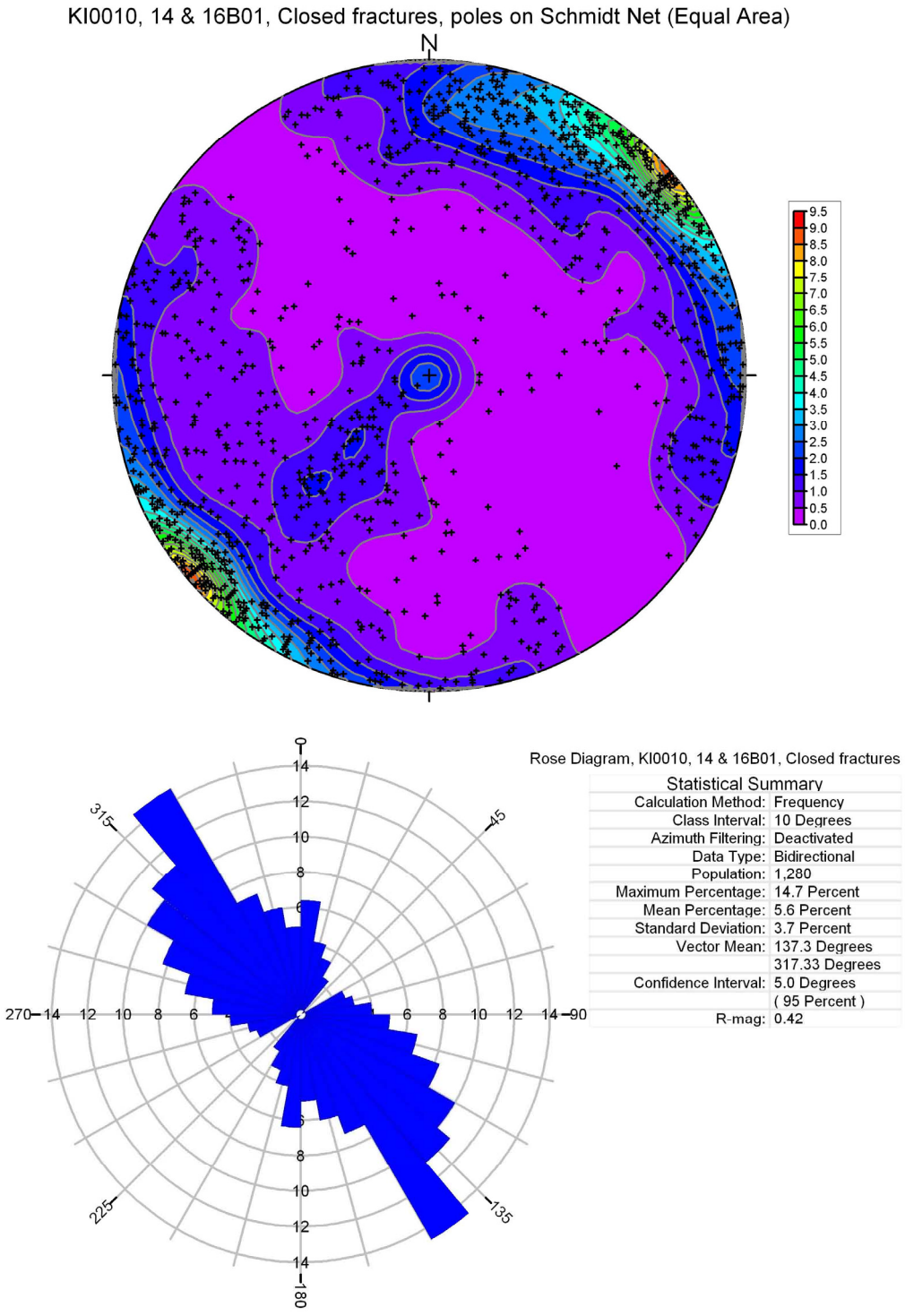

Figure 3-12. *Data from structural measurements in Boremap of all closed fractures in the boreholes KI0010B01, KI0014B01 and KI0016B01. The coordinate system is Äspö96. Top: Schmidt net stereogram (poles to fracture planes, strike/dip), contouring indicates concentration in % of total number per 1 % area, colour bar on right side in %. Bottom: Rose diagram (strike), including all fractures independent of dip.*

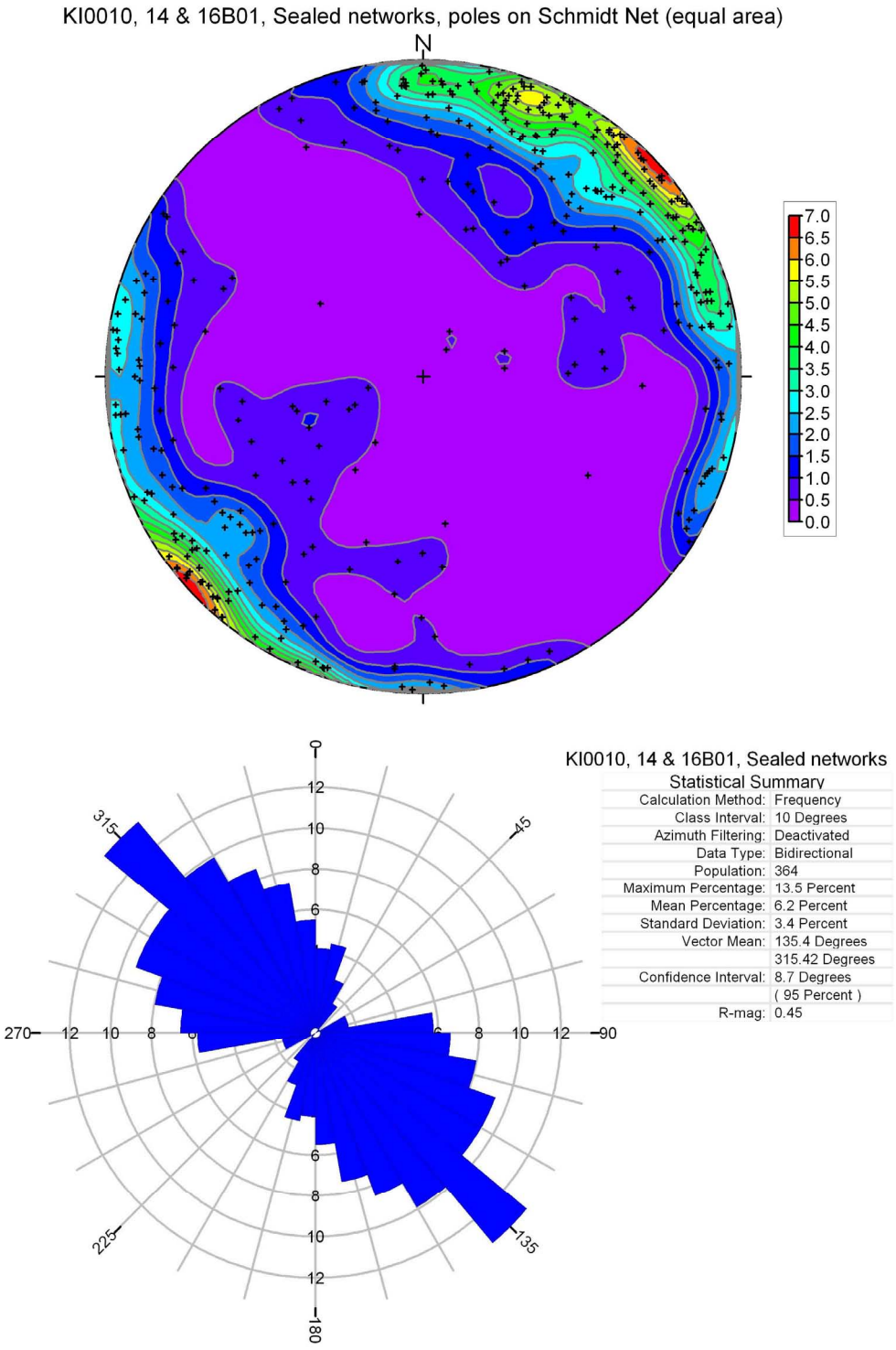

Figure 3-13. *Data from structural measurements in Boremap of all sealed networks in the boreholes KI0010B01, KI0014B01 and KI0016B01. The two assumed main fracture directions mapped within each network are plotted. The coordinate system is Äspö96. Top: Schmidt net stereogram (poles to fracture planes, strike/dip), contouring indicates concentration in % of total number per 1 % area, colour bar on right side in %. Bottom: Rose diagram (strike), including all fractures independent of dip.*

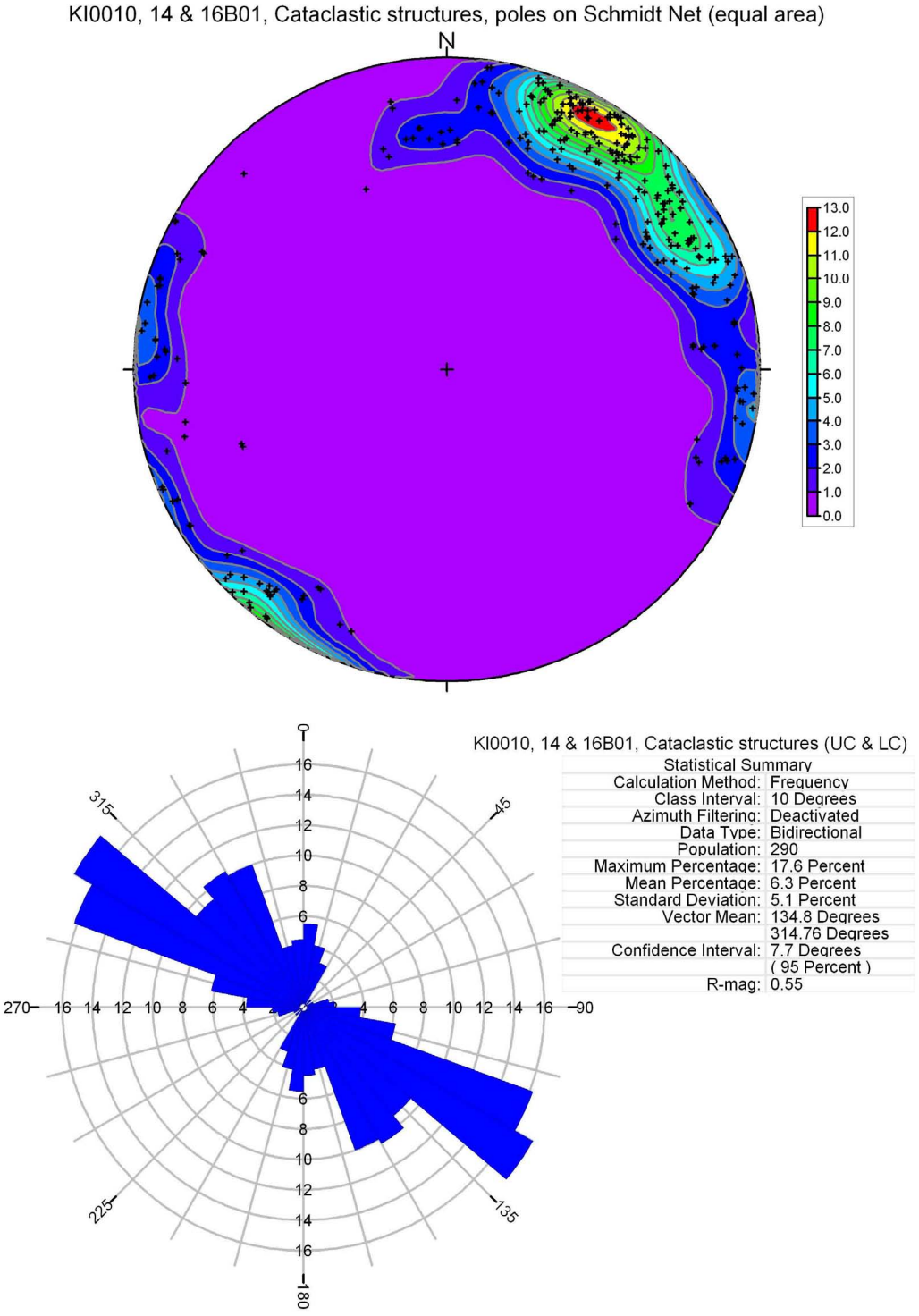

Figure 3-14. *Data from structural measurements in Boremap of all cataclastic structures in the boreholes KI0010B01, KI0014B01 and KI0016B01. Mapped upper and lower contact of rock occurrence containing the cataclastic structure is plotted. The coordinate system is Äspö96. Top: Schmidt net stereogram (poles to fracture planes, strike/dip), contouring indicates concentration in % of total number per 1 % area, colour bar on right side in %. Bottom: Rose diagram (strike), including all fractures independent of dip.*

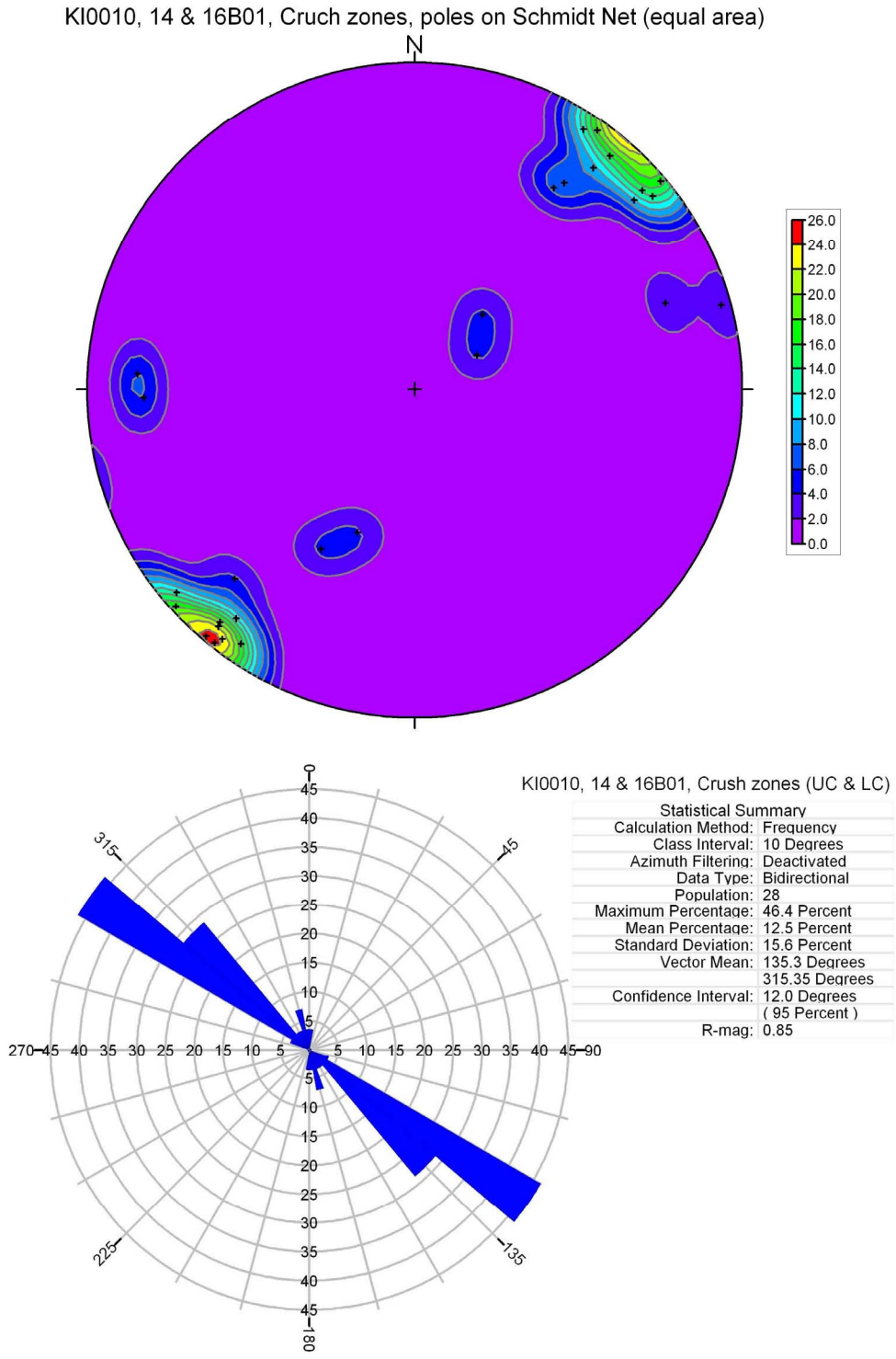

Figure 3-15. *Data from structural measurements in Boremap of all crush zones in the boreholes KI0010B01, KI0014B01 and KI0016B01. Mapped upper and lower contact of crush zones is plotted. The coordinate system is Äspö96. Top: Schmidt net stereogram (poles to fracture planes, strike/dip), contouring indicates concentration in % of total number per 1 % area, colour bar on right side in %. Bottom: Rose diagram (strike), including all fractures independent of dip.*

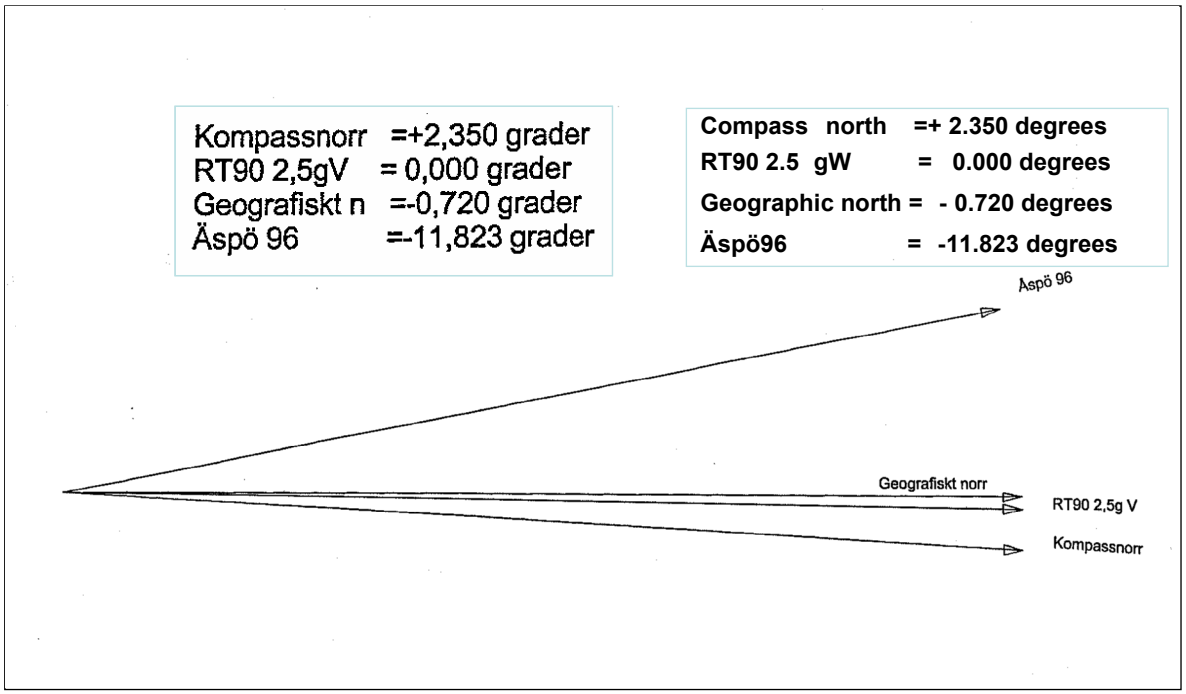

***Figure 3-16**. Relationship between the various geographical systems used at Äspö HRL (modified from drawing made by Gerry Johansson, Geocon AB for SKB, 2006).*

3.6 Summary and discussions concerning the core logging

The lithology dominating the drill cores of KI0010B01, KI0014B01 and KI0016B01 is Äspö diorite (see Tables 3-3, 3-4 and 3-5, as well as Figure 3-3). All cores except KI0010B01 carry minor amounts of fine-grained diorite-gabbro and all are cut by occasional pegmatite and fine-grained granite dykes and veins (see Tables 3-3, 3-4 and 3-5, as well as Figures 3-5, 3-6 and 3-7).

Both red staining (oxidation) and epidotization occurs in all three boreholes. Red staining occurs in approximately 90% of the rock in KI0010B01 where approximately 2% is of medium intensity, ca 33% of KI0014B01 (see Figure 3-5 and 3-7) with approximately 10% of medium intensity and ca 44% of KI0016B01 (see Figure 3-8) where approximately 3% is of medium intensity; see Table 3-6.

Epidotization makes up totally ca 91% of KI0010B01 of which most is weak, only approximately 2% of the core is of medium intensity. The amount of epidotization is approximately 84% in KI0014B01 and 69% in KI0016B01; see Table 3-6.

The Rose diagram in Figure 3-10 shows that the mean strike of fractures in the three boreholes is 135.5 degrees, while the Stereogram shows that steep dips dominate with a small gently dipping component. In the sub-horizontal boreholes the gently dipping fractures sometimes do not cut the centre of the drill core, see Figure 3-8. When comparing Figure 3-11 with Figure 3-12 it can be seen that the strike and dip of sealed fractures varies more than the open fractures.

Sealed networks usually occur as thin Epidote filled, sealed fractures that occur in the cores of all three boreholes. The fractures are too many and often so thin that they are too difficult to see in the core as well as being too irregular, to be mapped as individual fractures (see Figure 3-9). They are therefore mapped as zones of sealed networks with two main estimated fracture set orientations marked out. These two main fracture orientations mapped within each network plot in a very similar fashion to the closed fractures, as can be seen when comparing Figure 3-12 with 3-13.

Cataclastic bands are bands consisting of highly deformed rock dominated by secondary minerals, mainly Epidote and Prehnite. Fragments of host rock (i.e. Äspö diorite) can sometimes be seen floating in the matrix. They are mapped in Boremap as bands (rock occurrence) with an upper and a lower contact and in the approximate middle a cataclastic structure is marked (see also chapter 3.4.3). Approximately 50% of the cataclastic bands are less than 1 cm wide and ca 80% are less than 2 cm wide. Nevertheless occasional thicker cataclastic bands occur as can be seen in see Figure 3-9. The diagrams in Figure 3-14 show that the dominating strike direction is approximately northwest-southeast with steep dips to the southwest.

Several crush zones were mapped in the three boreholes; see Table 3-8. Their strike and dip can be seen from Figure 3-15 and one example of a probably water yielding crush zone is shown in Figure 3-4.

Measuring the aperture of broken fractures in the Boremap mapping is done both in the BIPS image and core. It is probable that broken fractures in the core can not always be fitted to their original apertures in the rock, making their measurement somewhat uncertain. The BIPS image on the other hand can be assumed to show the actual aperture of those fractures, so it is used to measure the true aperture of open fractures. The resolution of the BIPS image is approximately 1 mm, resulting in the practice that all open fractures with aperture less than 1 mm are assigned an aperture of 0.5 mm. Open fractures with measured aperture of 1 mm and more are measured in the BIPS image. All apertures of broken fractures are plotted against length of boreholes in Figure 3-17a-c (cf. Figure 5-20). The crush zones have varied apertures in the BIPS image but are not given a separate value in the Boremap mapping; only the zone width is recorded (see Table 3-8).

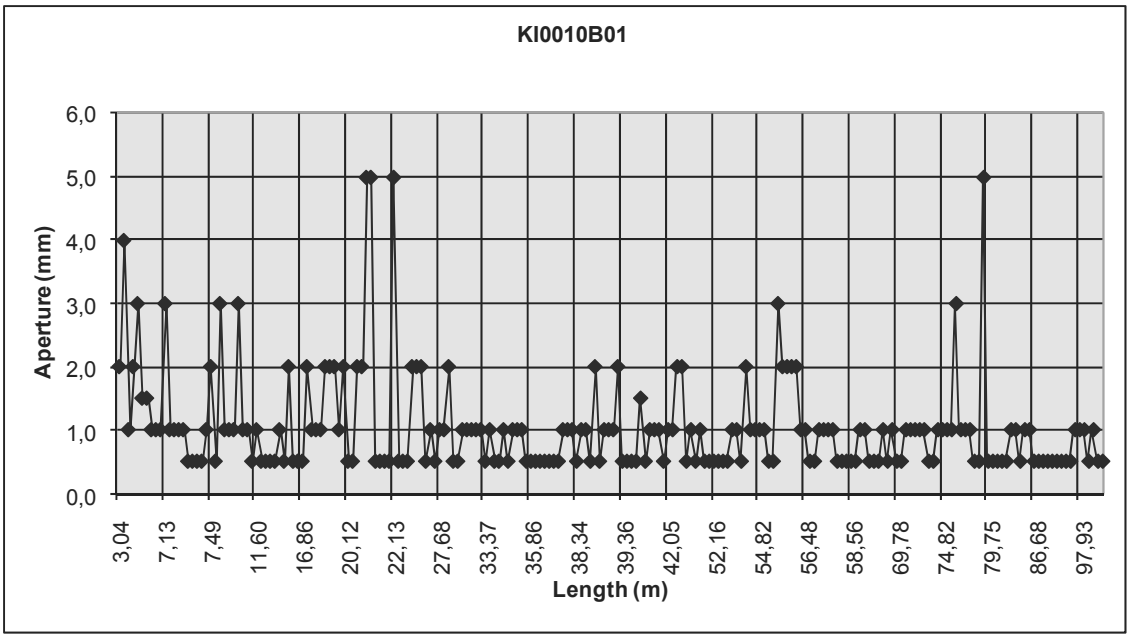
KI0010B01
Aperture (mm)
6,0
5,0
4,0
3,0
2,0
1,0
0,0
3,04
7,13
7,49
11,60
16,86
20,12
22,13
27,68
33,37
35,86
38,34
39,36
42,05
52,16
54,82
56,48
58,56
69,78
74,82
79,75
86,68
97,93
Length (m)

a)

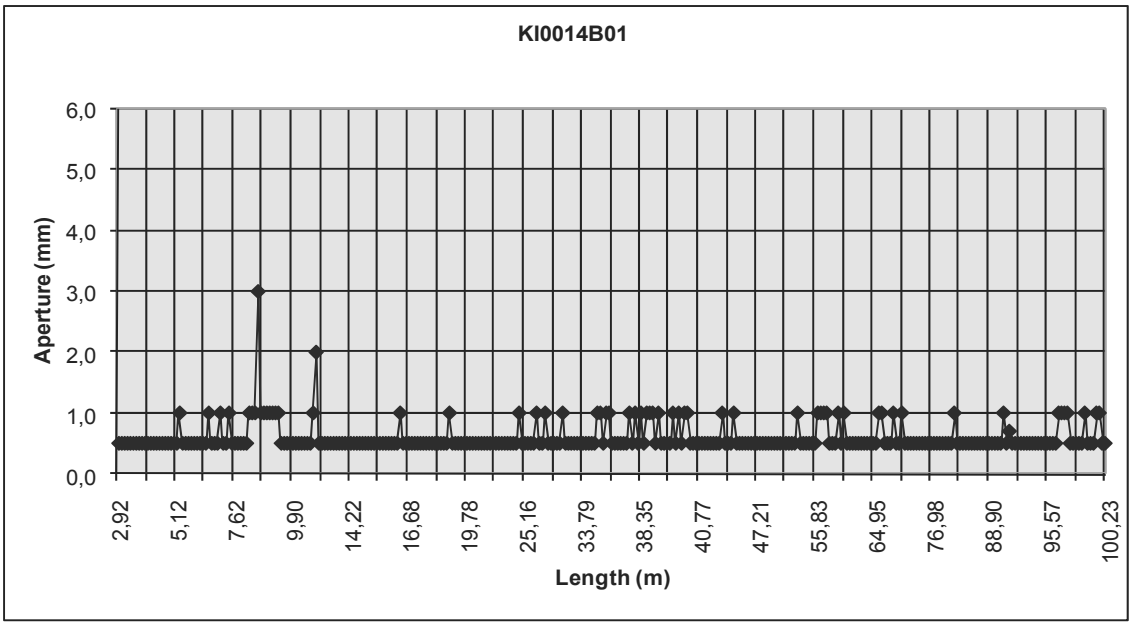
KI0014B01
Aperture (mm)
6,0
5,0
4,0
3,0
2,0
1,0
0,0
2,92
5,12
7,62
9,90
14,22
16,68
19,78
25,16
33,79
38,35
40,77
47,21
55,83
64,95
76,98
88,90
95,57
100,23
Length (m)

b)

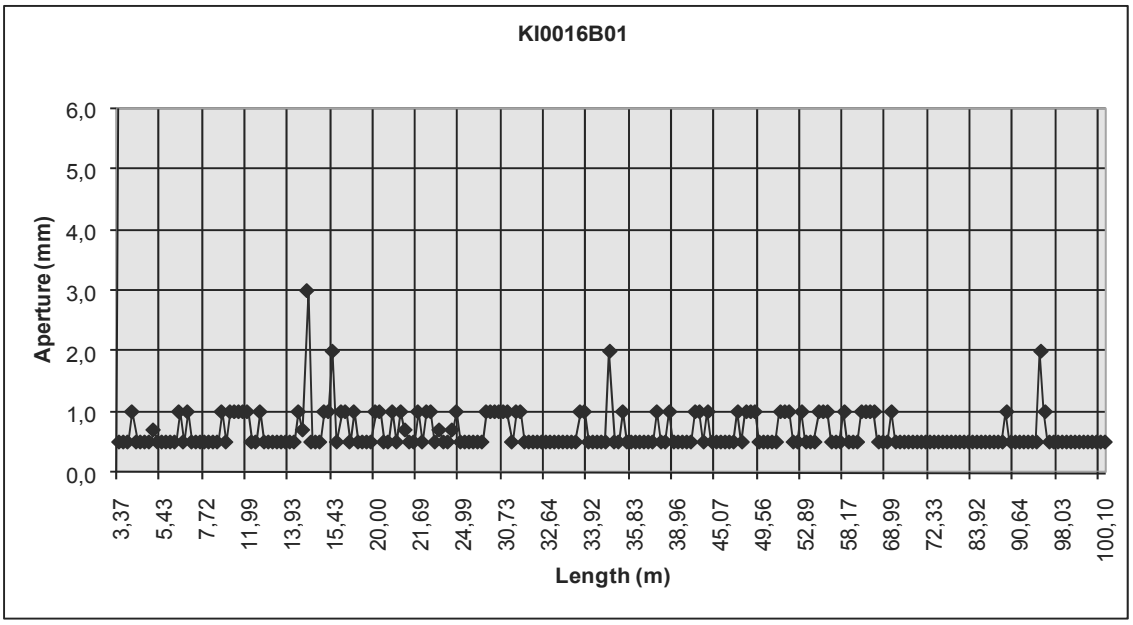

c)

Figure 3-17a-c*. Diagrams showing the apertures of broken fractures in mm against length of borehole in m. In general all apertures less than 1 mm are given the aperture of 0.5 mm, because the resolution of the BIPS images is approximately 1 mm. All data taken from Sicada, activity type GE041.* ***a)*** *KI0010B01,* ***b)*** *KI0014B01 and* ***c)*** *KI0016B01. Four fractures were deemed wider than 0.5 mm in the core and got the aperture of 0.7 mm.*

4 Hydrogeological investigations

The hydrogeological tests that were performed in all or some of the boreholes were pressure measurements, double packer flow logging and PFL-logging (PFL=Posiva Flow Log. Also called difference flow logging). All data that were achieved during the tests have been stored in the SKB Sicada database and is generally not included in this report. Chapter 5 of this report includes the hydrogeological evaluation based on the tests.

4.1 Pressure measurements

The initial plan to measure the water pressure in the boreholes is described in the internal SKB-document "AP TD SU32516-07-018 Kärnborrning av KI0010B01, KI0014B01 och KI0016B01". According to that the water pressure was meant to be measured after each core up-take (approximately every 3rd metre) by closing the valves on the casing (see Appendix 1A-C and Figure 2-6a and b). When this was done the valves should have been opened and the water flow was measured. It was, however, soon realized that this procedure was quite time consuming. Instead it was decided to measure the pressure in each of the three holes in 10 m sections as is described for KI0010B01 below and not in full-hole lengths. The pressure tests were, however, due to problems described below, not carried out fully according to this plan either.

1) KI0010B01 (11-21/4 -07): The hole was drilled and tested according to the adjusted plan. Every time the core was taken out of the hole, which was approximately every three meters, the inflow from the hole was measured. Every night the hole was closed and the pressure measured. Due to problems with the equipment the pressure had to be meassured in successively longer full-hole sections. After having finished the borehole KI0010B01 it was closed all the time during the drilling and testing of the other two boreholes. It was only open when the BIPS and PFL measurements took place in it which was not at the same time as the drilling/testing of the other two holes was performed.

2) KI0016B01 (1/6-8/6 -07): This hole too was drilled and tested as planned. In this borehole the pressure in the section that had been drilled during the preceeding day, about 10 m, was measured over the night. While the drilling and testing took place, there was an alarm from the research project Prototype that the pressure was rising in the Prototype repository located in a neighbouring rock volume in Äspö HRL. The reason for the pressure rise was discussed. It was considered that the high pressure from a fracture identified in the 55-60 m section of the borehole was transmitted through the borehole and via another structure into the Prototype rock volume. The first structure may be identical to structure # 7 in the TRUE Block Scale rock volume and the second one to TRUE Block Scale structure # *5* (Andersson et al, 2002a). Some of the TRUE Block Scale structures have been illustrated in Figure 2-8.

In order to deal with this, KI0016B01 was opened after it was drilled and tested. This led to a pressure drop to an acceptable level in the Prototype repository.

The pressure data from KI0016B01 is not useful for understanding the pressure profile in the rock volume under natural conditions. Once the first major structure (TRUE Block Scale structure # 5) that is intersecting both KI0016B01 and KI0010B01 had been passed while drilling KI0016B01 a water passage had opened up between the two holes. When the water pressure was measured in sections deeper in the borehole KI0016B01, behind structure #5, the water could escape from the measured section via minor structures into KI0010B01. Since the latter hole was closed at the opening the water then was believed to be transmitted along structure #5 back into KI0016B01 and out into the tunnel as illustrated in Figure 5-6 in the chapter on evaluations. Thus, the achieved pressures are not reliable.

3) KI0014B01 (14-18/6 -07): During the drilling of KI0014B01, the borehole KI0016B01 was left open until water was noticed in KI0014B01. Then borehole KI0016B01 could be closed. KI0014B01 was after this kept open during the drilling, of consideration for Prototype. Hence there are no pressure data from KI0014B01.

4.1.1 The effect on surrounding boreholes and rock mass

It was not only the Prototype repository that was affected by the drilling of the core holes KI0010B01, KI0014B01 and KI0016B01. Already while the drilling of borehole K0010B01 took place it was obvious that there was a pressure response in surrounding boreholes Figure 4-1 illustrates the array of boreholes that have been drilled from the -450 m level of the Äspö HRL.

When the boreholes were open during and after the drilling the ground water pressure in surrounding boreholes dropped by approximately 5-8 bars. When the boreholes were closed by the valves on the casing (Figure 2-6a and b) the pressure increased again in the surrounding holes. At the same time there was an increase of water inflow into the prototype repository as well as a pore pressure increase in the back filling material. Figure 4-2a and b illustrates the course of events in section 1 of boreholes KA3548A01 and KA3600F respectively. Both boreholes have been drilled from the part of the TASA-tunnel hosting the Prototype repository. The same type of pressure responses can be observed deep in the rock volume for example in the inner sections of the boreholes KI0025F, KI0025F03 and KA3600F (see the internal SKB document Fintätningsprojektet – Tryckresponser. PM Utredning av grundvattentryckresponser på Äspölaboratoriet. “The project sealing of narrow fractures - Pressure responses. PM Analyses of ground water pressure responces at the Äspö laboratory”. N. Bockgård, Golder Associates for SKB, 2008).

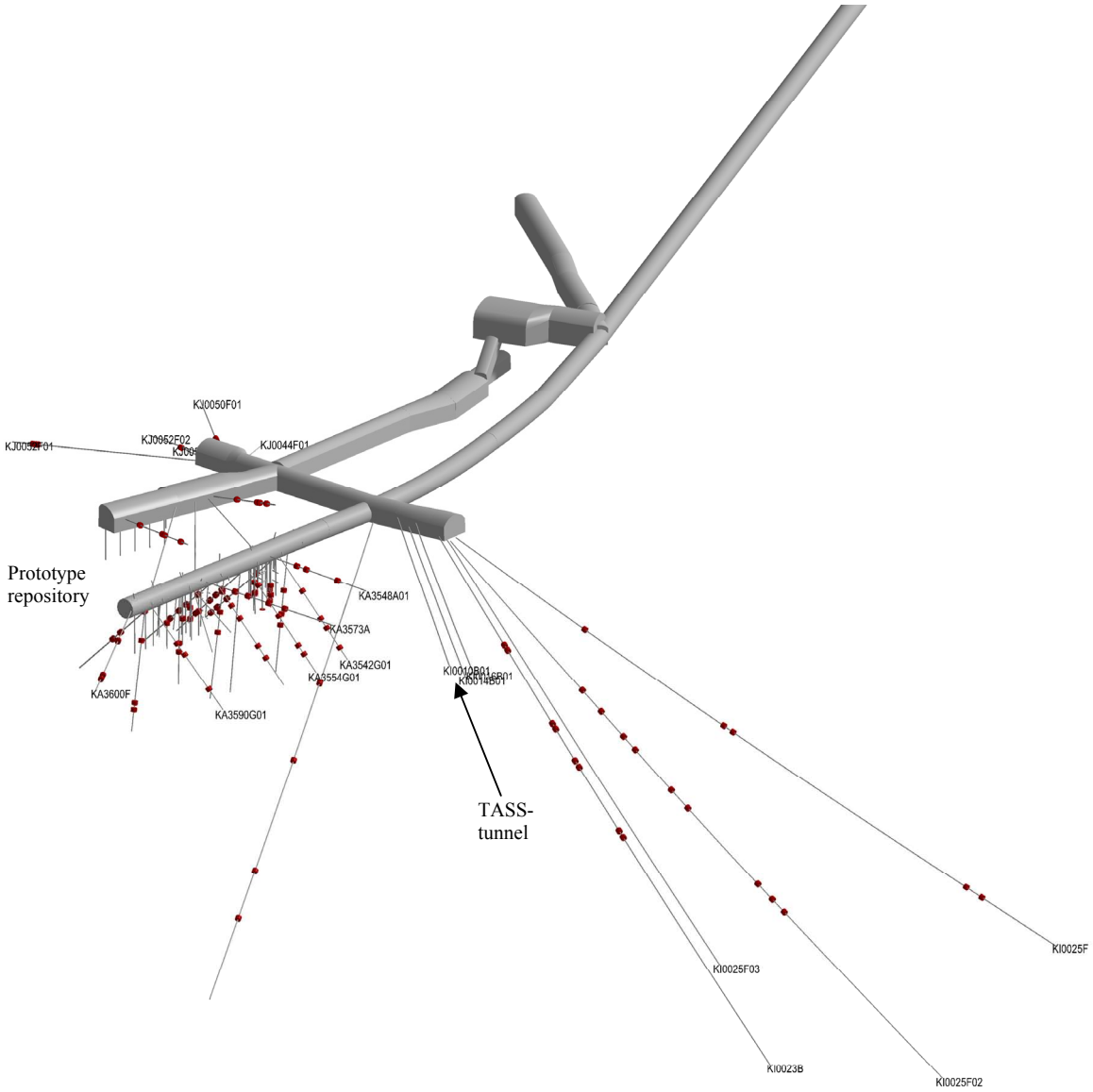

Figure 4-1. *Boreholes on the -450 m level of Äspö HRL. The view is seen from south west- Red dots or cylinders on the drill holes indicate packer locations. The TASS-tunnel is excavated where the boreholes KI0010B01, KI0014B01 and KI0016B01 are shown (slightly modified from N. Bockgård 2008, Fintätningsprojektet – Tryckresponser. PM Utredning av grundvattentryckresponser på Äspölaboratoriet. Internal SKB document).*

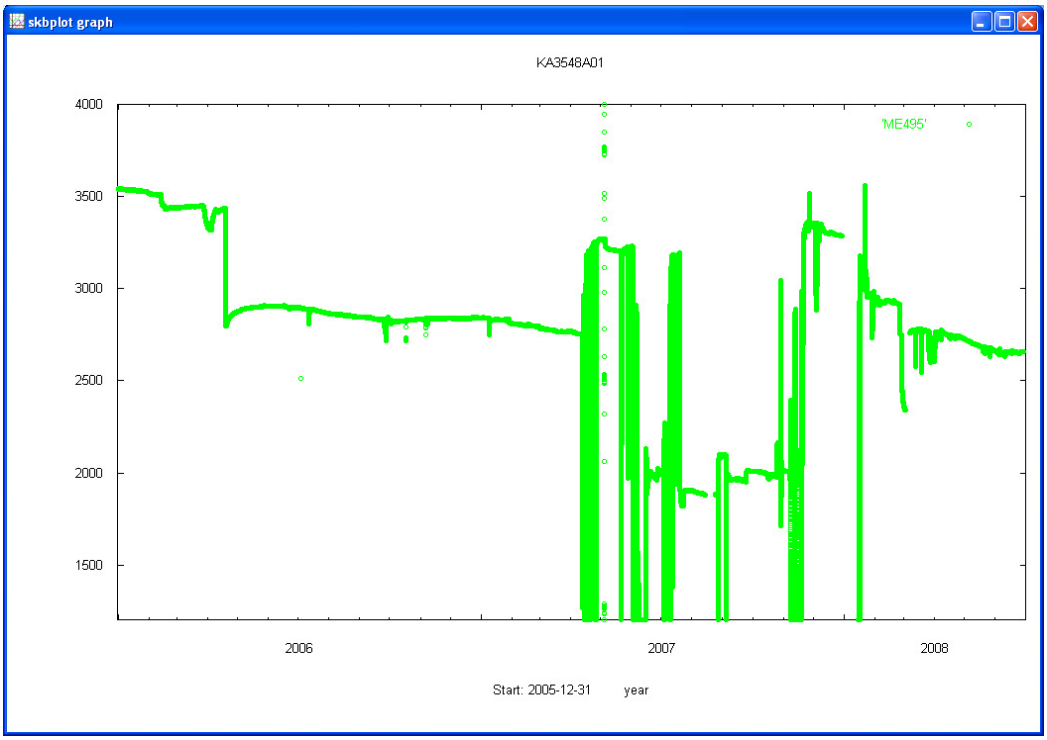

a)

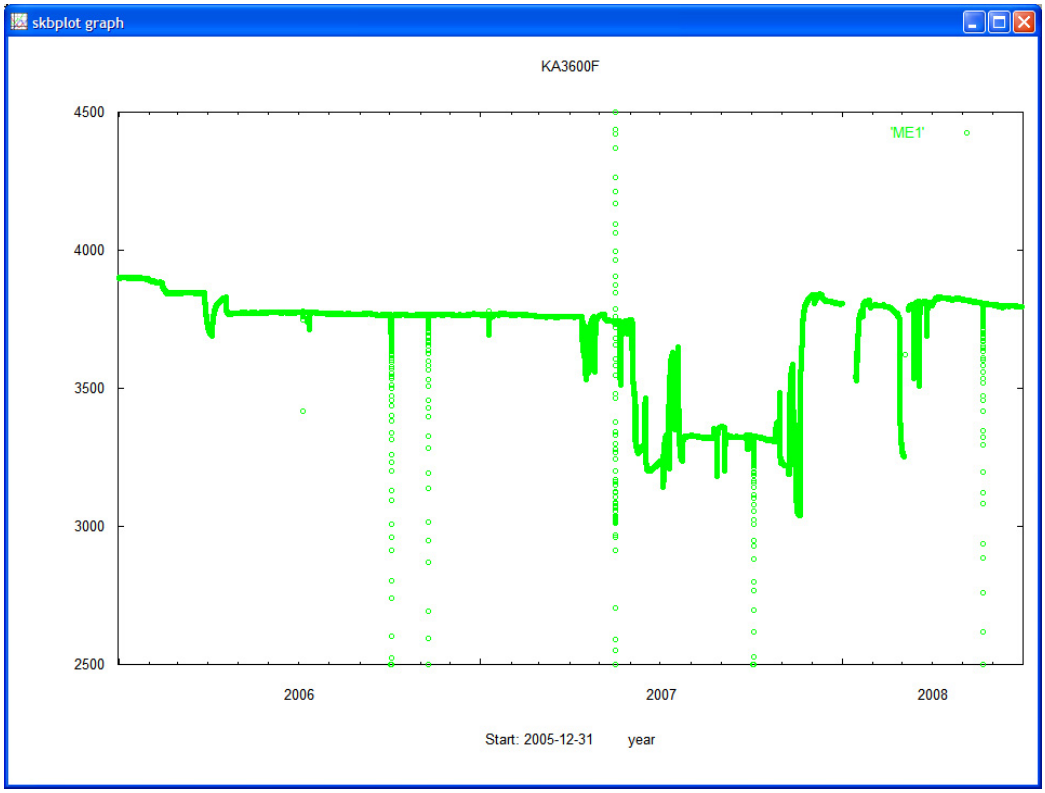

b)

Figure 4-2. *Ground water pressure, kPa (=0.01bar).* ***a)*** *Borehole KA3548A01, section 1.* ***b)*** *Borehole KA3600F, section 1 (from N. Bockgård 2008, Fintätningsprojektet – Tryckresponser. PM Utredning av grundvattentryckresponser på Äspölaboratoriet. Internal SKB document).*

4.2 Double packer flow logging

The double packer flow tests were performed by Kristoffer Gokall-Norman and Tomas Svensson of Geosigma AB during the summer 2007. They used SKB's UHT1-equipment (Underground Hydraulic Test sytem, version No. 1). The components and the operation of the test system is described in the document Hydrauliskt Testsystem för Underjordsmiljö ("Hydraulic Test system in an underground environment" Mansueto Morosini 1998, NR TD-98-04, internal SKB document). The controlling document for the tests in the three present boreholes is the activity plan AP TD SU32516-07-032 Flödesloggning med dubbelmanschetter i KI0010B01, KI0014B01 och KI0016B01 ("Flow logging with double packers in KI0010B01, KI0014B01 and KI0016B01" 2007, SKB internal document). Unfortunately one of the regulating valves of the equipment did not work properly during the tests and had to be adjusted manually at a few occasions. The principle test set up is shown in Figure 4-3 and the double packer in Figure 4-4a and b.

In short, the system is based on two packers separated by a 3 m long pipe, the measuring section. When the test unit (Figure 4-4a and b) has been inserted into the borehole and the packers have been inflated the pressure within the measuring section is kept on a constant level. While measuring, the pressure was kept at 10 bars below the observed original pressure in the section. The water inflow into the borehole section between the packers is then measured. In this way, the water inflow is measured in 3 m sections throughout the borehole. Evaluations of the measurements (T_{Moye}) are described in chapter 5.4.

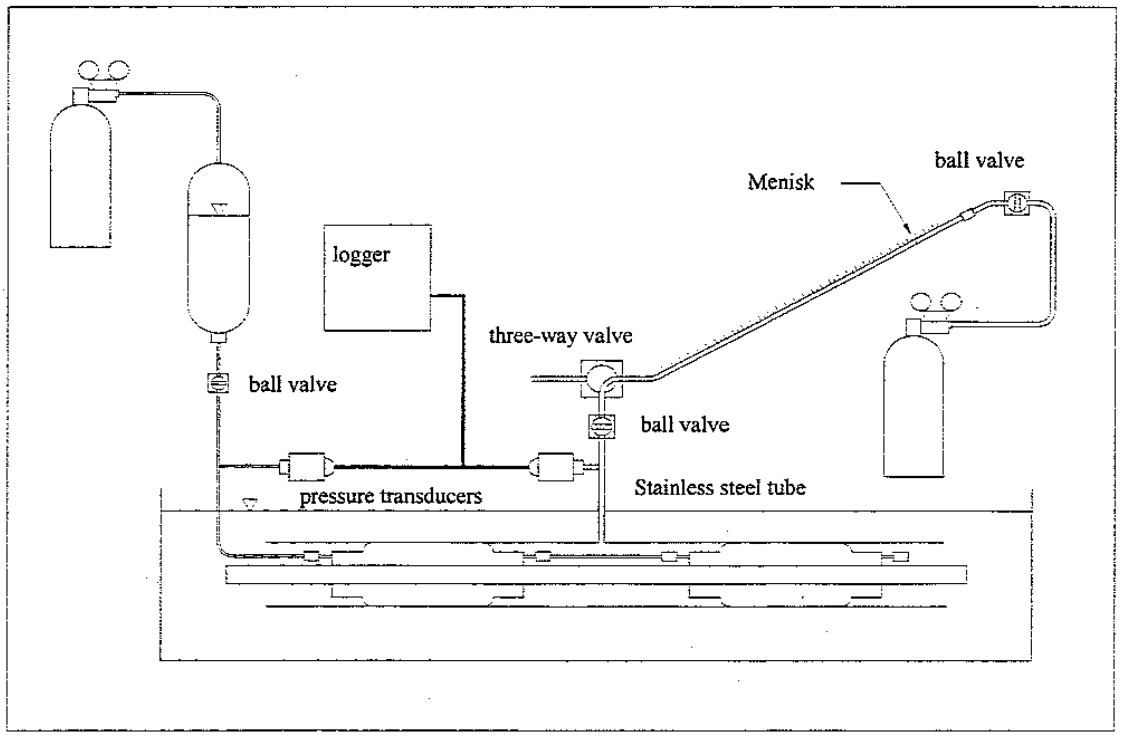

Figure 4-3. *Principle test set-up for double packer tests (from Kort avrapportering av tester utförda på system och komponenter tillhörande hydroutrustning UHT1, Wahlberg A., Stoor J., Lindström D. and Jansson F.,1997. Geosigma, internal document for SKB).*

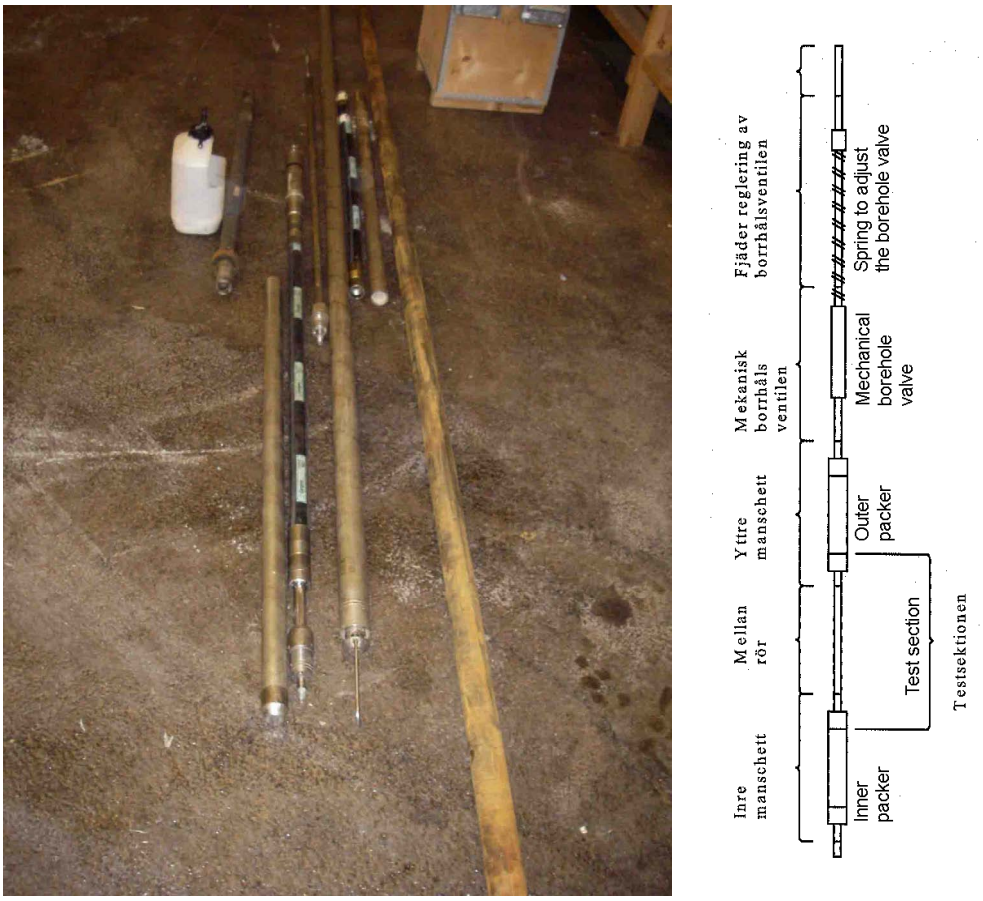

a) ***b)***

Figure 4-4. a) *Double packer to be used at the double packer tests. The packers are not assembled yet (photo: Oskar Sigurdsson).* ***b)*** *Principle sketch of the assembled double packer system, the test unit [modified from Hydrauliskt Testsystem för Underjordsmiljö ("Hydraulic Test system in an underground environment") Mansueto Morosini 1998, NR TD-98-04, internal SKB document].*

4.3 PFL difference flow logging

The PFL logging (Posiva Flow Log) was performed only in borehole KI0010B01. The controlling document is the AP TD SU32516-07-023 Difference flow logging in borehole KI0010B01 (Niclas Bockgård 2007, internal SKB document). The method is described in SKB's internal document MD 322.010e Method description for Difference flow logging (J-E. Ludvigson, P. Rouhiainen and N-Å. Larsson 2006).

The PFL-logging is used in the characterizing work concerning the hydraulic properties of the rock. The measuring probe is inserted in a borehole where for example hydraulic conductive sections and/or hydraulic conductive single fractures in the borehole wall are registered (Figure 4-5). By the help of the flow logging features such as transmissivity and the hydraulic head can be determined. Not only can the hydraulic properties be measured by the PLF-logging but also e.g. electric conductivity (EC) and temperature (Te). The difference flow logging is normally performed either as sequential logging or overlapping logging. The two logging modes are visualized in Figure 4-6.

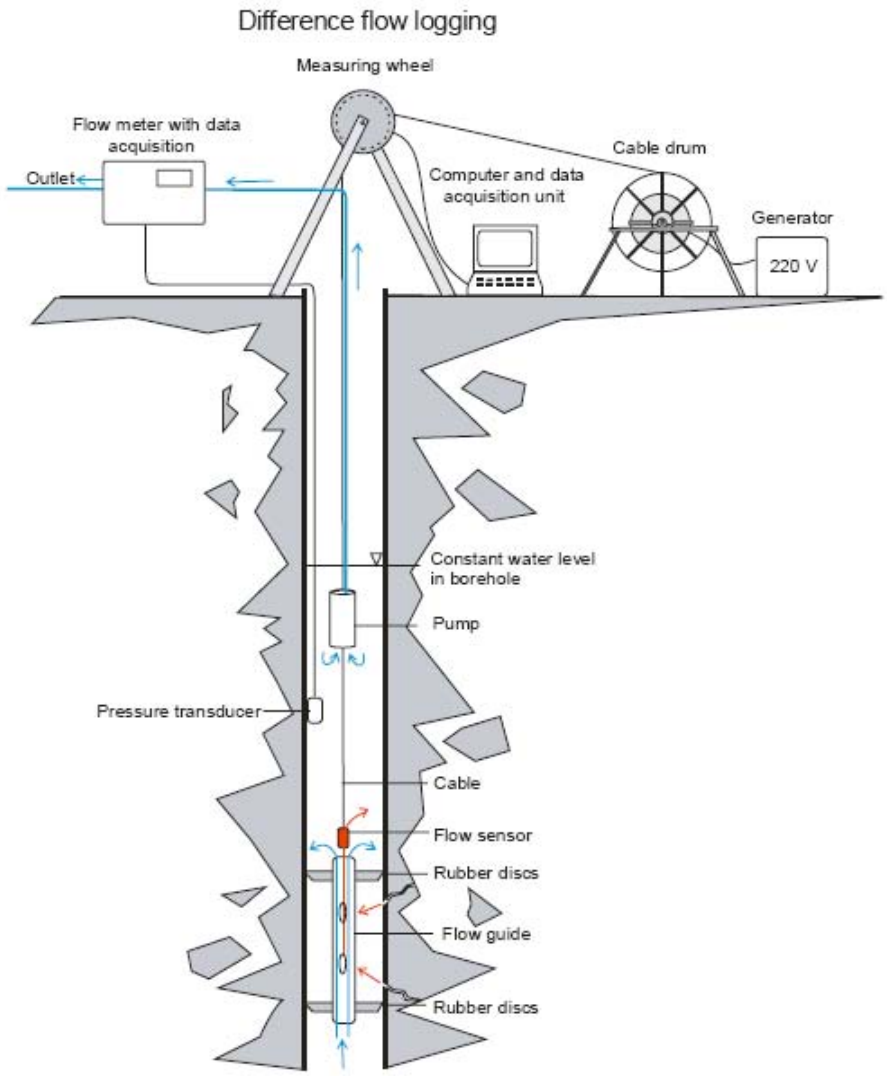

Figure 4-5. *Schematic drawing of the equipment used in difference flow logging, here in a vertical borehole (from MD 322.010e Method description for Difference flow logging (J-E. Ludvigson, P. Rouhiainen and N-Å. Larsson 2006, SKB internal document).*

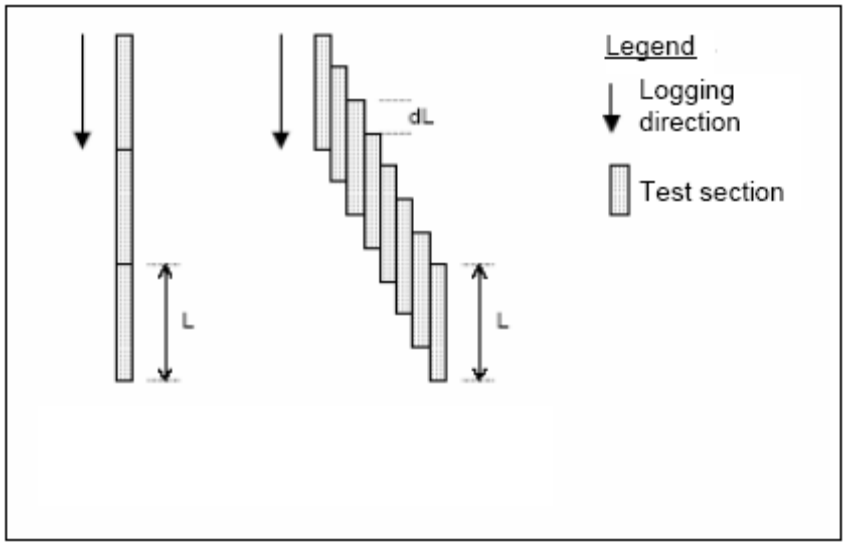

Figure 4-6. *Difference flow logging can be performed in basically two different ways. i.e. sequential and overlapping logging respectively (from MD 322.010e Method description for Difference flow logging (J-E. Ludvigson, P. Rouhiainen and N-Å. Larsson 2006, SKB internal document).*

The tests that were performed in May 2007 in the borehole KI0010B01 were executed by Posiva Oy as executive organisation with Mikael Sokolnicki and Stefan Kristiansson of PRG-Tec Oy as under-consultants. Overlapping flow logging with 1 m long test sections (L in Figure 4-6) that were measured in steps of 0.1 m (dL in Figure 4-6) was used in the tests. Before the tests took place the borehole was thoroughly cleaned by flushing water. The total water inflow into the hole was between about 40 l/min ("steady state" after the drilling was completed) and 50 l/min (transient measured when the valve on the borehole casing is opened). Besides the flow logging SPR (Single Point Resistance), EC (Electric Conductivity) and Te (Temperature) was measured.

According to the executing consultants of PRG-Tec Oy the noise level during the tests was exceptionally high (about 100 ml/hour compared to the normal 30 ml/hour). This may have been caused by;

- Drill-mud/cuttings that make the section to be measured leaky
- Gas bubbles, that due to the large pressure drop, have been released from dissolved gas in the water.

Figures 4-7 and 4-8 show some of the settings and equipment used while measuring the borehole KI0010B01. The results from the tests are shown in Appendix 5 as graphs.

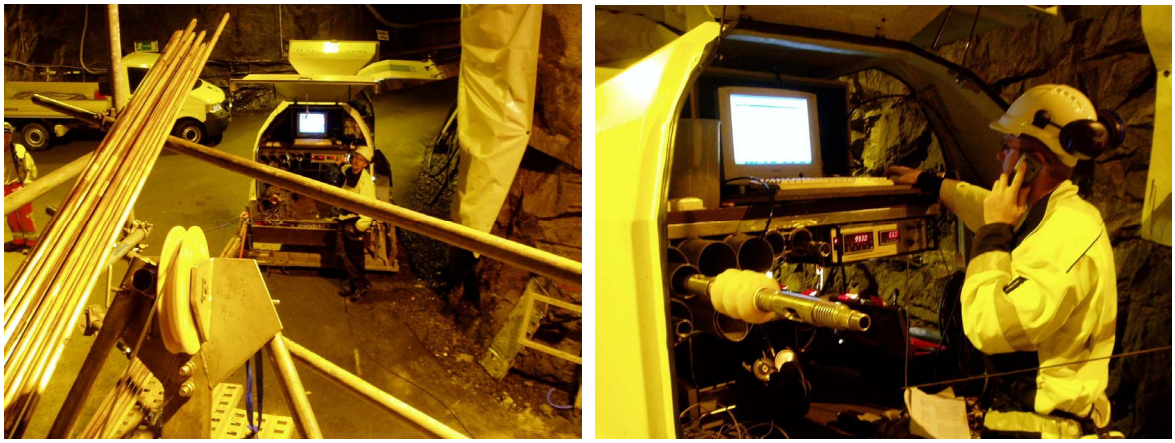

a) ***b)***

Figure 4-7. a) *The settings around borehole KI0010B01.* ***b)*** *A close up of the instrument and control trailer (photos: Elinor Örtendahl).*

a) ***b)***

Figure 4-8. a) *A close up of the rubber discs on the measuring device.* ***b)*** *The measuring device is almost fully inserted into the borehole via the casing valve and only the guides at the end are visible (photos: Elinor Örtendahl).*

5 Hydrogeological evaluation

5.1 Introduction

The hydraulic tests of the three parallel 100 m long cored boreholes have been evaluated. The location of the boreholes, KI0010B01, KI0014B01 and KI0016B01, are shown in Figure 5-1 (see also Figures 1-1 and 2-4). The aim of the tests was to characterize the rock volume to build a hydro-geologic model of the rock volume. This was needed as a base for the grouting design for the tunnel construction. The three holes have a 1% inclination downwards, in order to contain water rather than air. Since the tunnel is at an angle to the wall in which it starts, the starting point of the three holes (top of casing) differ compared to each other and compared to the length along the tunnel. The original data used in the evaluation below have been taken from SKB's database Sicada and is generally not included in the report. Appendix 6, however, contains a number of tables with data on which some of the diagrams further down have been based.

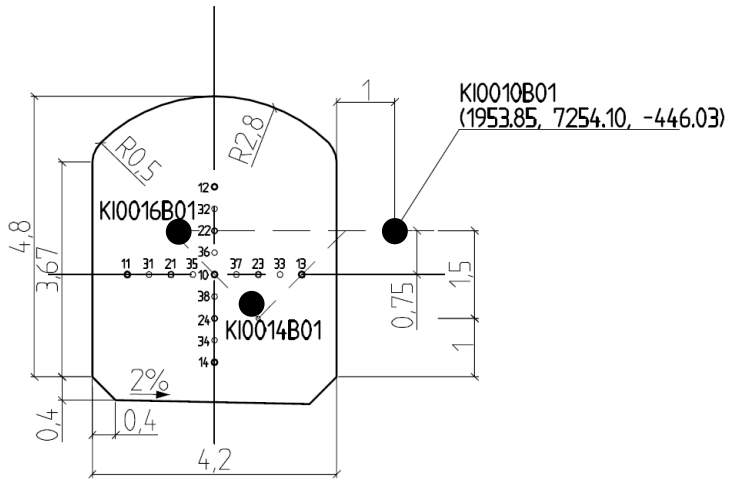

Figure 5-1: *The location of the three boreholes relative to the planned tunnel contour.*

5.2 Methods

One parameter shown to be useful when characterizing fractures, in the context of grouting and inflow, is the hydraulic aperture, *b*. Therefore that is the parameter presented as the result of the hydraulic evaluations.

b is calculated from the transmissivity *T* via the cubic law (Snow1968, see Zimmerman and Bodvarsson 1996),

$$T = \frac{\rho g b^3}{12\mu}, \qquad \textbf{Equation 1}$$

where ρ is the density of water [kg/m^3], g is the gravitational acceleration [m/s^2] and μ is the viscosity of water [Pa s].

T may be calculated in different ways depending on what tests are performed, but two input parameters which are always necessary are the inflow Q and the hydraulic head Δh. The simplest approximation of T is estimating it by the specific capacity

$$T \approx \frac{Q}{dh}, \qquad \textit{Equation 2}$$

which is shown to be useful for short duration hydraulic tests (Fransson 2001).

5.2.1 Equivalent hydraulic aperture b_{eq}

Transmissivity evaluations have been conducted for the three cored boreholes using data from three different measurements:

- Inflow and pressure during drilling, measured in app. 3 m sections (although, as described in the drilling chapter, the pressure was not measured in KI0014B01 and the data from KI0016B01 is difficult to interpret),
- Double packer tests in 3 m sections, and
- Posiva Flow Log (PFL) (done only on KI0010B01).

For the tests performed in sections (as in the first two of the three cases above), a transmissivity T_{sec} was calculated for every section. This T_{sec} was used to calculate an equivalent hydraulic aperture b_{eq} using the cubic law, *as if* all inflow within the section originated from one single fracture. b_{eq} is not to be interpreted as a true hydraulic aperture of a fracture. It is, rather, an estimation of the largest fracture within the section, since it has been found that with few fractures within an interval the largest fracture is of the same order of magnitude as T_{sec} (Gustafson 2009). On the other hand, b_{eq} says nothing about the size of small fractures within the interval.

It must also be considered that even though b_{eq} estimates the largest fracture in each measured interval, this is a local value which depends on the local aperture of the part of the fracture intersected by the evaluated borehole. If the borehole intersects the fracture in a part where it is open, then the measurement gives a good approximation of the effective hydraulic aperture for the whole fracture. If, however, the borehole intersects the fracture in a part where it is closed or narrow, then the obtained aperture only says something about the fracture aperture locally (Gustafson 2009).

Since it is not known whether a borehole intersects a fracture in a locally narrow or wide part, it must be taken into consideration that the fracture may have a larger hydraulic aperture than the local value that was measured.

The PFL measures 1 m sections of the boreholes, but is moved 0.1 m in each step, which means the resolution is 0.1 m. It is seen in the fracture mapping that most 0.1 m sections do not contain more than one fracture. The measurements are generally interpreted as if each interval contains only one fracture. Thus the calculated aperture is interpreted as the hydraulic aperture of one fracture. The above discussion on the local apertures at the point where the borehole intersects the fracture applies for these PFL-apertures too.

5.3 Evaluation of tests performed during drilling

The in-data to these evaluations originate from tests performed during drilling of the cored boreholes.

The aim was to verify the location of the planned tunnel, for which a set of demands was specified (see chapter 1.2.1), and also to give a preliminary picture of the rock volume, which gave important early information for the grouting design.

The in-data consist of the inflow measurements, pressure measurements and preliminary core mapping.

The inflow was measured as the full-hole inflow, with a section increase of about 3 m between measurements. It was expected that the inflow would remain unchanged or increase for each measurement, since each measurement included the inflow from the previously measured section plus the inflow into the added 3 m section. It was also expected that it would be harder and harder to distinguish the local inflow increase the longer the borehole was drilled, as an effect of the noise from the increasing total flow from the hole.

The section-wise transmissivities were estimated using ***Eq. 2***, and the equivalent hydraulic apertures using ***Eq. 1***. For this, the hydraulic head was one input-parameter, and the used pressure was the evaluated data from the first of the three boreholes (KI0010B01), described in the section on interpretation of pressure measured in a long section of a borehole.

The out-put of the analysis was a preliminary estimation of the equivalent hydraulic apertures along the borehole length.

The fracture frequency was also evaluated and compared to the initial demands for the location of the tunnel.

5.3.1 Interpretation of pressure measured in a long section of a borehole

When measuring the pressure in a section of a borehole, an important question is to understand what the result represents. The hydraulic head may vary along the borehole, for instance because the borehole starts in the wall of a tunnel (atmospheric pressure) and ends deep in the rock. It might be tempting to think that the pressure h_w of a measured section represents the pressure at the end of the section or the middle of it. This is not the case. The distance along the boreehole for which h_w is representative is derived below under the presented assumptions. In this case we consider a horizontal borehole, and the conceptual model is shown in Figure 5-2.

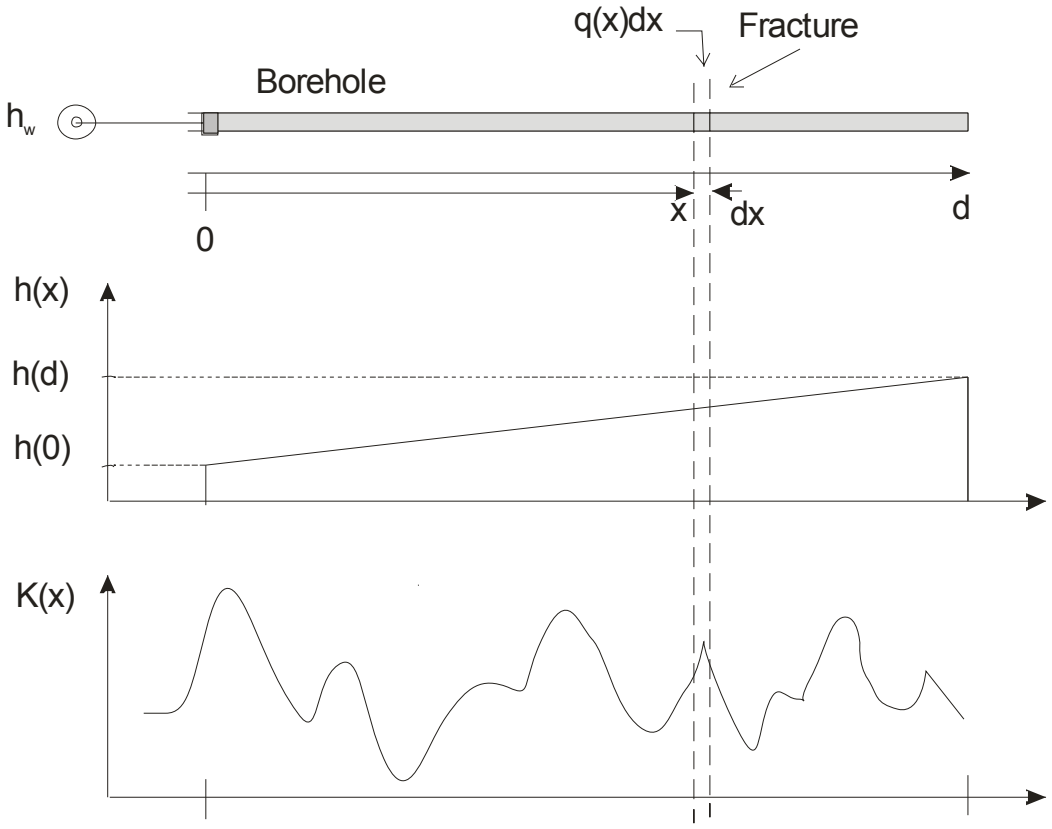

Figure 5-2: *The important parameters when measuring the hydraulic head in a section of a borehole. Top: A borehole section of length d is tested, resulting in the section pressure h_w. Middle: The hydraulic head is assumed to increase linearly along the test section. Bottom: The hydraulic conductivity varies along the borehole.*

d is the length of the tested section.

dx is the thickness of a fracture that intersects the borehole.

h_w is the hydraulic head obtained by measuring the pressure along a section of a borehole.

h(x) is the hydraulic head at different depths along the borehole line before the borehole was drillled, and *h(0)* and *h(d)* are the local values of the hydraulic head at the beginning and end of the measured section.

K(x) is the conductivity of the rock as a function of borehole depth. In crystalline rock it is low where no fractures intersect the borehole, and high in areas of conductive fractures.

The inflow into a borehole, intersecting a long conductive fracture, can be written according to Thiem's equation (Thiem 1906) as

$$\Delta h = \frac{Q}{2\pi T}\ln(\frac{R_0}{r_w}) \qquad \textbf{\textit{Equation 3}}$$

Inserting $T = KL$ and $q = Q/L$ into ***Eq. 3*** leads to

$$\Delta h = \frac{q}{2\pi K} \ln(\frac{R_0}{r_w}) .$$

The water flow into the borehole from a fracture, at position x along the borehole, as illustrated in the top of Figure 5-2, is thus

$$q(x) = \frac{2\pi K(x) \cdot [h_w - h(x)]}{\ln(R_0 / r_w)} \qquad \textbf{Equation 4}$$

where

h_w is the hydraulic head, achieved by measuring the pressure along a section of a borehole;

R_0 is the radius of influence, i.e., the radial distance from the borehole where there is no effect of the borehole and the hydraulic head equals $h(x)$;

r_w is the radius of the borehole.

During the measurements, the borehole is closed so no water is entering or leaving. This is expressed by

$$\int_0^d q(x)dx = 0 \qquad \textbf{Equation 5}$$

where d is the total length of the section.

Combining ***Eq. 4*** and ***Eq. 5*** results in

$$\int_0^d K(x)\big(h_w - h(x)\big)dx = 0$$

Equation 6

Assuming that the hydraulic head increases linearly within the test-section, as shown in the middle part of Figure 5-2, leads to

$$h(x) = h(0) + \frac{x}{d} \cdot [h(d) - h(0)] \qquad \textbf{Equation 7}$$

Inserting ***Eq. 7*** into ***Eq. 6*** yields

$$\int_0^d K(x)\left(h_w - h(0) - \frac{x}{d}[h(d) - h(0)]\right)dx = 0 .$$

Rearranging:

$$\big(h_w - h(0)\big) \cdot \int_0^d K(x)dx = \frac{1}{d}[h(d) - h(0)] \cdot \int_0^d K(x) \cdot x dx$$

$$\frac{\int_0^d K(x)\cdot x dx}{\int_0^d K(x)dx} = d\cdot\frac{h_w - h(0)}{h(d)-h(0)}$$

Imagining that *K(x)* is a mass distribution along $0 < x < d$, then the position of the centre of gravity , x_t, becomes

$$\frac{\int_0^d K(x)\cdot x dx}{\int_0^d K(x)dx} = x_t \qquad \textbf{\textit{Equation 8}}$$

(Grahn and Jansson, 1997).

Hence

$$x_t = d\cdot\frac{h_w - h(0)}{h(d)-h(0)}. \qquad \textbf{\textit{Equation 9}}$$

Rearranging ***Eq. 9*** leads to

$$h_w = h(0) + \frac{x_t}{d}\left[h(d)-h(0)\right]$$

The right hand side in this equation is recognized as the right hand side of ***Eq. 7***, and the conclusion is that the measured pressure is valid at the distance x_t according to

$$h_w = h(x_t) \qquad \textbf{\textit{Equation 10}}$$

5.4 Evaluation of double packer tests

The in-data from the double packer tests are pressure and inflow measured in 3 m sections.

The aim of this analysis was to supply a more accurate base for grouting design, than the initial analysis based on in-data from the drilling.

The section-wise transmissivities were estimated using Moye's formula (Moye 1967)

$$T = \frac{Q}{2\pi\Delta h}\cdot\left[1+\ln(\frac{L}{2r_w})\right] \qquad \textbf{\textit{Equation 11}}$$

and the equivalent hydraulic apertures using ***Eq. 1***.

The out-put of the analysis was an estimation of the equivalent hydraulic apertures along the borehole length.

5.5 Evaluation of Posiva Flow Log

Only the first of the three long boreholes was tested with PFL.

The aim of the PFL analysis was to provide a supplementary base for grouting design. It was expected that this would yield the most accurate picture of the fractures along the borehole, based on the short step length.

The in-data consist of flow rate during natural outflow from the hole. The tested section length was L = 1 m, and the step length was dL = 0.1 m. The single point resistance showed the location of the fractures. Since the step length was so short, it was generally assumed that each 0.1 m interval contained a maximum of one fracture. Hence the inflows were regarded as fracture inflows.

The transmissivities were estimated by the specific capacity using ***Eq. 2***, and also using Thiem's well equation (Thiem 1906)

$$T = \frac{Q}{2\pi\Delta h} \cdot \ln(\frac{R_0}{r_w}) \qquad \textit{Equation 12}$$

The hydraulic apertures obtained using ***Eq. 1*** was regarded as fracture hydraulic apertures, as opposed to the equivalent hydraulic apertures from section-wise data in the two previous test methods. The hydraulic head is one parameter in ***Eq. 1***, and the used pressure was the evaluated data from the first of the three boreholes (KI0010B01) described in the section on interpretation of pressure measured in a long section of a borehole.

The out-put of the analysis was hydraulic apertures along the borehole length.

5.6 Comparison of the results based on the different test methods for each of the boreholes

The described evaluation results were compared. Attention was put to the fact that the different methods are based on different conceptual models, and hence describe the fractures in different ways. The aim was to increase the understanding of the analyzed rock volume.

5.7 Results and discussion concerning the hydrogeological evaluations

5.7.1 Tests during drilling

The pressure profile

As explained in previous sections, the only pressure data really useful in estimating the pressure profile in the rock volume came from KI0010B01.

In KI0010B01 the pressure was measured in full-hole sections. The data is presented in Figure 5-3. In this chart, the length values along the x-axis are the current lengths of the hole, as far as it was drilled at each measuring moment.

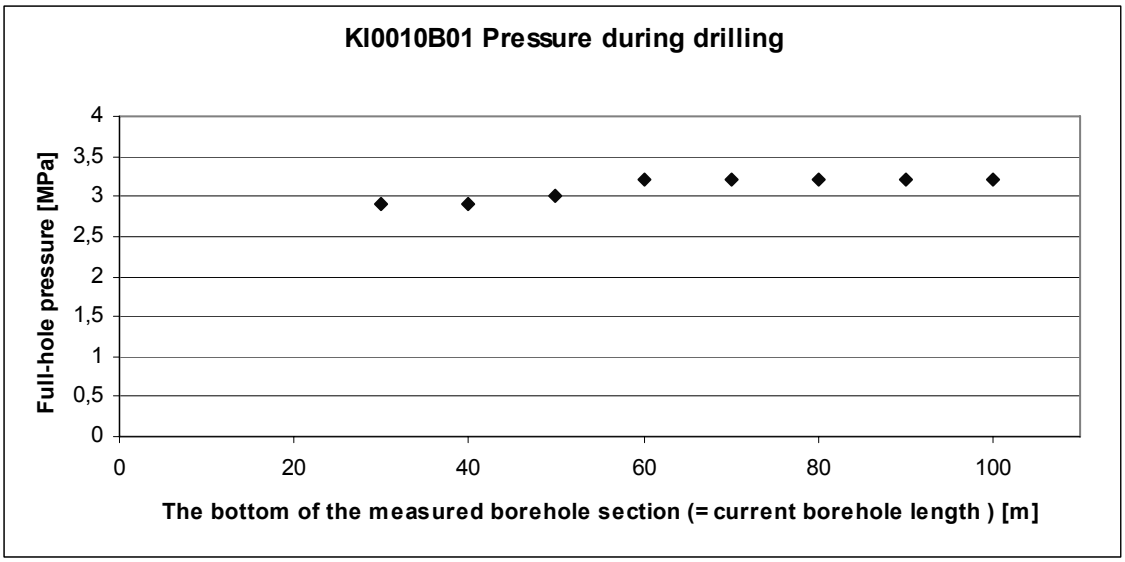

Figure 5-3: *The pressure measured in full-hole sections in KA0010B01.*

When interpreting full-hole pressure data, like this data set, it is important to understand that the measured pressure P (which is easily transformed to the hydraulic head h_w mentioned in the Methods section) does not represent the pressure at the end of the borehole, which would be the first glimpse interpretation of Figure 5-3. Instead it is a type of average pressure along the whole measured section. In order to calculate what distance along the borehole each measured *P* does represent, an analysis based on the transmissivities along the borehole, described in chapter 5.3.1 on interpretation of pressure measured in a long section of a borehole, has been done, , using Equations 8 and 10 . The resulting distances x_t obtained for each pressure h_w, have been extrapolated with a logarithmic trend line, shown in Figure 5-4. This is the pressure used for the evaluation of data obtained during drilling and for PFL-data.

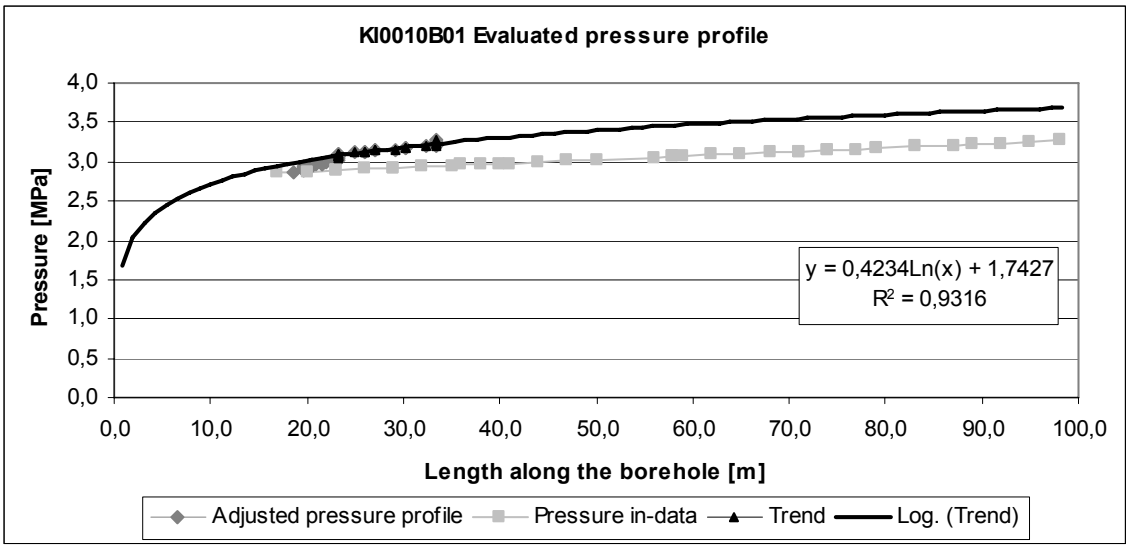

Figure 5-4: *The evaluated pressure profile of KI0010B01. The pressure in-data is a linear extrapolation of the measurements (Figure 5-3). The adjusted profile is the calculated position that each pressure value corresponds to; and the trend line is extrapolated logarithmically.*

The second borehole to be drilled and tested was KI0016B01. For this borehole the pressure testing proceeded according to the original plans, as described earlier. Since these measurements were done in sections, not in full-hole lengths, they represent well the pressure along the test section, and no special analysis of the data is needed.

However, the water took shortcuts through fractures connecting the tested hole to the previously drilled KI0010B01, which influenced the pressure situation to the extent that the data does not describe the pressure profile under natural conditions. The pressure profile is presented in Figure 5-5 and the explanations for its appearance are illustrated in Figure 5-6.

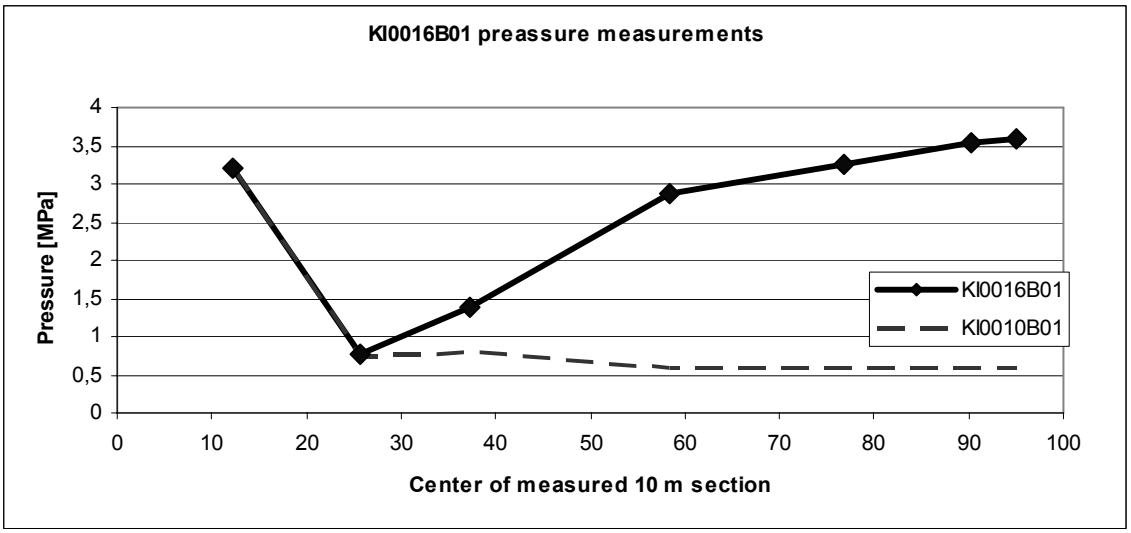

Figure 5-5: *The pressure in KI0016B01, measured in 10 m test sections. The pressure was measured in KI0010B01 simultaneously, to be able to see connections, and both are shown in the graph.*

The unexpected appearance of the pressure data in KI0016B01 leads to conclusions about water leaking through fractures connecting the borehole with the previously drilled (and during these measurements closed) KI0010B01, as illustrated in Figure 5-6. The first measured section in KI0016B01 showed equal pressure as the whole borehole KI0010B01, which confirmed that the full-hole pressure of KI0010B01 was transmitted through what is believed to be structure #5 of the TRUE Block Scale model (see the TRUE Block Scale hydro-structural model in Andersson et al 2002a and Figure 2-8) into the measured section of KI0016B01. During all the following measurements, deeper in KI0016B01, water was drained from KI0010B01 through structure #5 and out into the tunnel through the open entrance of KI0016B01, reducing the pressure in KI0010B01 to the low level of the bottom curve of Figure 5-5. During the second and third measurements this low pressure is transferred into the measured section of KI0016B01 through other connecting fractures. The last two measurements do not indicate any connecting fractures, thus the data here presumably represent the pressure under undisturbed conditions fairly well.

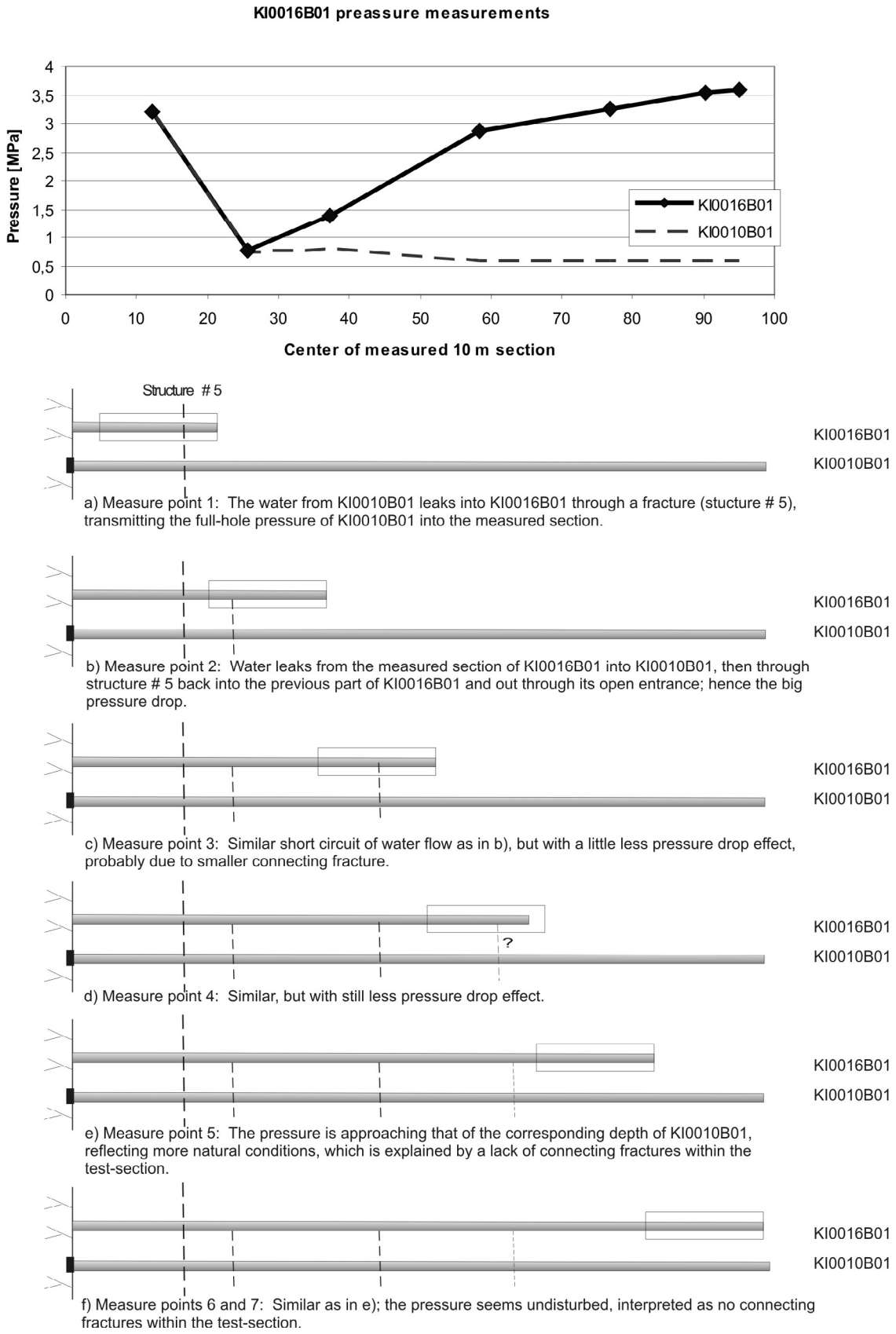

Figure 5-6: *Principal sketch illustrating an interpretation of how connecting fractures influence the pressure as measured in KI0016B01. The measured section is the white box.*

It is interesting to compare the deepest measure points of KI0016B01 (Figure 5-5) to the evaluated pressure profile of KI0010B01 (Figure 5-4). It is seen that the two deepest values, where pressure conditions are interpreted as uninfluenced by the existence of the previously drilled borehole, correspond well to the evaluated pressure profile; both curves indicate a pressure a little above 3.5 MPa in this region.

Inflow

The full-hole inflow was measured during drilling of the boreholes, as the holes were drilled. The intervals between the measurements varied a little, but were often 3 meters. The inflow is shown in Figure 5-7. The depth along the boreholes, along which the inflows are plotted, start at top of casing for each of the holes, and this differs up to four meters between the holes, because they are bored at an angle to the wall in which they start.

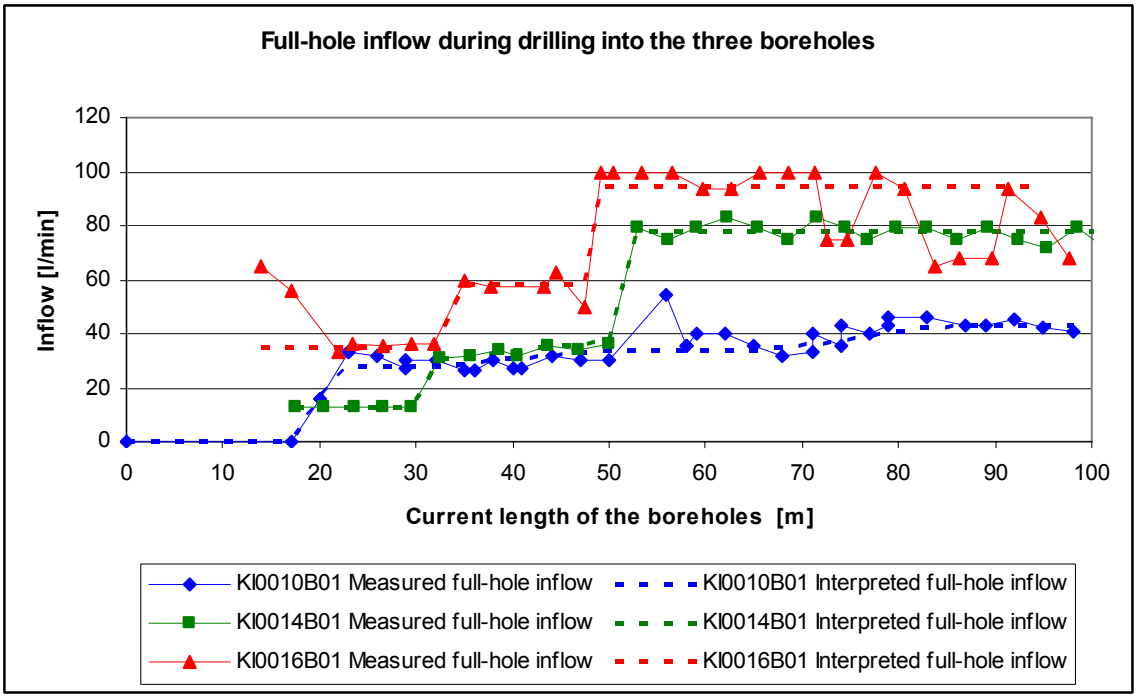

Figure 5-7: *The inflow during drilling into the three boreholes. The markers connected by the continuous line show the measured inflow. The broken lines show an interpretation based on the principle that the full-hole inflow should not decrease as the boreholes grow longer.*

At first sight it may seem a little strange that the total flow of water out of a borehole may decrease as the hole is drilled longer, as is seen in the chart. The HMS (Hydro Monitoring System) report for 2007 (internal SKB report) showed that no other activities could have had any influence on the site area. The reason for the behaviour of the water flow is thought to be that a volume close to the borehole is drained when the hole connects to it, but that the inflow to that volume from more remote parts of the rock is smaller. This time dependant behaviour is called transients.

When using the inflow data for a first estimation of the local hydraulic properties of the rock, it is the inflow in each section of the hole that is useful. Since negative inflows do not give a sensible interpretation, the full-hole inflow curves need not to have a negative inclination. Hence the curves are adjusted, showed by the broken lines in Figure 5-7, and then the inflow into each interval can be obtained and is presented in Figure 5-8. It should be kept in mind that the result is influenced by the way the adjustment is done.

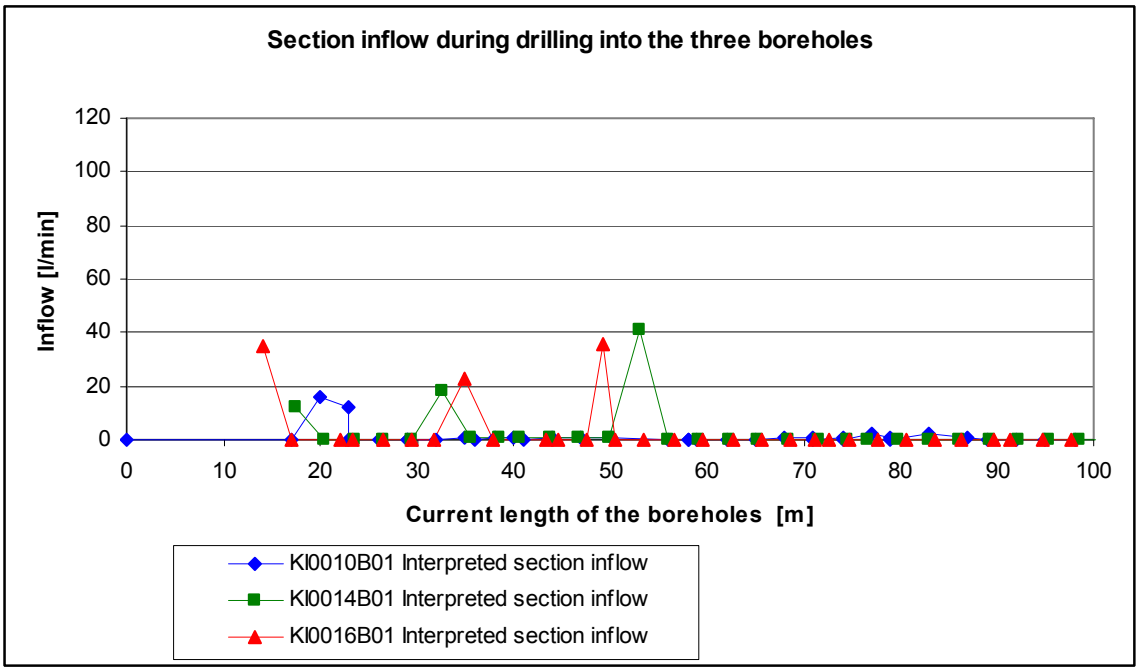

Figure 5-8: *An interpretation of the inflow into each section of the three boreholes, based on the interpreted full-hole inflow shown in Figure 5-7.*

Evaluation of hydraulic apertures along the three cored boreholes

As described in the methods section, the transmissivity T is needed for calculating the hydraulic aperture b. The transmissivity estimated by the specific capacity (***Eq. 2***) is shown in Figure 5-9. For this the inflows presented in Figure 5-8 and the evaluated pressure profile shown in Figure 5-4, transformed into hydraulic head, were used.

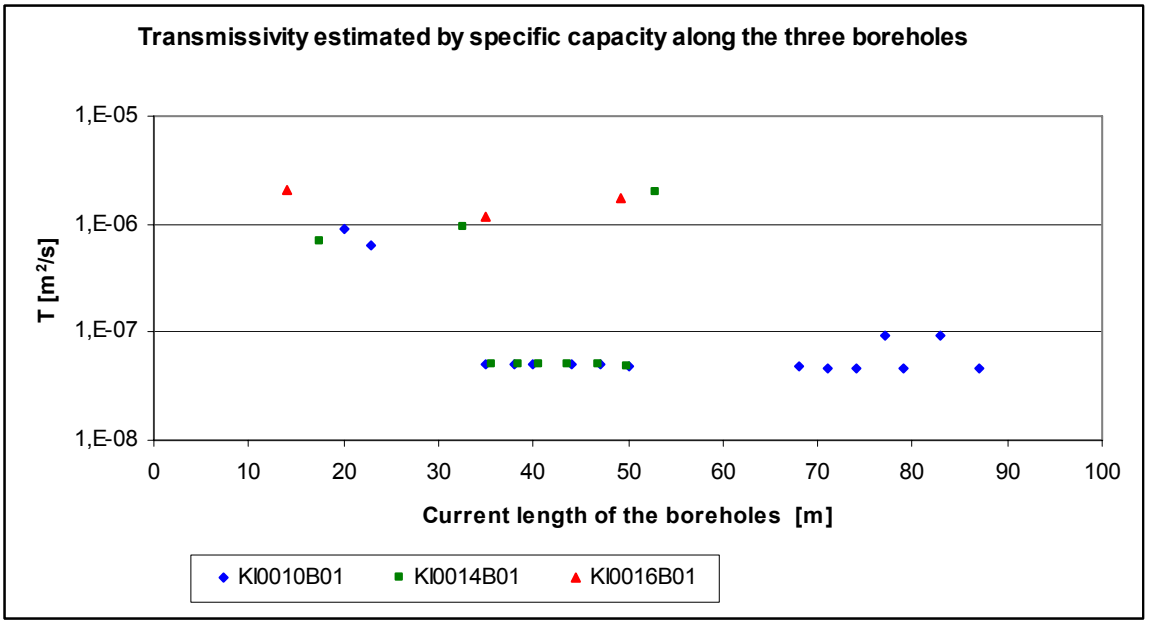

Figure 5-9: *Section transmissivities, as interpreted from the full-hole inflow measurements during drilling, along the three boreholes.*

Next, the hydraulic aperture *b* is calculated from the transmissivity *T* using the cubic law (***Eq. 1***). In the graphs illustrating the evaluations (Figure 5-10, Figure 5-11 and Figure 5-12. See Appendix 6 for data tables.), there are sometimes text boxes inserted, containing names of structures (for example #5) which are known from a neighbouring experiment, the TRUE block scale rock volume (see the TRUE Block Scale hydro-structural model in Andersson, P. et al, 2002a). The boxes mark the places of intersection between the boreholes and the extrapolated location of these structures (see also Figures 5-13 to 17). This does not have to mean that it is the TRUE-structures which have been found, but it shows the possibility that it could be.

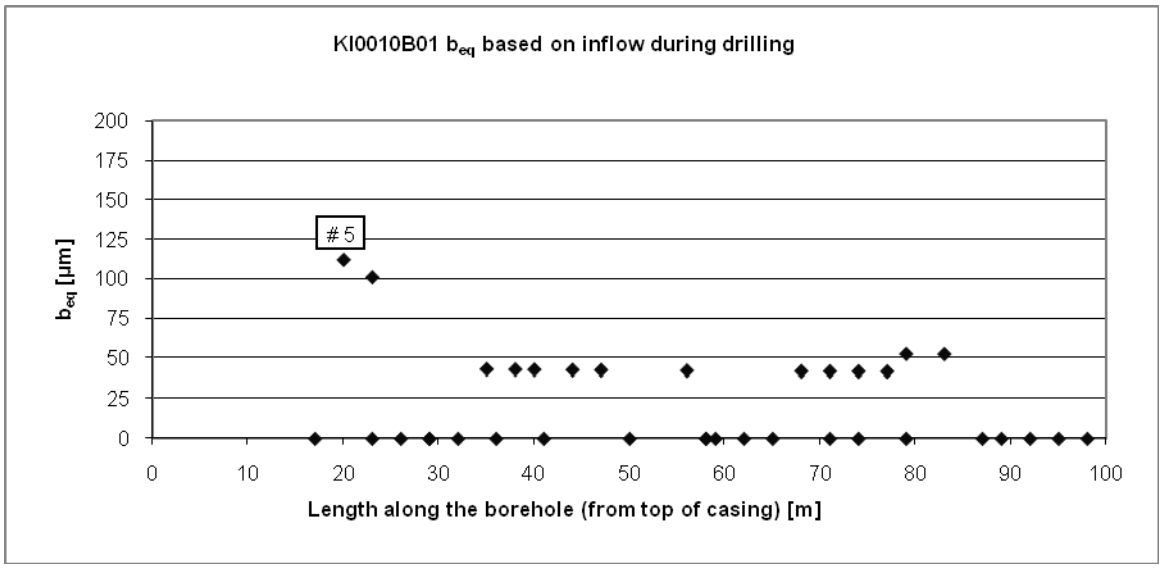

Figure 5-10: *The equivalent hydraulic aperture of KI0010B01 based on inflow during drilling.*

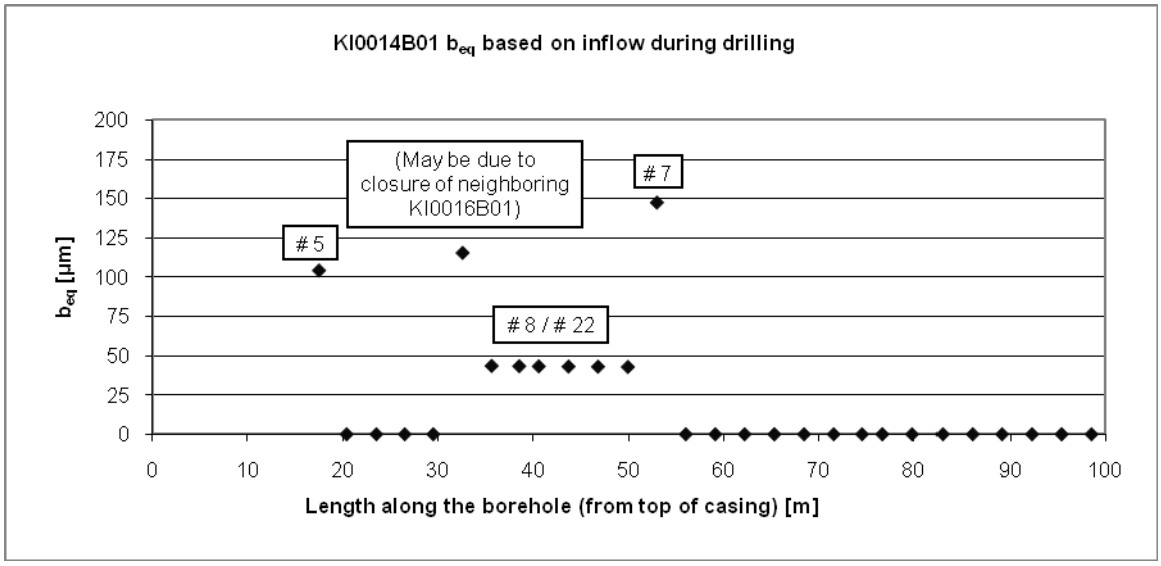

Figure 5-11: *The equivalent hydraulic aperture of KI0014B01 based on inflow during drilling.*

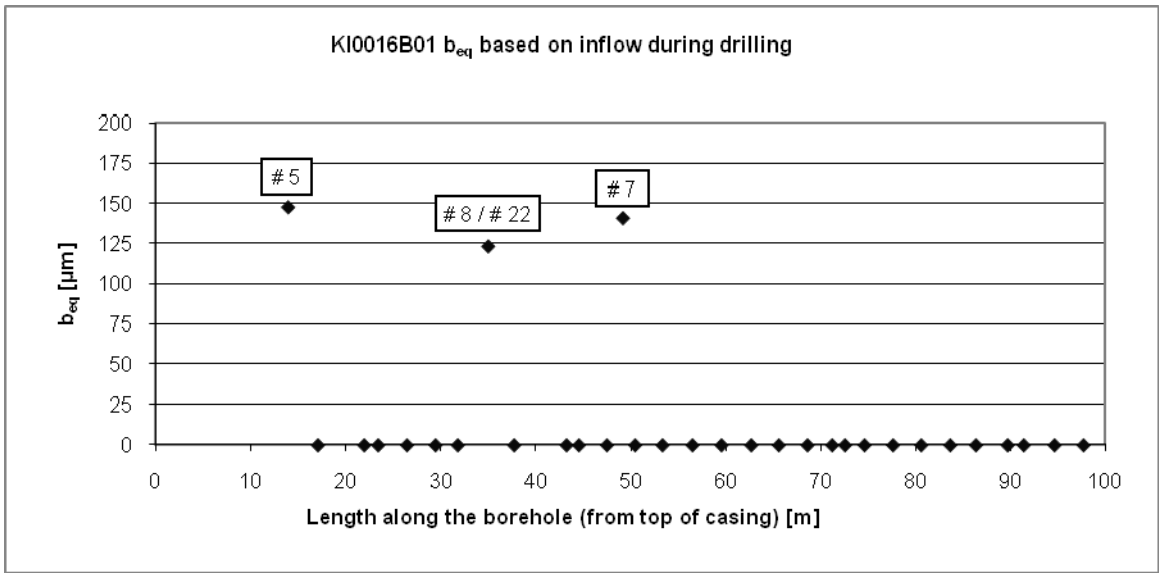

Figure 5-12: *The equivalent hydraulic aperture of KI0016B01 based on inflow during drilling.*

5.7.2 Double packer tests

The equivalent hydraulic apertures based on double packer tests are illustrated in the diagrams below (Figures 5-13, 5-14 and 5-15, see Appendix 6 for data tables)

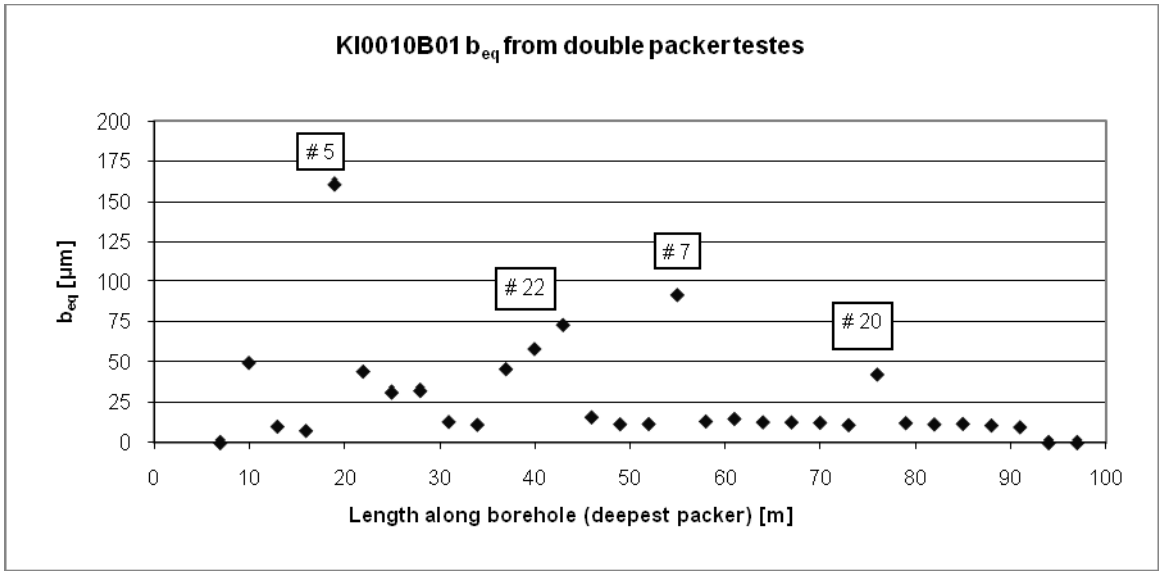

Figure 5-13: *The equivalent hydraulic aperture of KI0010B01 based on double packer tests.*

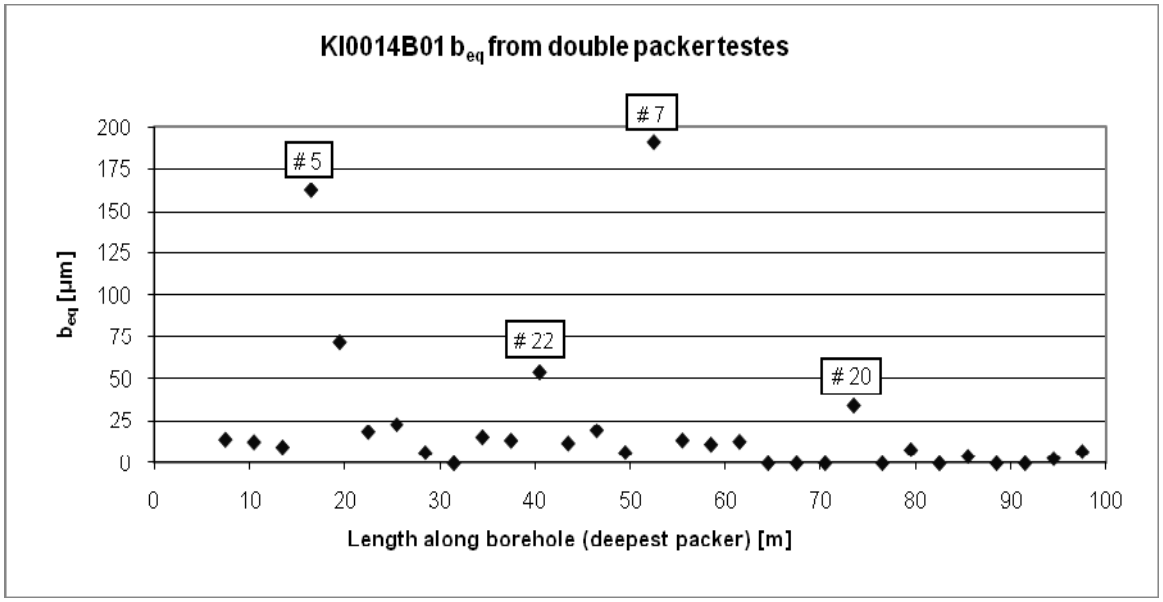

Figure 5-14: *The equivalent hydraulic aperture of KI0014B01 based on double packer tests.*

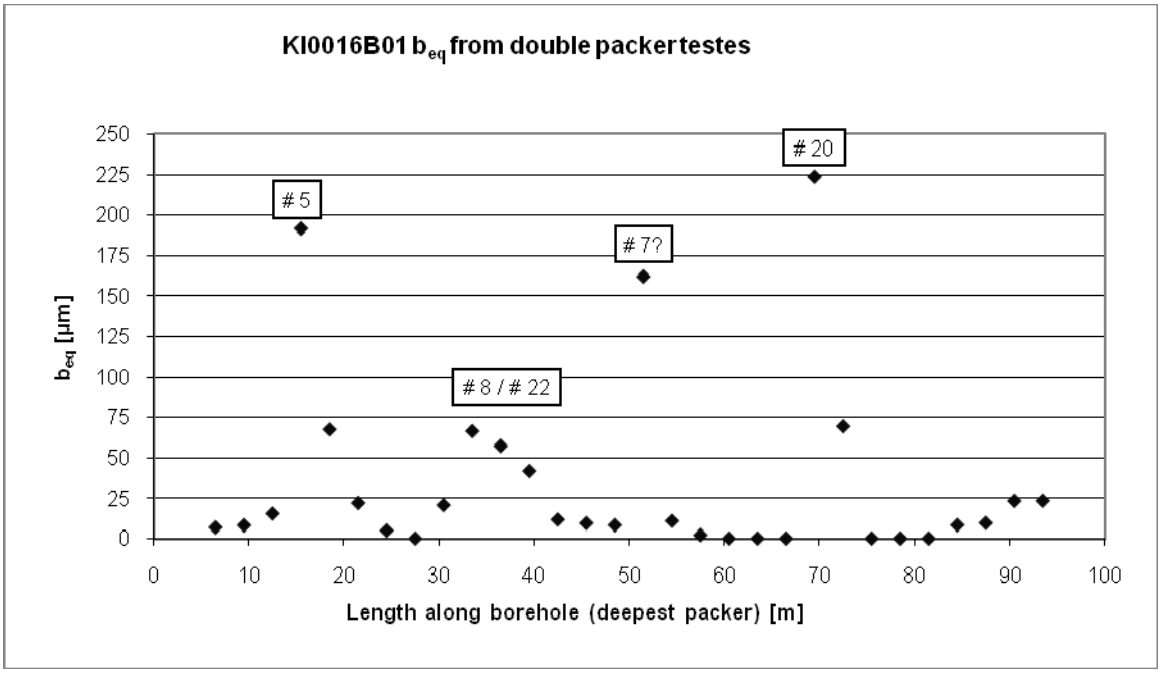

Figure 5-15: *The equivalent hydraulic aperture of KI0016B01 based on double packer tests.*

Note especially the fracture/inflow at around 70 m depth, which wasn't visible in the data from the drilling, and is in KI0016B01 (Figure 5-15) larger than any other inflow measured in the three long cored boreholes. This inflow surprised the hydrologist in charge of the measurements, and the section was measured twice as an extra check, with the same result. If this inflow is structure # 20, then it is much tighter where it is intersected by the other two boreholes (Figures 5-13 and 5-14).

5.7.3 PFL-logging

In the case of PFL-logging, the resolution is, as previously mentioned, dL = 0.1 m. This, combined with the fracture frequency of on average approximately two fractures per meter, means that each inflow can generally be regarded as the inflow from one single fracture. These calculated hydraulic apertures are therefore considered to represent local properties of the intersecting fractures, unlike the equivalent apertures which were the results of the measurements in 3 m sections.

The hydraulic aperture is, as described previously, calculated from the transmissivity by the cubic law (***Eq.1***). It was found that the simplest estimation of the transmissivity as the specific capacity, $T \approx Q/dh$ (***Eq. 2***), gave values which differed very little from the more complex Thiem's equation (***Eq. 4***). Here the evaluated pressure profile of the borehole, shown in Figure 5-4, transformed into hydraulic head, was used. For the PFL-data, hydraulic apertures from the simple formula were 99.6% of those achieved by using Thiem's well equation (with R_0/r_w = 500), and the former is presented.

PFL-measurements were performed only on the first of the three boreholes, KI0010B01, and the evaluated hydraulic apertures are presented in Figure 5-16 (see Appendix 6 for data table. See also Appendix 5 for additional data presented as graphs).

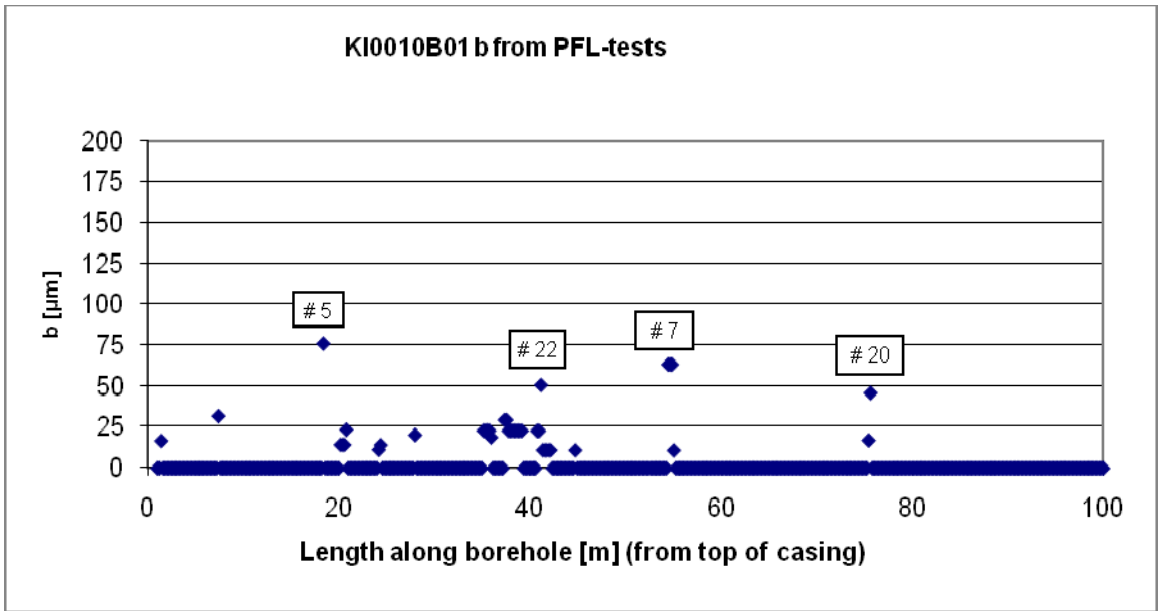

Figure 5-16: *The hydraulic aperture of KI0010B01 based on PFL.*

5.7.4 Comparison of the results based on the different test methods

It is interesting to compare the data from PFL and from the double packer. In Figure 5-17 both curves are shown: the double packer equivalent apertures and the largest PFL-aperture within each of the intervals defined by the double packer tests. The two sets give pictures of the borehole that looks generally much alike, although the apertures are not the same.

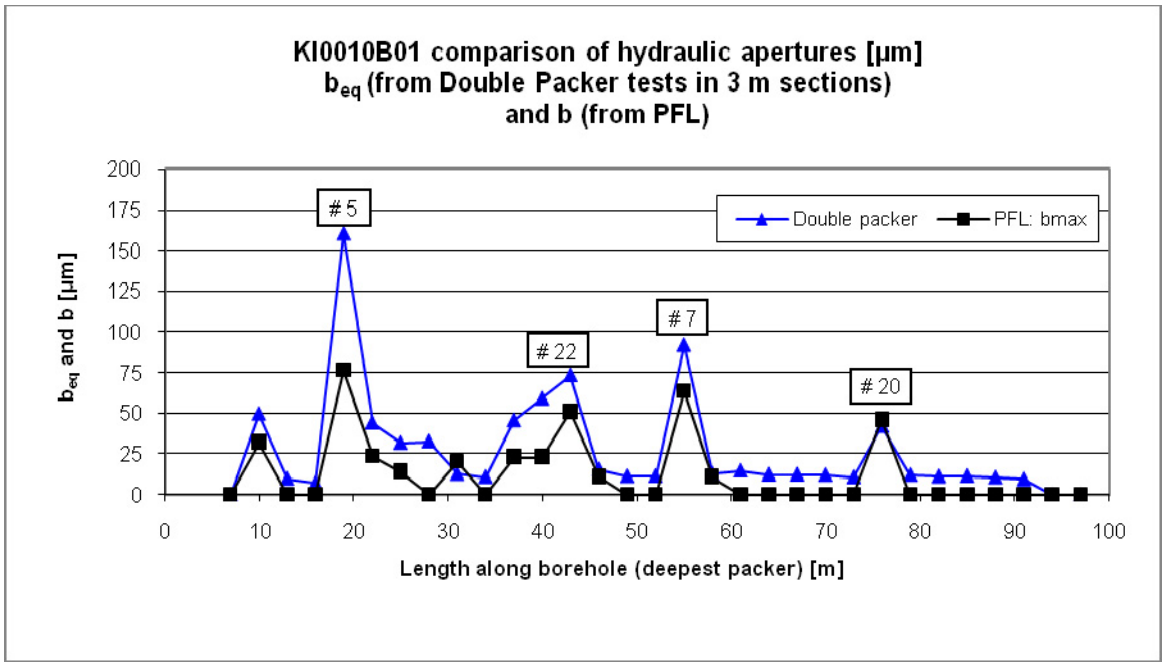

Figure 5-17: *Comparison between the largest b-value from PFL within each 3 m section, and the b_{eq} from double packer from the same sections.*

In 31 out of the 33 measured 3 m sections the double packer b_{eq} is larger than the PFL b-values. This is in accordance to expectations, since there are often several fractures contributing to the inflow into each 3 m section. Also if all PFL anomalies in each section are summed, the hydraulic apertures calculated from PFL measurements may be smaller than those calculated from the double packer measurements. This is due to potential turbulent flow at the open borehole during the PFL measurements. The double packer measurements were done at lower hydraulic gradients and thus lower flow velocities.

The *b*- and b_{eq}-values in Figure 5-17 are plotted against each other below, to illustrate the relation between them. The thin line shows the 1:1 relation; the thick line is a linear trend line (Figure 5-18).

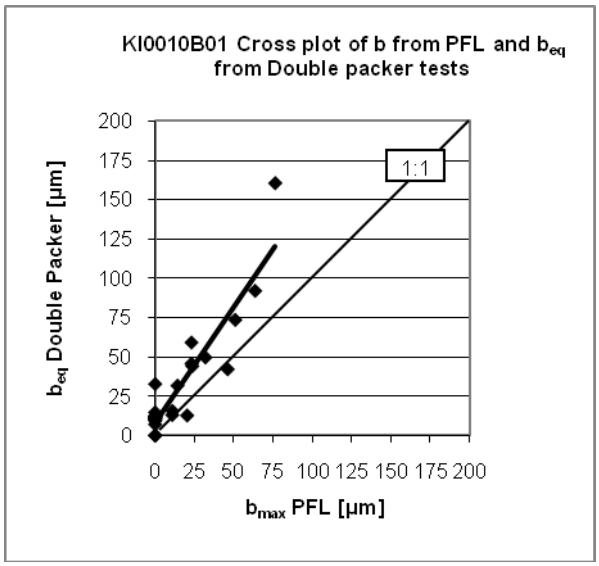

Figure 5-18: *Relation between PFL b-values and double packer b_{eq}-values (from KI0010B01)*

5.7.5 Open fracture positions

The positions of the open fractures along one of the boreholes (KI0010B01) are shown in Figure 5-19 (cf. Figure 3-17). The positions are shown according to two mapping methods: both the preliminary mapping in connection to the drilling (except for the first approximately 2 m) and Boremap. They are found to correspond quite well, and the small deviations in positions is accounted for by the fact that during the preliminary mapping the positions were measured on the cores, and in Boremap they are measured on the borehole images as well.

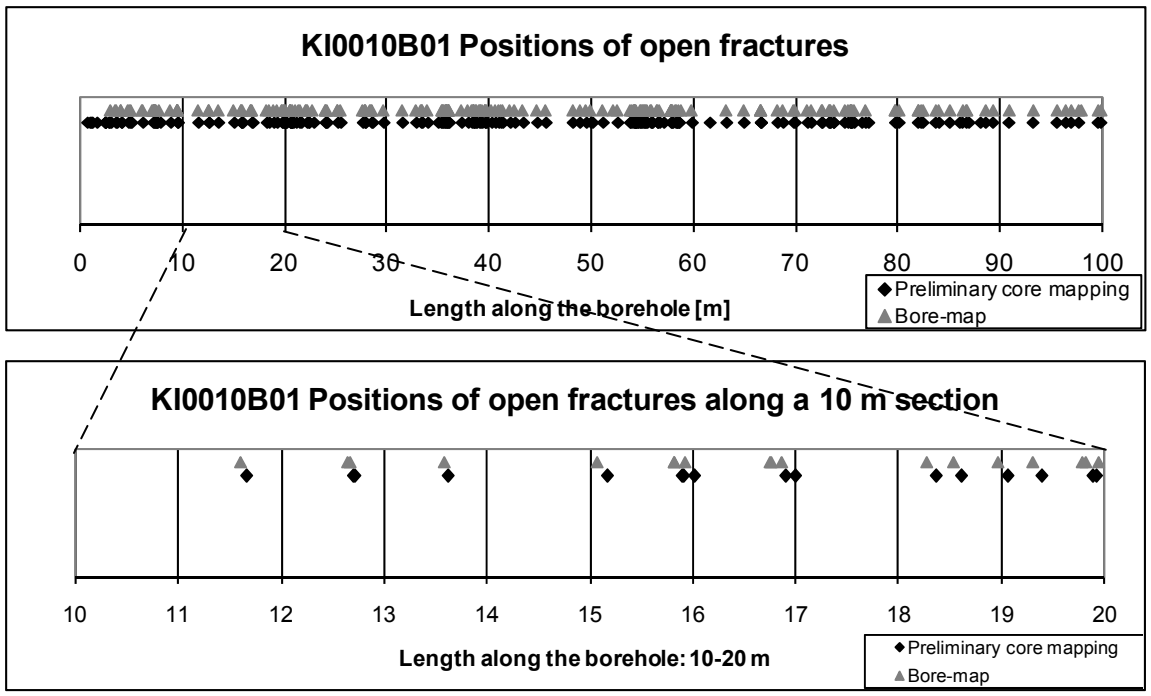

Figure 5-19: *The positions of open fractures along KI0010B01. The diamonds show the results from the preliminary mapping, and the triangles show the Boremap results. Note that the diagram does not show the dimension of the apertures. Top: The whole borehole. Bottom: A 10 m section shown for better resolution.*

The positions of the inflows, as found by PFL, into the same borehole are compared to the mapped open fractures in Figure 20 (cf. also Figure 3-17). It is found that there are mapped open fractures in the vicinity of each PFL inflow, which seems quite logical. On the other hand, it can be seen in the chart that there are a lot of open fractures in which no inflow has been measured.

Note that in Boremap the smallest aperture to be recorded is 0.5 mm (500 µm). This means that all fractures with apertures <1 mm will be recorded as 0.5 mm. Since the hydraulic apertures are much smaller than 0.5 mm only the positions of the apertures recorded with Boremap have been market out in Figure 5-20.

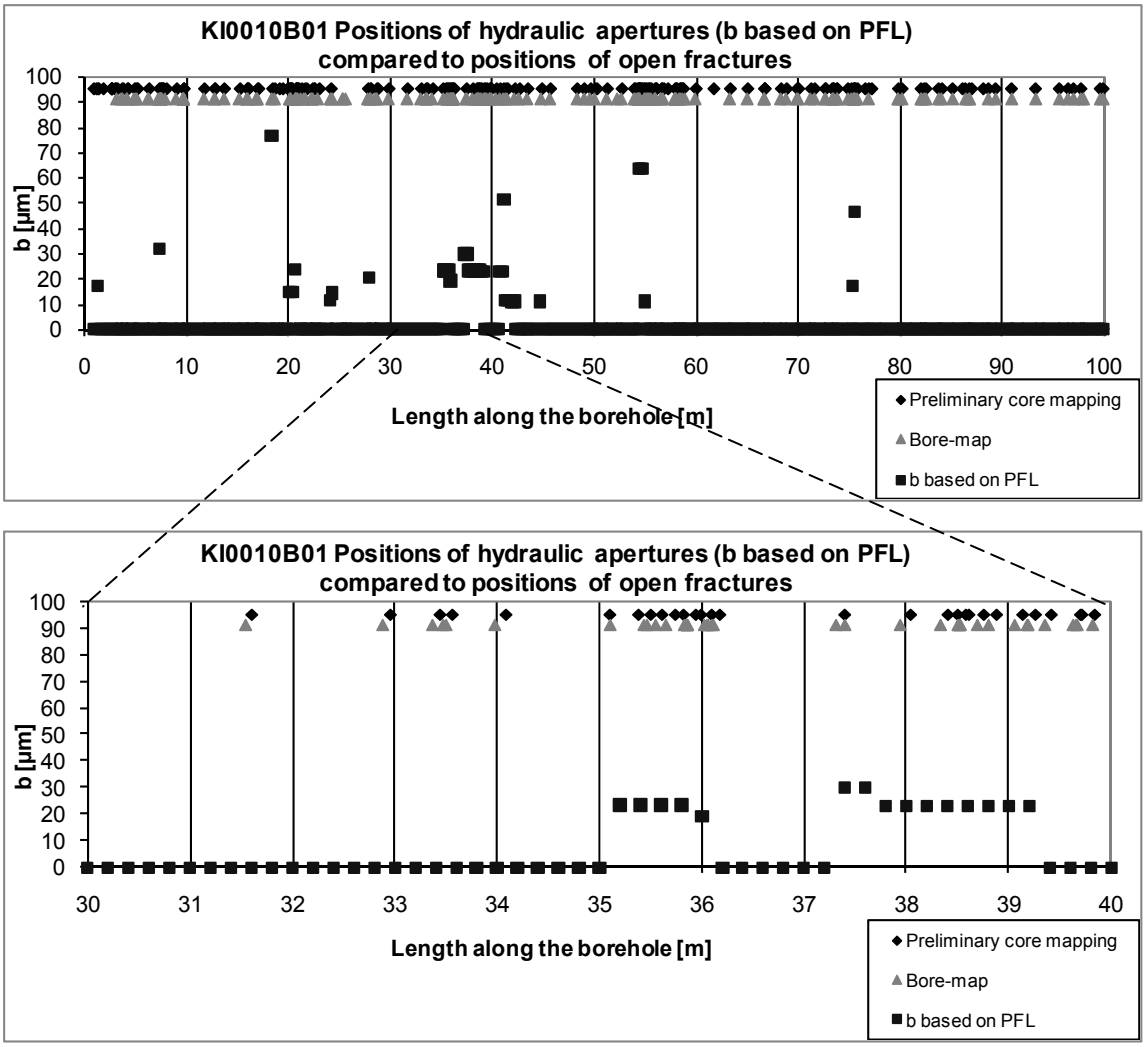

Figure 5-20: *The PFL b-values and the open fractures plotted along KI0010B01. The diamonds show the fracture positions based on the preliminary core mapping; the triangles show the fracture positions based on Boremap results; and the squares show positions of inflow and also the dimension of hydraulic apertures. Top: The whole borehole. Bottom: A 10 m section shown for better resolution.*

6 Predictions and outcome in relation to the TRUE Block Scale model

6.1 Predictions and outcome based on core logging

The TRUE Block Scale model is a 200x250x100 m rock volume characterised with the purpose of furnishing the basis for tracer experiments in a network of conductive structures in the block scale, i.e. 10-100 m, see Figure 6-1 (from Anderson et.al. 2002a). The hydraulic measurements of the three boreholes KI0010B01, KI0014B01 and KI0016B01 were compared with the structural Block Scale model. Points of inflow were identified as possible intersections between boreholes and the extrapolated water conductive structures from the TRUE Block Scale model.

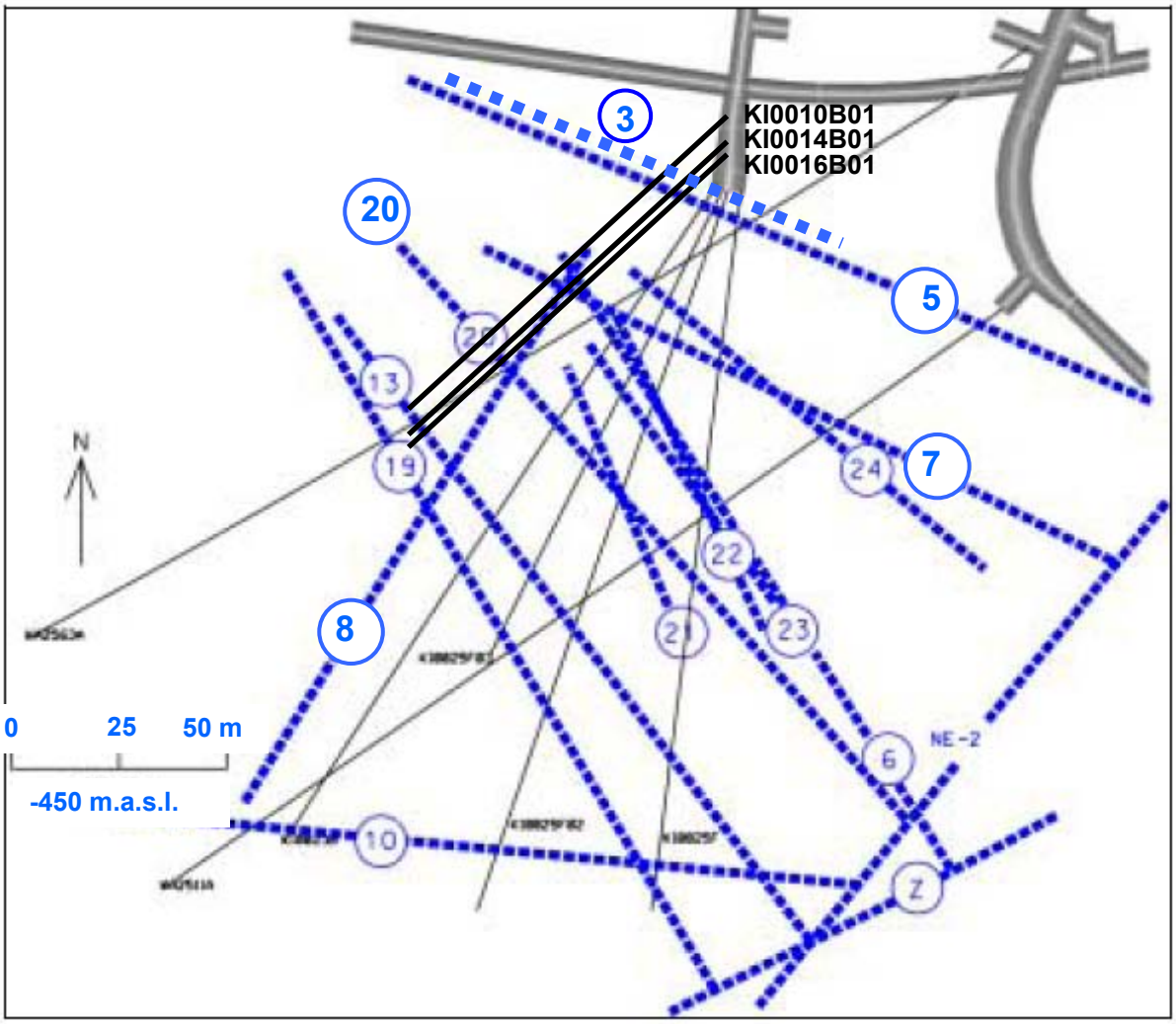

Figure 6-1. *Plan view of the TRUE Block Scale hydro-structural model (modified from Figure 4-6 in Andersson, P. et al, 2002a). Structure #3 has been added (sub parallel and in close proximity to structure #5) as well as the approximate location of the boreholes KI0010B01, KI0014B01 and KI0016B01*

The structures #5, #7, #8, #20 and #22 are believed to be identified in the hydraulic measurements in chapter 5. Their occurrences along length of the borehole, as shown in Figure 5-17, are compared with the BIPS images and mapping in Boremap. Identified open fractures and crush zones at lengths along the borehole that approximate the location of inflow in Figure 5-17 are interpreted as the possible intercepts of the appropriate TRUE Block Scale model structures. In addition the possible location of a part of structure #3 is interpreted in the three boreholes. The results are presented in Figures 6-2 to 6-5 and in Tables 6-1 to 6-5.

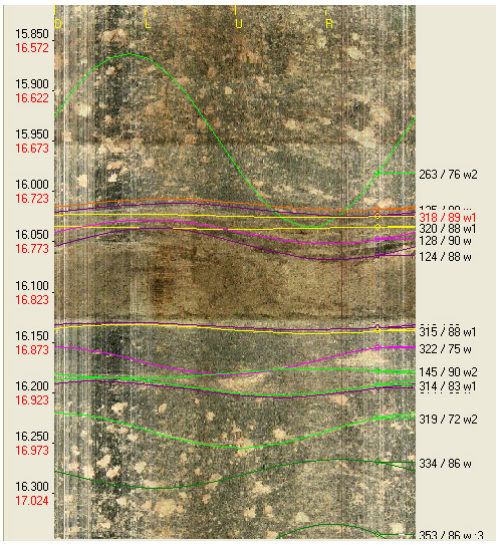

KI0010B01, open fract. & cataclastic band:

borehole length: ~16.74-16.92 m (adj.length), orientation: ~128/90 (ÄSPÖ96)

possibly structure #5 (and #3?)

a)

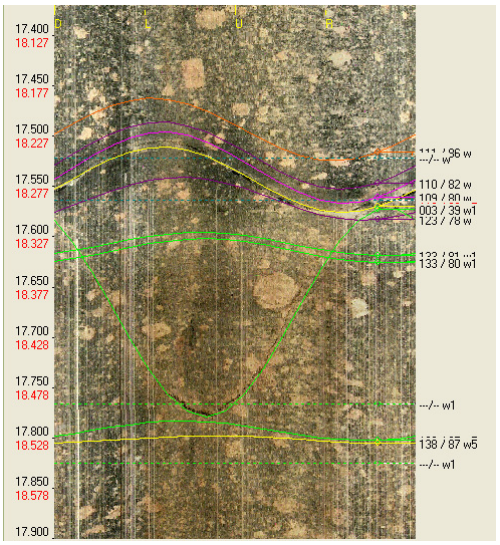

KI0010B01, open fracture:

borehole length: ~18.27 m (adj.length), orientation: ~110/82 (ÄSPÖ96),

possibly structure #5

b)

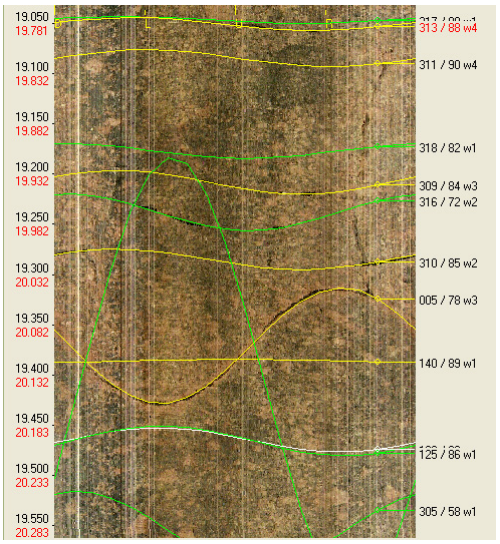

KI0010B01, open fractures:

borehole length: ~19.78 m (adj.length), orientation: ~131/88 (ÄSPÖ96),

borehole length: ~19.82 m (adj.length), orientation: ~311/90 (ÄSPÖ96),

borehole length: 20.02 m (adj.length), orientation: 310/85 (ÄSPÖ96),

borehole length: 20.10 m (adj.length),

orientation: 005/78 (ÄSPÖ96),

possibly part of structure #5

c)

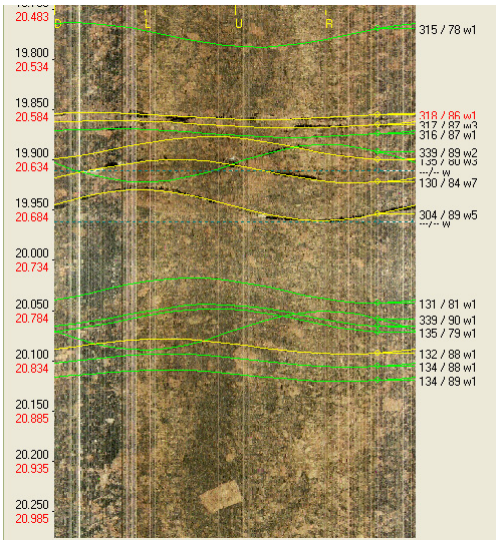

KI0010B01, open fractures:

borehole length: 20.6 m (adj.length), orientation: 317/87 (ÄSPÖ96),

borehole length: 20.65 m (adj.length), orientation: 130/84 (ÄSPÖ96),

borehole length: 20.68 m (adj.length), orientation: 304/89 (ÄSPÖ96),

are all possibly part of structure #5

d)

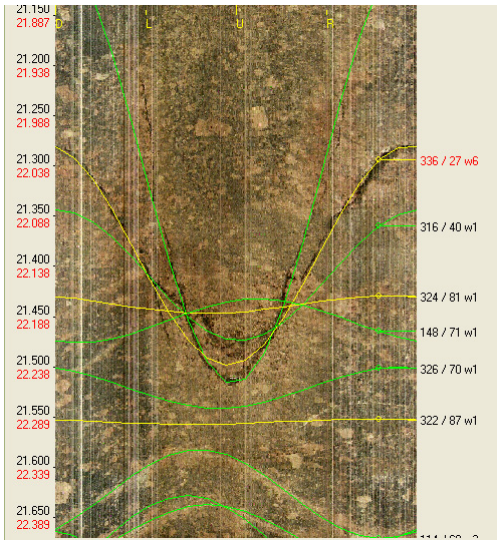

KI0010B01, open fractures:

borehole length: 22.13 m (adj.length), orientation: 356/27 (ÄSPÖ96),

borehole length: 22.18 m (adj.length), orientation: 324/81 (ÄSPÖ96),

are also possibly part of structure #5

e)

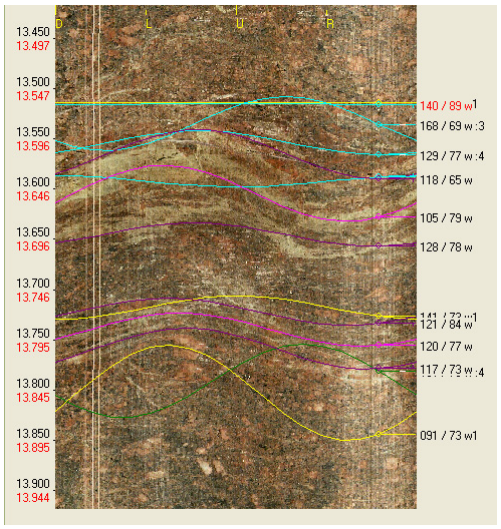

KI0014B01, crush zone:

borehole length: 13.56-13.64 m (adj.length) marked as blue lines orientation: 140/89-319/81 (ÄSPÖ96),

possibly structure #5 (and part of structure #3?)

f)

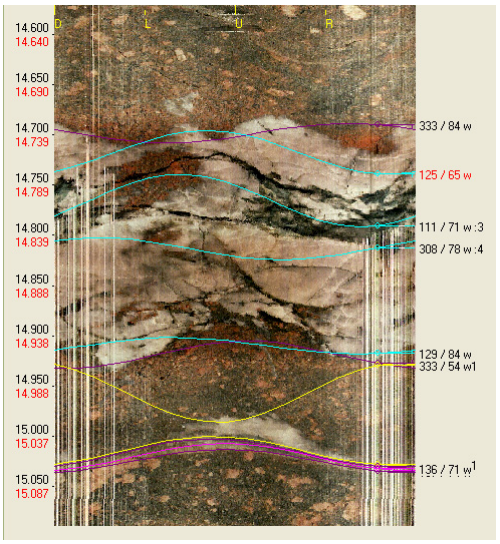

KI0014B01, crush zone:

borehole length: 14.8-14.9 m (adj.length) marked as blue lines orientation: 125/65 (ÄSPÖ96),

are possibly structure #5 (and even part of structure #3?)

g)

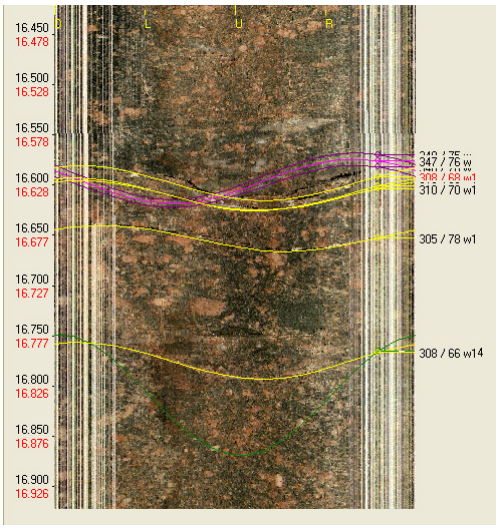

KI0014B01, open fractures

(marked as yellow lines):

borehole length: ~16.63 m (adj.length) orientation: ~309/69 (ÄSPÖ96),

borehole length: 16.68 m (adj.length), orientation: 305/78 (ÄSPÖ96),

borehole length: 16.80 m (adj.length), orientation: 308/66 (ÄSPÖ96),

possibly structure #5

h)

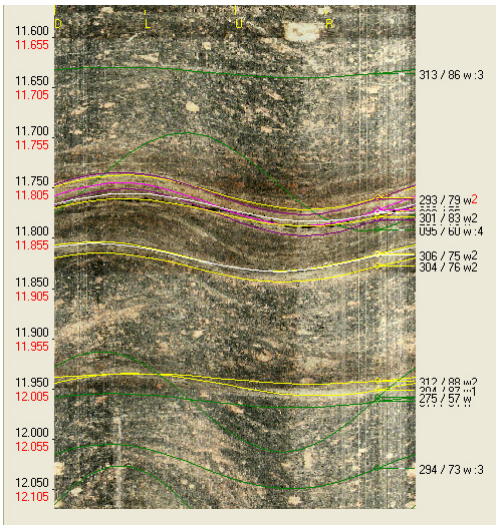

KI0016B01, open fractures

(marked as yellow lines):

borehole length: ~11.82 m (adj.length)
orientation: ~299/82 (ÄSPÖ96),

borehole length: 11.88 m (adj.length),
orientation: 305/75 (ÄSPÖ96),

borehole length: 12.00 m (adj.length),
orientation: 308/88 (ÄSPÖ96),

possibly structure #5 (and even part of structure #3?)

i)

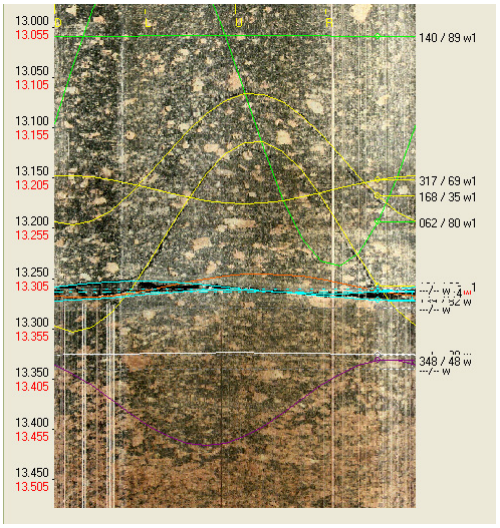

KI0016B01, crush zone

(marked as blue lines):

borehole length: 13.31 m (adj.length)
orientation: 310/89 (ÄSPÖ96),

probably structure #5

j)

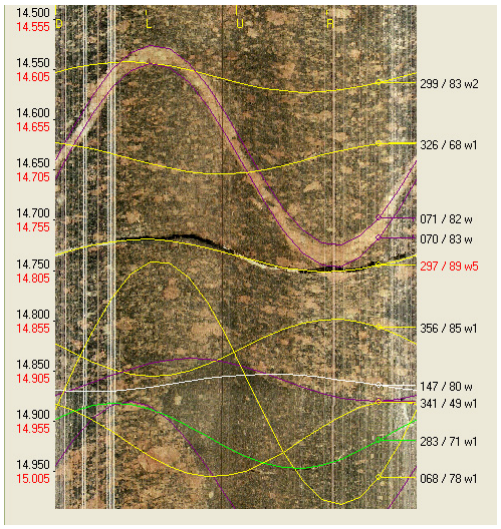

KI0016B01, open fracture

(marked as yellow line):

borehole length: 14.79 m (adj.length)
orientation: 297/89 (ÄSPÖ96),

possibly structure #5

k)

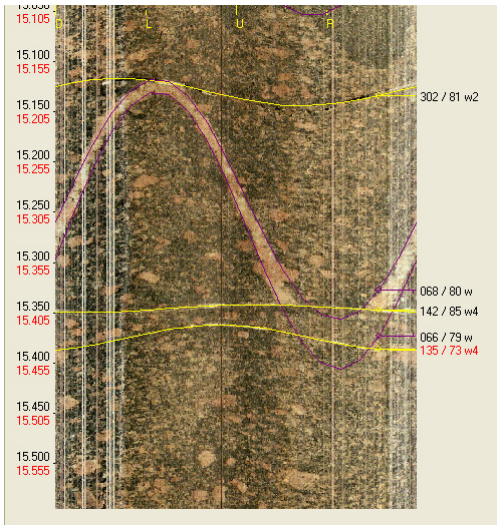

KI0016B01, open fractures

(marked as yellow lines):

borehole length: 15.19 m (adj.length)
orientation: 302/81 (ÄSPÖ96),

borehole length: 15.4 m (adj.length)
orientation: 142/85 (ÄSPÖ96),

borehole length: 15,43 m (adj.length)
orientation: 135/73 (ÄSPÖ96),

possibly structure #5

l)

Figure 6-2 a-l. *Possible intercepts of structure #5 and in some cases possibly structure #3 with boreholes KI0010B01, KI0014B01 and KI0016B01.* ***a-e)*** *KI0010B01, showing possible intercepts along adjusted lengths: 16.74-22.18 m, consisting of open fractures.* ***f-h)*** *KI0014B01, showing possible intercepts along adjusted lengths: 13.56-16.80 m, consisting of crush zones and open fractures.* ***i-l)*** *KI0016B01, showing possible intercepts along adjusted lengths: 11.82-15.43 m, consisting of open fractures and crush zones.*

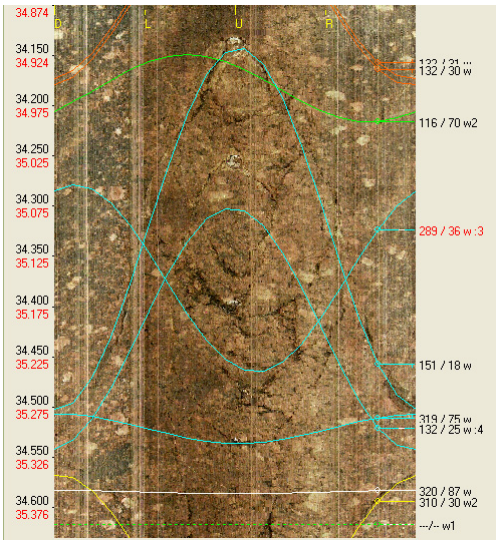

KI0010B01, crush zone

(marked as blue lines):

borehole length: 35.1-35.3 m (adj.length) orientation: 151/18 (ÄSPÖ96),

possibly part of structure #22 (and even part of structure #8?)

a)

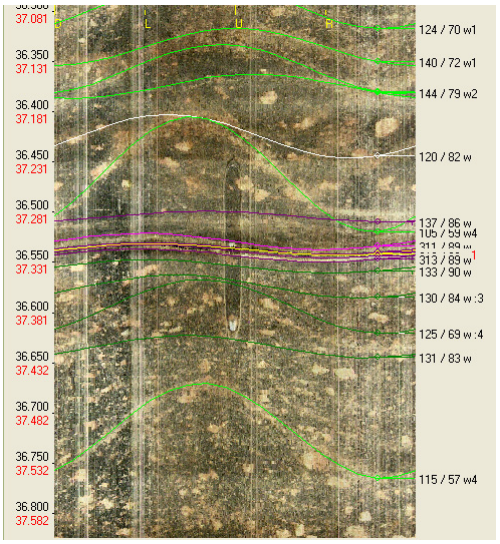

KI0010B01, open fracture

(marked as yellow line):

borehole length: 37.32 m (adj.length) orientation: 134/90 (ÄSPÖ96),

possibly part of structure #22 (and even part of structure #8?)

b)

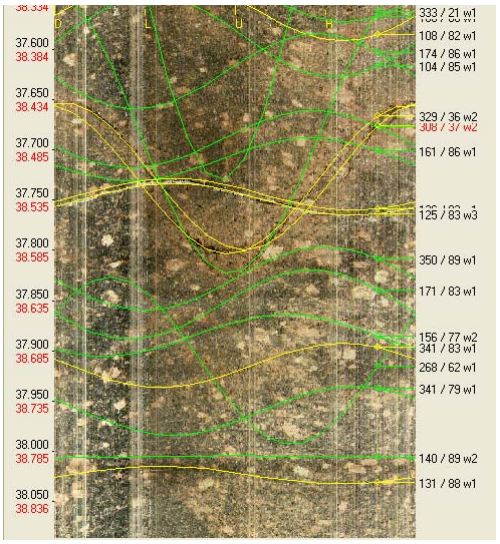

c)

KI0010B01, open fractures

(marked as yellow lines):

borehole length: 38.51 m (adj.length)
orientation: 319/37 (ÄSPÖ96),

borehole length: 38.53 m (adj.length)
orientation: 126/83 (ÄSPÖ96),

borehole length: 38.7 m (adj.length)
orientation: 341/83 (ÄSPÖ96),

borehole length: 38.81 m (adj.length)
orientation: 131/88 (ÄSPÖ96),

possibly part of structure #22 (and even part of structure #8?)

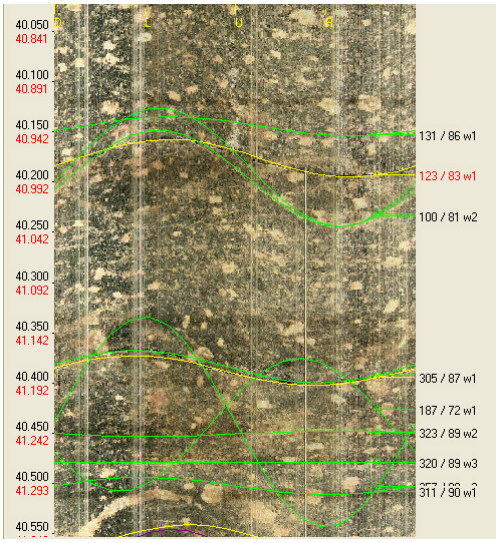

d)

KI0010B01, open fractures

(marked as yellow lines):

borehole length: 40.97 m (adj.length)
orientation: 123/83 (ÄSPÖ96),

borehole length: 41.18 m (adj.length)
orientation: 305/87 (ÄSPÖ96),

possibly part of structure #22 (and even part of structure #8?)

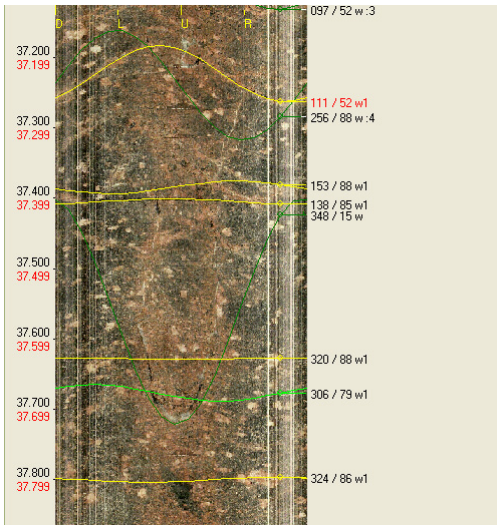

e)

KI0014B01, open fractures

(marked as yellow lines):

borehole length: 37.22 m (adj.length)
orientation: 111/52 (ÄSPÖ96),

borehole length: 37.38 m (adj.length)
orientation: 153/88 (ÄSPÖ96),

borehole length: 37.4 m (adj.length)
orientation: 138/85 (ÄSPÖ96),

borehole length: 37.63 m (adj.length)
orientation: 320/88 (ÄSPÖ96),

borehole length: 37.8 m (adj.length)
orientation: 324/86 (ÄSPÖ96),

possibly part of structure #22 (and even part of structure #8?)

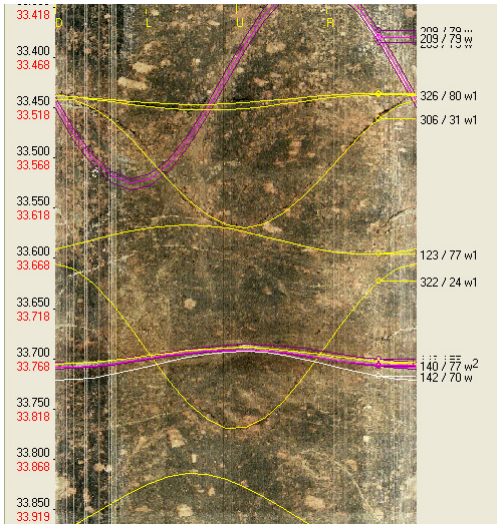

f)

KI0016B01, open fractures

(marked as yellow lines):

borehole length: 33.51 m (adj.length)
orientation: 326/82 (ÄSPÖ96),

borehole length: 33.57 m (adj.length)
orientation: 306/31 (ÄSPÖ96),

borehole length: 33.65 m (adj.length)
orientation: 123/77 (ÄSPÖ96),

borehole length: 33.76 m (adj.length)
orientation: 322/24 (ÄSPÖ96),

borehole length: 33.77 m (adj.length)
orientation: 141/79 (ÄSPÖ96),

possibly part of structure #22 (and even part of structure #8?)

Figure 6-3 a-f. *Possible intercepts of structure #22 and in some cases possibly structure #8 with boreholes KI0010B01, KI0014B01 and KI0016B01.* ***a-d)*** *KI0010B01, showing possible intercepts along adjusted lengths: 35.10-41.18 m, consisting of open fractures and a crush zone.* ***e)*** *KI0014B01, showing possible intercepts along adjusted lengths: 37.22-37.80 m, consisting of open fractures.* ***f)*** *KI0016B01, showing possible intercepts along adjusted lengths: 33.51-33.77 m, consisting of open fractures.*

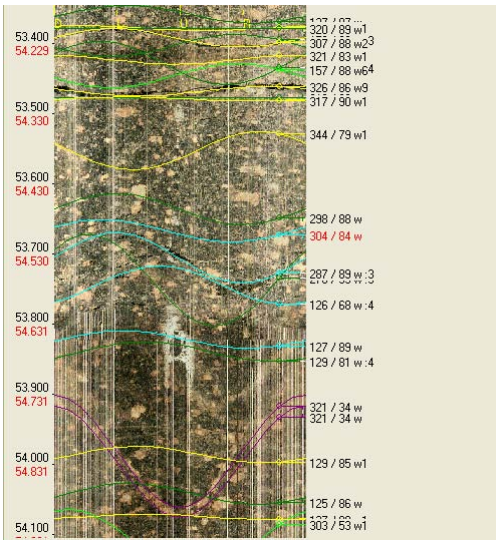

KI0010B01, open fracture

(marked as yellow line):

borehole length: 54.3 m (adj.length)
orientation: 326/86 (ÄSPÖ96),

crush zone (marked as blue line):
borehole length: 54.5-54.65 m (adj.length)

orientation: 304/84 (ÄSPÖ96),

possibly part of structure #7

a)

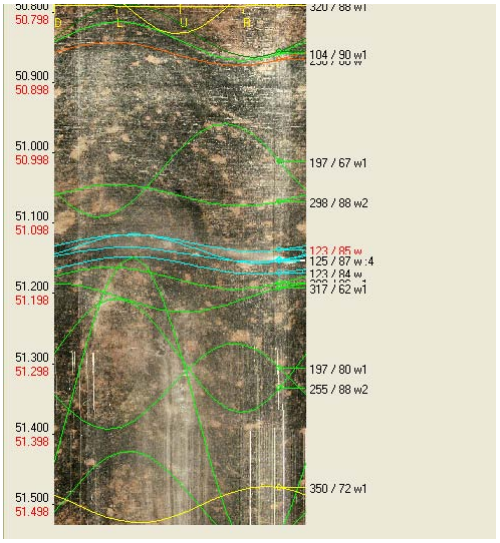

KI0014B01, crush zone

(marked as blue lines):

borehole length: 51.13-51.16 m (adj.length)

orientation: 123/85 (ÄSPÖ96),

possibly part of structure #7

b)

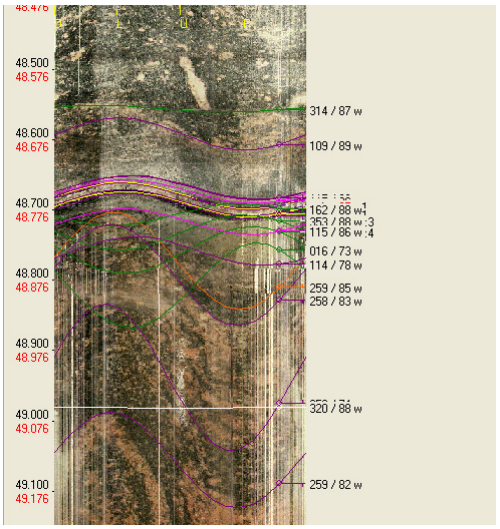

KI0016B01, open fractures

(marked as yellow lines):

borehole length: 48.76m (adj.length)

orientation: 113/87 (ÄSPÖ96),

borehole length: 48.77m (adj.length)

orientation: 114/87 (ÄSPÖ96),

possibly part of structure #7

c)

Figure 6-4 a-c. *Possible intercepts of structure #7 with boreholes KI0010B01, KI0014B01 and KI0016B01.* ***a)*** *KI0010B01, showing possible intercepts along adjusted lengths: 54.30-54.65 m, consisting of open fractures and a crush zone.* ***b)*** *KI0014B01, showing possible intercepts along adjusted lengths: 51.13-51.16 m, consisting of a crush zone.* ***c)*** *KI0016B01, showing possible intercepts along adjusted lengths: 48.76-48.77 m, consisting of open fractures.*

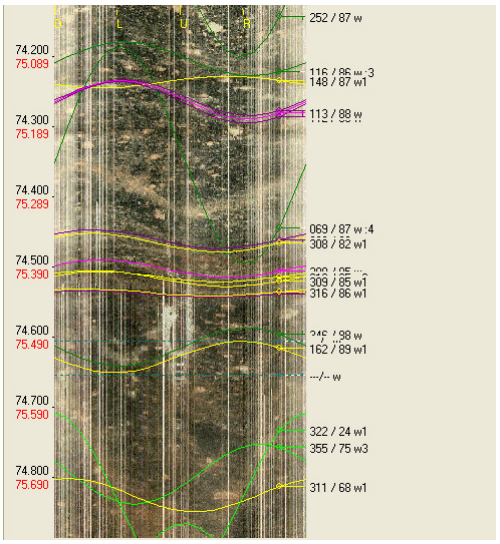

a)

KI0010B01, open fractures

(marked as yellow lines):

borehole length: 75.13 m (adj.length)
orientation: 148/87 (ÄSPÖ96),

borehole length: 75.35m (adj.length)
orientation: 308/82 (ÄSPÖ96),

borehole length: ~75.41 m (adj.length)
orientation: ~313/85 (ÄSPÖ96),

borehole length: 75.52 m (adj.length)
orientation: 162/89 (ÄSPÖ96),

borehole length: 75.72 m (adj.length)
orientation: 311/68 (ÄSPÖ96),

possibly part of structure #20

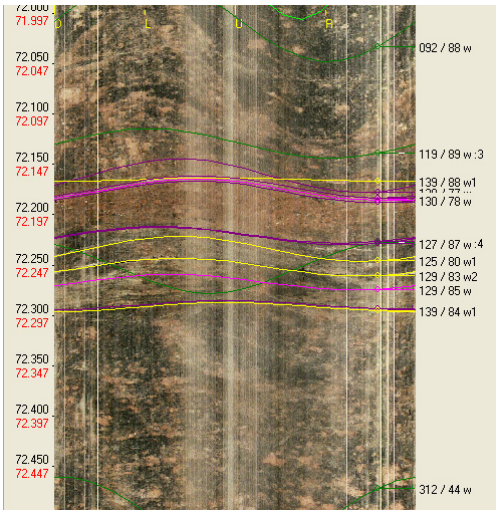

b)

KI0014B01, open fractures

(marked as yellow lines):

borehole length: 72.16 m (adj.length)
orientation: 139/88 (ÄSPÖ96),

borehole length: 72.23 m (adj.length)
orientation: 125/80 (ÄSPÖ96),

borehole length: 72.25 m (adj.length)
orientation: 129/83 (ÄSPÖ96),

borehole length: 72.29 m (adj.length)
orientation: 139/84 (ÄSPÖ96),

possibly part of structure #20

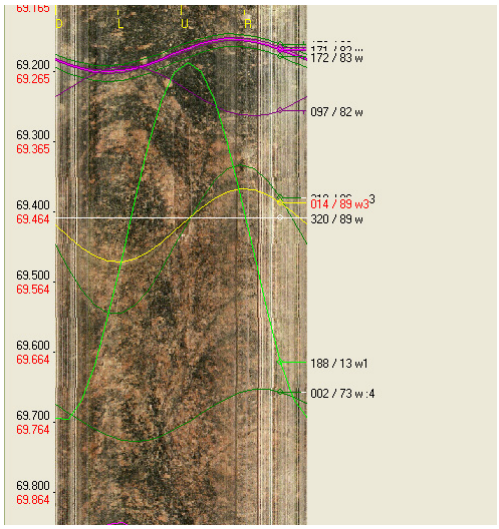

KI0016B01, open fracture

(marked as yellow line):

borehole length: 69.48 m (adj.length)
orientation: 14/90 (ÄSPÖ96),

possibly part of structure #20

c)

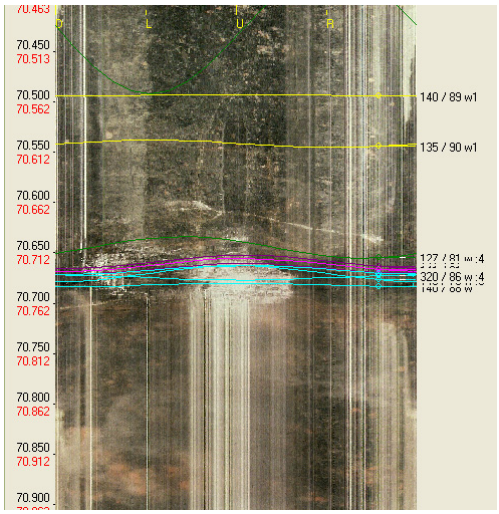

KI0016B01, crush zone

(marked as blue lines):

borehole length: 70.73-70.74 m (adj.length)

orientation: 141/84 (ÄSPÖ96),

possibly part of structure #20

d)

Figure 6-5 a-d. *Possible intercepts of structure #20 with boreholes KI0010B01, KI0014B01 and KI0016B01.* ***a)*** *KI0010B01, showing possible intercepts along adjusted lengths: 75.13-75.72 m, consisting of open fractures.* ***b)*** *KI0014B01, showing possible intercepts along adjusted lengths: 72.16-72.29 m, consisting of open fractures.* ***c-d)*** *KI0016B01, showing possible intercepts along adjusted lengths: 69.48-70.74 m, consisting of open fractures and a crush zone.*

The possible intercepts of the various structures is limited to open fractures and crush zones, except for structure #3 which is interpreted as part of cataclastic bands mapped in the boreholes (Figure 6-2a, f, i and Table 6-1).

Some of the structures in the BIPS images show features that are interpreted as indications that they yield water, in Figure 6-2 g the number of impurities on the lower side of the camera glass decreases up hole from a crush zone indicating that water comes into the hole there, the same occurs to a lesser extent in Figure 6-2 h and also in Figure 6-2 j. In Figure 6-3 b a pattern occurs that could be interpreted as a bubble at the upper side of the protective glass of the BIPS camera, indicating that water flows into the hole. In Figure 6-4 a this pattern of bubbles at upper side of BIPS camera as well as decreased amount of impurities on the protective glass indicate that water comes into the hole, the same seems to be the case in Figure 6-4 b and to a smaller extend in 6-4 c. The pattern in Figure 6-5 a is of the same kind and especially in Figure 6-5 d, where the BIPS image shows mud in suspension below the suspected water yielding crush zone.

Table 6-1. Interpreted intercepts of structure #3 with boreholes.

Borehole ID	Adj.length (m)	Type of structures	Figure ID
KI0010B01	16.7-16.9	Cataclastic band	6-2 a
KI0014B01	13.6-13.8	Cataclastic bands	6-2 f
KI0016B01	11.8-12.0	Cataclastic bands	6-2 i

Table 6-2. Interpreted intercepts of structure #5 with boreholes.

Borehole ID	Adj.length (m)	Type of structures	Figure ID
KI0010B01	16.7-22.2	Open fractures	6-2 a-e
KI0014B01	13.6-16.8	Crush zone & open fractures	6-2 f-h
KI0016B01	11.8-15.4	Open fractures & crush zone	6-2 i-l

Table 6-3. Interpreted intercepts of structure #22 (and possibly structure #8) with boreholes.

Borehole ID	Adj.length (m)	Type of structures	Figure ID
KI0010B01	35.1-41.2	Open fractures & crush zone	6-3 a-d
KI0014B01	37.2-37.8	Open fractures	6-3 e
KI0016B01	33.5-33.8	Open fractures	6-3 f

Table 6-4. Interpreted intercepts of structure #7 with boreholes.

Borehole ID	Adj.length (m)	Type of structures	Figure ID
KI0010B01	54.3-54.7	Open fractures & crush zone	6-4 a
KI0014B01	51.1-51.2	Crush zone	6-4 b
KI0016B01	48.8	Open fractures	6-4 c

Table 6-5. .Interpreted intercepts of structure #20 with boreholes.

Borehole ID	Adj.length (m)	Type of structures	Figure ID
KI0010B01	75.1-75.7	Open fractures	6-5 a
KI0014B01	72.2-72.3	Open fractures	6-5 b
KI0016B01	69.5-70.7	Open fractures & crush zone	6-5 c-d

6.2 Predictions and outcome based on hydro-geological responses

One way to verify the intercepts with the TRUE Block Scale structures in the boreholes KI0010B01, KI0014B01, and KI0016B01 is to evaluate the groundwater pressure interferences in the structures due to the drilling of the boreholes. Borehole sections in the True Block Scale area that are known to contain the TRUE Block Scale structures #3, #5, and #7 (Andersson et al. 2007) were analysed. For location of the structures see Figure 6-1.

The observed pressure responses were evaluated in terms of normalised drawdown, s/Q, where s is the drawdown due to drilling through the structure and Q is the estimated outflow from the structure. The responses were classified according to the class limits applied by Andersson et al. (2007) for the TRUE BS structures (TR-06-42):

$s/Q > 1 \cdot 10^5$ s/m^2 Excellent (Red)
$3 \cdot 10^4 < s/Q \leq 1 \cdot 10^5$ s/m^2 High (Yellow)
$1 \cdot 10^4 < s/Q \leq 3 \cdot 10^4$ s/m^2 Medium (Green)
$s/Q \leq 1 \cdot 10^4$ s/m^2 Low (Blue)

The result for structure #3 was unclear since this structure was present only in one observation section (KA3510A:5). The drilling of KI0010B01 caused no drawdown but only some noise in the pressure signal, and for KI0014B01 and KI0016B01 the response in the possible structure #3 could not be separated from structure #5. The responses in structure #5 and #7 were generally fast and clear (Tables 6-6 and 6-7). For most sections the pressure response was classified as Excellent or High. It can thus be assumed that the interpreted intercepts in the boreholes KI0010B01, KI0014B01, and KI0016B01 have a distinct hydraulic connection to the structures #5 and #7, respectively.

See also chapter 5.7 for further attempts to identify possible TRUE-structures.

Table 6-6. Groundwater pressure responses in structure #5 due to drilling. Colour code for response: Red = Excellent, Yellow = High, Green = Medium, Blue = Low, Gray = No response.

Borehole ID	Interpreted intercept (m)	Drilling secup (m)	Drilling seclow (m)	Drilling start	Drilling stop	Normalised drawdown s/Q (s/m^2)			
						KA3510A:5 (4.5–50 m)	KI0023B:9 (4.6–40.45 m)	KI0025F:6 (5–41.5 m)	KI0025F02:10 (3.4–55.1 m)
KI0010B01	16.7–22.2	14.27	23.35	2007-04-12 14:42	2007-04-13 11:05	$3.4{\cdot}10^5$	$3.4{\cdot}10^5$	$5.2{\cdot}10^4$	$5.4{\cdot}10^4$
KI0014B01	13.6–16.8	13.37	17.50	2007-06-14 12:50	2007-06-14 16:40	$7.0{\cdot}10^4$	$7.2{\cdot}10^4$	n/a	$9.6{\cdot}10^3$
KI0016B01	11.8–15.4	11.52	17.13	2007-06-02 15:15	2007-06-02 17:45	$4.1{\cdot}10^5$	$3.9{\cdot}10^5$	$8.5{\cdot}10^4$	$6.7{\cdot}10^4$

Table 6-7. Groundwater pressure responses in structure #7 due to drilling. Colour code for response: Red = Excellent, Yellow = High, Green = Medium, Blue = Low, Gray = No response.

Borehole ID	Interpreted intercept (m)	Drilling secup (m)	Drilling seclow (m)	Drilling start	Drilling stop	Normalised drawdown s/Q (s/m^2)				
						KA2511A:8 (6-64 m)	KA2563A:5 (146-186)	KI0023B:8 (41.45-42.45	KI0025F:5 (42.5-86.5)	KI0025F02:10 (3.4-55.1 m)
KI0010B01	54.3–54.7	53.01	56.05	2007-04-16 10:46	2007-04-16 11:15	$9{,}4{\cdot}10^4$	$6{,}9{\cdot}10^4$	$9{,}4{\cdot}10^4$	$1{,}1{\cdot}10^5$	$1{,}2{\cdot}10^5$
KI0014B01	51.1–51.2	49.96	53.01	2007-06-16 09:30	2007-06-16 10:10	$4{,}0{\cdot}10^4$	$3{,}4{\cdot}10^4$	$7{,}3{\cdot}10^4$	$6{,}4{\cdot}10^4$	$6{,}3{\cdot}10^4$
KI0016B01	48.8	47.55	49.23	2007-06-05 11:06	2007-06-05 11:36	$3{,}2{\cdot}10^4$	$2{,}5{\cdot}10^4$	$4{,}1{\cdot}10^4$	$4{,}1{\cdot}10^4$	$4{,}1{\cdot}10^4$

7 Concluding remarks

One of the risks with the choice of location for the new tunnel (TASS) was the proximity to the True Block Scale Experiment site, TASI. Since this experiment had introduced minor amount of radioactive nuclides there was a risk that the site could be contaminated. Although this possibility was quite small no risks could be taken to expose the staff to any remaining radioactivity. Nor was it acceptable to pollute the tunnel water with radioactive substances. The checks that were performed did not interfere too much on the regular work at the site. Eventually it could be shown that the area was free of radioactive nuclides and thus this issue was not an obstacle for the new tunnel.

Due to the expected high ground water pressures a sturdy casing had to be installed in the outer end (approximately two meters) of the boreholes. Outside the boreholes the casing was equipped with valves that could be opened and closed depending on the situation. It was experienced that the casing worked well during the drilling and the period after. Before the the blasting of the new tunnel begun the casing of the boreholes had to be removed and the holes sealed with grout.

The core drilling went well. When the drilling of first borehole (KI0010B01) was completed the drillrigg was moved to be used at another location in the Äspö HRL while preparations for the next hole were going on. Unfortunately the rig was delayed at the alternative location and a new one had to be brought down to the -450 m level to drill the next two boreholes there.

The core logging with Boremap combined with a BIPS-image gives very good results. By plotting the logging with the help of the software WellCAD good illustrations and summaries of the core logging has been obtained. The cores did not contain any major zones of deformation and the rock can be regarded as normal according to Äspö HRL standards. The fracture frequency in the cores varied between 2.2-3.5/m (open fractures) and 2.2-5.7/m (healed fractures). The location of known major deformation zones such as the NE-2 had been checked already before the pre-investigation started and were regarded to be at a safe distance (100-150 m) from the tunnel entrance and thus not expected to be found in the cores.

Software from RockWare was used to plot the orientations of planar structures in stereograms. It is interesting to see that the orientations of fractures follow the common pattern at Äspö HRL where most fractures strike NW and dip steeply to the NE or SW. This means that the TASS-tunnel will be excavated at a large angle to the dominating fracture orientation which normally is regarded as favourable.

The pressure measurements that were performed in the boreholes showed that there were structures connecting the holes. For example borehole KI0016B01 was draining KI0010B01 via what was interpreted as structure #5 in the TRUE Block Scale Experiment. The measured full borehole water pressure in borehole KI0010B01 was almost 3.5 MPa before KI0016B01 was drilled but dropped to about 0.5 MPa afterwards when the latter was kept open. The increasing pressure in the Prototype repository while drilling e.g. KI0016B01 was an indication too that there was a connection between the boreholes and the surrounding areas.

The tests on water inflow, pressure etc were used to make interpretations on where TRUE Block Scale Experiment structures might intersect the new boreholes. It was concluded that structures #5, #7, #8, #20 and #22 could be identified through the hydraulic tests. An attempt was made to identify the same structures in the drill cores. Open fractures and minor crush zones in the cores were interpreted to represent the five True Block Scale structures and in addition possibly True Block Scale structure #3. Some of the structures in the boreholes appeared in the BIPS-images to be water bearing.

It should, however, be remembered that each of the water bearing structures that have been identified in the True Block Scale Experiment most probably does not represent just a single plane but a number of sub-parallel planes between which the water migrates.

7.1 Conclusion

It is the authors' opinion that the various tests that have been presented in this report have verified that the choice of location for the TASS-tunnel is suitable for the project Sealing of tunnel at great depth. All the requirements that were listed in chapter 1.2 have been regarded to be fulfilled:

1. No known major deformation zones such as NE-2 is found in the vicinity of the planned TASS-tunnel
2. Each of the test holes were drilled to a length/depth of approximately 100 m
3. The core logging showed that the fracture frequency exceeded the requirement of 1-2 fractures/m
4. The main orientation of the fractures is at a large angle (almost perpendicular) to the planned tunnel
5. A large number of the fractures have hydraulic apertures between 10-300 μm
6. The ground water pressure was, in spite of the trouble to measure it, considered to have fulfilled the requirements (30-35 bar measured over the full length of a borehole.

Acknowledgements

Johan Berglund (Vattenfall Power Consultans AB) who consentrated on geological matters and Mansueto Morosini (SKB) who consentrated on hydro-geological matters are greatly acknowledged for their critical review of the report.

References

Andersson, P., Byegård, J., Dershowitz, B., Doe, T., Hermanson, J., Meier, P., Tullborg, E-L., and Winberg, A. (ed) 2002a: Final report of the TRUE Block Scale project. 1 Characterisation and model development (SKB TR-02-13)

Andersson, P., Byegård, J. and Winberg, A. 2002b: Final report of the TRUE Block Scale project. 2 Tracer tests in the block scale (SKB TR-02-14)

Andersson, P., Byegård, J., Billaux, D., Cvetkovic, V., Dershowitz, W., Doe, T., Hermanson, J., Poteri, A., Tullborg, E.-L. and Winberg, A. 2007: TRUE Block Scale Continuation Project. Final report. (SKB TR-06-42)

Fransson, Å. 2001: Characterisation of fractured rock for grouting using hydrogeological methods. Chalmers Tekniska Högskola (Chalmers University of Technology)

Grahn, R. and Jansson, P-Å. 1997: Mekanik: statik och dynamik. Studentlitteratur, Lund, 1997

Gustafson, G. 2009: Hydrogeologi för bergbyggare. Forskningsrådet för miljö, areella näringar och samhällsbyggande (Formas), Stockholm.

Gustafsson, J and Gustafsson, Ch. 2005: Oskarshamn site investigation. RAMAC and BIPS logging in boreholes KLX07A, KLX07B, HLX34 and HLX35 and deviation logging in boreholes KLX07B, HLX34 and HLX35 (SKB P-05-231, 2005)

Moye, D.G. 1967: Diamond Drilling for Foundation Exploration. Civil Engineering Transactions, 1967. **April**: p. 95-100

Snow, D.T. **1968:** Rock fracture spacings, openings, and porosities. Journal of the Soil Mechanics and Foundation Division, 1968. 94: p. 73-91

Thiem, G. 1906: Hydrologische Metoden. Gebhardt, Leipzig, 1906

Zimmerman, R.W. and Bodvarsson, G.S. 1996: Hydraulic conductivity of rock fractures. Transport in Porous Media, 1996. 23(1): p. 1-30

Appendices

Appendix 1

Design and modified design of the casing by Rickard Bäck, SKB
All sketches drawn by Christer Solberg, Elajo Mekanik
Components partially from the "shelf" and partially manufactured by Elajo Mekanik
All parts of the casing was assembled by SKB

- A: Principle sketch of the casing for the boreholes KI0010B01, KI0014B01 and KI0016B01
- B: Casing detail, principle sketch
- C: Casing detail, T-piece, principle sketch

Appendix 2

- A: Geology in KI0010B01; core log
- B: The BIPS image of borehole KI0010B01
- C: Stereonets & rose-diagrams of all logged fractures, all open fractures, all closed fractures, sealed networks and cataclastic structures in borehole KI0010B01

Appendix 3

- A: Geology in KI0014B01; core log
- B: The BIPS image of borehole KI0014B01
- C: Stereonets & rose-diagrams of all logged fractures, all open fractures, all closed fractures, sealed networks and cataclastic structures in borehole KI0014B01

Appendix 4

- A: Geology in KI0016B01; core log
- B: The BIPS image of borehole KI0016B01
- C: Stereonets & rose-diagrams of all logged fractures, all open fractures, all closed fractures, sealed networks and cataclastic structures in borehole KI0016B01

Appendix 5

Graphs showing the results of the PFL difference flow logging (created by Posiva Oy/PRG-Tec Oy):

KI0010B01.1.1-5 Flow rate and single point resistance

KI0010B01.2.1 Electric conductivity of borehole water

KI0010B01.2.2 Temperature of borehole water

KI0010B01.3 Flow rate out from the borehole during flow logging

Appendix 6

Tables and diagrams referring to the the hydro-geological diagrams in chapter 5

- A: KI0010B01: Transmissivities in sections - tests during drilling (see Figure 5-10)
- B: KI0010B01: Transmissivities in 3 m sections based on Double packer tests (see Figure 5-13)
- C: KI0010B01: Transmissivities based on PFL-anomalies (see Figure 5-16)
- D: KI0014B01: Transmissivities in sections - tests during drilling (see Figure 5-11
- E: KI0014B01: Transmissivities in 3 m sections based on Double packer tests (see Figure 5-14)
- F: KI0016B01: Transmissivities in sections - tests during drilling (see Figure 5-12)
- G: KI0016B01: Transmissivities in 3 m sections based on Double packer tests (see Figure 5-15)

Appendix 1 A

Principle sketch of the casing for the boreholes KI0010B01, KI0014B01 and KI0016B01

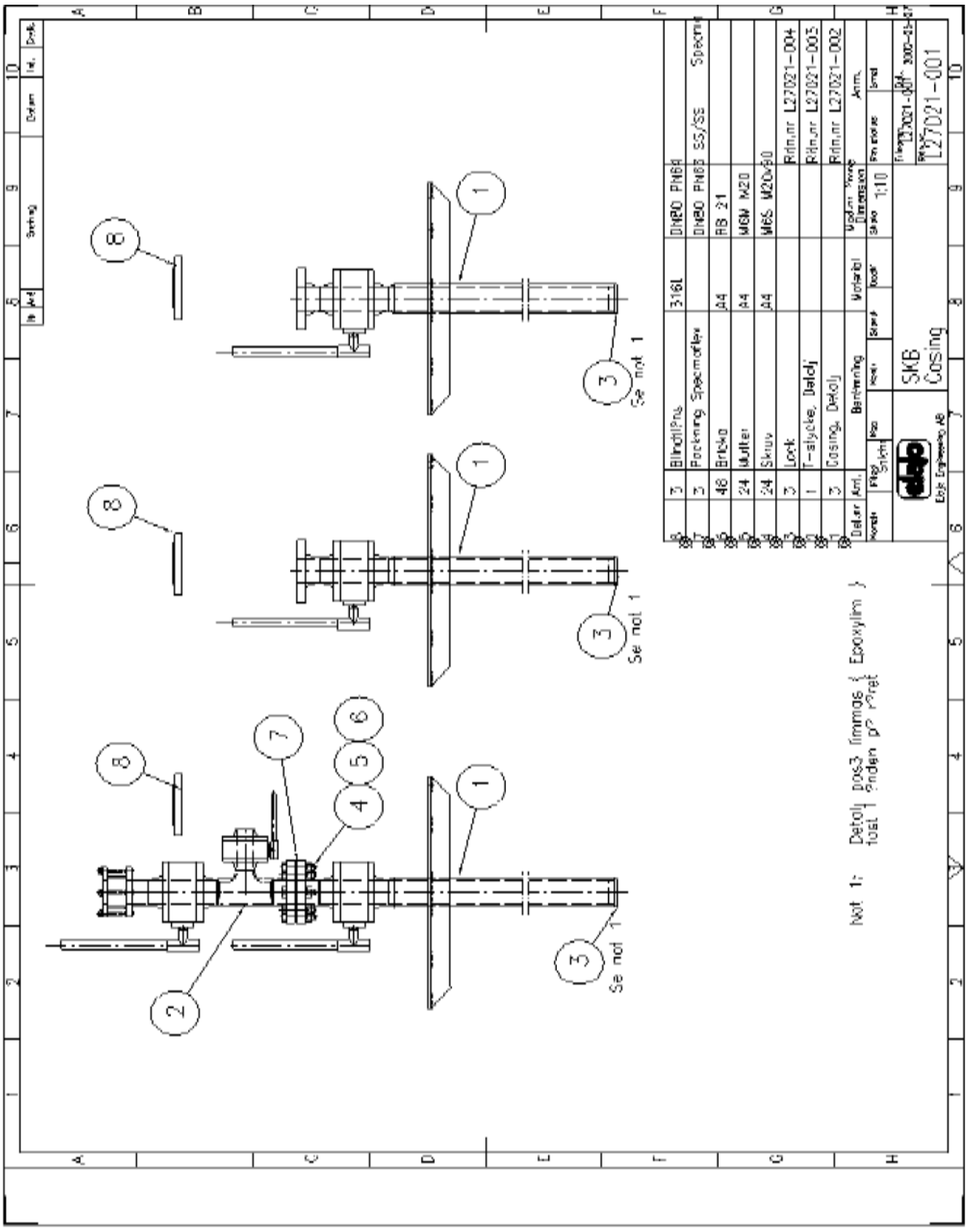

Appendix 1 B

Casing detail, principle sketch

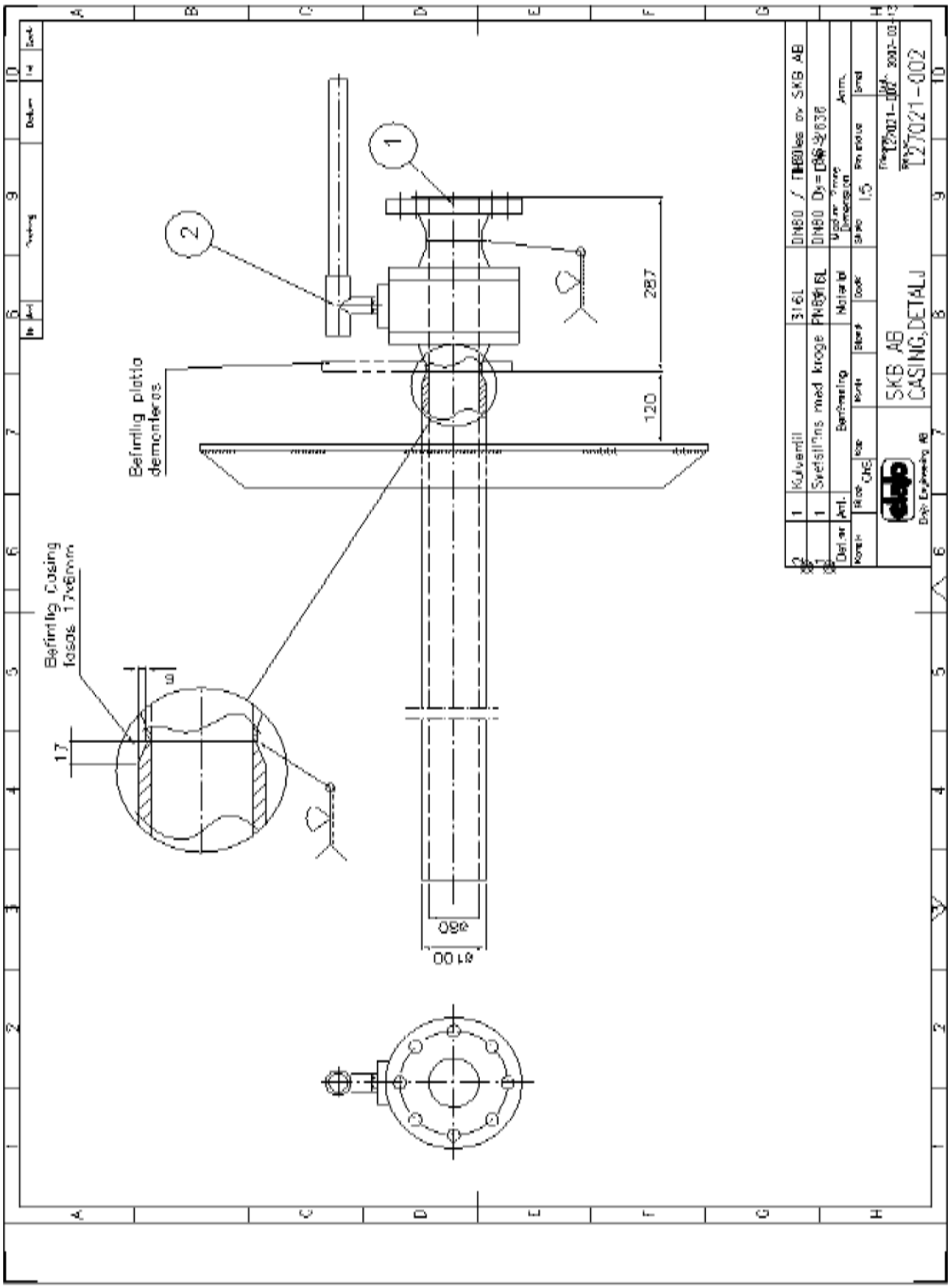

Appendix 1 C

Casing detail, "T-piece"

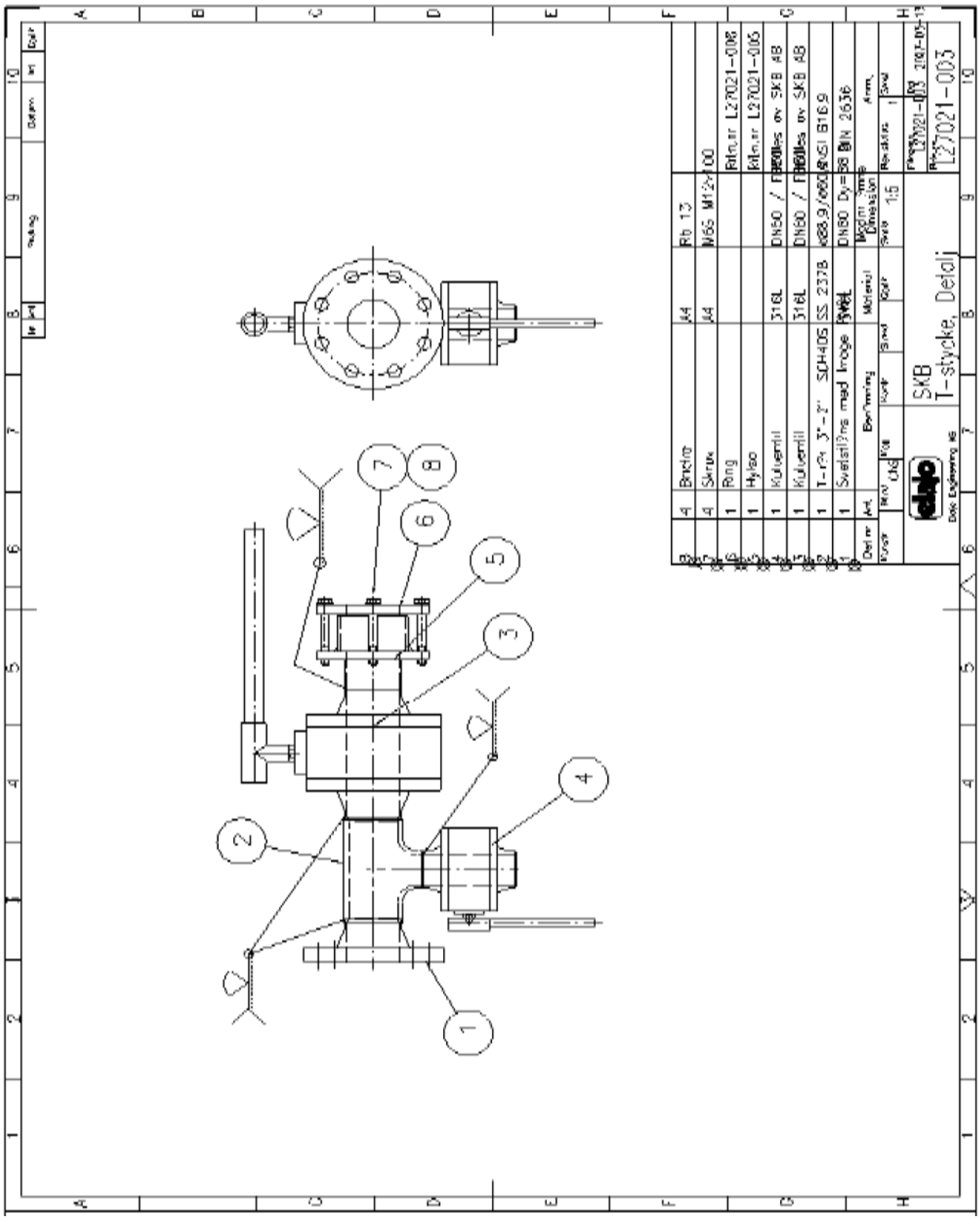

Appendix 2 A

Geology in KI0010B01; core log

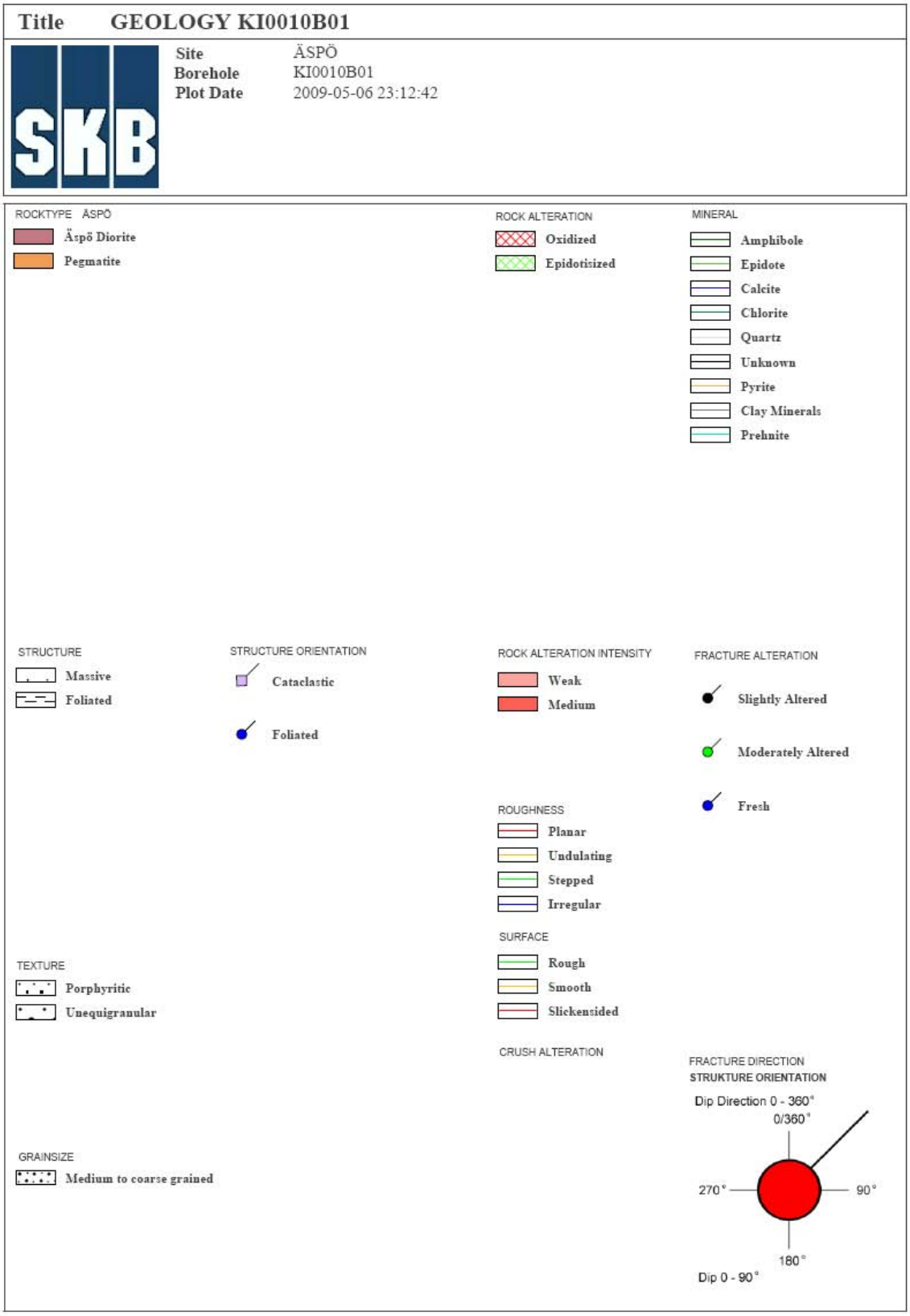

Title GEOLOGY IN KI0010B01 **Appendix: 2A**

Site	ÄSPÖ	**Coordinate System**	ÄSPÖ96
Borehole	KI0010B01	**Northing [m]**	7254.30
Diameter [mm]	76	**Easting [m]**	1954.09
Length [m]	100.640	**Elevation [m.a.s.l.]**	-446.00
Bearing [°]	229.84	**Drilling Start Date**	2007-03-12 10:10:00
Inclination [°]	-0.54	**Drilling Stop Date**	2007-03-12 15:30:00
Date of coremapping	2007-05-05 11:37:00	**Plot Date**	2007-11-13 22:03:06
Rocktype data from	p_rock	**Signed data**	

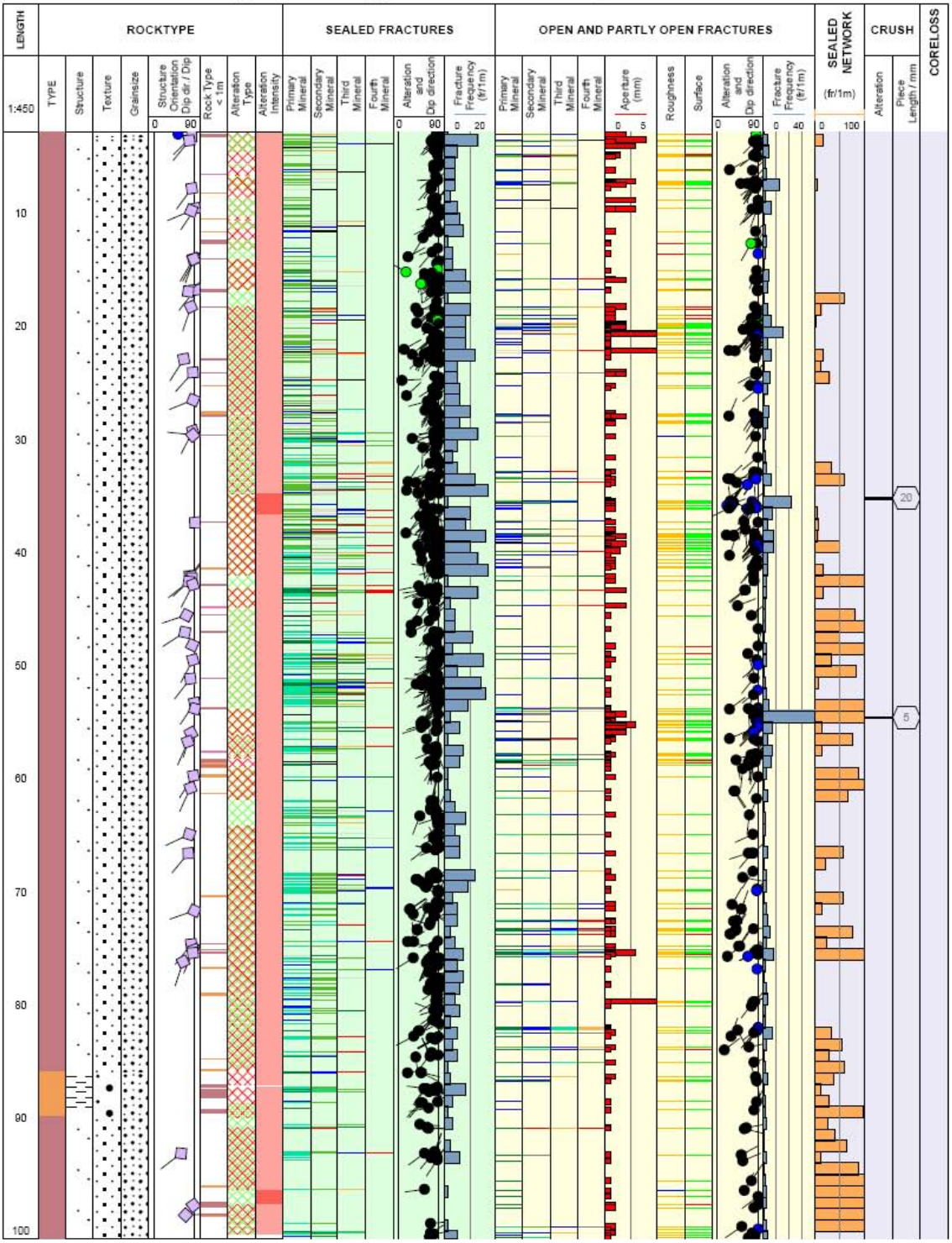

Appendix 2 B

The BIPS image of borehole KI0010B01

Project name: ÄSPÖ HRL

Image file	: c:\work\r56xxs~2\data\ki0010~2.bip
BDT file	:
Locality	: ASPO HRL
Bore hole number	: KI010B01
Date	: 07/04/26
Time	: 10:11:00
Depth range	: 2.045 - 99.400 m
Azimuth	: 0
Inclination	: -90
Diameter	: 76.0 mm
Magnetic declination	: 0.0
Span	: 4
Scan interval	: 0.25
Scan direction	: To entrance
Scale	: 1/25
Aspect ratio	: 175 %
Pages	: 5
Color	: +0 +0 +0

Project name: ÄSPÖ HRL
Bore hole No.: KI010B01 Azimuth: 0 Inclination: -90

Depth range: 0.000 - 20.000 m

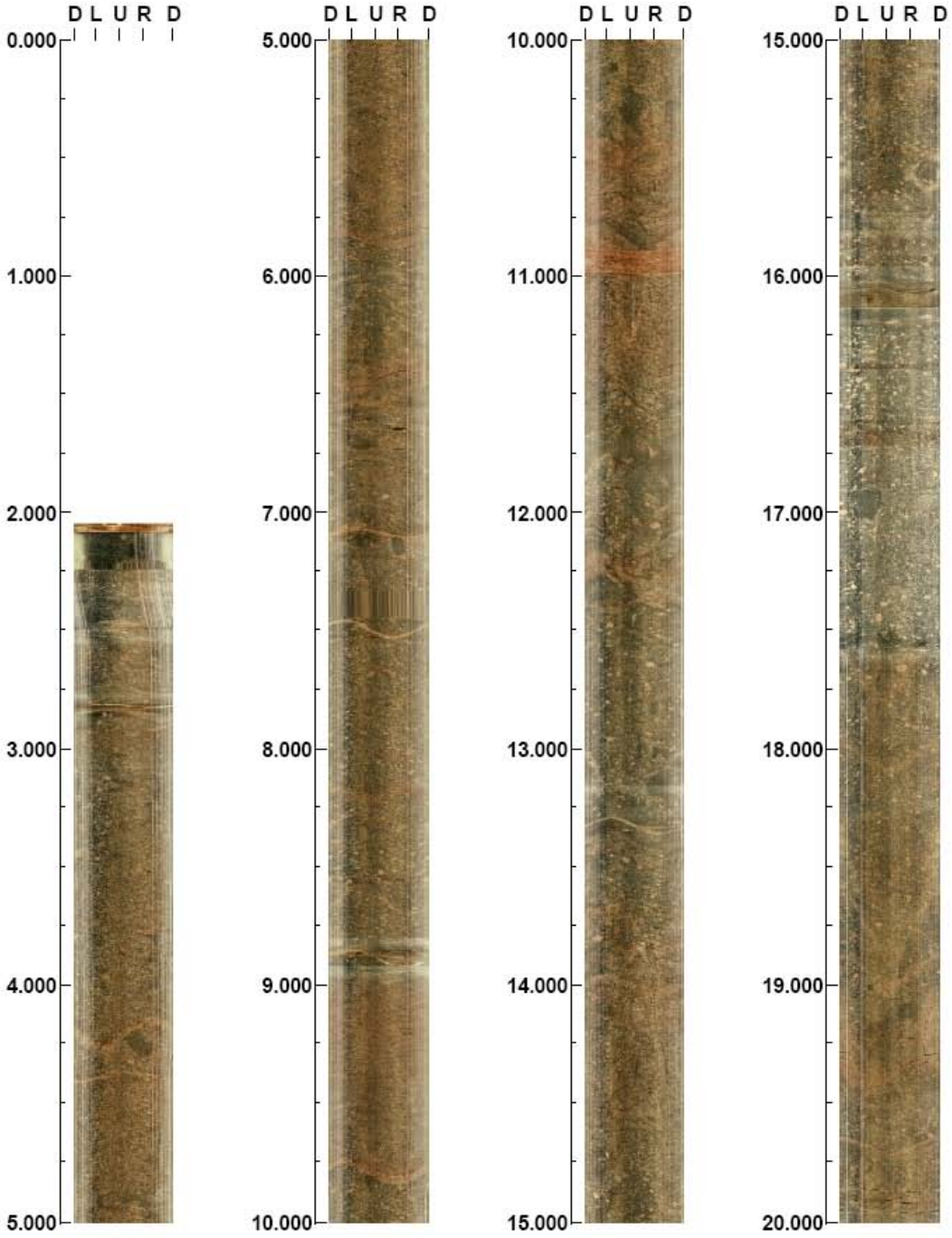

(1 / 5) Scale: 1/25 Aspect ratio: 175 %

Project name: ÄSPÖ HRL
Bore hole No.: KI010B01 Azimuth: 0 Inclination: -90

Depth range: 20.000 - 40.000 m

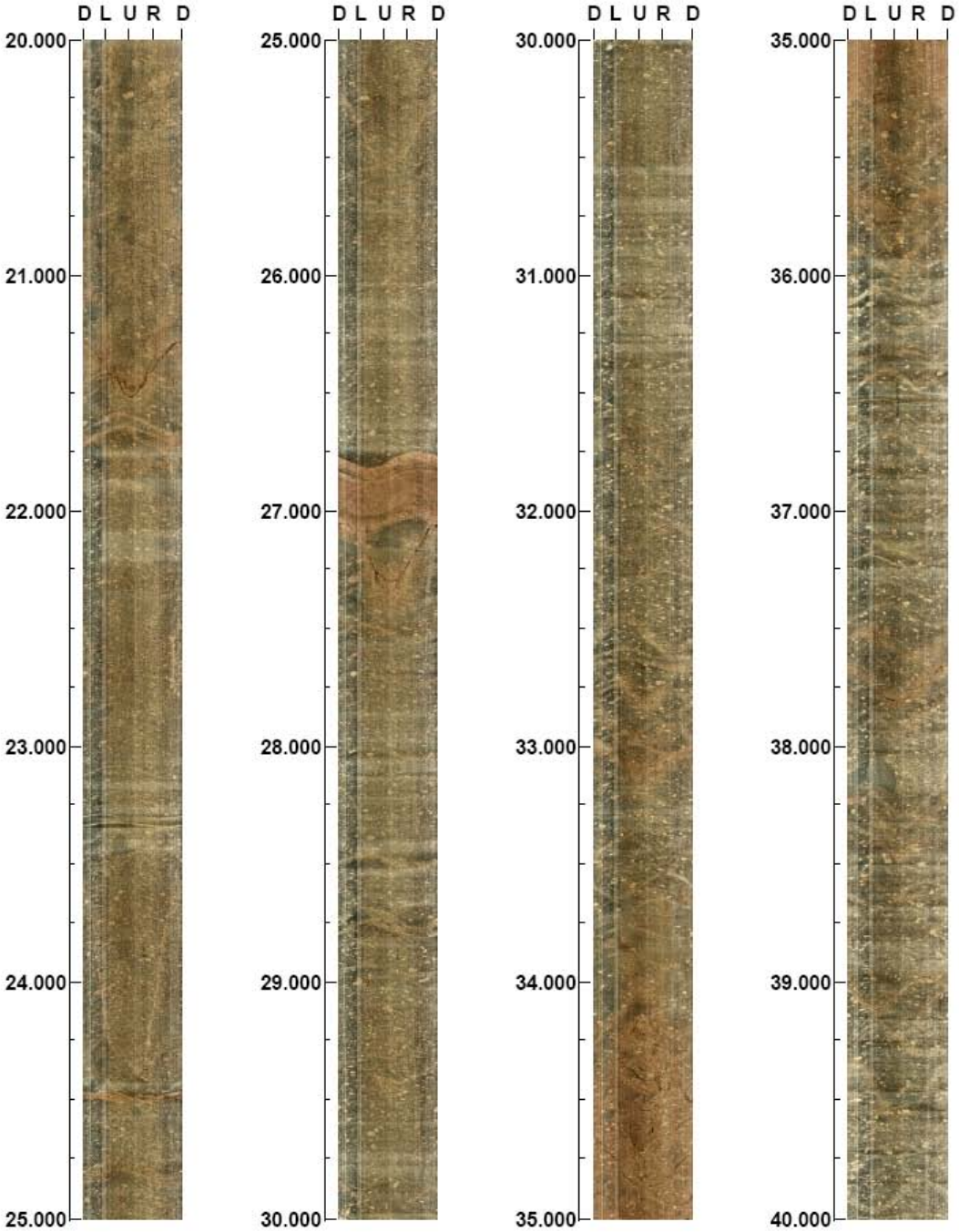

(2 / 5) Scale: 1/25 Aspect ratio: 175 %

Project name: ÄSPÖ HRL
Bore hole No.: KI010B01 **Azimuth: 0** **Inclination: -90**

Depth range: 40.000 - 60.000 m

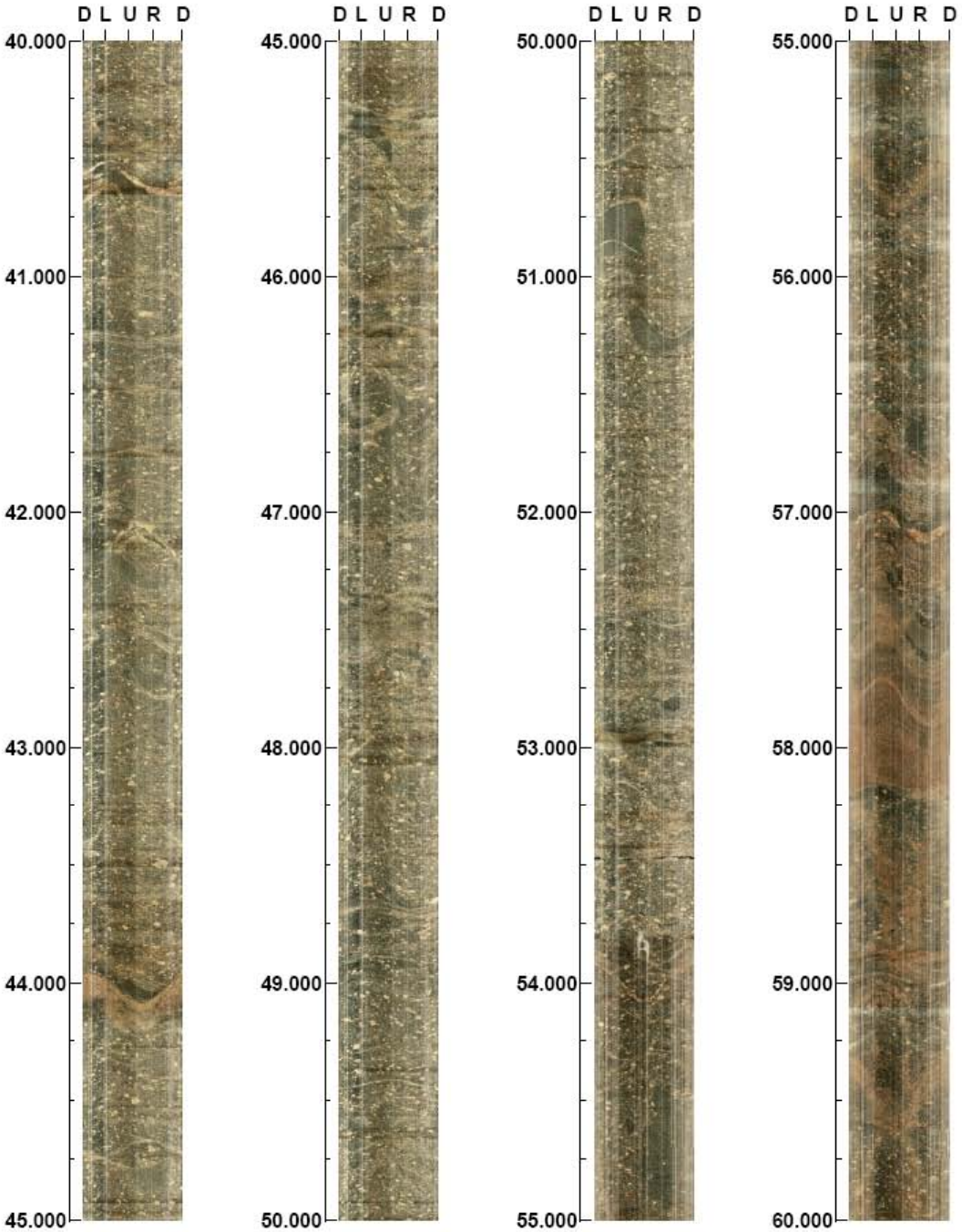

(3 / 5) **Scale: 1/25** **Aspect ratio: 175 %**

Project name: ÄSPÖ HRL
Bore hole No.: KI010B01 Azimuth: 0 Inclination: -90

Depth range: 60.000 - 80.000 m

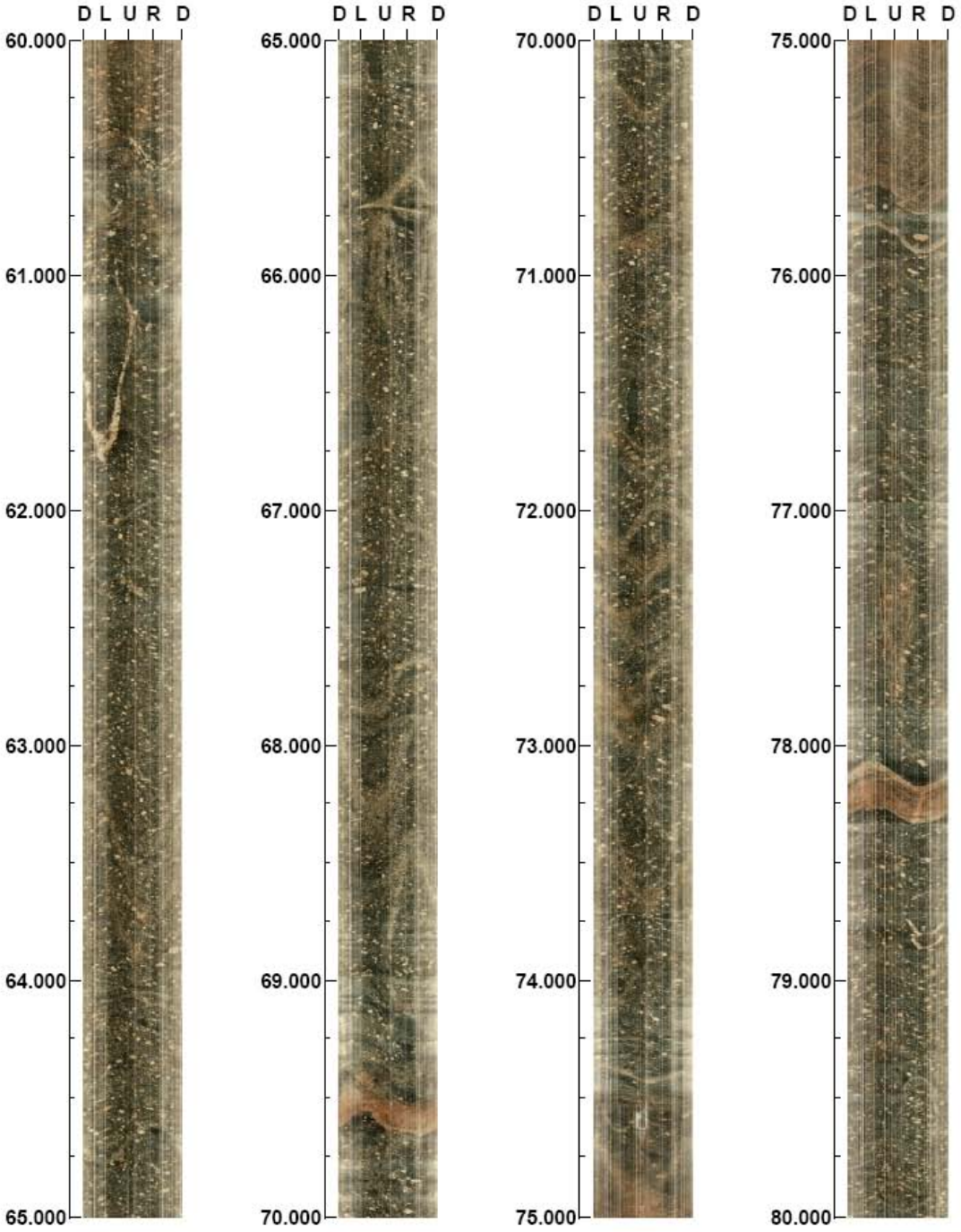

(4 / 5) Scale: 1/25 Aspect ratio: 175 %

Project name: ÄSPÖ HRL
Bore hole No.: KI010B01 Azimuth: 0 Inclination: -90

Depth range: 80.000 - 99.400 m

(5 / 5) Scale: 1/25 Aspect ratio: 175 %

Appendix 2 C

Stereonets & rose-diagrams of all logged fractures, all open fractures, all closed fractures, sealed networks and cataclastic structures in borehole KI0010B01

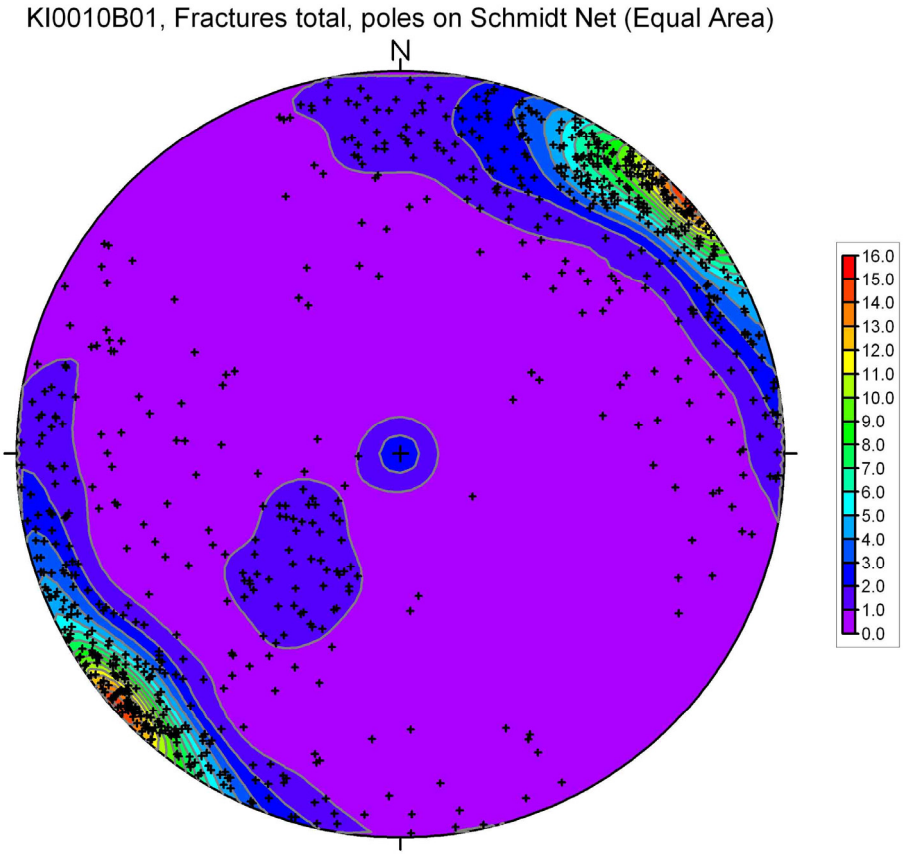

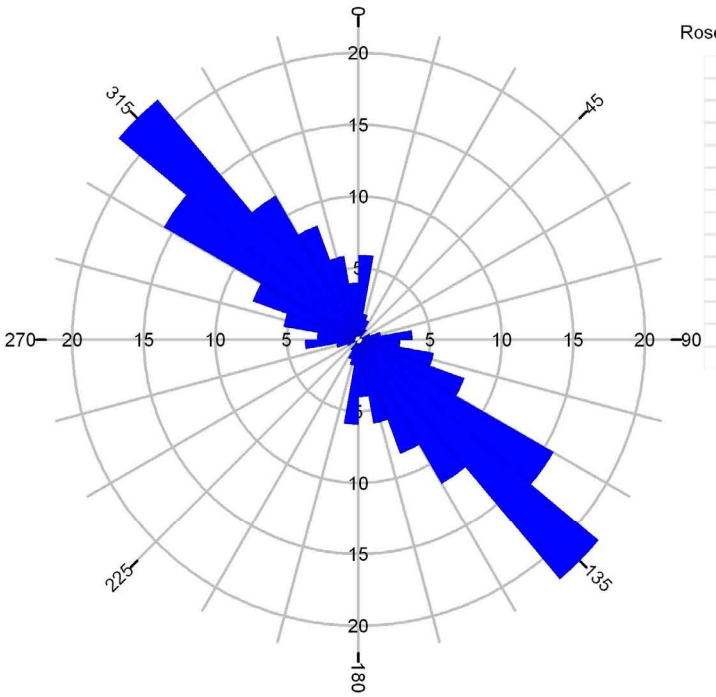

Rose Diagram, KI0010B01, Fractures total

Statistical Summary	
Calculation Method:	Frequency
Class Interval:	10 Degrees
Azimuth Filtering:	Deactivated
Data Type:	Bidirectional
Population:	828
Maximum Percentage:	21.9 Percent
Mean Percentage:	5.9 Percent
Standard Deviation:	5.8 Percent
Vector Mean:	136.9 Degrees
	316.94 Degrees
Confidence Interval:	4.0 Degrees
	(95 Percent)
R-mag:	0.61

KI0010B01 Open fractures, poles on Schmidt Net (Equal Area)

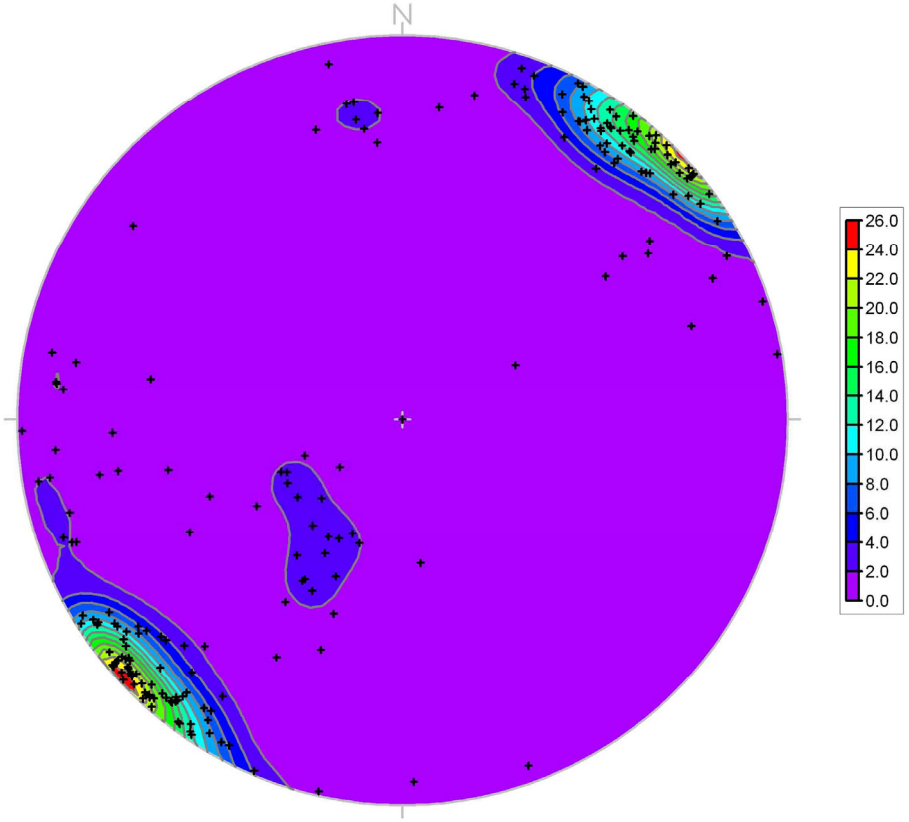

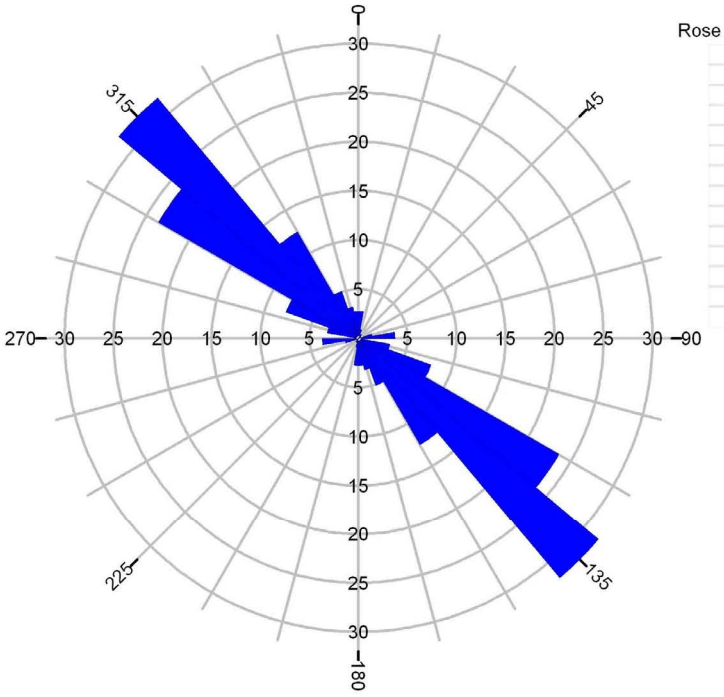

Rose Diagram, KI0010B01, Open fractures

Statistical Summary	
Calculation Method:	Frequency
Class Interval:	10 Degrees
Azimuth Filtering:	Deactivated
Data Type:	Bidirectional
Population:	216
Maximum Percentage:	31.9 Percent
Mean Percentage:	7.1 Percent
Standard Deviation:	9.3 Percent
Vector Mean:	134.1 Degrees
	314.12 Degrees
Confidence Interval:	5.5 Degrees
	(95 Percent)
R-mag:	0.77

KI0010B01, Closed fractures, poles on Schmidt Net (Equal Area)

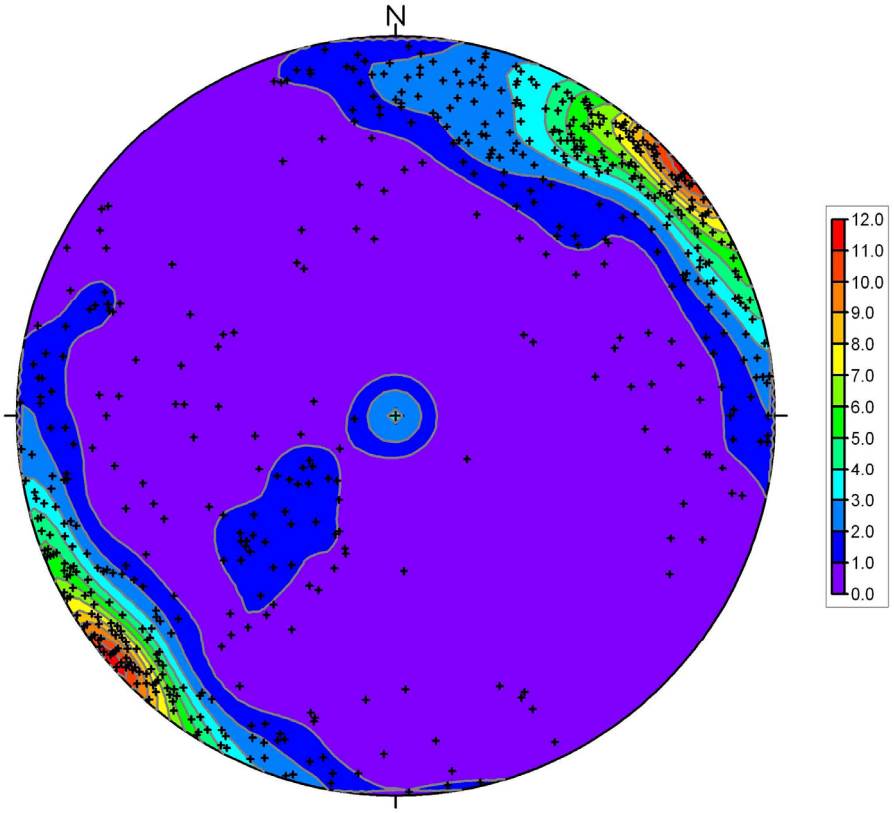

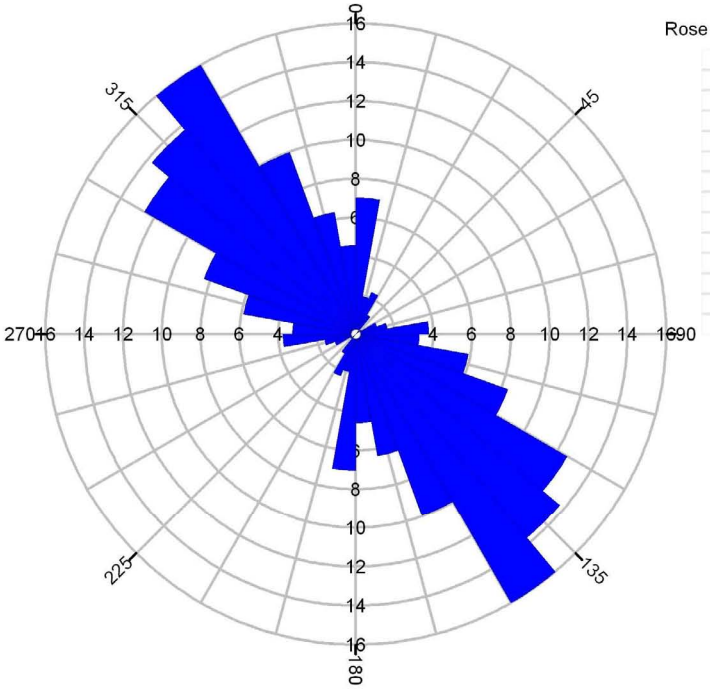

Rose Diagram, KI0010B01, Closed fractures

Statistical Summary	
Calculation Method:	Frequency
Class Interval:	10 Degrees
Azimuth Filtering:	Deactivated
Data Type:	Bidirectional
Population:	612
Maximum Percentage:	16.0 Percent
Mean Percentage:	5.9 Percent
Standard Deviation:	4.7 Percent
Vector Mean:	138.4 Degrees
	318.35 Degrees
Confidence Interval:	5.2 Degrees
	(95 Percent)
R-mag:	0.56

KI0010B01, Sealed Networks (UC), poles on Schmidt Net (Equal Area)

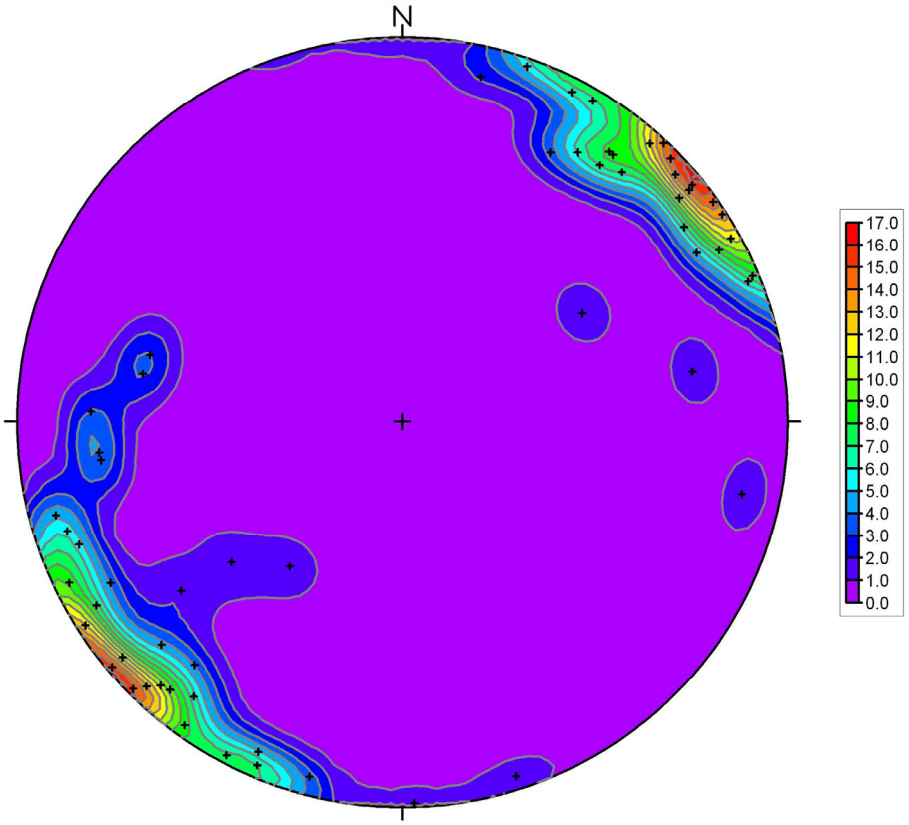

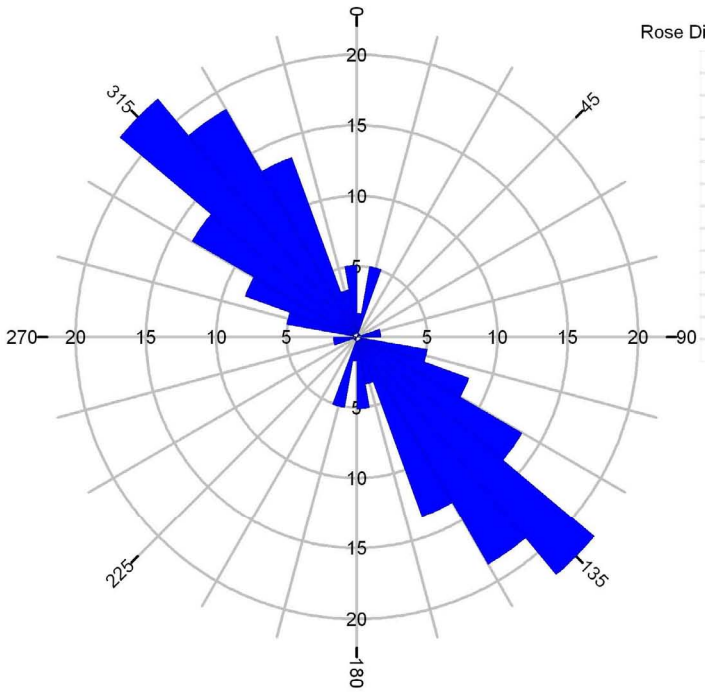

Rose Diagram, KI0010B01, Sealed Networks (UC)

Statistical Summary	
Calculation Method:	Frequency
Class Interval:	10 Degrees
Azimuth Filtering:	Deactivated
Data Type:	Bidirectional
Population:	59
Maximum Percentage:	22.0 Percent
Mean Percentage:	8.3 Percent
Standard Deviation:	6.8 Percent
Vector Mean:	139.4 Degrees
	319.4 Degrees
Confidence Interval:	11.5 Degrees
	(95 Percent)
R-mag:	0.73

KI0010B01, Cataclastic structures, poles on Schmidt Net (Equal Area)

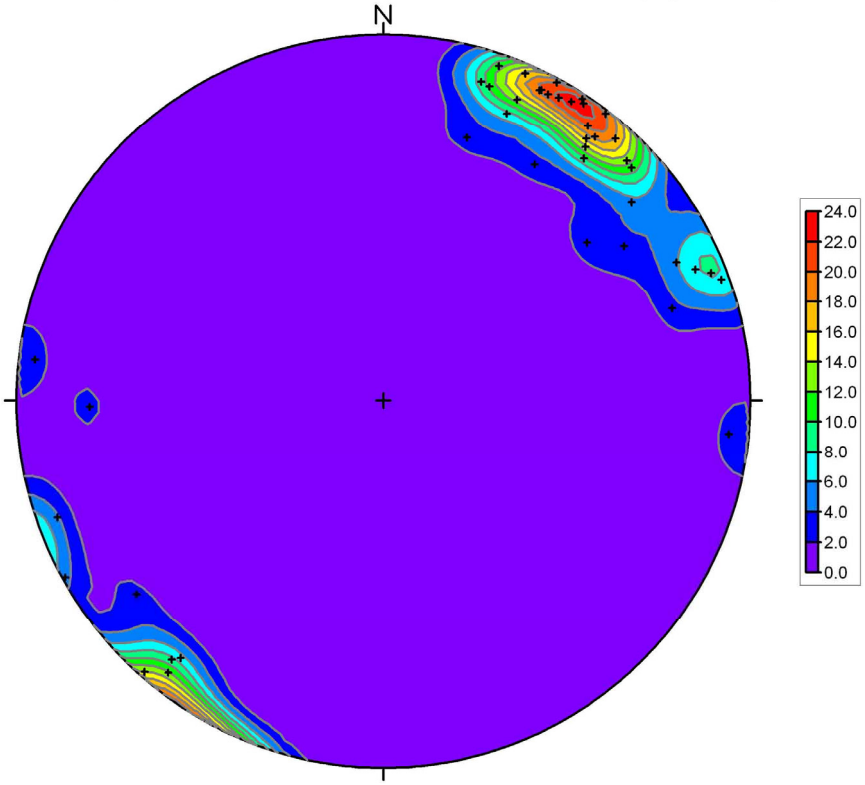

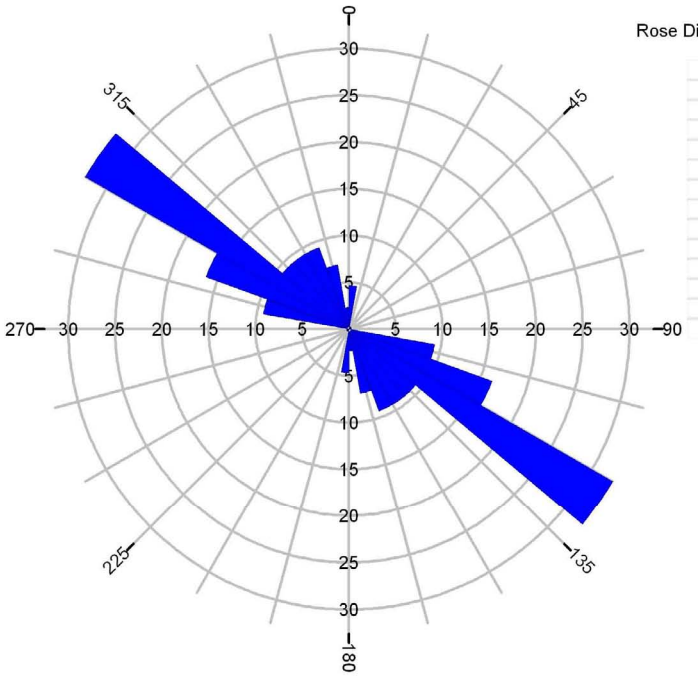

Rose Diagram, KI0010B01, Cataclastic structures

Statistical Summary	
Calculation Method:	Frequency
Class Interval:	10 Degrees
Azimuth Filtering:	Deactivated
Data Type:	Bidirectional
Population:	43
Maximum Percentage:	32.6 Percent
Mean Percentage:	11.1 Percent
Standard Deviation:	8.6 Percent
Vector Mean:	132.5 Degrees
	312.48 Degrees
Confidence Interval:	11.9 Degrees
	(95 Percent)
R-mag:	0.78

Appendix 3 A

Geology in KI0014B01; core log

Title GEOLOGY IN KI0014B01 **Appendix: 3A**

Site	ÄSPÖ	**Coordinate System**	ÄSPÖ96
Borehole	KI0014B01	**Northing [m]**	7250.84
Diameter [mm]	120	**Easting [m]**	1953.61
Length [m]	100.270	**Elevation [m.a.s.l.]**	-447.55
Bearing [°]	229.75	**Drilling Start Date**	2007-03-19 13:15:00
Inclination [°]	-0.64	**Drilling Stop Date**	2007-03-20 12:00:00
Date of coremapping	2007-07-26 10:31:00	**Plot Date**	2007-11-13 22:03:06
Rocktype data from	p_rock	**Signed data**	

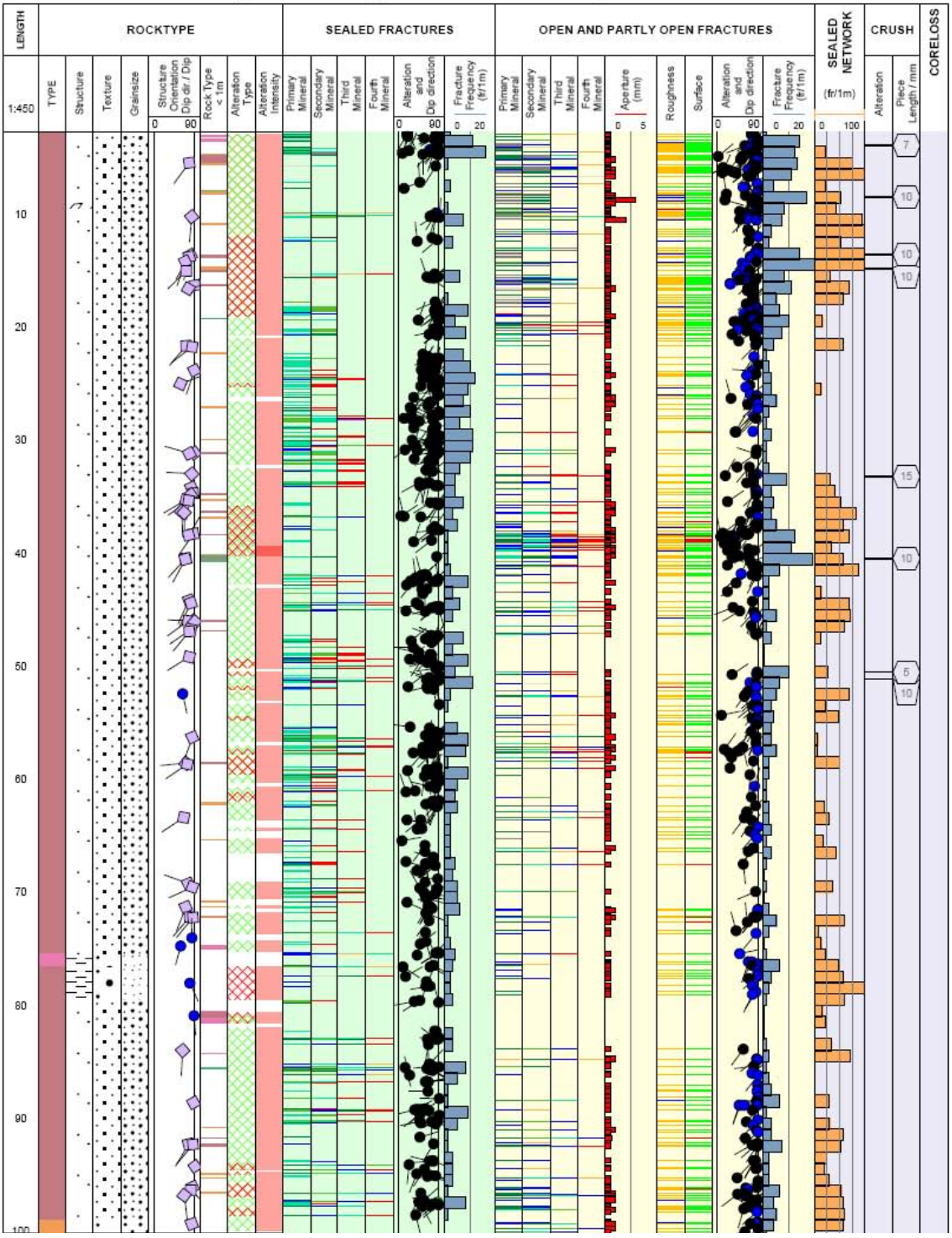

Appendix 3 B

The BIPS image of borehole KI0014B01

Project name: SKB HRL

Image file	: c:\work\r5612s~1\bips20~2\ki0014~1.bip
BDT file	: c:\work\r5612s~1\bips20~2\ki0014~1.bdt
Locality	: ASPOHRL
Bore hole number	: KI014B01
Date	: 07/07/04
Time	: 12:25:00
Depth range	: 1.996 - 100.000 m
Azimuth	: 230
Inclination	: -1
Diameter	: 76.0 mm
Magnetic declination	: 0.0
Span	: 4
Scan interval	: 0.25
Scan direction	: To entrance
Scale	: 1/25
Aspect ratio	: 175 %
Pages	: 5
Color	: +0 +0 +0

Project name: SKB HRL
Bore hole No.: KI014B01 Azimuth: 230 Inclination: -1

Depth range: 0.000 - 20.000 m

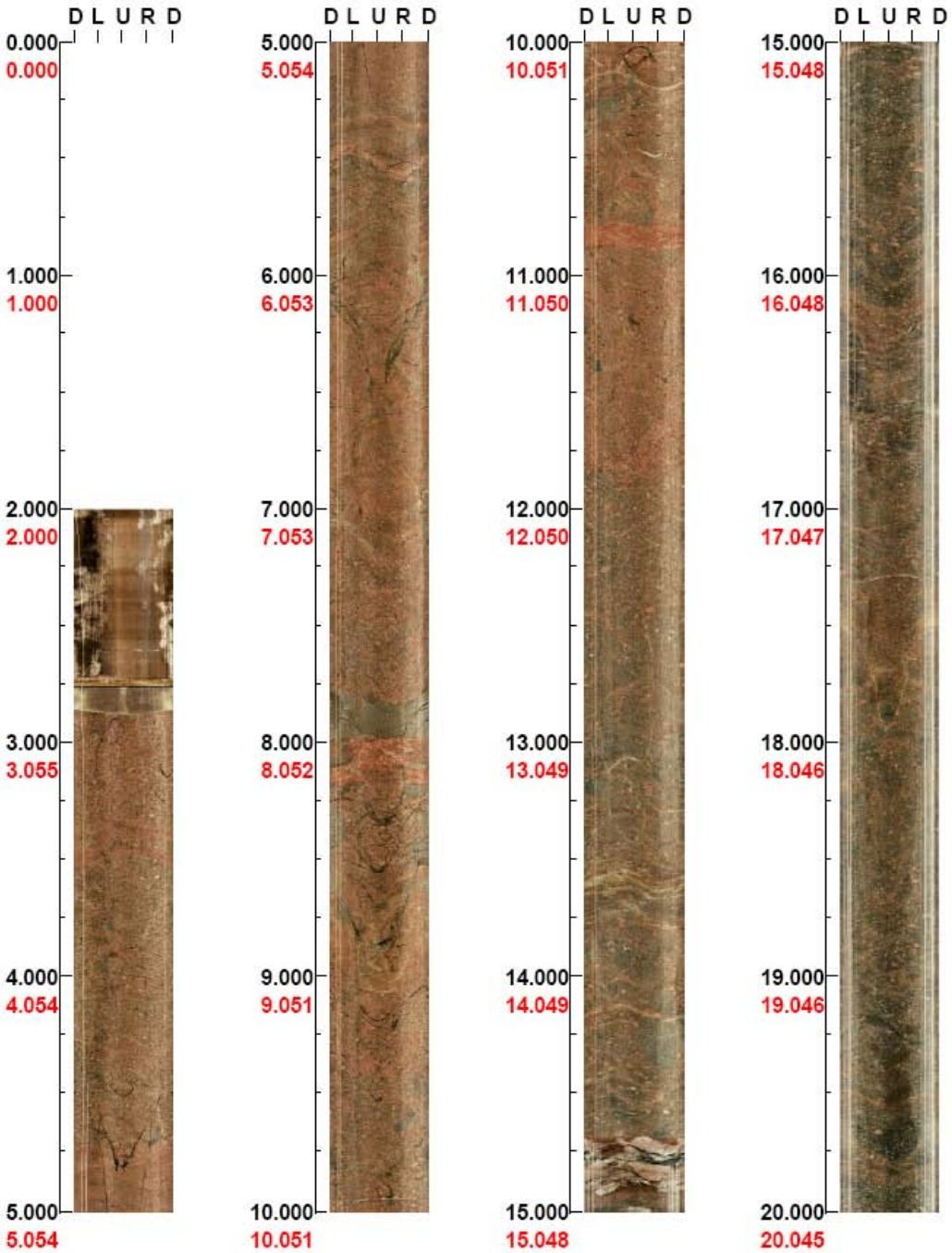

(1 / 5) Scale: 1/25 Aspect ratio: 175 %

Project name: SKB HRL
Bore hole No.: KI014B01 Azimuth: 230 Inclination: -1

Depth range: 20.000 - 40.000 m

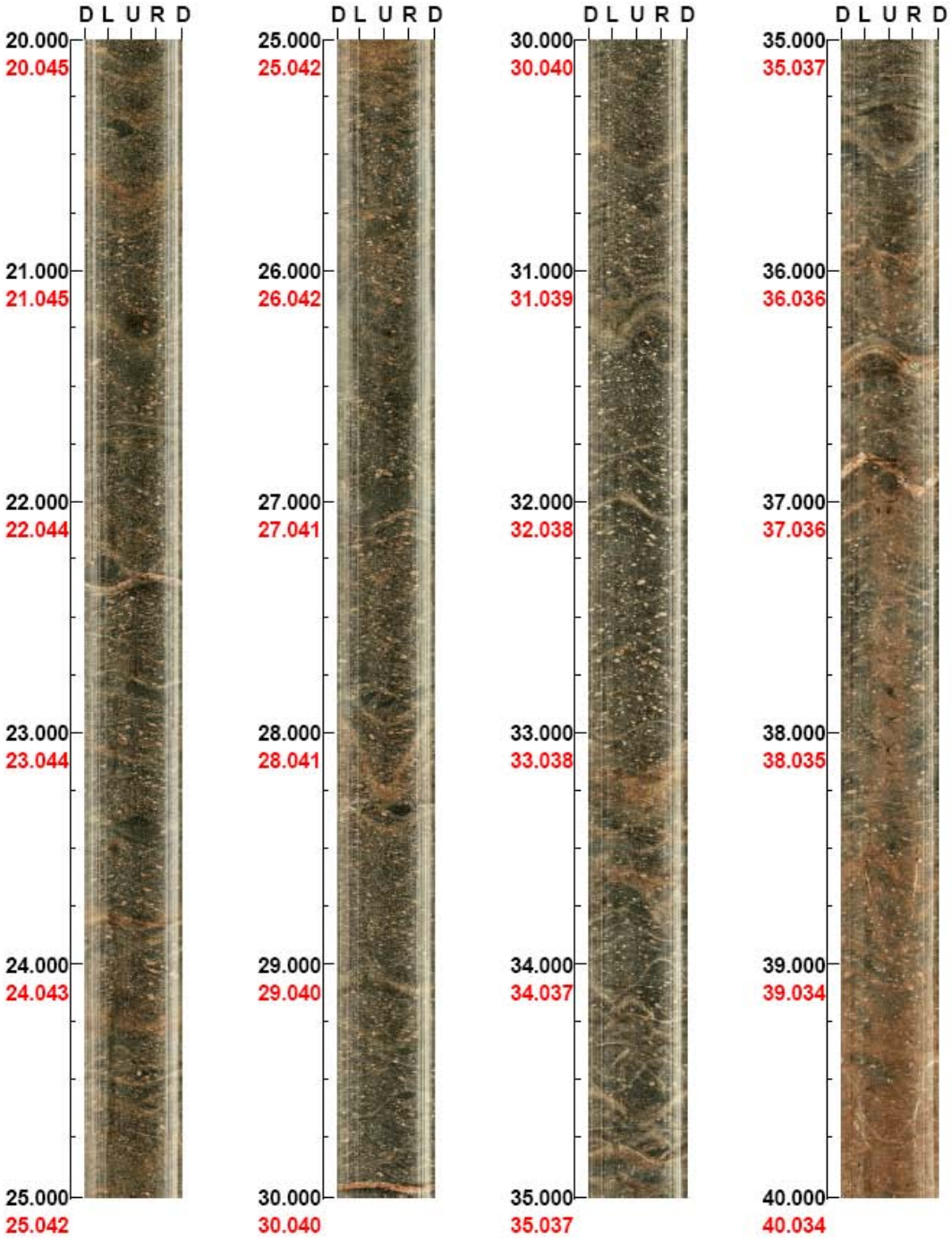

(2 / 5) Scale: 1/25 Aspect ratio: 175 %

Project name: SKB HRL
Bore hole No.: KI014B01 Azimuth: 230 Inclination: -1

Depth range: 40.000 - 60.000 m

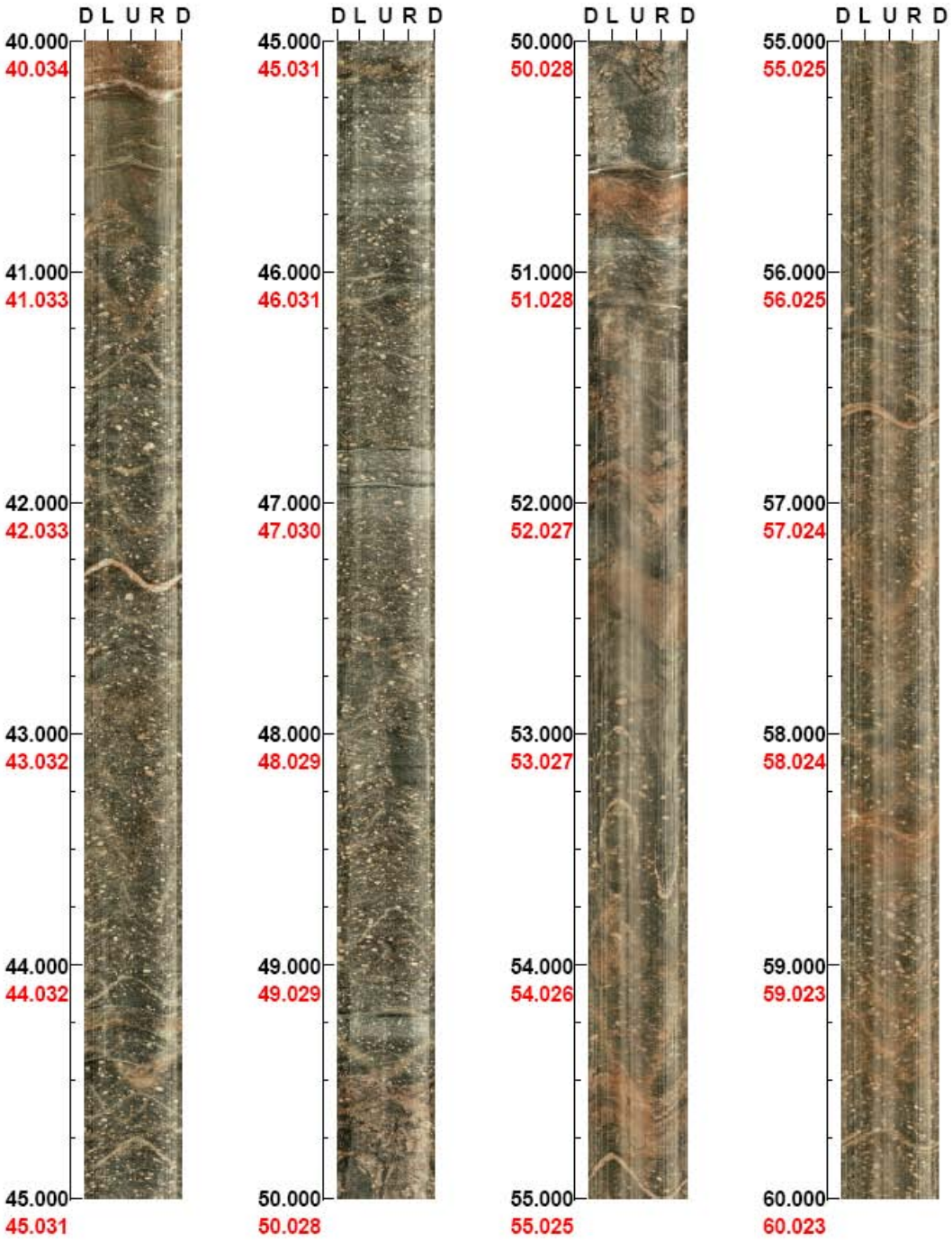

(3 / 5) Scale: 1/25 Aspect ratio: 175 %

Project name: SKB HRL
Bore hole No.: KI014B01 Azimuth: 230 Inclination: -1

Depth range: 60.000 - 80.000 m

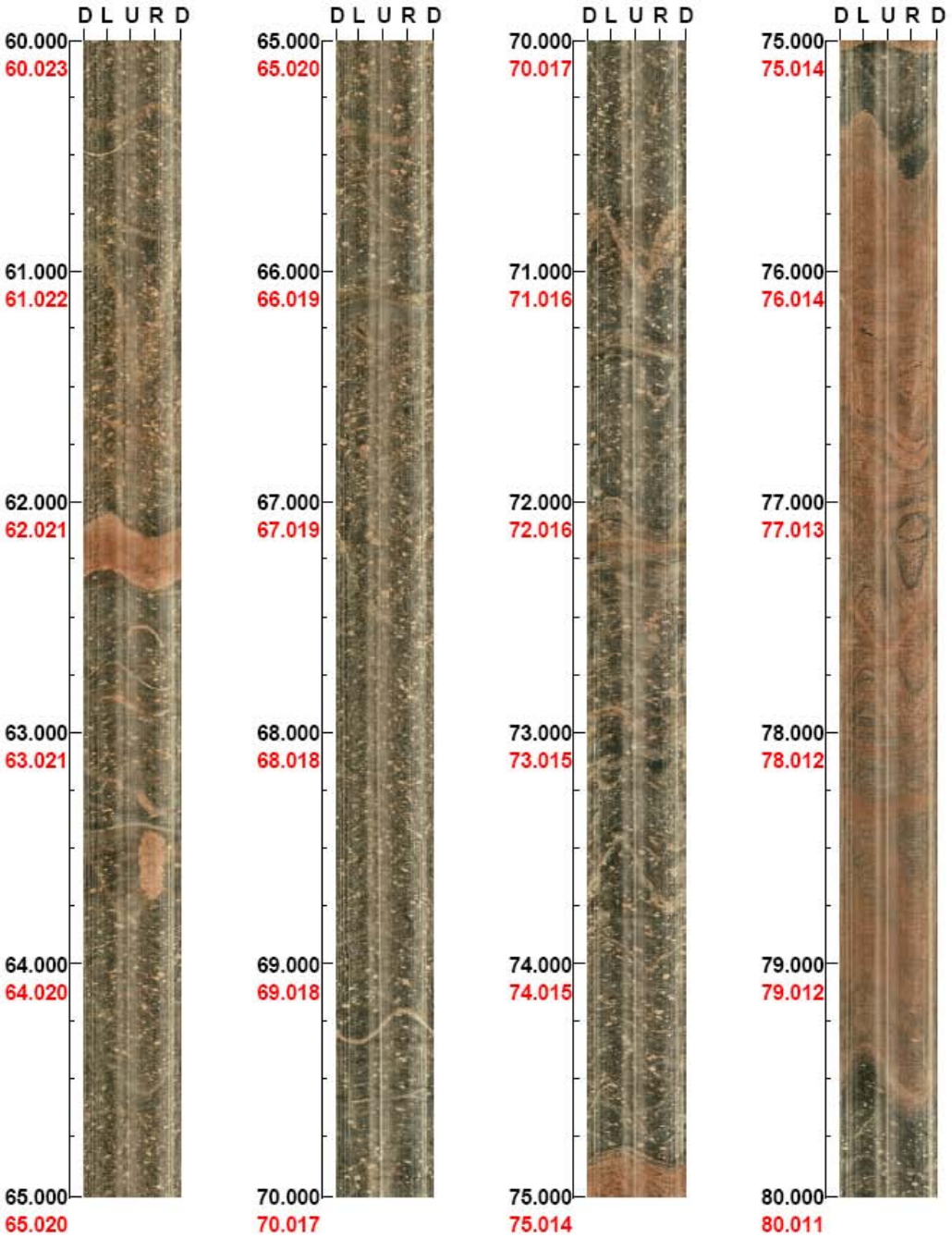

(4 / 5) Scale: 1/25 Aspect ratio: 175 %

Project name: SKB HRL
Bore hole No.: KI014B01 Azimuth: 230 Inclination: -1

Depth range: 80.000 - 100.000 m

(5 / 5) Scale: 1/25 Aspect ratio: 175 %

Appendix 3 C

Stereonets & rose-diagrams of all logged fractures, all open fractures, all closed fractures, sealed networks and cataclastic structures in borehole KI0014B01

KI0014B01, Fractures total, poles on Schmidt Net (Equal Area)

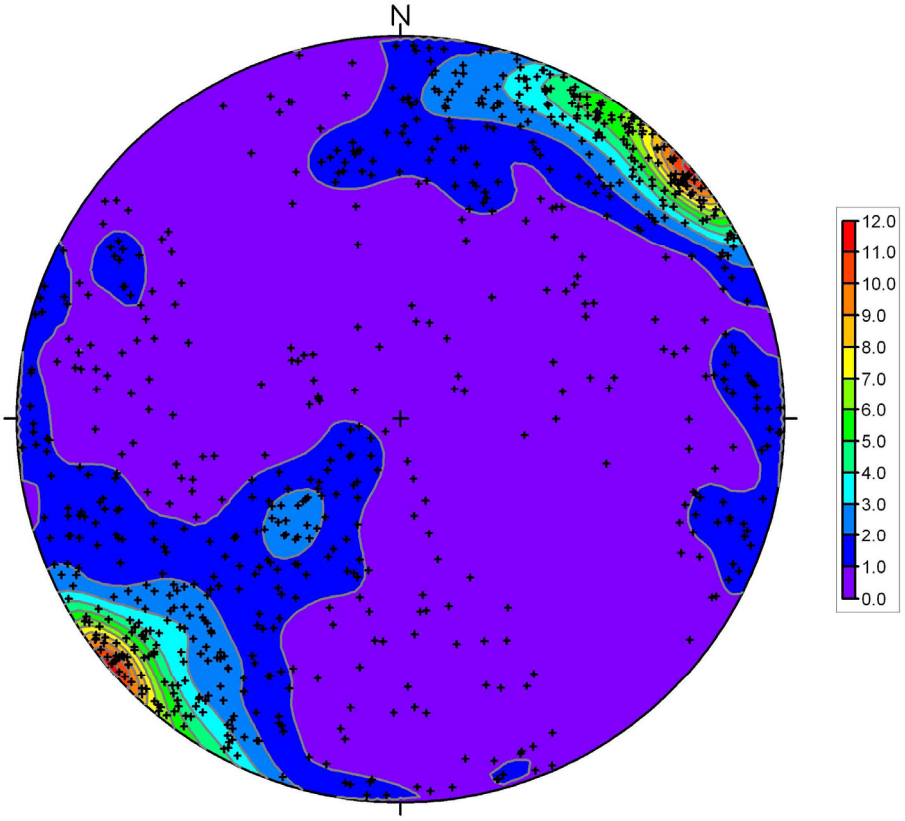

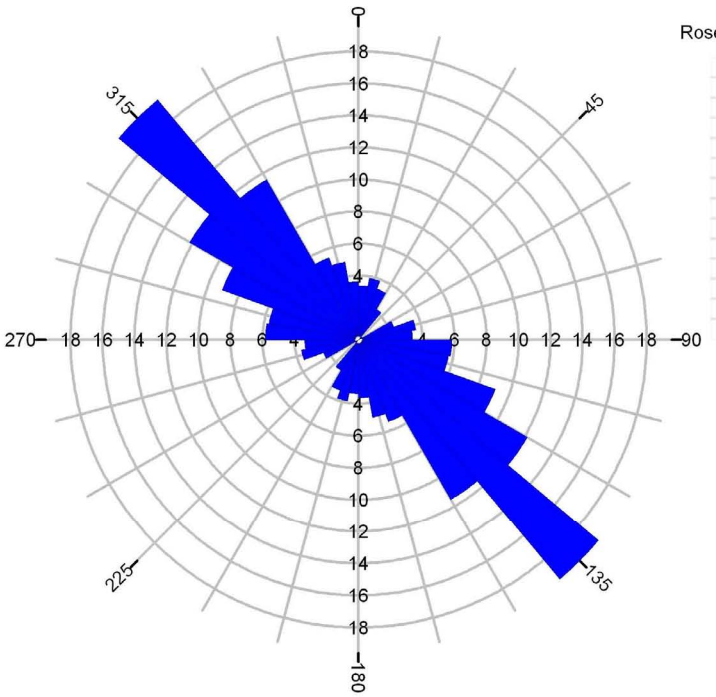

Rose Diagram, KI0014B01, Fractures total

Statistical Summary	
Calculation Method:	Frequency
Class Interval:	10 Degrees
Azimuth Filtering:	Deactivated
Data Type:	Bidirectional
Population:	772
Maximum Percentage:	19.6 Percent
Mean Percentage:	6.2 Percent
Standard Deviation:	4.6 Percent
Vector Mean:	133.2 Degrees
	313.22 Degrees
Confidence Interval:	5.5 Degrees
	(95 Percent)
R-mag:	0.49

KI0014B01, Open fractures, poles on Schmidt Net (Equal Area)

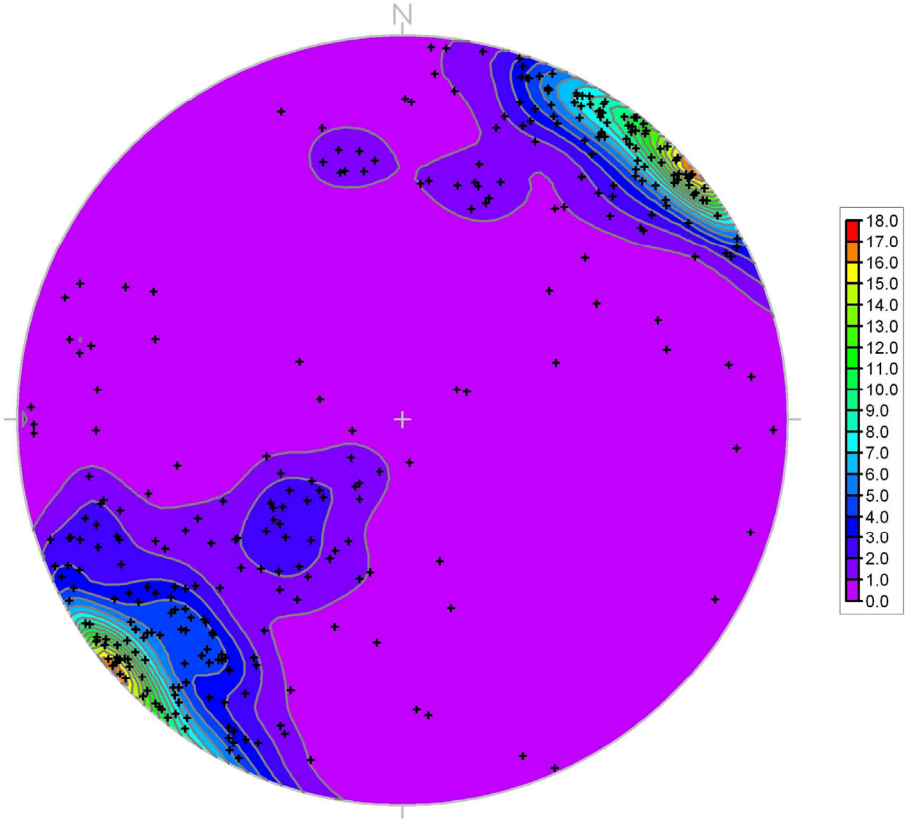

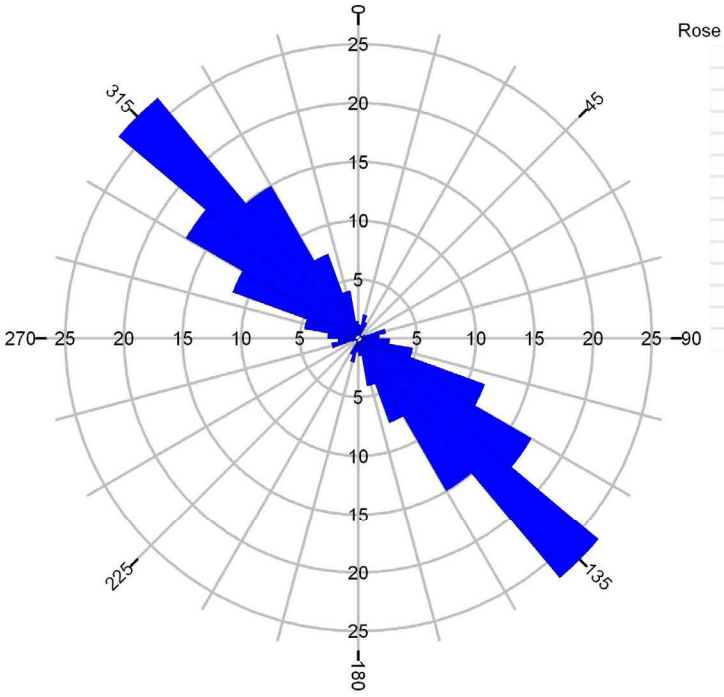

Rose Diagram, KI0014B01, Open fractures

Statistical Summary	
Calculation Method:	Frequency
Class Interval:	10 Degrees
Azimuth Filtering:	Deactivated
Data Type:	Bidirectional
Population:	341
Maximum Percentage:	26.7 Percent
Mean Percentage:	6.7 Percent
Standard Deviation:	7.5 Percent
Vector Mean:	133.5 Degrees
	313.49 Degrees
Confidence Interval:	4.9 Degrees
	(95 Percent)
R-mag:	0.72

KI0010, 14 & 16B01, Closed fractures, poles on Schmidt Net (Equal Area)

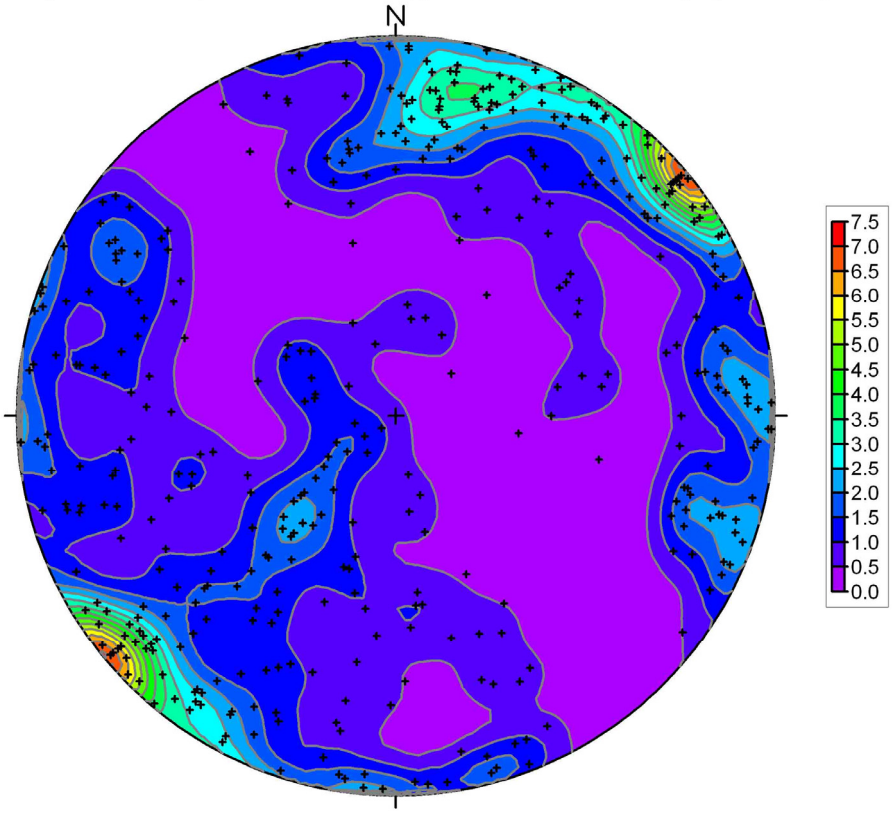

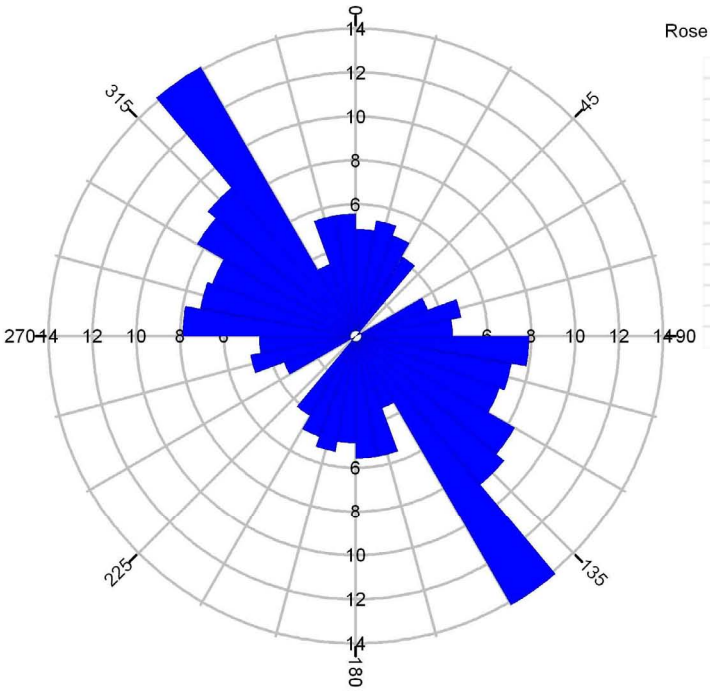

Rose Diagram, KI0014B01, Closed fractures

Statistical Summary	
Calculation Method:	Frequency
Class Interval:	10 Degrees
Azimuth Filtering:	Deactivated
Data Type:	Bidirectional
Population:	431
Maximum Percentage:	14.2 Percent
Mean Percentage:	6.3 Percent
Standard Deviation:	2.6 Percent
Vector Mean:	132.8 Degrees
	312.76 Degrees
Confidence Interval:	12.5 Degrees
	(95 Percent)
R-mag:	0.3

KI0014B01, Sealed Networks (UC), poles on Schmidt Net (Equal Area)

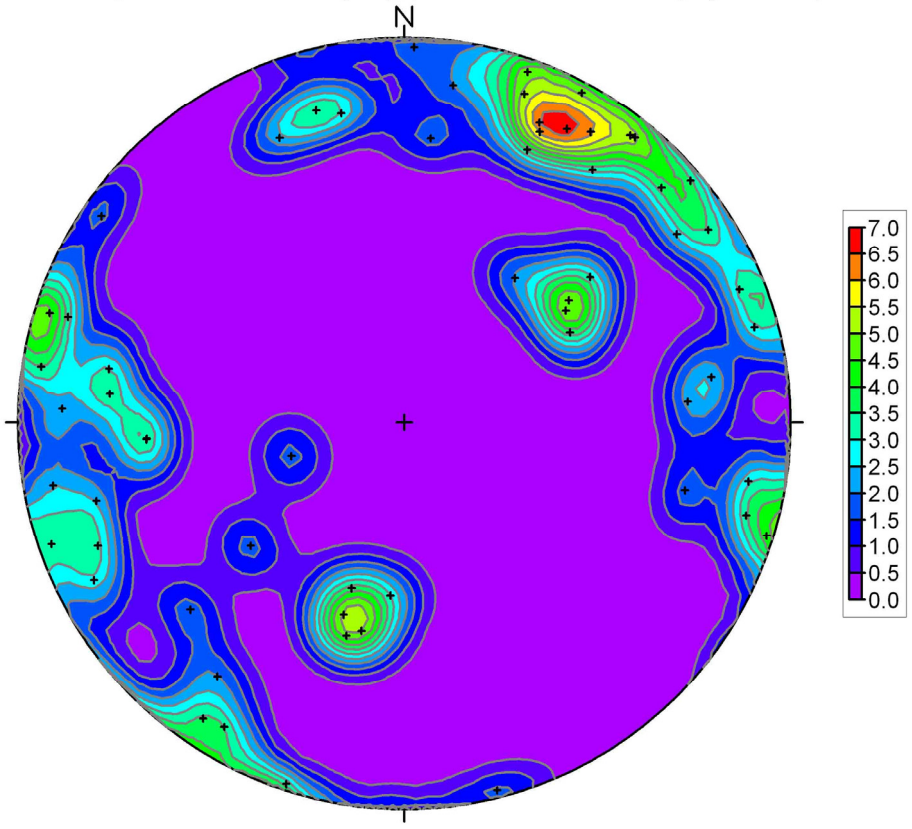

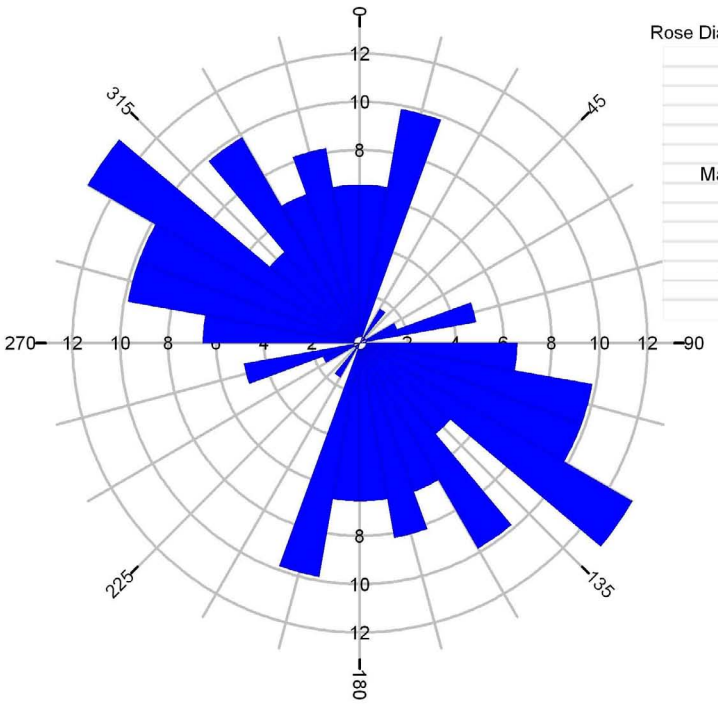

Rose Diagram, KI0014B01, Sealed Networks (UC)

Statistical Summary	
Calculation Method:	Frequency
Class Interval:	10 Degrees
Azimuth Filtering:	Deactivated
Data Type:	Bidirectional
Population:	61
Maximum Percentage:	13.1 Percent
Mean Percentage:	7.1 Percent
Standard Deviation:	3.2 Percent
Vector Mean:	139.5 Degrees
	319.47 Degrees
Confidence Interval:	24.4 Degrees
	(95 Percent)
R-mag:	0.4

KI0014B01, Cataclastic structures, poles on Schmidt Net (Equal Area)

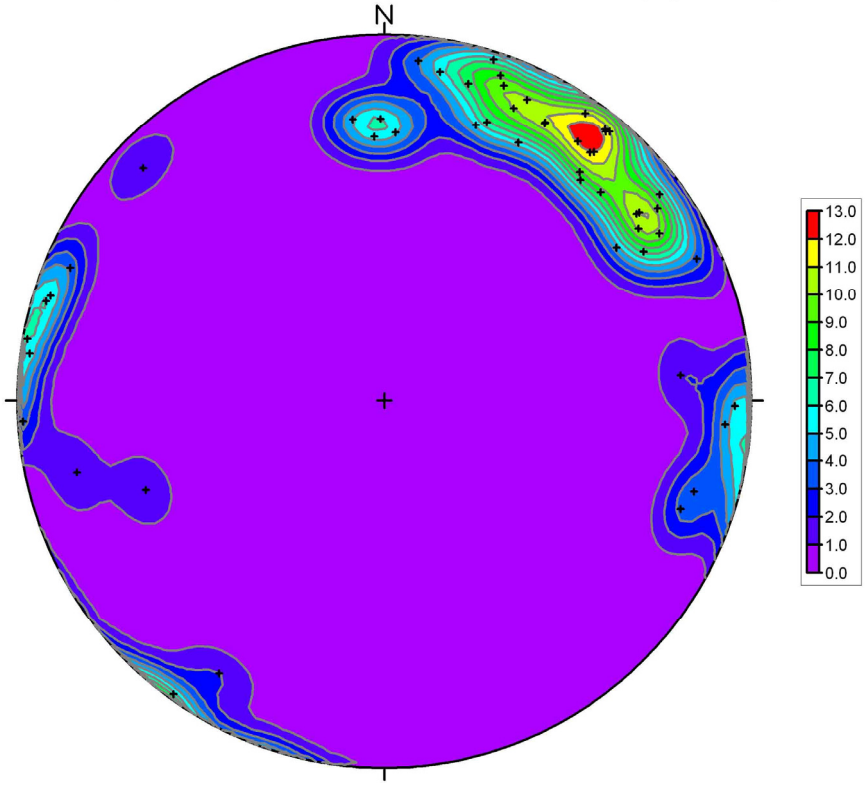

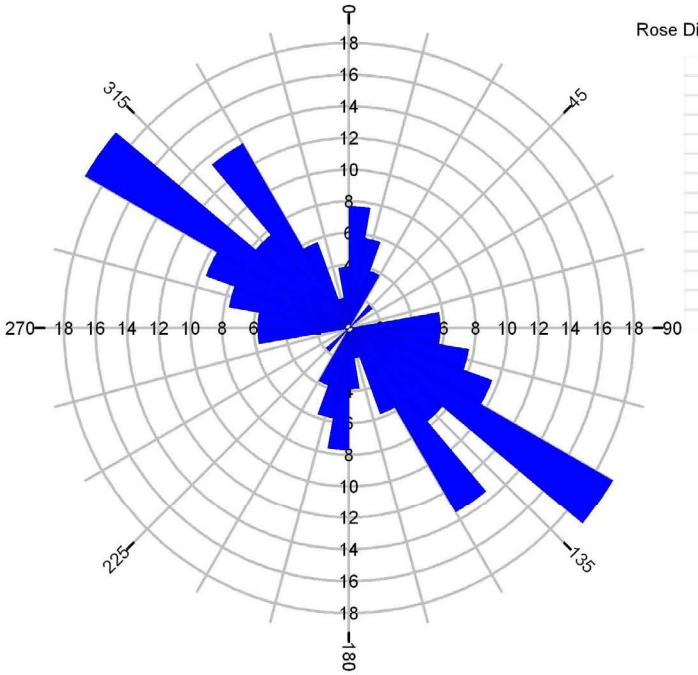

Rose Diagram, KI0014B01, Cataclastic structures

Statistical Summary	
Calculation Method:	Frequency
Class Interval:	10 Degrees
Azimuth Filtering:	Deactivated
Data Type:	Bidirectional
Population:	52
Maximum Percentage:	19.2 Percent
Mean Percentage:	7.1 Percent
Standard Deviation:	4.5 Percent
Vector Mean:	133.8 Degrees
	313.75 Degrees
Confidence Interval:	22.0 Degrees
	(95 Percent)
R-mag:	0.47

Appendix 4 A

Geology in KI0016B01; core log

Title GEOLOGY IN KI0016B01 **Appendix: 4A**

Site	ÄSPÖ	**Coordinate System**	ÄSPÖ96
Borehole	KI0016B01	**Northing [m]**	7248.80
Diameter [mm]	76	**Easting [m]**	1953.49
Length [m]	100.240	**Elevation [m.a.s.l.]**	-446.05
Bearing [°]	229.79	**Drilling Start Date**	2007-03-13 13:30:00
Inclination [°]	-0.52	**Drilling Stop Date**	2007-03-14 14:30:00
Date of coremapping	2007-09-24 10:50:00	**Plot Date**	2007-11-13 22:03:06
Rocktype data from	p_rock	**Signed data**	

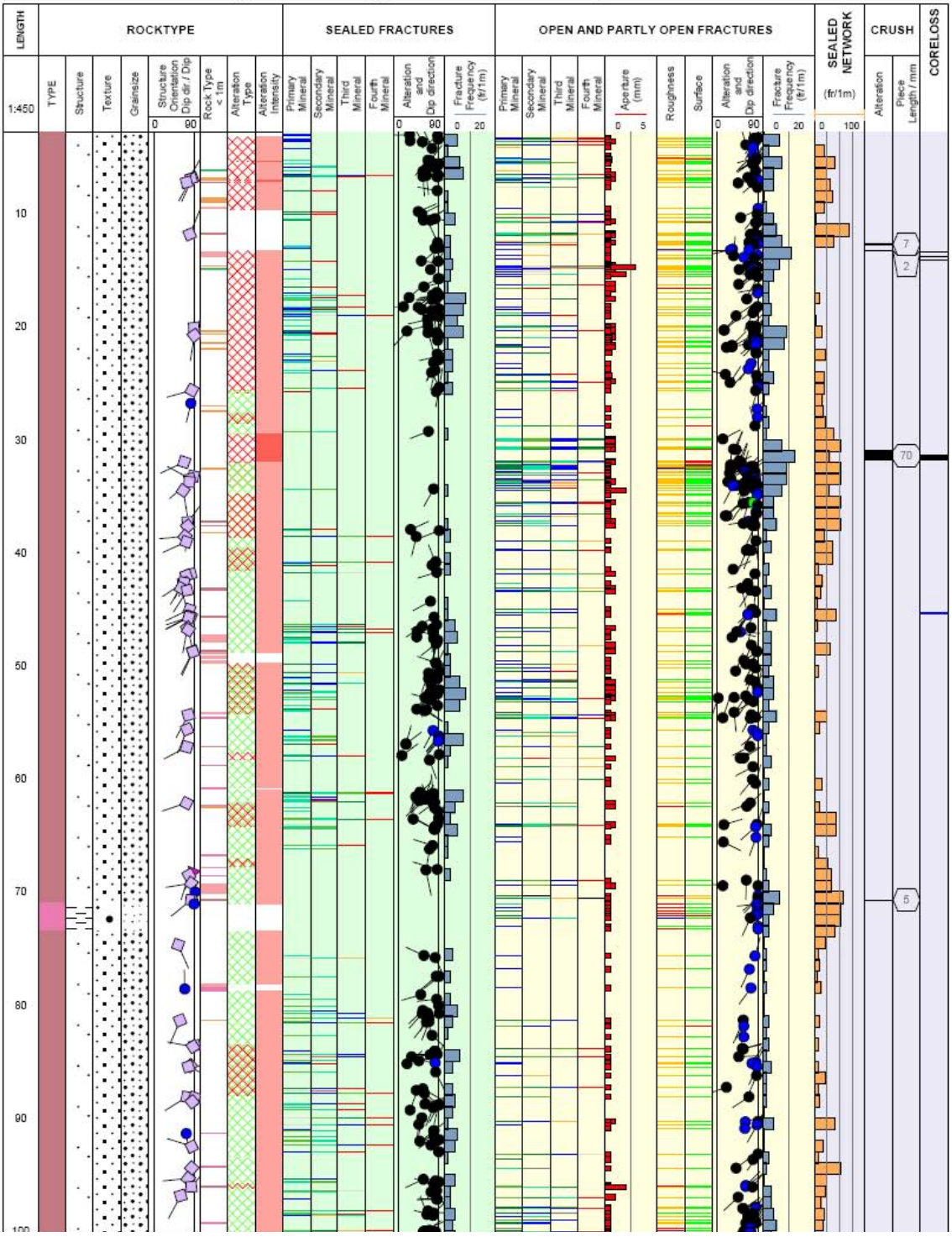

Appendix 4 B

The BIPS image of borehole KI0016B01

Project name: SKB HRL

Image file	: c:\work\r5612s~1\bips20~2\ki0016~1.bip
BDT file	: c:\work\r5612s~1\bips20~2\ki0016~1.bdt
Locality	: ASPOHRL
Bore hole number	: KI016B01
Date	: 07/07/04
Time	: 10:44:00
Depth range	: 1.990 - 100.000 m
Azimuth	: 230
Inclination	: -1
Diameter	: 76.0 mm
Magnetic declination	: 0.0
Span	: 4
Scan interval	: 0.25
Scan direction	: To entrance
Scale	: 1/25
Aspect ratio	: 175 %
Pages	: 5
Color	: +0 +0 +0

Project name: SKB HRL
Bore hole No.: KI016B01 Azimuth: 230 Inclination: -1

Depth range: 0.000 - 20.000 m

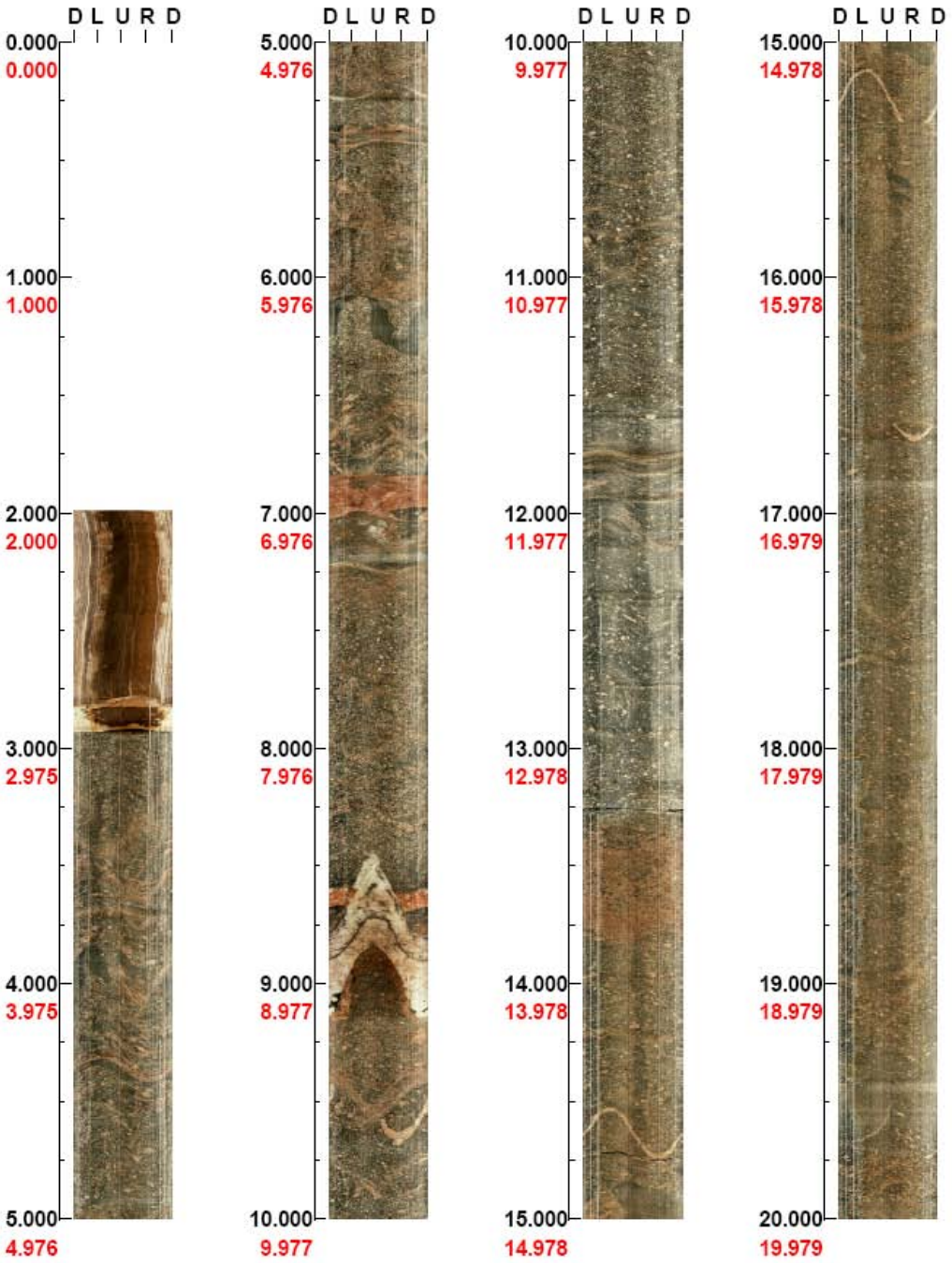

(1 / 5) Scale: 1/25 Aspect ratio: 175 %

Project name: SKB HRL
Bore hole No.: KI016B01 Azimuth: 230 Inclination: -1

Depth range: 20.000 - 40.000 m

(2 / 5) Scale: 1/25 Aspect ratio: 175 %

Project name: SKB HRL
Bore hole No.: KI016B01 Azimuth: 230 Inclination: -1

Depth range: 40.000 - 60.000 m

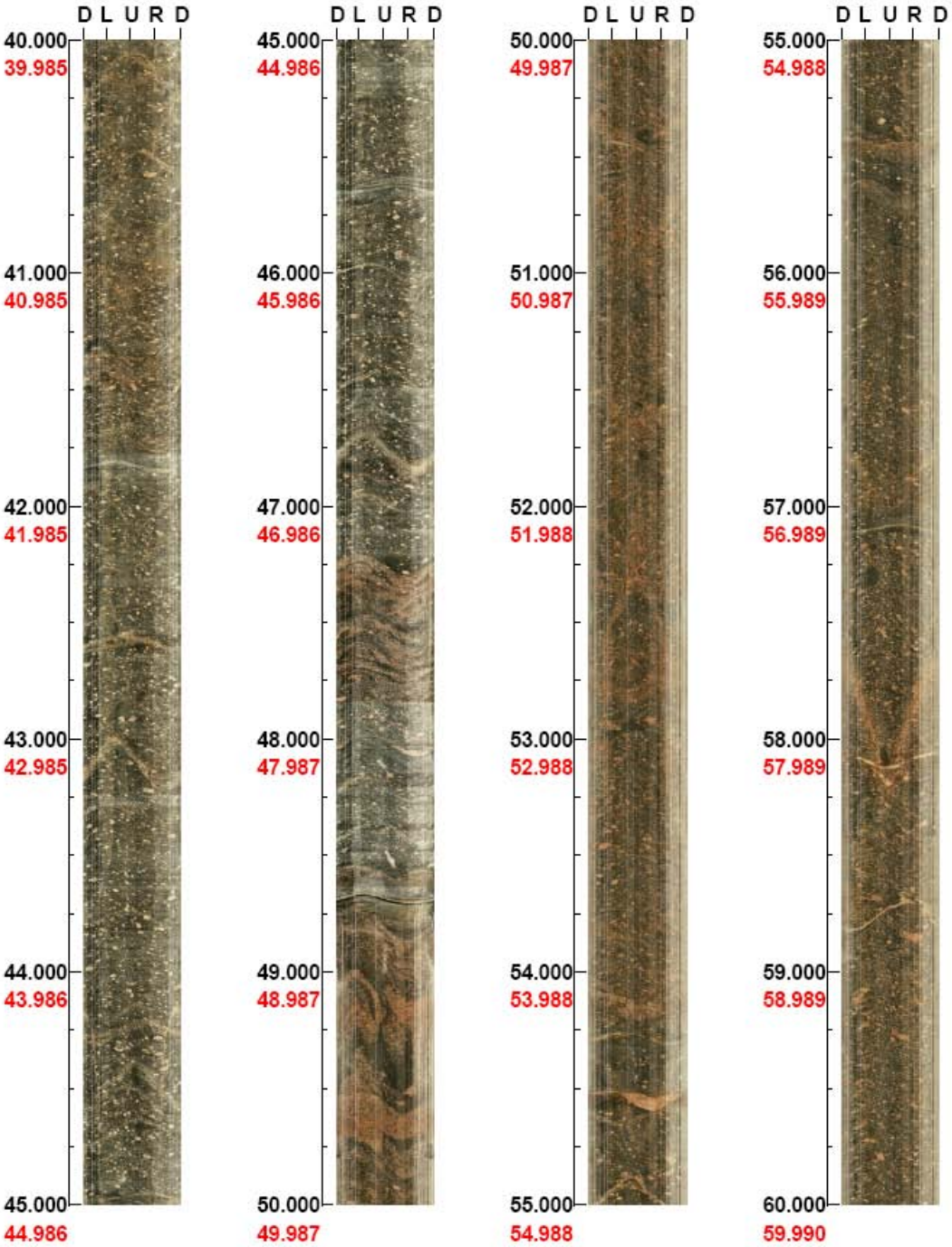

(3 / 5) Scale: 1/25 Aspect ratio: 175 %

Project name: SKB HRL
Bore hole No.: KI016B01 Azimuth: 230 Inclination: -1

Depth range: 60.000 - 80.000 m

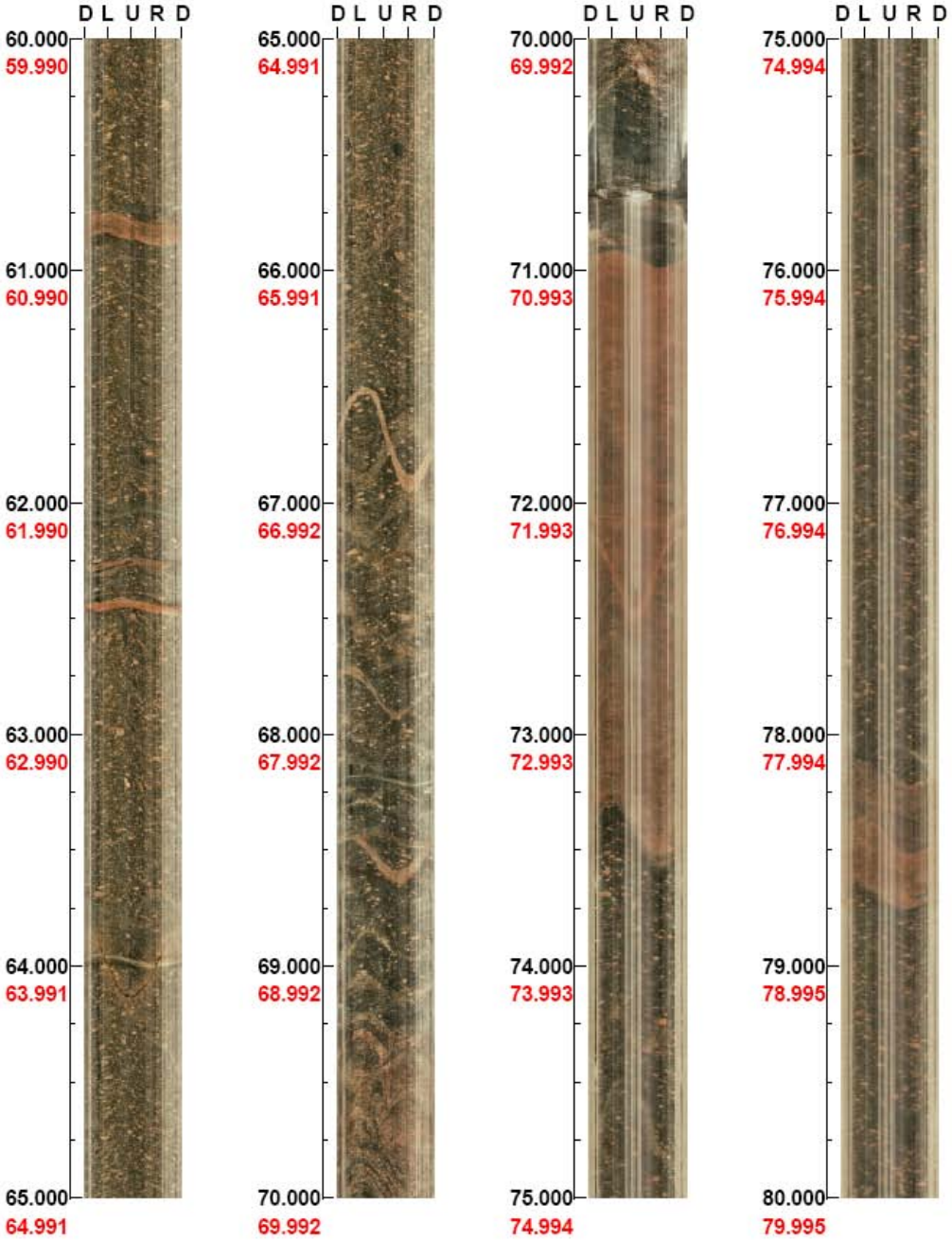

(4 / 5) Scale: 1/25 Aspect ratio: 175 %

Project name: SKB HRL
Bore hole No.: KI016B01 Azimuth: 230 Inclination: -1

Depth range: 80.000 - 100.000 m

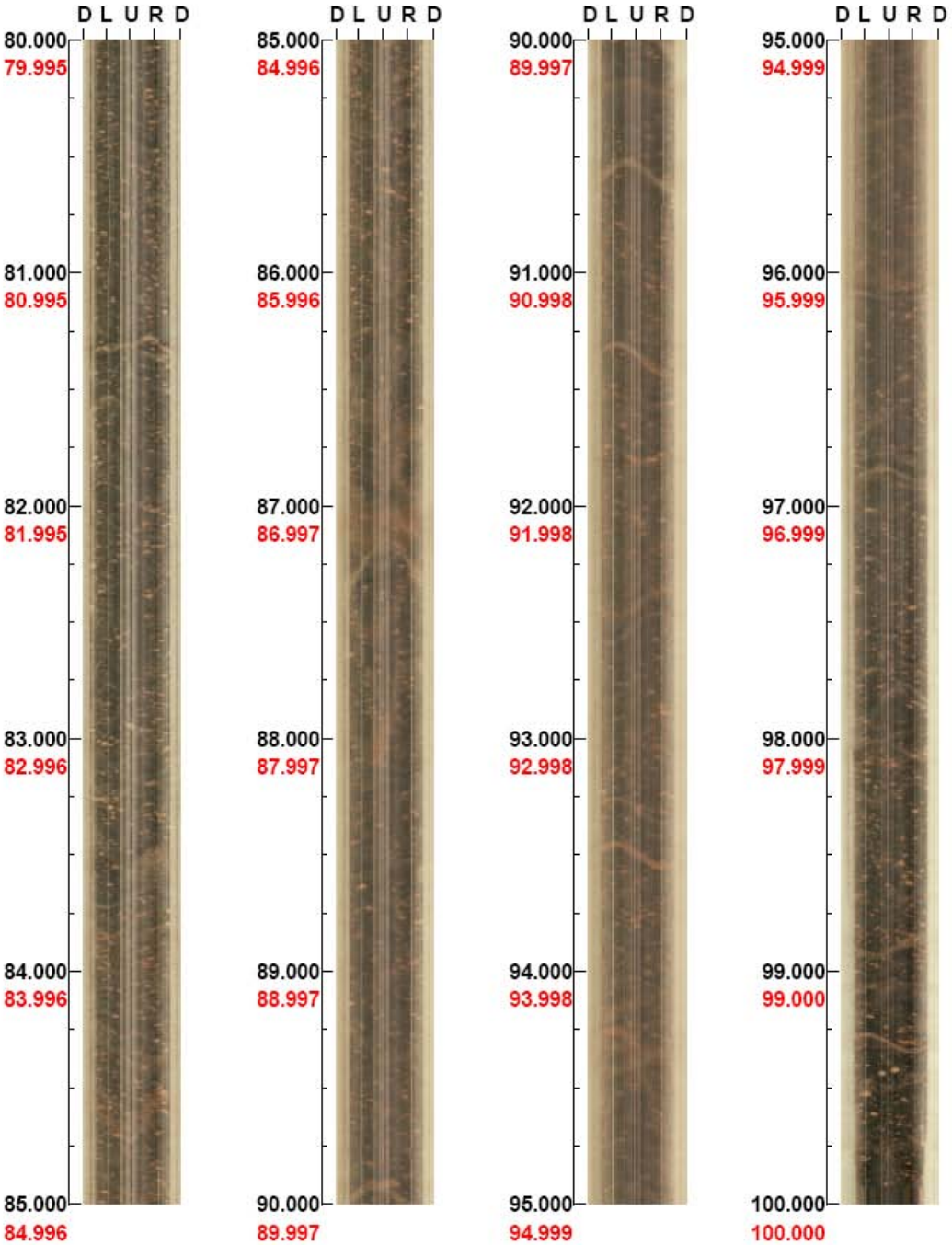

(5 / 5) Scale: 1/25 Aspect ratio: 175 %

Appendix 4 C

Stereonets & rose-diagrams of all logged fractures, all open fractures, all closed fractures, sealed networks and cataclastic structures in borehole KI0016B01

KI0016B01, Fractures total, poles on Schmidt Net (Equal Area)

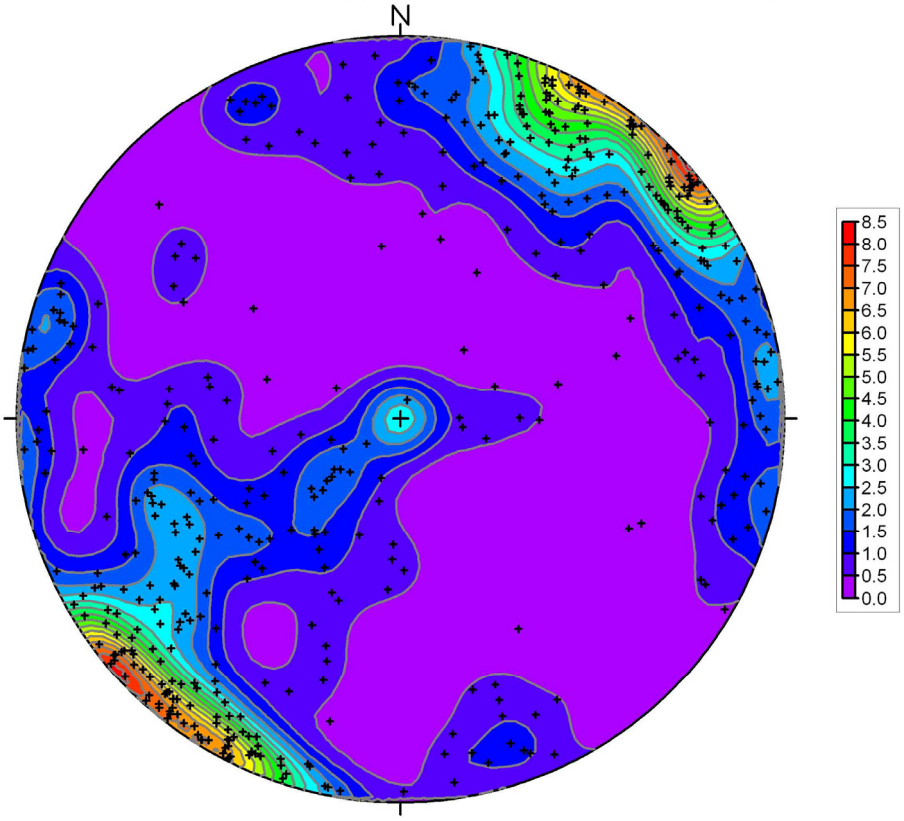

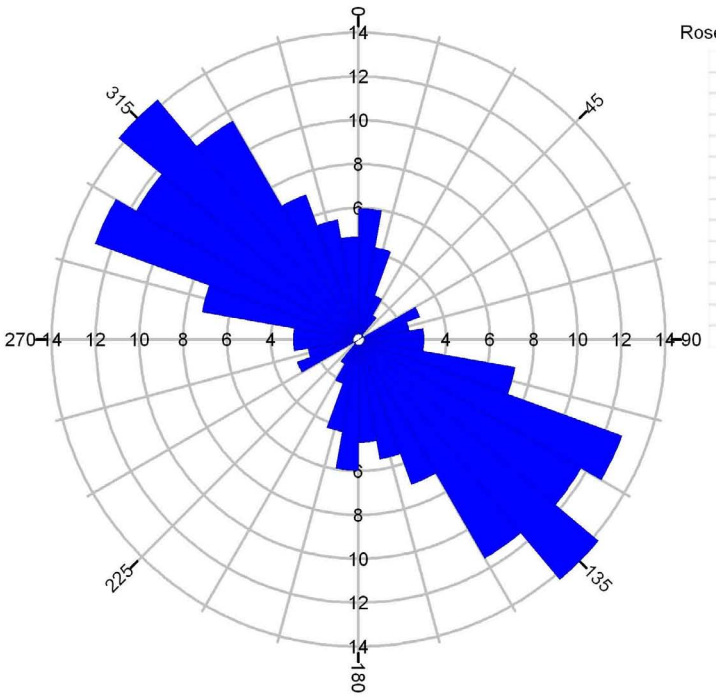

Rose Diagram, KI0016B01, Fractures total

Statistical Summary	
Calculation Method:	Frequency
Class Interval:	10 Degrees
Azimuth Filtering:	Deactivated
Data Type:	Bidirectional
Population:	469
Maximum Percentage:	14.3 Percent
Mean Percentage:	5.9 Percent
Standard Deviation:	4.2 Percent
Vector Mean:	135.9 Degrees
	315.87 Degrees
Confidence Interval:	6.8 Degrees
	(95 Percent)
R-mag:	0.5

KI0016B01, Open fractures, poles on Schmidt Net (Equal Area)

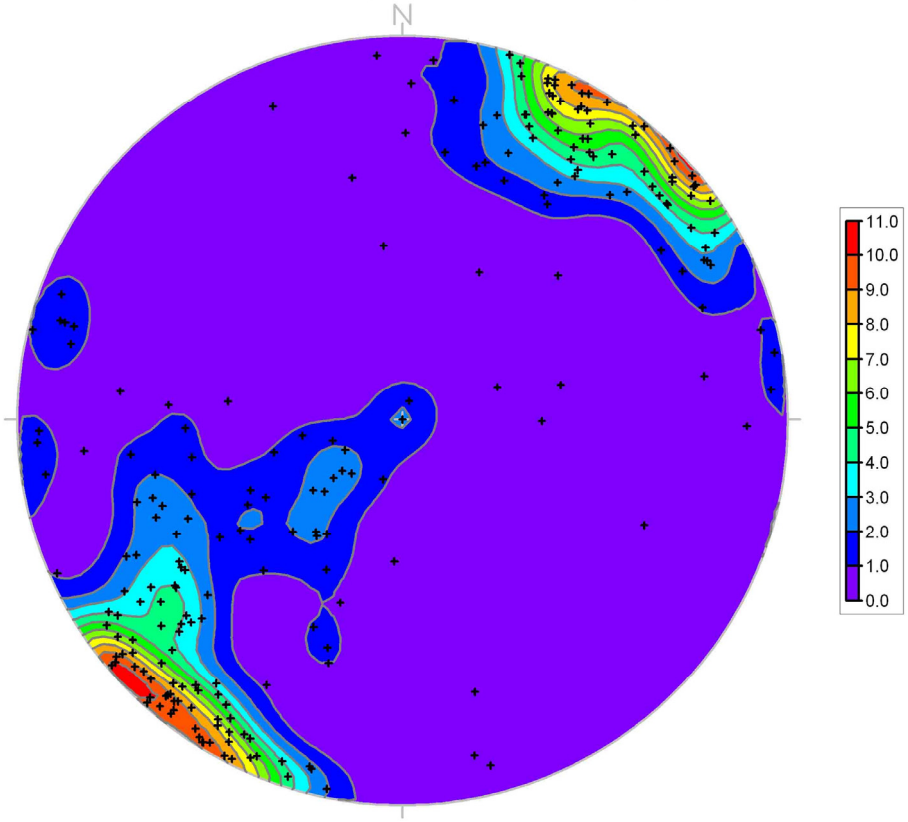

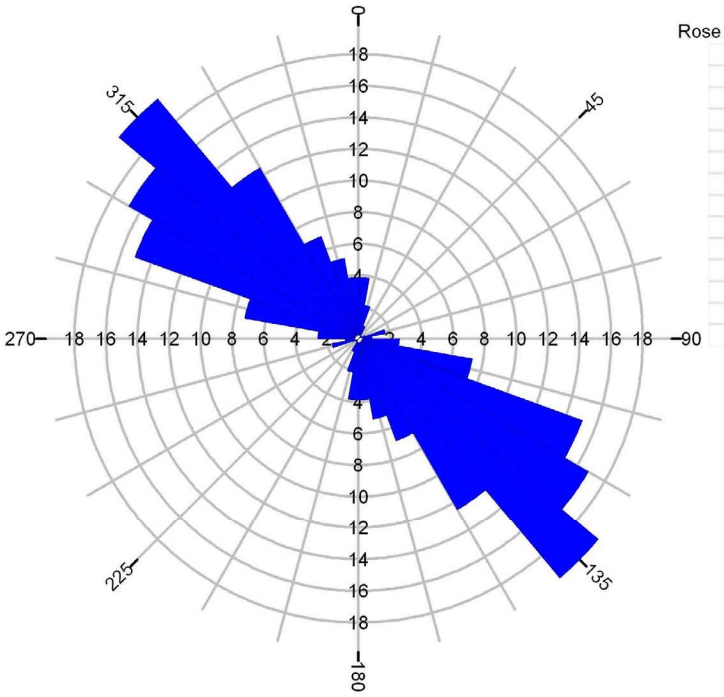

Rose Diagram, KI0016B01, Open fractures

Statistical Summary	
Calculation Method:	Frequency
Class Interval:	10 Degrees
Azimuth Filtering:	Deactivated
Data Type:	Bidirectional
Population:	232
Maximum Percentage:	19.8 Percent
Mean Percentage:	6.7 Percent
Standard Deviation:	6.3 Percent
Vector Mean:	133.8 Degrees
	313.79 Degrees
Confidence Interval:	6.3 Degrees
	(95 Percent)
R-mag:	0.69

KI0016B01, Closed fractures, poles on Schmidt Net (Equal Area)

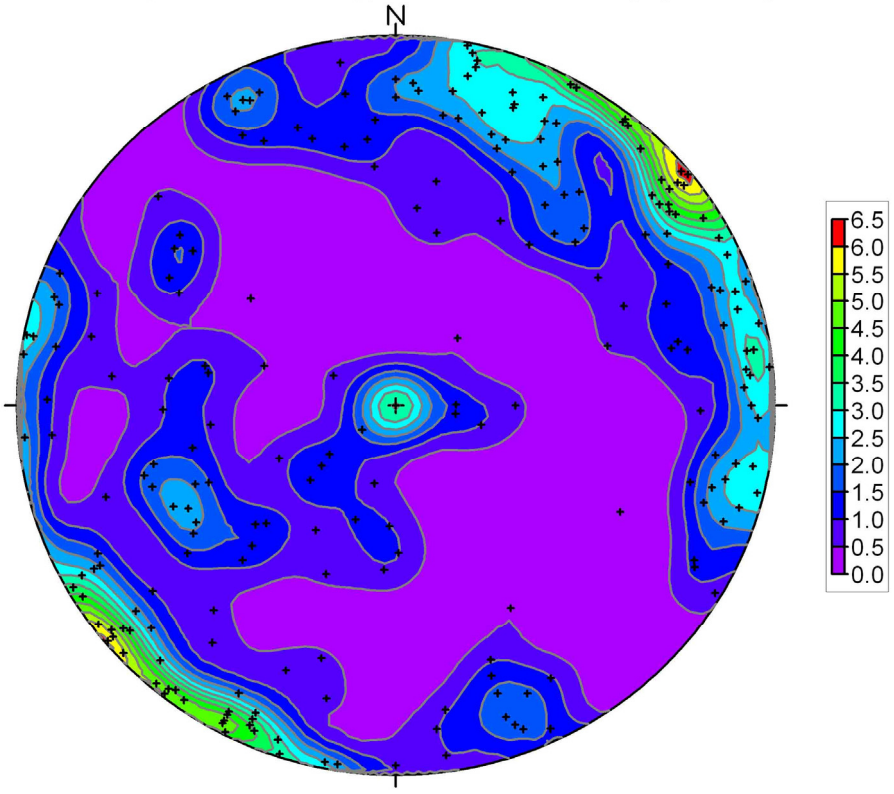

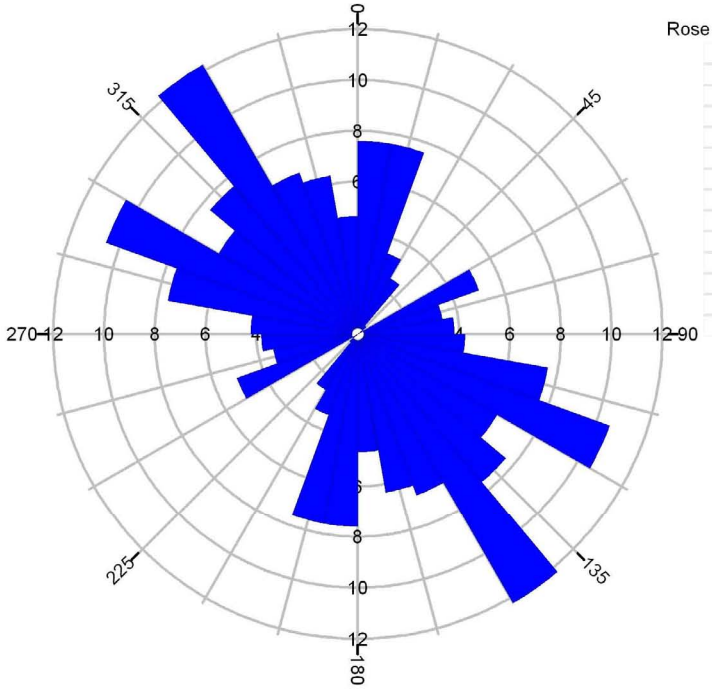

Rose Diagram, KI0016B01, Closed fractures

Statistical Summary

Calculation Method:	Frequency
Class Interval:	10 Degrees
Azimuth Filtering:	Deactivated
Data Type:	Bidirectional
Population:	237
Maximum Percentage:	12.2 Percent
Mean Percentage:	5.9 Percent
Standard Deviation:	2.9 Percent
Vector Mean:	140.5 Degrees
	320.46 Degrees
Confidence Interval:	16.2 Degrees
	(95 Percent)
R-mag:	0.31

KI0016B01, Sealed Networks (UC), poles on Schmidt Net (Equal Area)

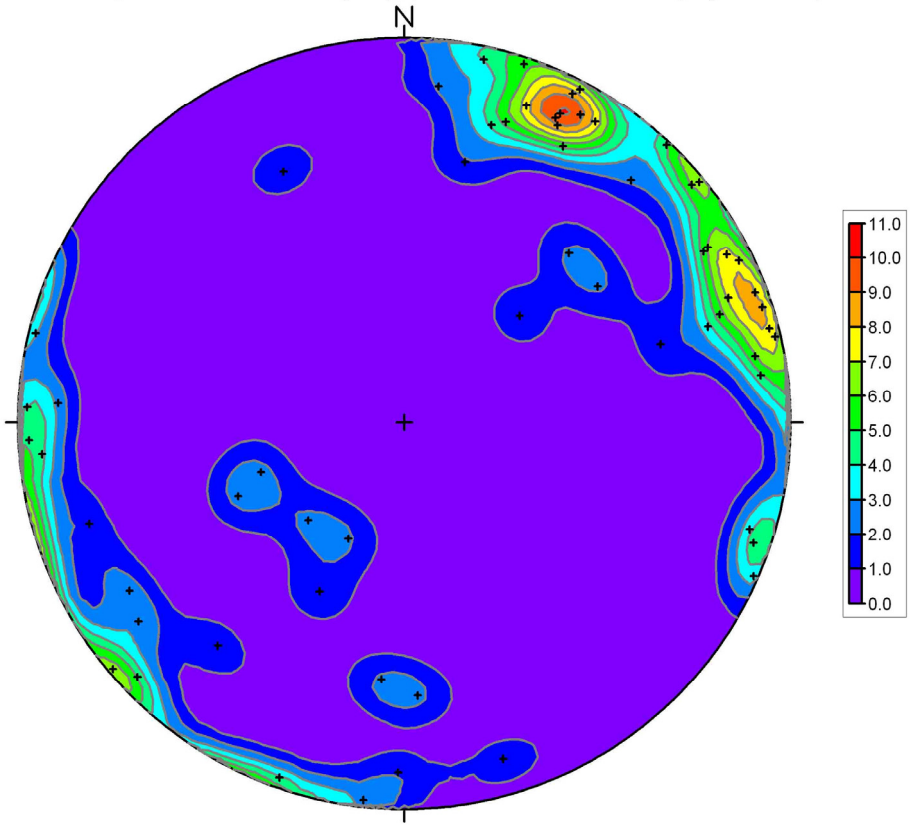

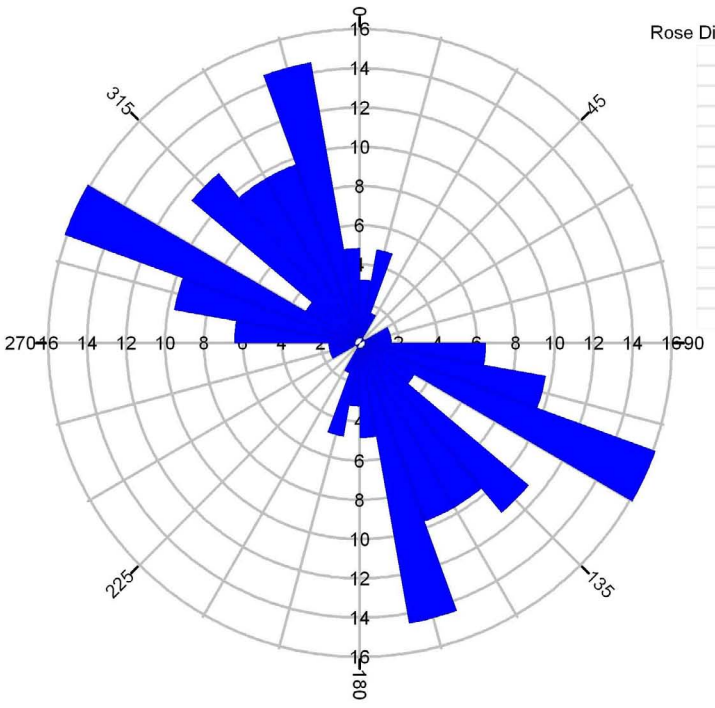

Rose Diagram, KI0016B01, Sealed Networks (UC)

Statistical Summary	
Calculation Method:	Frequency
Class Interval:	10 Degrees
Azimuth Filtering:	Deactivated
Data Type:	Bidirectional
Population:	62
Maximum Percentage:	16.1 Percent
Mean Percentage:	6.7 Percent
Standard Deviation:	4.8 Percent
Vector Mean:	138.2 Degrees
	318.2 Degrees
Confidence Interval:	17.8 Degrees
	(95 Percent)
R-mag:	0.52

KI0016B01, Cataclastic structures, poles on Schmidt Net (Equal Area)

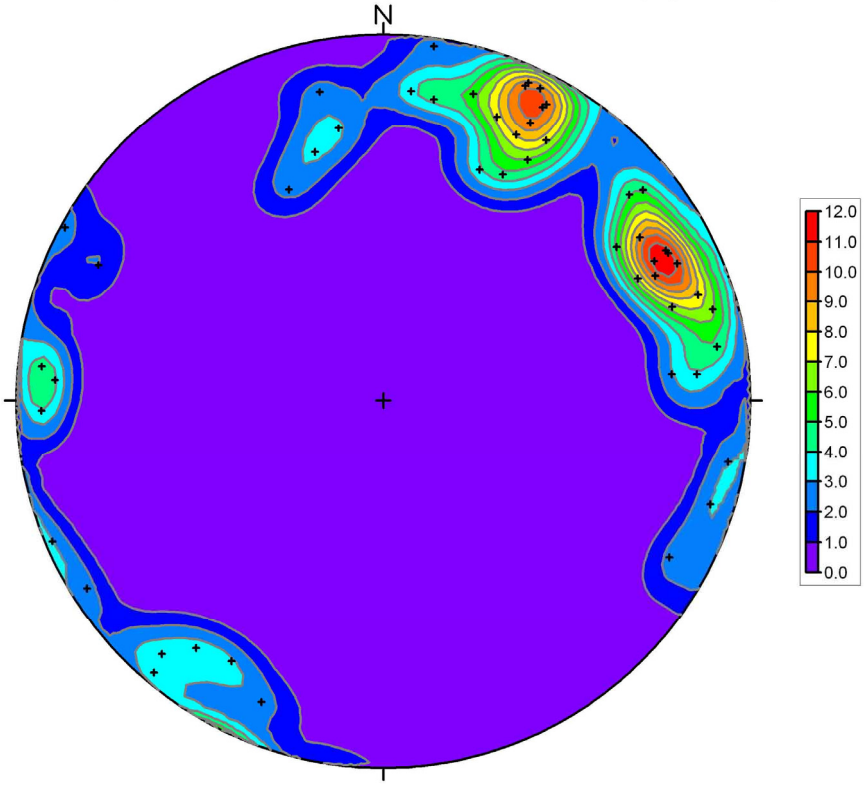

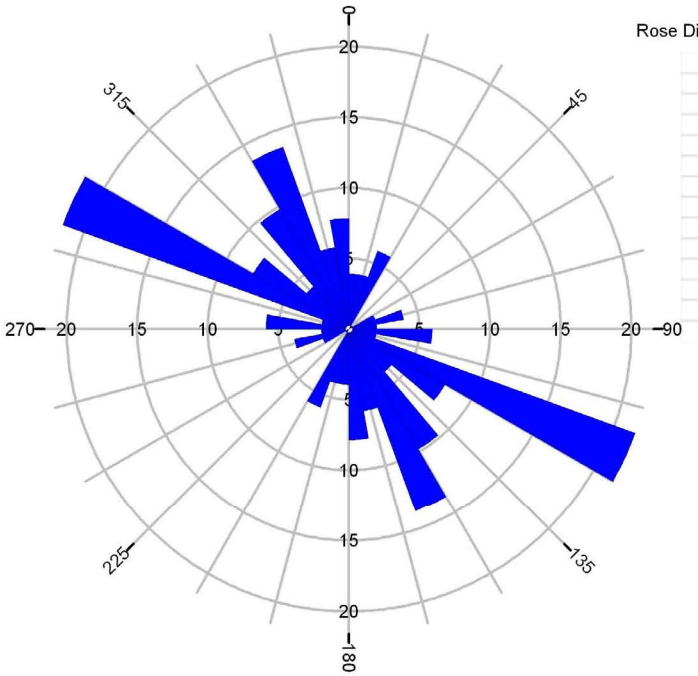

Rose Diagram, KI0016B01, Cataclastic structures

Statistical Summary	
Calculation Method:	Frequency
Class Interval:	10 Degrees
Azimuth Filtering:	Deactivated
Data Type:	Bidirectional
Population:	51
Maximum Percentage:	21.6 Percent
Mean Percentage:	6.7 Percent
Standard Deviation:	5.1 Percent
Vector Mean:	137.2 Degrees
	317.22 Degrees
Confidence Interval:	23.9 Degrees
	(95 Percent)
R-mag:	0.44

Appendix 5

Graphs showing the results of the PFL difference flow logging

Äspö, borehole KI0010B01
Flow rate and single point resistance

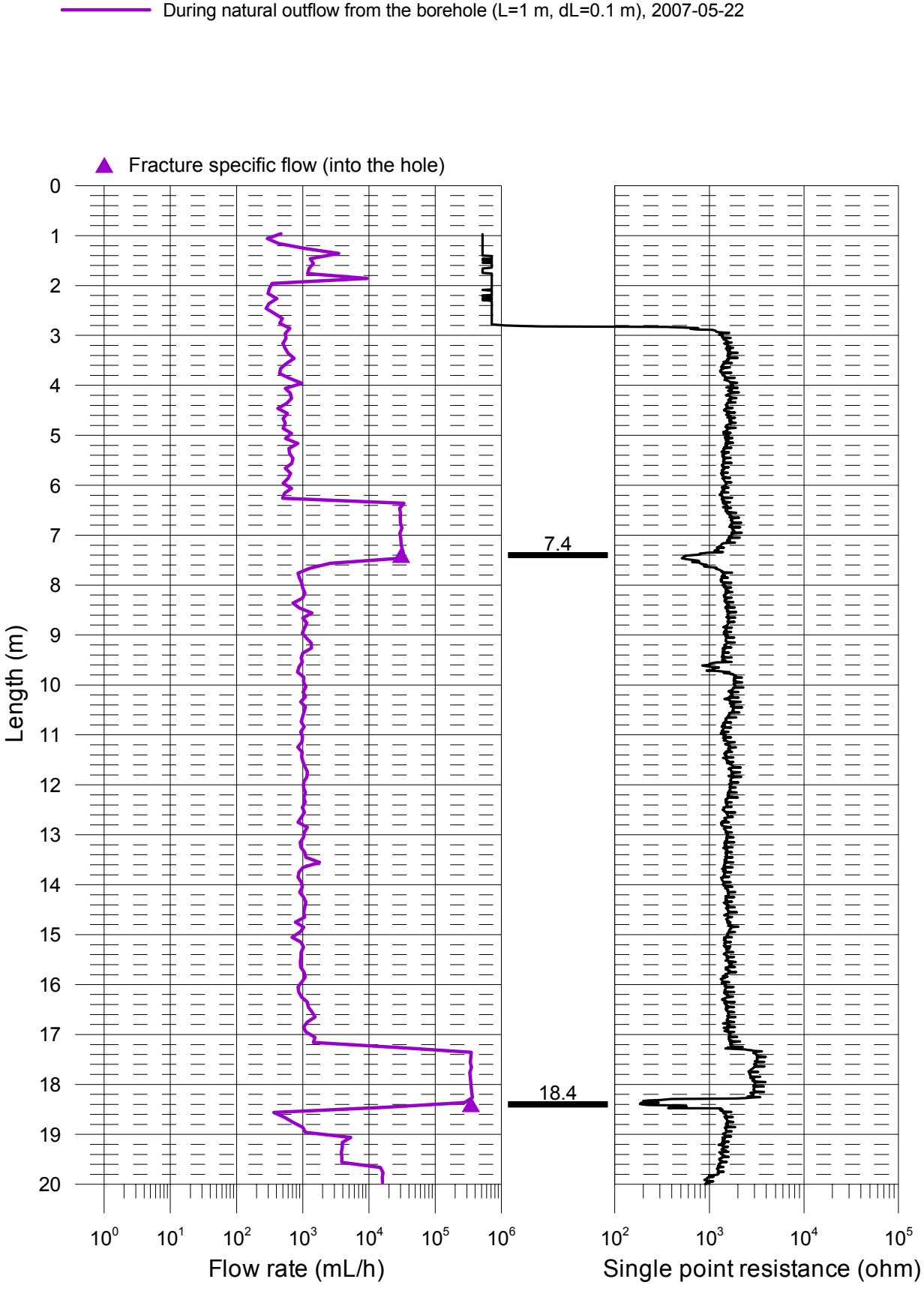

Äspö, borehole KI0010B01
Flow rate and single point resistance

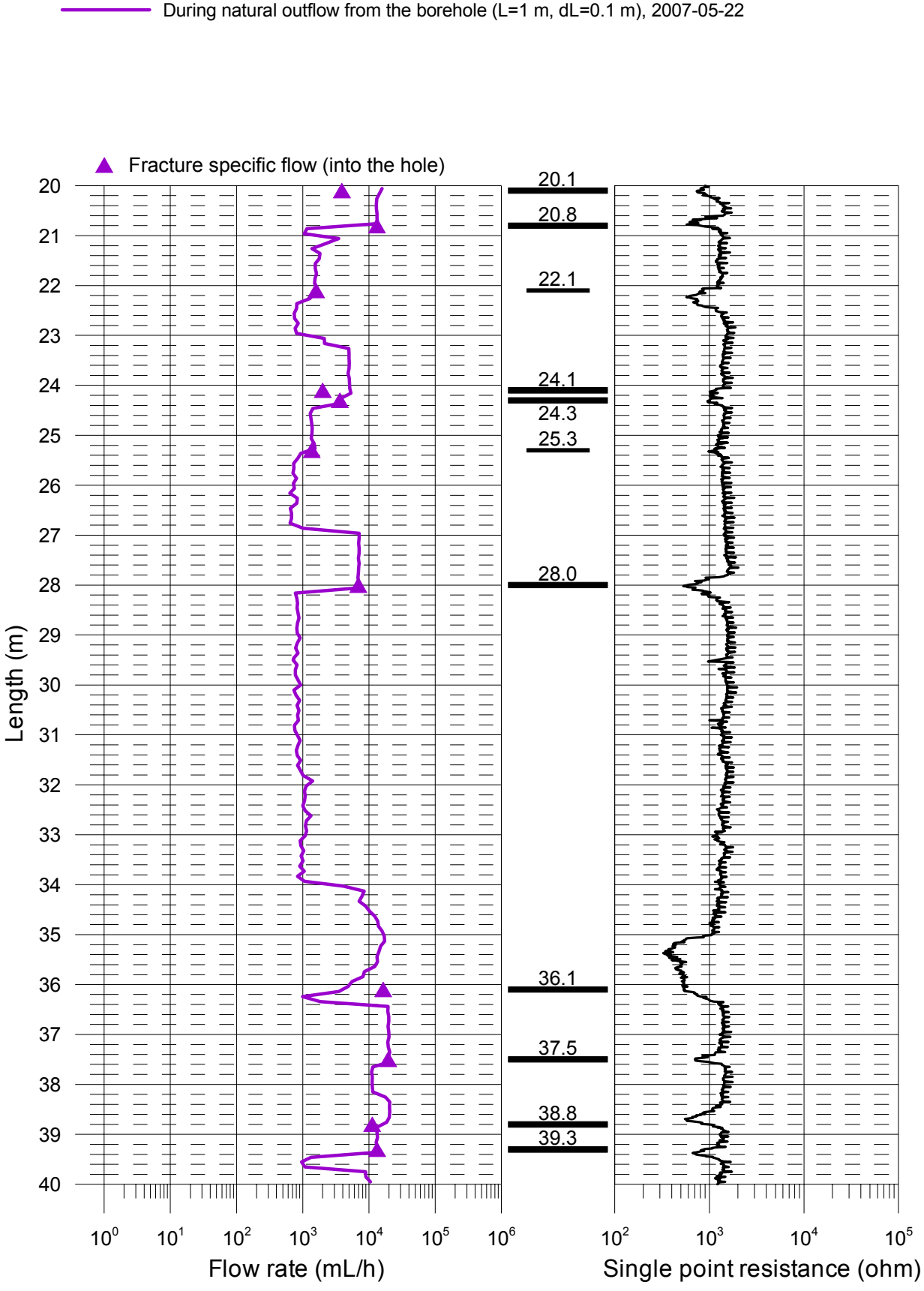

Äspö, borehole KI0010B01
Flow rate and single point resistance

During natural outflow from the borehole (L=1 m, dL=0.1 m), 2007-05-22

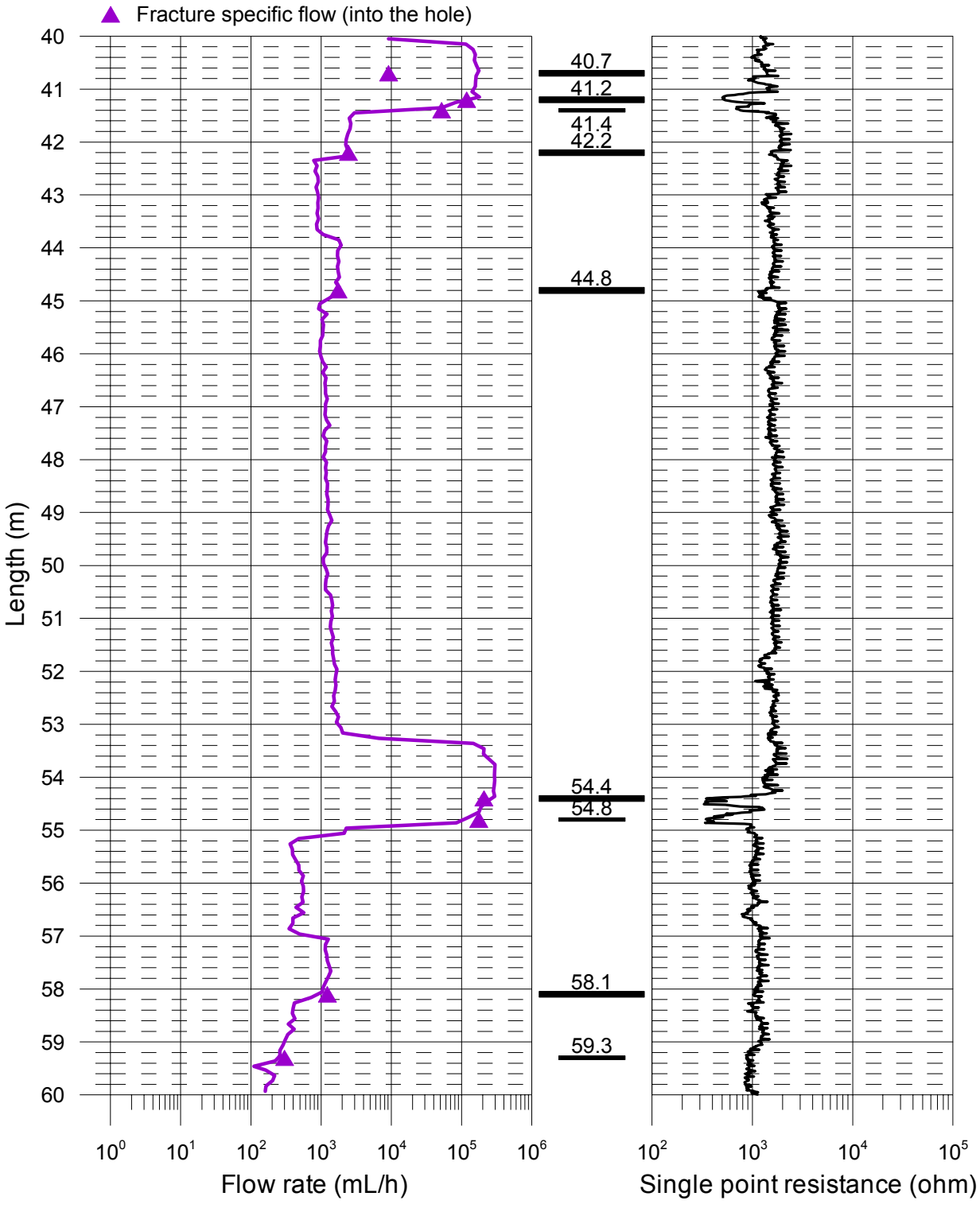

Äspö, borehole KI0010B01
Flow rate and single point resistance

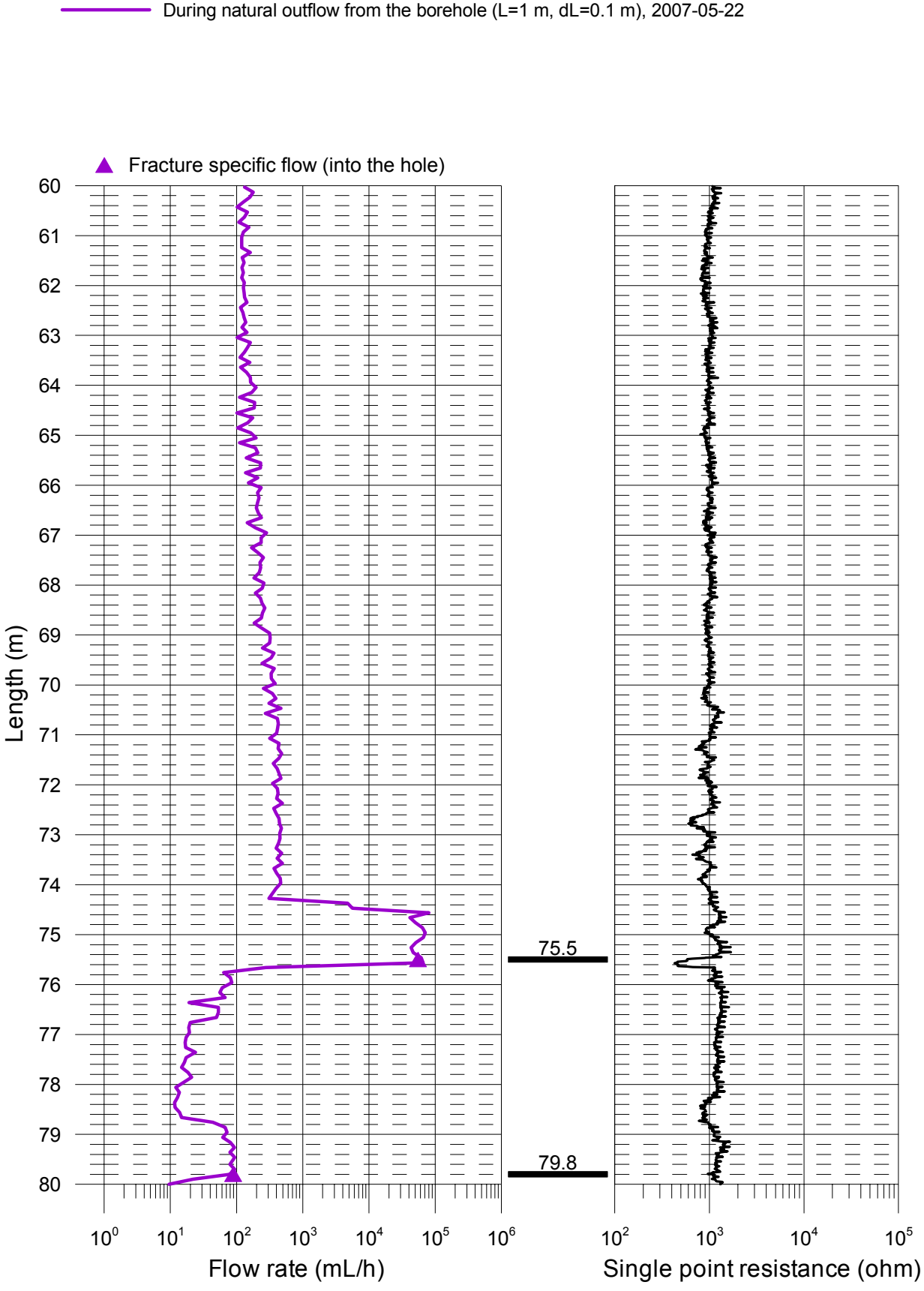

Äspö, borehole KI0010B01
Flow rate and single point resistance

During natural outflow from the borehole (L=1 m, dL=0.1 m), 2007-05-22

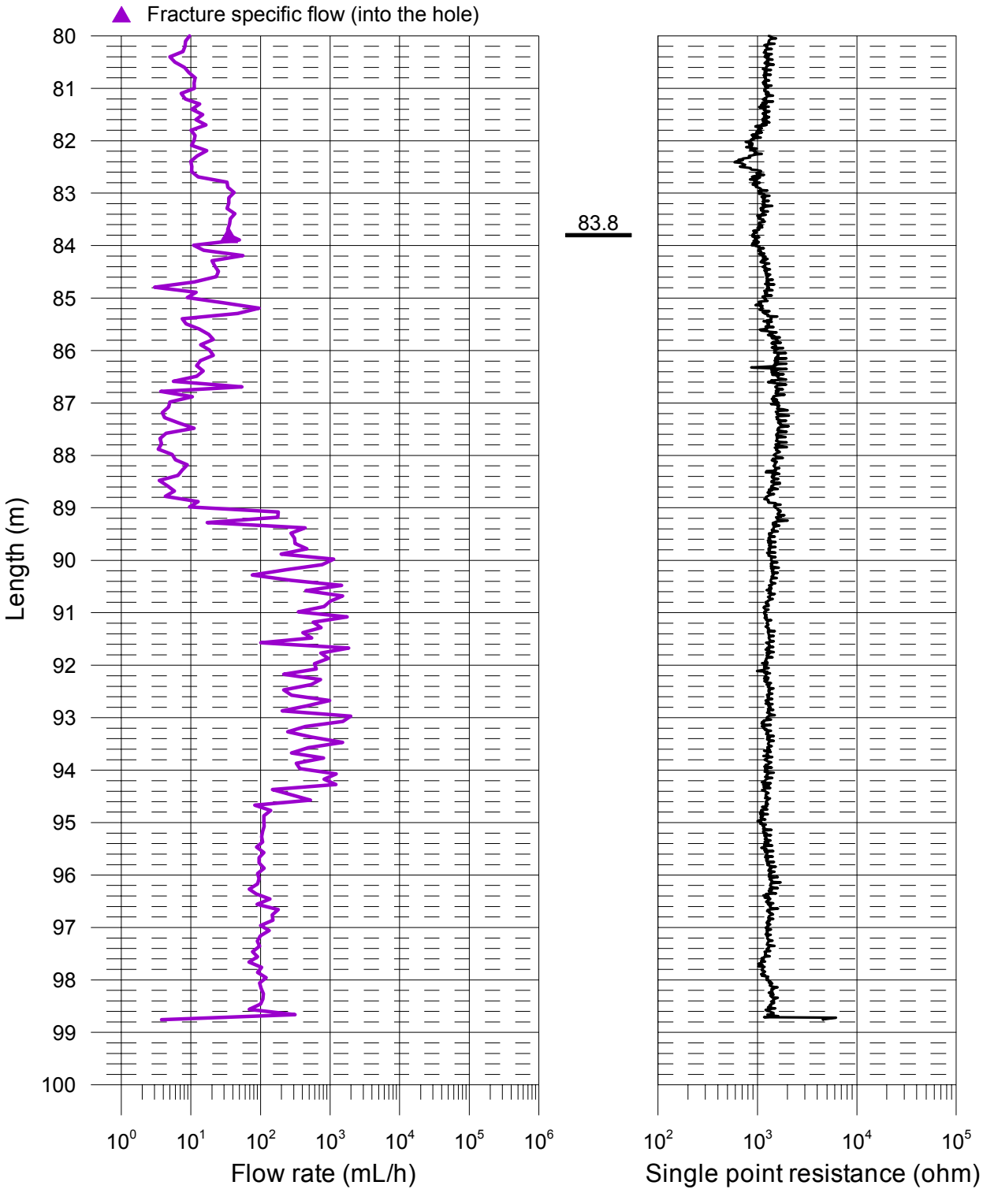

Äspö, borehole KI0010B01
Electric conductivity of borehole water

Measured with lower rubber disks:
During natural outflow from the borehole, 2007-05-22

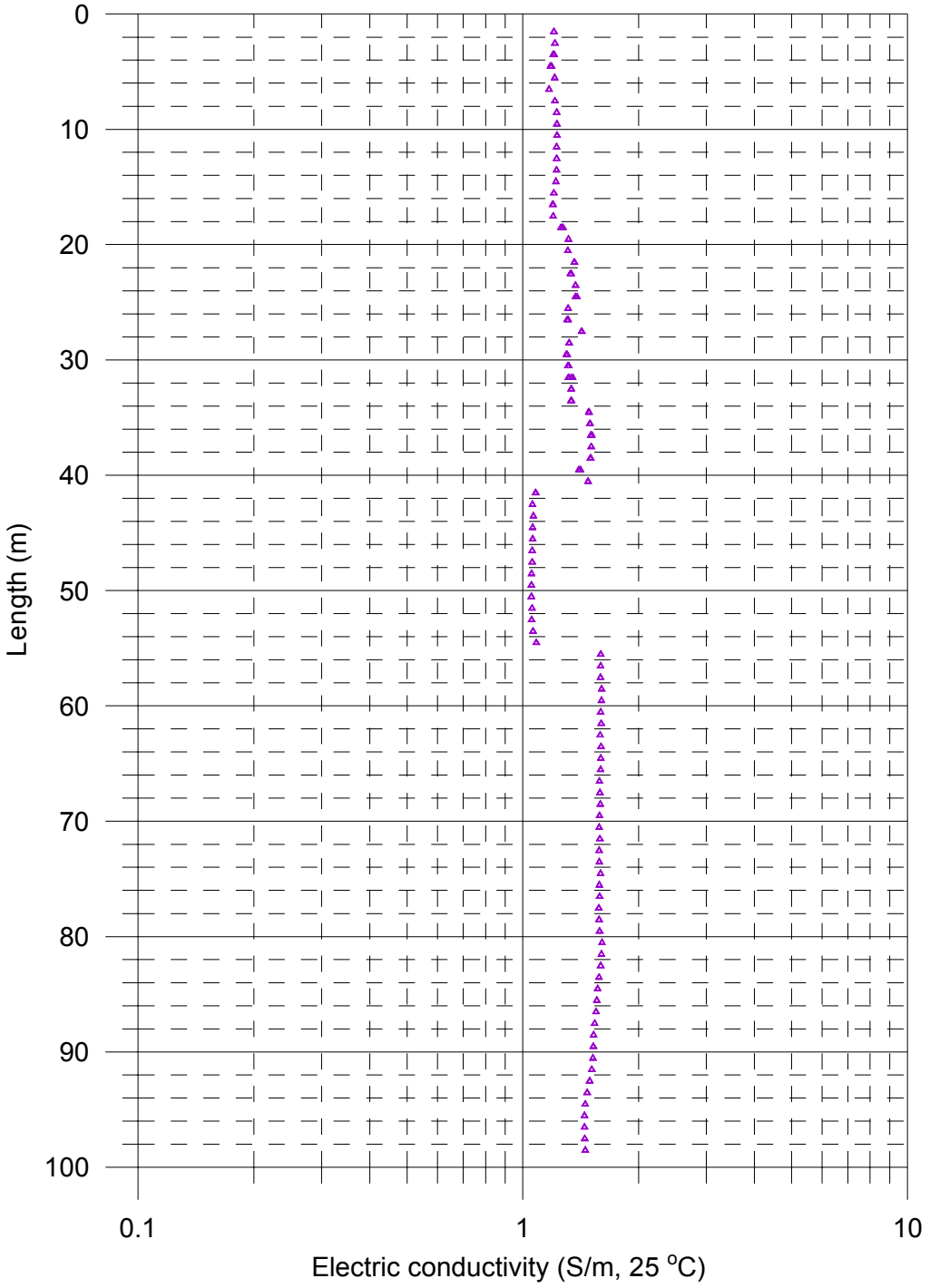

Äspö, borehole KI0010B01
Temperature of borehole water

Measured with lower rubber disks:
During natural outflow from the borehole, 2007-05-22

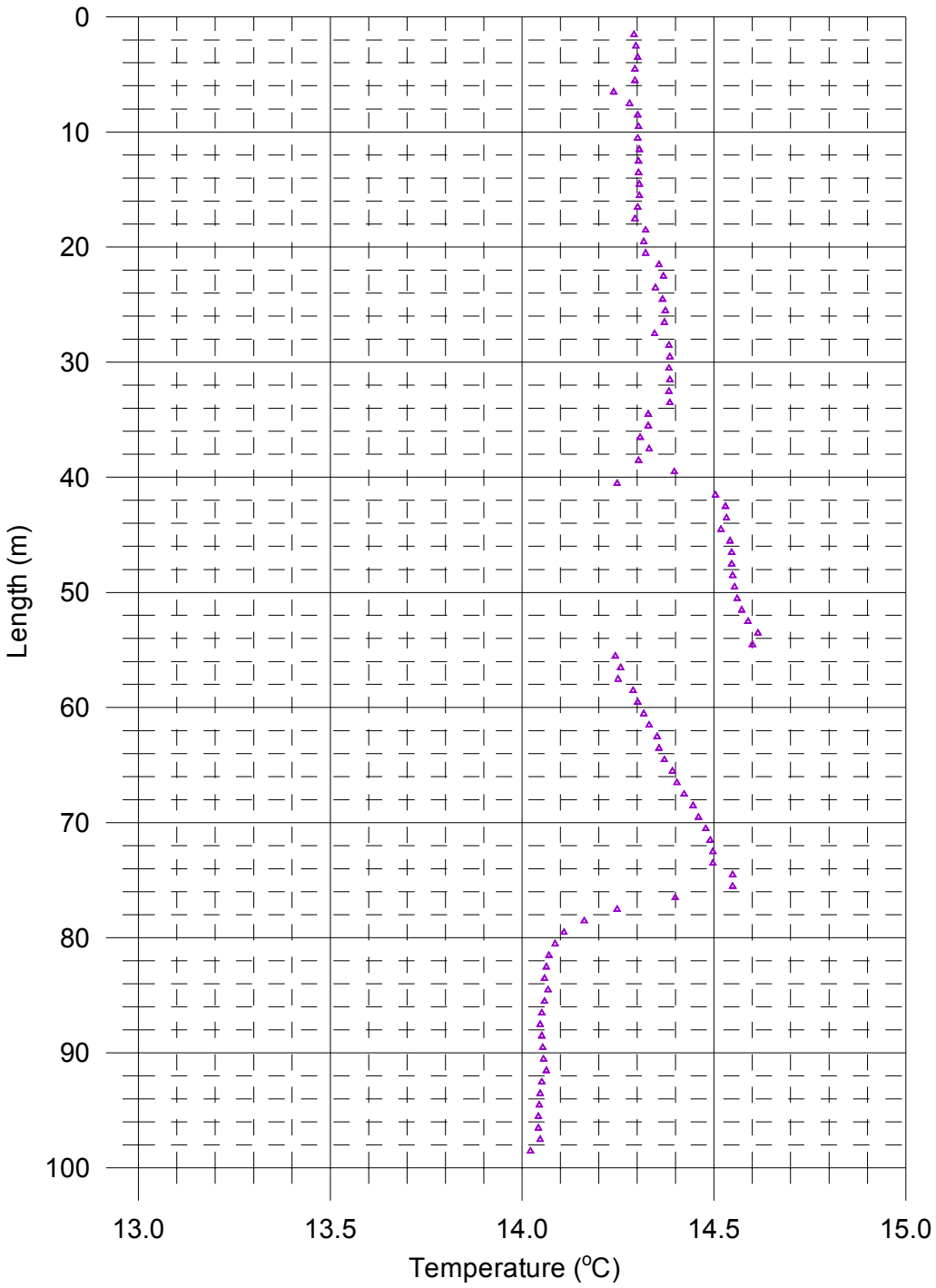

Äspö, borehole KI001B01
Flow rate out from the borehole during flow logging

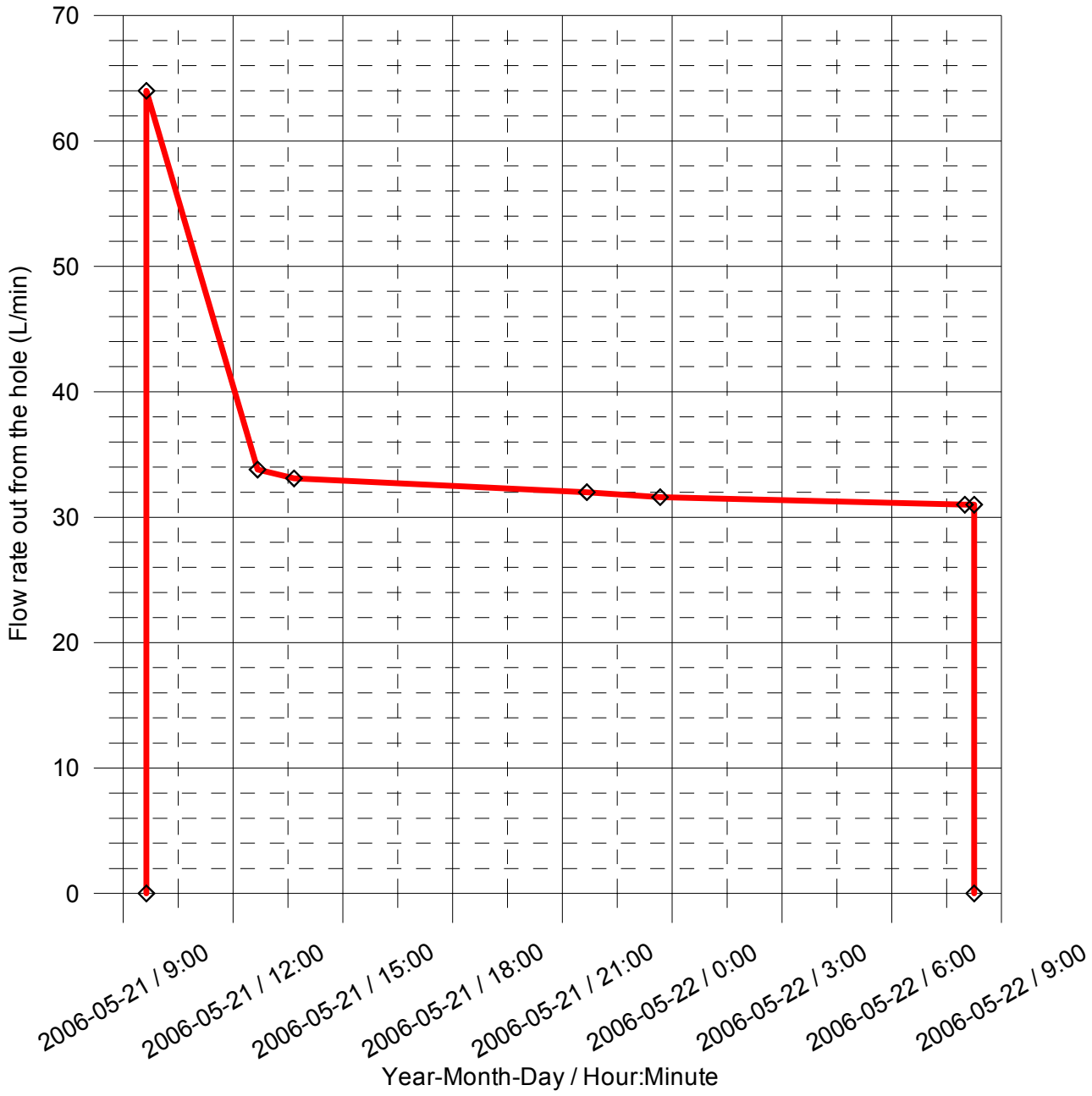

Appendix 6

Tables and diagrams referring to the the hydro-geological diagrams in chapter 5

KI0010B01: Transmissivities in sections - tests during drilling (see Figure 5-10)

KI0010B01 Transmissiviteter i sektioner
Analys baserad på de första indata från tester under borrning, alltså helhålsinflöde allteftersom hålet borrades.
Inflödena är anpassade så att ingen sektion får negativt flöde.
Trycket är anpassat med separat analys (se kapitel 5.3.1).
T approximerad som T≈Q/dh

KI0010B01 Transmissivity in sections
Analyses based on the first data delivered from tests during drilling, meaning full-hole inflow while drilling the borehole.
The inflow is adjusted to give all sections a positive flow.
The pressure is adjusted by using a separate analysis (see chapter 5.3.1).
T is approximated as T≈Q/dh

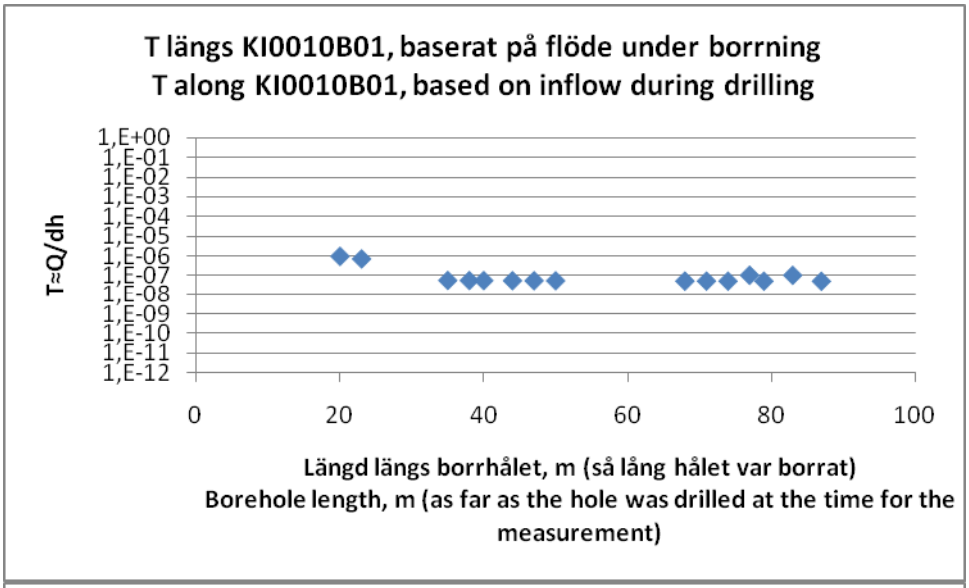

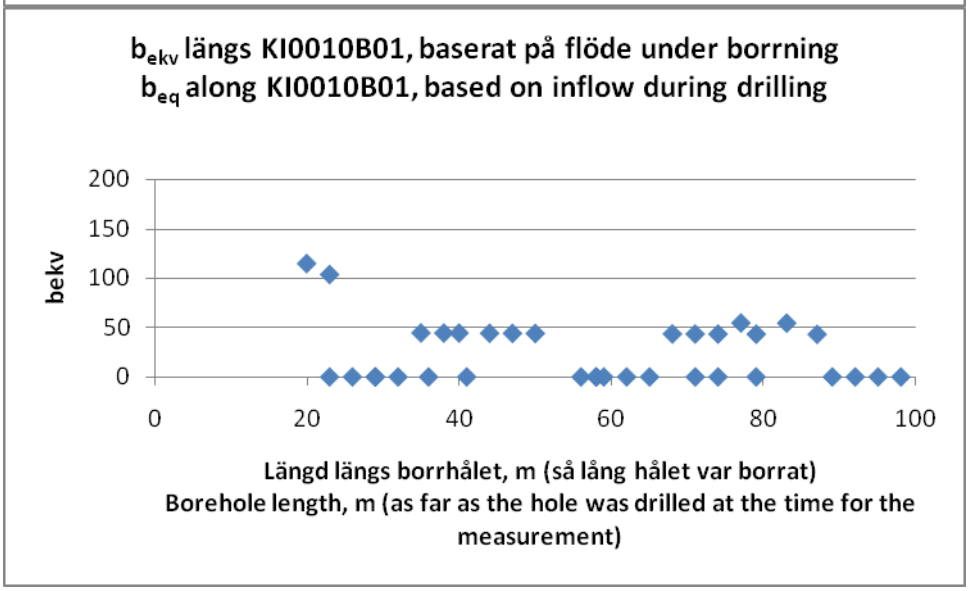

Appendix 6A

Borehole: KI0010B01

Bh length (m) Bhlängd (m)	T ≈ Q/dh [m^2/s]	b_{eq} [µm]
0		
17		
20	9,34E-07	114,09
23	6,89E-07	103,09
23	0,00E+00	0,00
26	0,00E+00	0,00
29	0,00E+00	0,00
29	0,00E+00	0,00
32	0,00E+00	0,00
35	5,47E-08	44,31
36	0,00E+00	0,00
38	5,42E-08	44,18
40	5,39E-08	44,09
41	0,00E+00	0,00
44	5,34E-08	43,94
47	5,30E-08	43,84
50	5,26E-08	43,74
56	0,00E+00	0,00
58	0,00E+00	0,00
58	0,00E+00	0,00
59	0,00E+00	0,00
62	0,00E+00	0,00
65	0,00E+00	0,00
68	5,09E-08	43,27
71	5,07E-08	43,20
71	0,00E+00	0,00
74	5,05E-08	43,14
74	0,00E+00	0,00
77	1,01E-07	54,28
79	5,02E-08	43,04
79	0,00E+00	0,00
83	9,98E-08	54,14
87	4,97E-08	42,90
89	0,00E+00	0,00
92	0,00E+00	0,00
95	0,00E+00	0,00
98	0,00E+00	0,00

KI0010B01: Transmissivities in 3 m sections based on Double packer tests - (see Figure 5-13)

KI0010B01 Transmissiviteter i 3 m-sektioner

Analys baserad på dubbelmanschettmätningarna.
T beräknad med Moye's formel

KI0010B01 Transmissivities in 3 m sections

Analyses based on double packer tests
T calculated by using Moye's formula

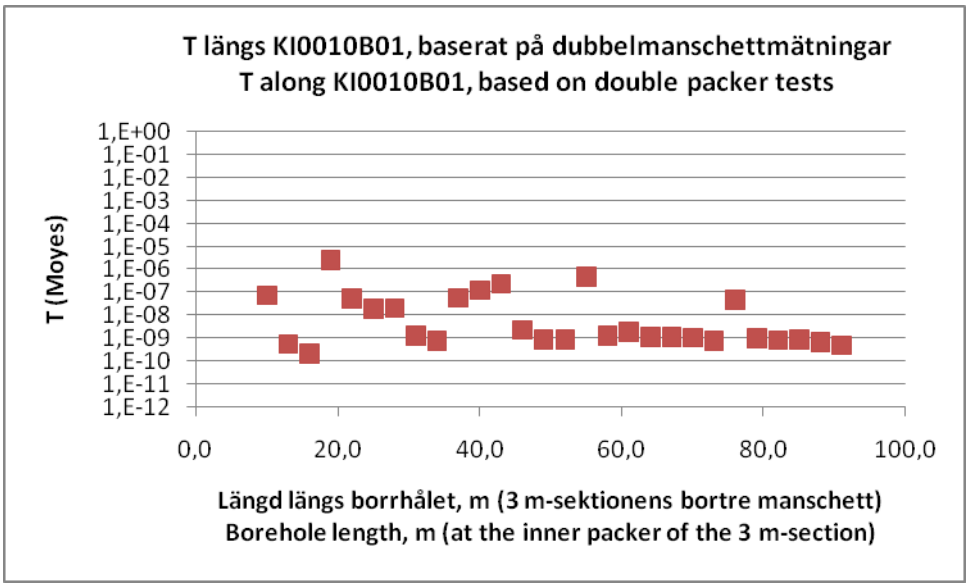

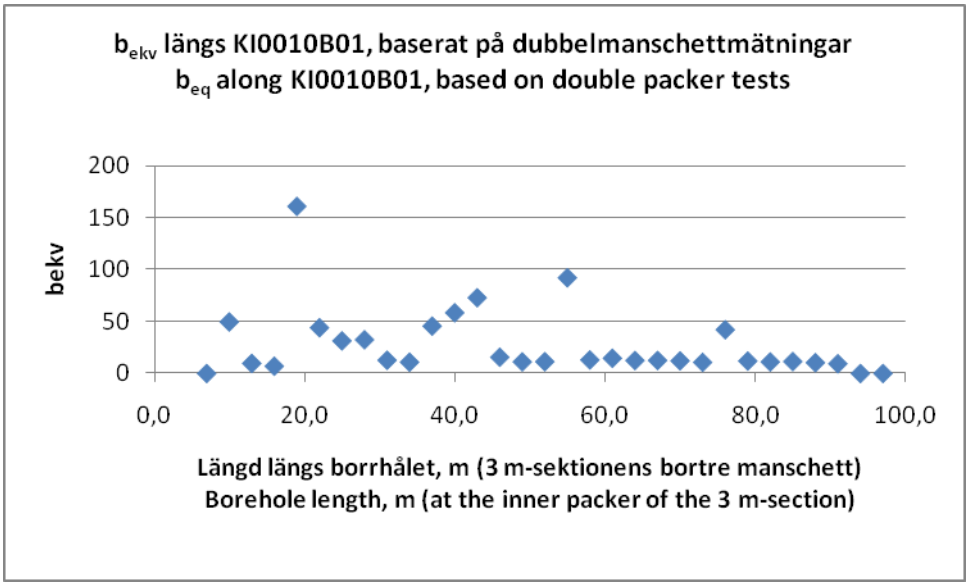

Appendix 6B

Borehole: KI0010B01

Borehole length (m) Bhlängd (m)		T (Moyes) [m^2/s]	b_{eq} [µm]
Upper Övre	Lower Nedre		
94,0	97,0	0,0E+00	0,00
91,0	94,0	0,0E+00	0,00
88,0	91,0	5,2E-10	9,39
85,0	88,0	7,3E-10	10,51
82,0	85,0	9,6E-10	11,53
79,0	82,0	8,8E-10	11,18
76,0	79,0	1,1E-09	12,04
73,0	76,0	4,7E-08	42,25
70,0	73,0	7,9E-10	10,77
67,0	70,0	1,1E-09	12,22
64,0	67,0	1,2E-09	12,52
61,0	64,0	1,2E-09	12,57
58,0	61,0	2,0E-09	14,69
55,0	58,0	1,4E-09	13,08
52,0	55,0	4,9E-07	92,28
49,0	52,0	9,4E-10	11,42
46,0	49,0	9,0E-10	11,28
43,0	46,0	2,4E-09	15,72
40,0	43,0	2,5E-07	73,08
37,0	40,0	1,3E-07	58,57
34,0	37,0	6,0E-08	45,70
31,0	34,0	8,2E-10	10,93
28,0	31,0	1,3E-09	12,79
25,0	28,0	2,2E-08	32,56
22,0	25,0	2,0E-08	31,46
19,0	22,0	5,4E-08	44,17
16,0	19,0	2,6E-06	161,17
13,0	16,0	2,2E-10	7,07
10,0	13,0	5,9E-10	9,78
7,0	10,0	7,7E-08	49,70
4,0	7,0	0,0E+00	0,00

KI0010B01: Transmissivities based on PFL-anomalies (see Figure 5-16)

KI0010B01 Transmissiviteter baserat på PFL-anomalier

Trycket är anpassat med separat analys.
Kolumn C: T approximerad som T≈Q/dh
Kolumn F: T beräknat med Thiems ekvation

KI0010B Transmissivities based on PFL-anomalies

The pressure is adjusted by a separate anaysis.
Column C: T is approximated to T≈Q/dh
Column F: T has been calculated with Thiem´s equation

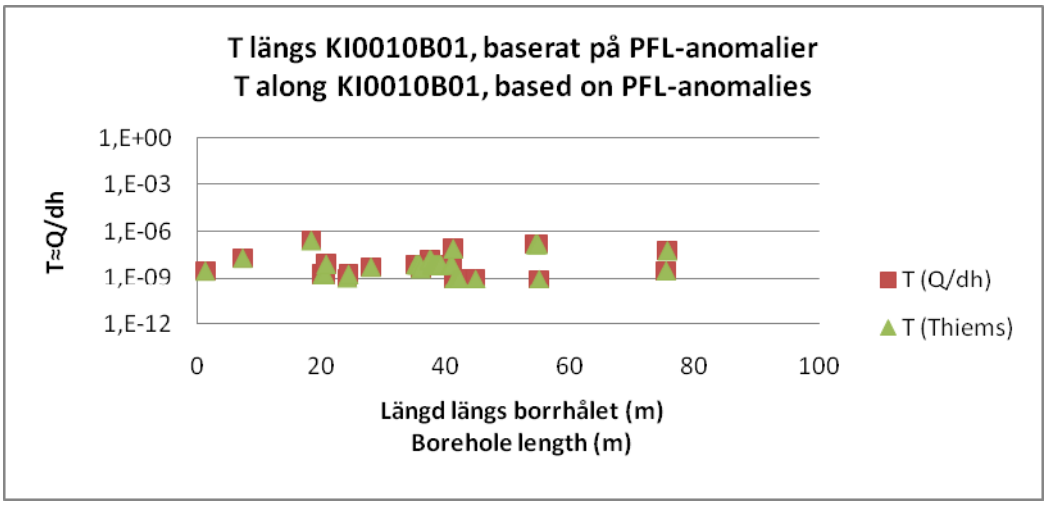

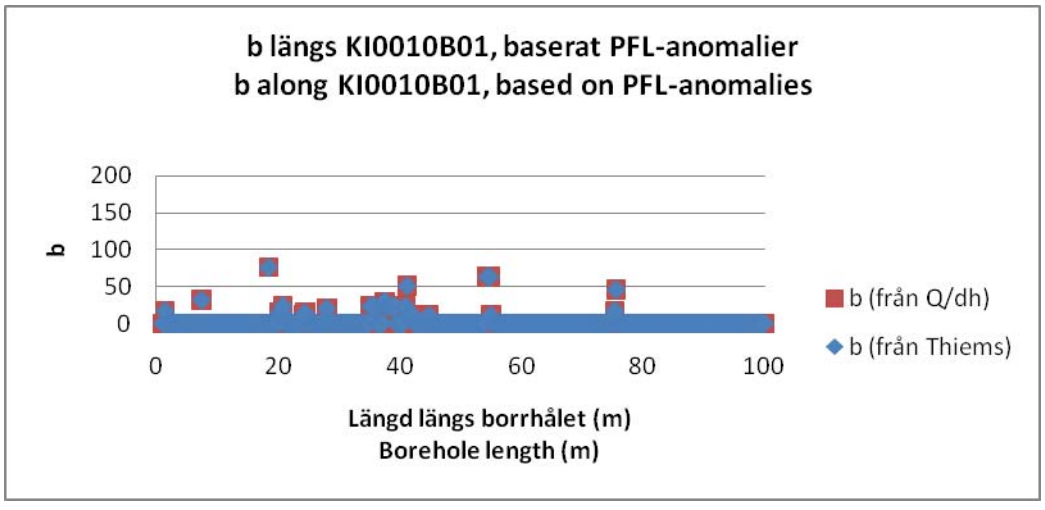

Appendix 6C

Borehole: KI0010B01

Evaluation using Thiem´s equation
in stead of T ≈ Q/dh
Utvärdering med Thiems ekvation
i stället för T ≈ Q/dh

Borehole length (m) Borrålslängd [m]		column C T≈Q/dh [m^2/s]	b [µm]		column F T [m^2/s]	b [µm]
1		0,00E+00	0		0,00E+00	0
1,2		0,00E+00	0		0,00E+00	0
1,4		2,95E-09	16,73445		2,91E-09	16,67334
1,6		0,00E+00	0		0,00E+00	0
1,8		0,00E+00	0		0,00E+00	0
2		0,00E+00	0		0,00E+00	0
2,2		0,00E+00	0		0,00E+00	0
2,4		0,00E+00	0		0,00E+00	0
2,6		0,00E+00	0		0,00E+00	0
2,8		0,00E+00	0		0,00E+00	0
3		0,00E+00	0		0,00E+00	0
3,2		0,00E+00	0		0,00E+00	0
3,4		0,00E+00	0		0,00E+00	0
3,6		0,00E+00	0		0,00E+00	0
3,8		0,00E+00	0		0,00E+00	0
4		0,00E+00	0		0,00E+00	0
4,2		0,00E+00	0		0,00E+00	0
4,4		0,00E+00	0		0,00E+00	0
4,6		0,00E+00	0		0,00E+00	0
4,8		0,00E+00	0		0,00E+00	0
5		0,00E+00	0		0,00E+00	0
5,2		0,00E+00	0		0,00E+00	0
5,4		0,00E+00	0		0,00E+00	0
5,6		0,00E+00	0		0,00E+00	0
5,8		0,00E+00	0		0,00E+00	0
6		0,00E+00	0		0,00E+00	0
6,2		0,00E+00	0		0,00E+00	0
6,4		0,00E+00	0		0,00E+00	0
6,6		0,00E+00	0		0,00E+00	0
6,8		0,00E+00	0		0,00E+00	0
7		0,00E+00	0		0,00E+00	0
7,2		0,00E+00	0		0,00E+00	0
7,4		2,04E-08	31,88075		2,02E-08	31,76434
7,6		0,00E+00	0		0,00E+00	0
7,8		0,00E+00	0		0,00E+00	0

Appendix 6C

Borehole length (m) Borrålslängd [m]		column C T≈Q/dh [m^2/s]	b [µm]		column F T [m^2/s]	b [µm]
8		0,00E+00	0		0,00E+00	0
8,2		0,00E+00	0		0,00E+00	0
8,4		0,00E+00	0		0,00E+00	0
8,6		0,00E+00	0		0,00E+00	0
8,8		0,00E+00	0		0,00E+00	0
9		0,00E+00	0		0,00E+00	0
9,2		0,00E+00	0		0,00E+00	0
9,4		0,00E+00	0		0,00E+00	0
9,6		0,00E+00	0		0,00E+00	0
9,8		0,00E+00	0		0,00E+00	0
10		0,00E+00	0		0,00E+00	0
10,2		0,00E+00	0		0,00E+00	0
10,4		0,00E+00	0		0,00E+00	0
10,6		0,00E+00	0		0,00E+00	0
10,8		0,00E+00	0		0,00E+00	0
11		0,00E+00	0		0,00E+00	0
11,2		0,00E+00	0		0,00E+00	0
11,4		0,00E+00	0		0,00E+00	0
11,6		0,00E+00	0		0,00E+00	0
11,8		0,00E+00	0		0,00E+00	0
12		0,00E+00	0		0,00E+00	0
12,2		0,00E+00	0		0,00E+00	0
12,4		0,00E+00	0		0,00E+00	0
12,6		0,00E+00	0		0,00E+00	0
12,8		0,00E+00	0		0,00E+00	0
13		0,00E+00	0		0,00E+00	0
13,2		0,00E+00	0		0,00E+00	0
13,4		0,00E+00	0		0,00E+00	0
13,6		0,00E+00	0		0,00E+00	0
13,8		0,00E+00	0		0,00E+00	0
14		0,00E+00	0		0,00E+00	0
14,2		0,00E+00	0		0,00E+00	0
14,4		0,00E+00	0		0,00E+00	0
14,6		0,00E+00	0		0,00E+00	0
14,8		0,00E+00	0		0,00E+00	0
15		0,00E+00	0		0,00E+00	0
15,2		0,00E+00	0		0,00E+00	0
15,4		0,00E+00	0		0,00E+00	0
15,6		0,00E+00	0		0,00E+00	0
15,8		0,00E+00	0		0,00E+00	0
16		0,00E+00	0		0,00E+00	0

Appendix 6C

Borehole length (m) Borrålslängd [m]		column C T≈Q/dh [m^2/s]	b [µm]		column F T [m^2/s]	b [µm]
16,2		0,00E+00	0		0,00E+00	0
16,4		0,00E+00	0		0,00E+00	0
16,6		0,00E+00	0		0,00E+00	0
16,8		0,00E+00	0		0,00E+00	0
17		0,00E+00	0		0,00E+00	0
17,2		0,00E+00	0		0,00E+00	0
17,4		0,00E+00	0		0,00E+00	0
17,6		0,00E+00	0		0,00E+00	0
17,8		0,00E+00	0		0,00E+00	0
18		0,00E+00	0		0,00E+00	0
18,2		0,00E+00	0		0,00E+00	0
18,4		2,79E-07	76,27942		2,76E-07	76,00089
18,6		0,00E+00	0		0,00E+00	0
18,8		0,00E+00	0		0,00E+00	0
19		0,00E+00	0		0,00E+00	0
19,2		0,00E+00	0		0,00E+00	0
19,4		0,00E+00	0		0,00E+00	0
19,6		0,00E+00	0		0,00E+00	0
19,8		0,00E+00	0		0,00E+00	0
20		0,00E+00	0		0,00E+00	0
20,2		1,84E-09	14,30926		1,82E-09	14,25701
20,4		1,84E-09	14,30267		1,82E-09	14,25044
20,6		1,84E-09	14,29615		1,82E-09	14,24395
20,8		8,26E-09	23,59179		8,17E-09	23,50565
21		0,00E+00	0		0,00E+00	0
21,2		0,00E+00	0		0,00E+00	0
21,4		0,00E+00	0		0,00E+00	0
21,6		0,00E+00	0		0,00E+00	0
21,8		0,00E+00	0		0,00E+00	0
22		0,00E+00	0		0,00E+00	0
22,2		0,00E+00	0		0,00E+00	0
22,4		0,00E+00	0		0,00E+00	0
22,6		0,00E+00	0		0,00E+00	0
22,8		0,00E+00	0		0,00E+00	0
23		0,00E+00	0		0,00E+00	0
23,2		0,00E+00	0		0,00E+00	0
23,4		0,00E+00	0		0,00E+00	0
23,6		0,00E+00	0		0,00E+00	0
23,8		0,00E+00	0		0,00E+00	0
24		0,00E+00	0		0,00E+00	0
24,2		8,98E-10	11,26282		8,89E-10	11,22169

Appendix 6C

Borehole length (m) Borrålslängd [m]		column C T≈Q/dh [m^2/s]	b [µm]		column F T [m^2/s]	b [µm]
24,4		1,79E-09	14,18494		1,78E-09	14,13314
24,6		0,00E+00	0		0,00E+00	0
24,8		0,00E+00	0		0,00E+00	0
25		0,00E+00	0		0,00E+00	0
25,2		0,00E+00	0		0,00E+00	0
25,4		0,00E+00	0		0,00E+00	0
25,6		0,00E+00	0		0,00E+00	0
25,8		0,00E+00	0		0,00E+00	0
26		0,00E+00	0		0,00E+00	0
26,2		0,00E+00	0		0,00E+00	0
26,4		0,00E+00	0		0,00E+00	0
26,6		0,00E+00	0		0,00E+00	0
26,8		0,00E+00	0		0,00E+00	0
27		0,00E+00	0		0,00E+00	0
27,2		0,00E+00	0		0,00E+00	0
27,4		0,00E+00	0		0,00E+00	0
27,6		0,00E+00	0		0,00E+00	0
27,8		0,00E+00	0		0,00E+00	0
28		5,29E-09	20,33143		5,23E-09	20,25719
28,2		0,00E+00	0		0,00E+00	0
28,4		0,00E+00	0		0,00E+00	0
28,6		0,00E+00	0		0,00E+00	0
28,8		0,00E+00	0		0,00E+00	0
29		0,00E+00	0		0,00E+00	0
29,2		0,00E+00	0		0,00E+00	0
29,4		0,00E+00	0		0,00E+00	0
29,6		0,00E+00	0		0,00E+00	0
29,8		0,00E+00	0		0,00E+00	0
30		0,00E+00	0		0,00E+00	0
30,2		0,00E+00	0		0,00E+00	0
30,4		0,00E+00	0		0,00E+00	0
30,6		0,00E+00	0		0,00E+00	0
30,8		0,00E+00	0		0,00E+00	0
31		0,00E+00	0		0,00E+00	0
31,2		0,00E+00	0		0,00E+00	0
31,4		0,00E+00	0		0,00E+00	0
31,6		0,00E+00	0		0,00E+00	0
31,8		0,00E+00	0		0,00E+00	0
32		0,00E+00	0		0,00E+00	0
32,2		0,00E+00	0		0,00E+00	0
32,4		0,00E+00	0		0,00E+00	0

Appendix 6C

Borehole length (m) Borrålslängd [m]		column C T≈Q/dh [m^2/s]	b [µm]		column F T [m^2/s]	b [µm]
32,6		0,00E+00	0		0,00E+00	0
32,8		0,00E+00	0		0,00E+00	0
33		0,00E+00	0		0,00E+00	0
33,2		0,00E+00	0		0,00E+00	0
33,4		0,00E+00	0		0,00E+00	0
33,6		0,00E+00	0		0,00E+00	0
33,8		0,00E+00	0		0,00E+00	0
34		0,00E+00	0		0,00E+00	0
34,2		0,00E+00	0		0,00E+00	0
34,4		0,00E+00	0		0,00E+00	0
34,6		0,00E+00	0		0,00E+00	0
34,8		0,00E+00	0		0,00E+00	0
35		0,00E+00	0		0,00E+00	0
35,2		7,69E-09	23,04009		7,61E-09	22,95596
35,4		7,69E-09	23,03442		7,60E-09	22,95032
35,6		7,68E-09	23,0288		7,60E-09	22,94471
35,8		7,67E-09	23,02321		7,59E-09	22,93914
36		4,26E-09	18,92214		4,21E-09	18,85304
36,2		0,00E+00	0		0,00E+00	0
36,4		0,00E+00	0		0,00E+00	0
36,6		0,00E+00	0		0,00E+00	0
36,8		0,00E+00	0		0,00E+00	0
37		0,00E+00	0		0,00E+00	0
37,2		0,00E+00	0		0,00E+00	0
37,4		1,61E-08	29,47921		1,59E-08	29,37157
37,6		1,61E-08	29,47244		1,59E-08	29,36482
37,8		7,62E-09	22,96924		7,54E-09	22,88537
38		7,62E-09	22,96403		7,53E-09	22,88017
38,2		7,61E-09	22,95884		7,53E-09	22,87501
38,4		7,61E-09	22,9537		7,52E-09	22,86988
38,6		7,60E-09	22,94858		7,52E-09	22,86478
38,8		7,59E-09	22,94349		7,51E-09	22,85972
39		7,59E-09	22,93844		7,51E-09	22,85468
39,2		7,58E-09	22,93341		7,50E-09	22,84967
39,4		0,00E+00	0		0,00E+00	0
39,6		0,00E+00	0		0,00E+00	0
39,8		0,00E+00	0		0,00E+00	0
40		0,00E+00	0		0,00E+00	0
40,2		0,00E+00	0		0,00E+00	0
40,4		0,00E+00	0		0,00E+00	0
40,6		0,00E+00	0		0,00E+00	0

Appendix 6C

Borehole length (m) Borrålslängd [m]		column C T≈Q/dh [m^2/s]	b [µm]		column F T [m^2/s]	b [µm]
40,8		7,55E-09	22,89426		7,46E-09	22,81066
41		7,54E-09	22,88949		7,46E-09	22,80591
41,2		8,29E-08	50,89524		8,20E-08	50,7094
41,4		8,37E-10	10,99958		8,28E-10	10,95941
41,6		8,36E-10	10,99732		8,27E-10	10,95717
41,8		8,36E-10	10,99508		8,27E-10	10,95493
42		8,35E-10	10,99285		8,26E-10	10,95272
42,2		8,35E-10	10,99064		8,26E-10	10,95051
42,4		0,00E+00	0		0,00E+00	0
42,6		0,00E+00	0		0,00E+00	0
42,8		0,00E+00	0		0,00E+00	0
43		0,00E+00	0		0,00E+00	0
43,2		0,00E+00	0		0,00E+00	0
43,4		0,00E+00	0		0,00E+00	0
43,6		0,00E+00	0		0,00E+00	0
43,8		0,00E+00	0		0,00E+00	0
44		0,00E+00	0		0,00E+00	0
44,2		0,00E+00	0		0,00E+00	0
44,4		0,00E+00	0		0,00E+00	0
44,6		0,00E+00	0		0,00E+00	0
44,8		8,29E-10	10,96291		8,20E-10	10,92288
45		0,00E+00	0		0,00E+00	0
45,2		0,00E+00	0		0,00E+00	0
45,4		0,00E+00	0		0,00E+00	0
45,6		0,00E+00	0		0,00E+00	0
45,8		0,00E+00	0		0,00E+00	0
46		0,00E+00	0		0,00E+00	0
46,2		0,00E+00	0		0,00E+00	0
46,4		0,00E+00	0		0,00E+00	0
46,6		0,00E+00	0		0,00E+00	0
46,8		0,00E+00	0		0,00E+00	0
47		0,00E+00	0		0,00E+00	0
47,2		0,00E+00	0		0,00E+00	0
47,4		0,00E+00	0		0,00E+00	0
47,6		0,00E+00	0		0,00E+00	0
47,8		0,00E+00	0		0,00E+00	0
48		0,00E+00	0		0,00E+00	0
48,2		0,00E+00	0		0,00E+00	0
48,4		0,00E+00	0		0,00E+00	0
48,6		0,00E+00	0		0,00E+00	0
48,8		0,00E+00	0		0,00E+00	0

Appendix 6C

Borehole length (m) Borrålslängd [m]		column C T≈Q/dh [m^2/s]	b [µm]		column F T [m^2/s]	b [µm]
49		0,00E+00	0		0,00E+00	0
49,2		0,00E+00	0		0,00E+00	0
49,4		0,00E+00	0		0,00E+00	0
49,6		0,00E+00	0		0,00E+00	0
49,8		0,00E+00	0		0,00E+00	0
50		0,00E+00	0		0,00E+00	0
50,2		0,00E+00	0		0,00E+00	0
50,4		0,00E+00	0		0,00E+00	0
50,6		0,00E+00	0		0,00E+00	0
50,8		0,00E+00	0		0,00E+00	0
51		0,00E+00	0		0,00E+00	0
51,2		0,00E+00	0		0,00E+00	0
51,4		0,00E+00	0		0,00E+00	0
51,6		0,00E+00	0		0,00E+00	0
51,8		0,00E+00	0		0,00E+00	0
52		0,00E+00	0		0,00E+00	0
52,2		0,00E+00	0		0,00E+00	0
52,4		0,00E+00	0		0,00E+00	0
52,6		0,00E+00	0		0,00E+00	0
52,8		0,00E+00	0		0,00E+00	0
53		0,00E+00	0		0,00E+00	0
53,2		0,00E+00	0		0,00E+00	0
53,4		0,00E+00	0		0,00E+00	0
53,6		0,00E+00	0		0,00E+00	0
53,8		0,00E+00	0		0,00E+00	0
54		0,00E+00	0		0,00E+00	0
54,2		0,00E+00	0		0,00E+00	0
54,4		1,61E-07	63,48969		1,59E-07	63,25786
54,6		1,61E-07	63,48012		1,59E-07	63,24833
54,8		1,61E-07	63,47059		1,59E-07	63,23883
55		8,08E-10	10,86984		7,99E-10	10,83015
55,2		0,00E+00	0		0,00E+00	0
55,4		0,00E+00	0		0,00E+00	0
55,6		0,00E+00	0		0,00E+00	0
55,8		0,00E+00	0		0,00E+00	0
56		0,00E+00	0		0,00E+00	0
56,2		0,00E+00	0		0,00E+00	0
56,4		0,00E+00	0		0,00E+00	0
56,6		0,00E+00	0		0,00E+00	0
56,8		0,00E+00	0		0,00E+00	0
57		0,00E+00	0		0,00E+00	0

Appendix 6C

Borehole length (m) Borrålslängd [m]		column C T≈Q/dh [m^2/s]	b [µm]		column F T [m^2/s]	b [µm]
57,2		0,00E+00	0		0,00E+00	0
57,4		0,00E+00	0		0,00E+00	0
57,6		0,00E+00	0		0,00E+00	0
57,8		0,00E+00	0		0,00E+00	0
58		0,00E+00	0		0,00E+00	0
58,2		0,00E+00	0		0,00E+00	0
58,4		0,00E+00	0		0,00E+00	0
58,6		0,00E+00	0		0,00E+00	0
58,8		0,00E+00	0		0,00E+00	0
59		0,00E+00	0		0,00E+00	0
59,2		0,00E+00	0		0,00E+00	0
59,4		0,00E+00	0		0,00E+00	0
59,6		0,00E+00	0		0,00E+00	0
59,8		0,00E+00	0		0,00E+00	0
60		0,00E+00	0		0,00E+00	0
60,2		0,00E+00	0		0,00E+00	0
60,4		0,00E+00	0		0,00E+00	0
60,6		0,00E+00	0		0,00E+00	0
60,8		0,00E+00	0		0,00E+00	0
61		0,00E+00	0		0,00E+00	0
61,2		0,00E+00	0		0,00E+00	0
61,4		0,00E+00	0		0,00E+00	0
61,6		0,00E+00	0		0,00E+00	0
61,8		0,00E+00	0		0,00E+00	0
62		0,00E+00	0		0,00E+00	0
62,2		0,00E+00	0		0,00E+00	0
62,4		0,00E+00	0		0,00E+00	0
62,6		0,00E+00	0		0,00E+00	0
62,8		0,00E+00	0		0,00E+00	0
63		0,00E+00	0		0,00E+00	0
63,2		0,00E+00	0		0,00E+00	0
63,4		0,00E+00	0		0,00E+00	0
63,6		0,00E+00	0		0,00E+00	0
63,8		0,00E+00	0		0,00E+00	0
64		0,00E+00	0		0,00E+00	0
64,2		0,00E+00	0		0,00E+00	0
64,4		0,00E+00	0		0,00E+00	0
64,6		0,00E+00	0		0,00E+00	0
64,8		0,00E+00	0		0,00E+00	0
65		0,00E+00	0		0,00E+00	0
65,2		0,00E+00	0		0,00E+00	0

Appendix 6C

Borehole length (m) Borrålslängd [m]		column C T≈Q/dh [m^2/s]	b [µm]		column F T [m^2/s]	b [µm]
65,4		0,00E+00	0		0,00E+00	0
65,6		0,00E+00	0		0,00E+00	0
65,8		0,00E+00	0		0,00E+00	0
66		0,00E+00	0		0,00E+00	0
66,2		0,00E+00	0		0,00E+00	0
66,4		0,00E+00	0		0,00E+00	0
66,6		0,00E+00	0		0,00E+00	0
66,8		0,00E+00	0		0,00E+00	0
67		0,00E+00	0		0,00E+00	0
67,2		0,00E+00	0		0,00E+00	0
67,4		0,00E+00	0		0,00E+00	0
67,6		0,00E+00	0		0,00E+00	0
67,8		0,00E+00	0		0,00E+00	0
68		0,00E+00	0		0,00E+00	0
68,2		0,00E+00	0		0,00E+00	0
68,4		0,00E+00	0		0,00E+00	0
68,6		0,00E+00	0		0,00E+00	0
68,8		0,00E+00	0		0,00E+00	0
69		0,00E+00	0		0,00E+00	0
69,2		0,00E+00	0		0,00E+00	0
69,4		0,00E+00	0		0,00E+00	0
69,6		0,00E+00	0		0,00E+00	0
69,8		0,00E+00	0		0,00E+00	0
70		0,00E+00	0		0,00E+00	0
70,2		0,00E+00	0		0,00E+00	0
70,4		0,00E+00	0		0,00E+00	0
70,6		0,00E+00	0		0,00E+00	0
70,8		0,00E+00	0		0,00E+00	0
71		0,00E+00	0		0,00E+00	0
71,2		0,00E+00	0		0,00E+00	0
71,4		0,00E+00	0		0,00E+00	0
71,6		0,00E+00	0		0,00E+00	0
71,8		0,00E+00	0		0,00E+00	0
72		0,00E+00	0		0,00E+00	0
72,2		0,00E+00	0		0,00E+00	0
72,4		0,00E+00	0		0,00E+00	0
72,6		0,00E+00	0		0,00E+00	0
72,8		0,00E+00	0		0,00E+00	0
73		0,00E+00	0		0,00E+00	0
73,2		0,00E+00	0		0,00E+00	0
73,4		0,00E+00	0		0,00E+00	0

Appendix 6C

Borehole length (m) Borrålslängd [m]		column C T≈Q/dh [m^2/s]	b [µm]		column F T [m^2/s]	b [µm]
73,6		0,00E+00	0		0,00E+00	0
73,8		0,00E+00	0		0,00E+00	0
74		0,00E+00	0		0,00E+00	0
74,2		0,00E+00	0		0,00E+00	0
74,4		0,00E+00	0		0,00E+00	0
74,6		0,00E+00	0		0,00E+00	0
74,8		0,00E+00	0		0,00E+00	0
75		0,00E+00	0		0,00E+00	0
75,2		0,00E+00	0		0,00E+00	0
75,4		3,11E-09	17,03705		3,08E-09	16,97484
75,6		6,14E-08	46,04734		6,07E-08	45,8792
75,8		0,00E+00	0		0,00E+00	0
76		0,00E+00	0		0,00E+00	0
76,2		0,00E+00	0		0,00E+00	0
76,4		0,00E+00	0		0,00E+00	0
76,6		0,00E+00	0		0,00E+00	0
76,8		0,00E+00	0		0,00E+00	0
77		0,00E+00	0		0,00E+00	0
77,2		0,00E+00	0		0,00E+00	0
77,4		0,00E+00	0		0,00E+00	0
77,6		0,00E+00	0		0,00E+00	0
77,8		0,00E+00	0		0,00E+00	0
78		0,00E+00	0		0,00E+00	0
78,2		0,00E+00	0		0,00E+00	0
78,4		0,00E+00	0		0,00E+00	0
78,6		0,00E+00	0		0,00E+00	0
78,8		0,00E+00	0		0,00E+00	0
79		0,00E+00	0		0,00E+00	0
79,2		0,00E+00	0		0,00E+00	0
79,4		0,00E+00	0		0,00E+00	0
79,6		0,00E+00	0		0,00E+00	0
79,8		0,00E+00	0		0,00E+00	0
80		0,00E+00	0		0,00E+00	0
80,2		0,00E+00	0		0,00E+00	0
80,4		0,00E+00	0		0,00E+00	0
80,6		0,00E+00	0		0,00E+00	0
80,8		0,00E+00	0		0,00E+00	0
81		0,00E+00	0		0,00E+00	0
81,2		0,00E+00	0		0,00E+00	0
81,4		0,00E+00	0		0,00E+00	0
81,6		0,00E+00	0		0,00E+00	0

Appendix 6C

Borehole length (m) Borrålslängd [m]		column C T≈Q/dh [m^2/s]	b [µm]		column F T [m^2/s]	b [µm]
81,8		0,00E+00	0		0,00E+00	0
82		0,00E+00	0		0,00E+00	0
82,2		0,00E+00	0		0,00E+00	0
82,4		0,00E+00	0		0,00E+00	0
82,6		0,00E+00	0		0,00E+00	0
82,8		0,00E+00	0		0,00E+00	0
83		0,00E+00	0		0,00E+00	0
83,2		0,00E+00	0		0,00E+00	0
83,4		0,00E+00	0		0,00E+00	0
83,6		0,00E+00	0		0,00E+00	0
83,8		0,00E+00	0		0,00E+00	0
84		0,00E+00	0		0,00E+00	0
84,2		0,00E+00	0		0,00E+00	0
84,4		0,00E+00	0		0,00E+00	0
84,6		0,00E+00	0		0,00E+00	0
84,8		0,00E+00	0		0,00E+00	0
85		0,00E+00	0		0,00E+00	0
85,2		0,00E+00	0		0,00E+00	0
85,4		0,00E+00	0		0,00E+00	0
85,6		0,00E+00	0		0,00E+00	0
85,8		0,00E+00	0		0,00E+00	0
86		0,00E+00	0		0,00E+00	0
86,2		0,00E+00	0		0,00E+00	0
86,4		0,00E+00	0		0,00E+00	0
86,6		0,00E+00	0		0,00E+00	0
86,8		0,00E+00	0		0,00E+00	0
87		0,00E+00	0		0,00E+00	0
87,2		0,00E+00	0		0,00E+00	0
87,4		0,00E+00	0		0,00E+00	0
87,6		0,00E+00	0		0,00E+00	0
87,8		0,00E+00	0		0,00E+00	0
88		0,00E+00	0		0,00E+00	0
88,2		0,00E+00	0		0,00E+00	0
88,4		0,00E+00	0		0,00E+00	0
88,6		0,00E+00	0		0,00E+00	0
88,8		0,00E+00	0		0,00E+00	0
89		0,00E+00	0		0,00E+00	0
89,2		0,00E+00	0		0,00E+00	0
89,4		0,00E+00	0		0,00E+00	0
89,6		0,00E+00	0		0,00E+00	0
89,8		0,00E+00	0		0,00E+00	0

Appendix 6C

Borehole length (m) Borrålslängd [m]		column C T≈Q/dh [m^2/s]	b [µm]		column F T [m^2/s]	b [µm]
90		0,00E+00	0		0,00E+00	0
90,2		0,00E+00	0		0,00E+00	0
90,4		0,00E+00	0		0,00E+00	0
90,6		0,00E+00	0		0,00E+00	0
90,8		0,00E+00	0		0,00E+00	0
91		0,00E+00	0		0,00E+00	0
91,2		0,00E+00	0		0,00E+00	0
91,4		0,00E+00	0		0,00E+00	0
91,6		0,00E+00	0		0,00E+00	0
91,8		0,00E+00	0		0,00E+00	0
92		0,00E+00	0		0,00E+00	0
92,2		0,00E+00	0		0,00E+00	0
92,4		0,00E+00	0		0,00E+00	0
92,6		0,00E+00	0		0,00E+00	0
92,8		0,00E+00	0		0,00E+00	0
93		0,00E+00	0		0,00E+00	0
93,2		0,00E+00	0		0,00E+00	0
93,4		0,00E+00	0		0,00E+00	0
93,6		0,00E+00	0		0,00E+00	0
93,8		0,00E+00	0		0,00E+00	0
94		0,00E+00	0		0,00E+00	0
94,2		0,00E+00	0		0,00E+00	0
94,4		0,00E+00	0		0,00E+00	0
94,6		0,00E+00	0		0,00E+00	0
94,8		0,00E+00	0		0,00E+00	0
95		0,00E+00	0		0,00E+00	0
95,2		0,00E+00	0		0,00E+00	0
95,4		0,00E+00	0		0,00E+00	0
95,6		0,00E+00	0		0,00E+00	0
95,8		0,00E+00	0		0,00E+00	0
96		0,00E+00	0		0,00E+00	0
96,2		0,00E+00	0		0,00E+00	0
96,4		0,00E+00	0		0,00E+00	0
96,6		0,00E+00	0		0,00E+00	0
96,8		0,00E+00	0		0,00E+00	0
97		0,00E+00	0		0,00E+00	0
97,2		0,00E+00	0		0,00E+00	0
97,4		0,00E+00	0		0,00E+00	0
97,6		0,00E+00	0		0,00E+00	0
97,8		0,00E+00	0		0,00E+00	0
98		0,00E+00	0		0,00E+00	0

Appendix 6C

Borehole length (m) Borrålslängd [m]		column C T≈Q/dh [m^2/s]	b [µm]		column F T [m^2/s]	b [µm]
98,2		0,00E+00	0		0,00E+00	0
98,4		0,00E+00	0		0,00E+00	0
98,6		0,00E+00	0		0,00E+00	0
98,8		0,00E+00	0		0,00E+00	0
99		0,00E+00	0		0,00E+00	0
99,2		0,00E+00	0		0,00E+00	0
99,4		0,00E+00	0		0,00E+00	0
99,6		0,00E+00	0		0,00E+00	0
99,8		0,00E+00	0		0,00E+00	0
100		0,00E+00	0		0,00E+00	0

KI0014B01: Transmissivities in sections - tests during drilling (see Figure 5-11)

KI0014B01 Transmissiviteter i sektioner
Analys baserad på de första indata från tester under borrning, alltså helhålsinflöde allteftersom hålet borrades.
Inflödena är anpassade så att ingen sektion får negativt flöde.
Trycket är anpassat med separat analys (se kapitel 5.3.1).
T approximerad som T≈Q/dh

KI0014B01 Transmissivity in sections
Analyses based on the first data delivered from tests during drilling, meaning full-hole inflow while drilling the borehole.
The inflow is adjusted to give all sections a positive flow.
The pressure is adjusted by using a separate analysis (see chapter 5.3.1).
T is approximated as T≈Q/dh

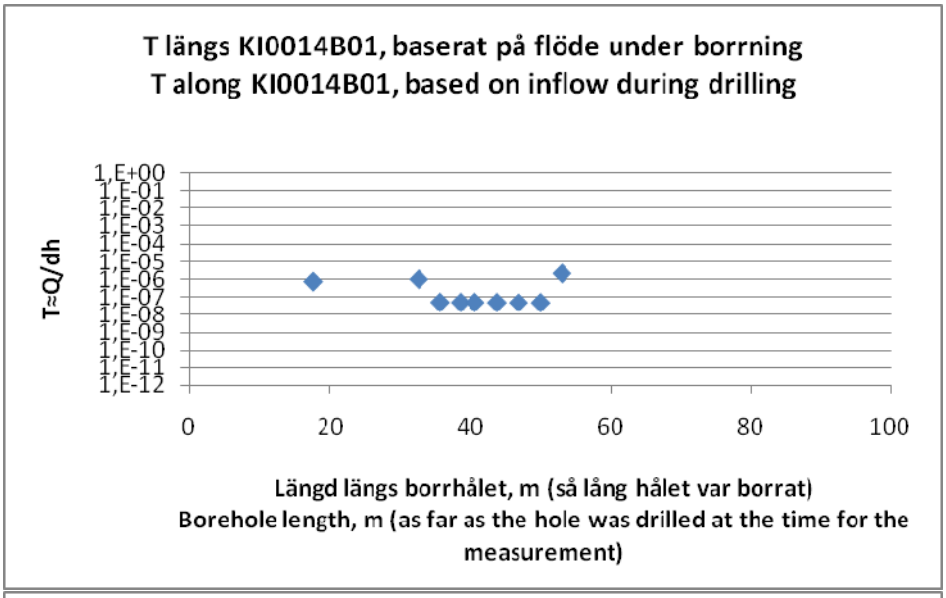

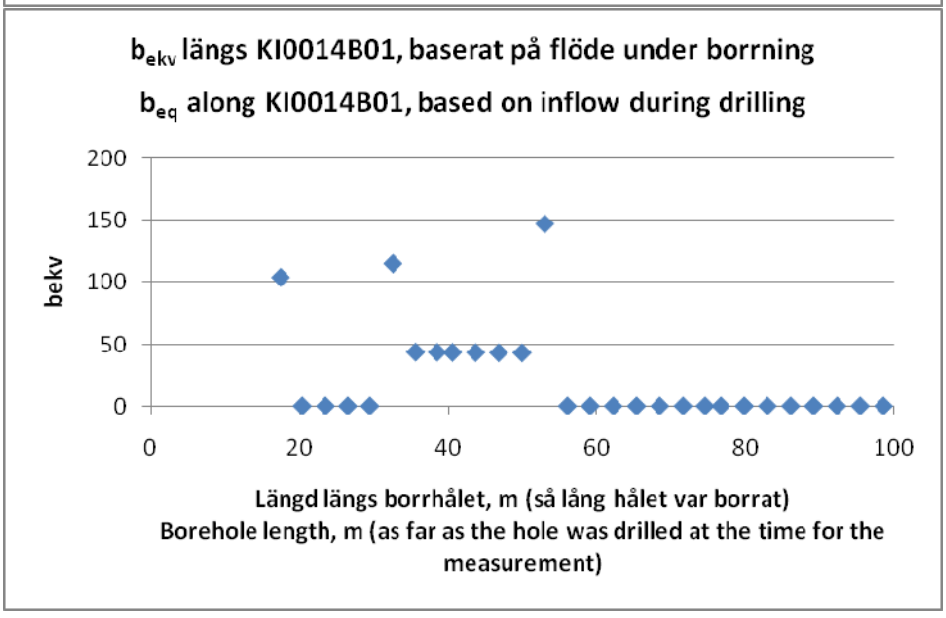

Appendix 6D

Borehole: KI0014B01

Bh length (m) Bhlängd (m)	T ≈ Q/dh [m^2/s]	b_{eq} [µm]
17,5	7,05E-07	103,8901
20,4	0	0
23,53	0	0
26,51	0	0
29,5	0	0
32,59	9,58E-07	115,0724
35,64	5,12E-08	43,33975
38,54	5,07E-08	43,19376
40,59	5,03E-08	43,09813
43,72	4,99E-08	42,96251
46,82	4,94E-08	42,83894
49,96	4,9E-08	42,72316
53,01	2E-06	146,958
56,05	0	0
59,14	0	0
62,22	0	0
65,35	0	0
68,47	0	0
71,59	0	0
74,57	0	0
76,70	0	0
79,83	0	0
82,94	0	0
86,07	0	0
89,16	0	0
92,30	0	0
95,41	0	0
98,55	0	0
100,27	0	0

KI0014B01: Transmissivities in 3 m sections based on Double packer tests - (see Figure 5-14)

KI0014B01 Transmissiviteter i 3 m-sektioner

Analys baserad på dubbelmanschettmätningarna.
T beräknad med Moye's formel

KI0014B01 Transmissivities in 3 m sections

Analyses based on double packer tests
T calculated by using Moye's formula

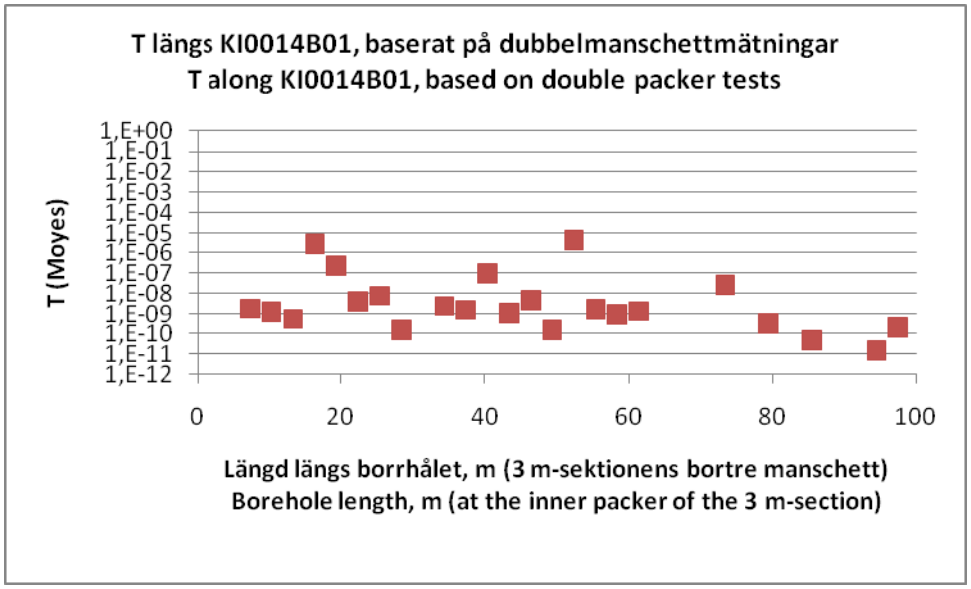

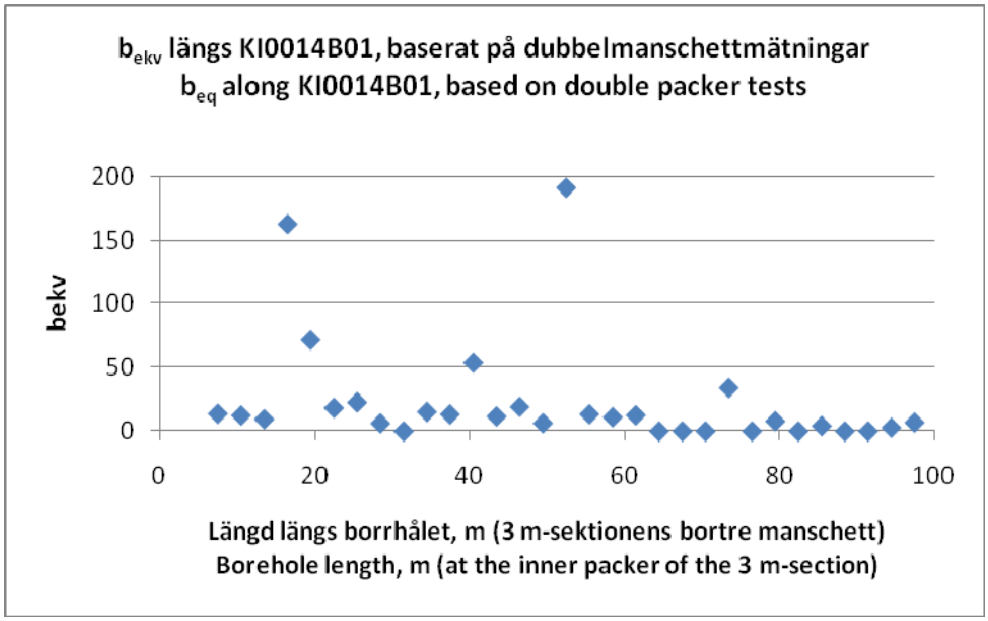

Appendix 6E

Borehole: KI0014B01

Borehole length (m) Bhlängd (m)		T (Moyes) [m2/s]	b_{eq} [µm]
Upper Övre	Lower Nedre		
94,5	97,5	2,1E-10	6,94
91,5	94,5	1,5E-11	2,88
88,5	91,5	0,0E+00	0,00
85,5	88,5	0,0E+00	0,00
82,5	85,5	4,8E-11	4,25
79,5	82,5	0,0E+00	0,00
76,5	79,5	3,3E-10	8,05
73,5	76,5	0,0E+00	0,00
70,5	73,5	2,5E-08	34,34
67,5	70,5	0,0E+00	0,00
64,5	67,5	0,0E+00	0,00
61,5	64,5	0,0E+00	0,00
58,5	61,5	1,3E-09	12,84
55,5	58,5	8,9E-10	11,25
52,5	55,5	1,6E-09	13,63
49,5	52,5	4,4E-06	191,36
46,5	49,5	1,7E-10	6,41
43,5	46,5	4,6E-09	19,45
40,5	43,5	1,1E-09	11,90
37,5	40,5	1,0E-07	54,10
34,5	37,5	1,6E-09	13,52
31,5	34,5	2,3E-09	15,43
28,5	31,5	0,0E+00	0,00
25,5	28,5	1,6E-10	6,32
22,5	25,5	7,6E-09	23,00
19,5	22,5	4,0E-09	18,58
16,5	19,5	2,3E-07	71,96
13,5	16,5	2,7E-06	162,58
10,5	13,5	5,6E-10	9,61
7,5	10,5	1,3E-09	12,62
4,5	7,5	1,7E-09	14,04

Appendix 6F

KI0016B01: Transmissivities in sections - tests during drilling (see Figure 5-12)

KI0016B01 Transmissiviteter i sektioner
Analys baserad på de första indata från tester under borrning, alltså helhålsinflöde allteftersom hålet borrades.
Inflödena är anpassade så att ingen sektion får negativt flöde.
Trycket är anpassat med separat analys (se kapitel 5.3.1).
T approximerad som T≈Q/dh

KI0016B01 Transmissivity in sections
Analyses based on the first data delivered from tests during drilling, meaning full-hole inflow while drilling the borehole.
The inflow is adjusted to give all sections a positive flow.
The pressure is adjusted by using a separate analysis (see chapter 5.3.1).
T is approximated as T≈Q/dh

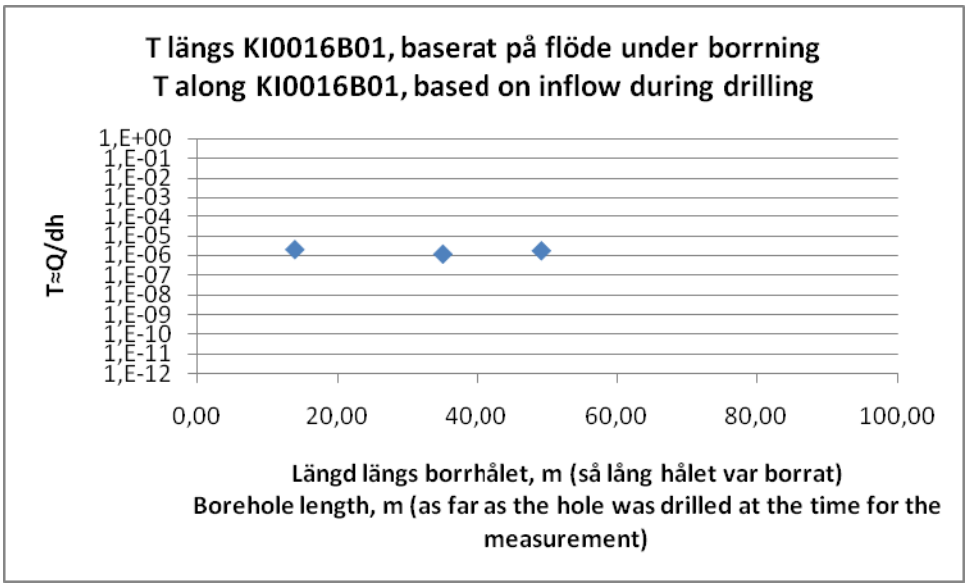

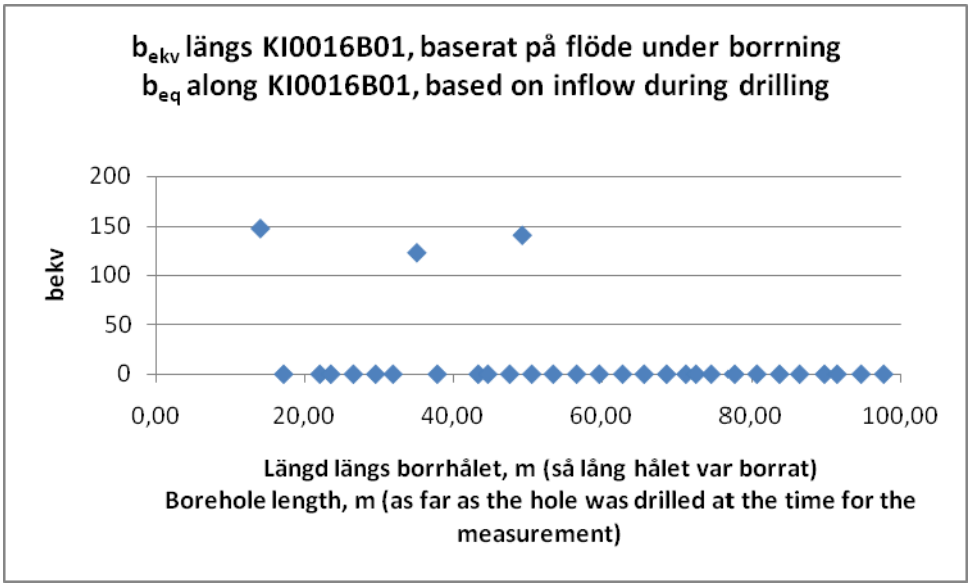

Appendix 6F

Borehole: KI0016B01

Bh length Bhlängd (m)	T ≈ Q/dh [m^2/s]	b_{eq} [µm]
14,00	2,04E-06	148,0238
17,13	0	0
22,00	0	0
23,47	0	0
26,51	0	0
29,50	0	0
31,85	0	0
35,05	1,18E-06	123,3418
37,79	0	0
43,30	0	0
44,60	0	0
47,55	0	0
49,23	1,77E-06	141,1551
50,51	0	0
53,40	0	0
56,55	0	0
59,60	0	0
62,73	0	0
65,63	0	0
68,65	0	0
71,25	0	0
72,60	0	0
74,65	0	0
77,65	0	0
80,63	0	0
83,67	0	0
86,38	0	0
89,72	0	0
91,42	0	0
94,65	0	0
97,70	0	0

KI0016B01: Transmissivities in 3 m sections based on Double packer tests - (see Figure 5-15)

KI0016B01 Transmissiviteter i 3 m-sektioner

Analys baserad på dubbelmanschettmätningarna.
T beräknad med Moye's formel

KI0016B01 Transmissivities in 3 m sections

Analyses based on double packer tests
T calculated by using Moye's formula

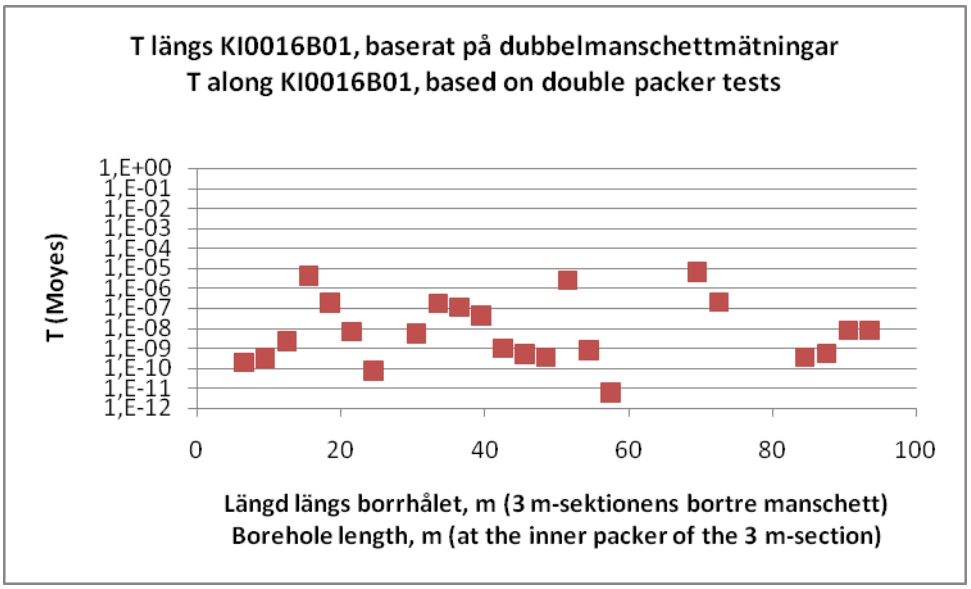

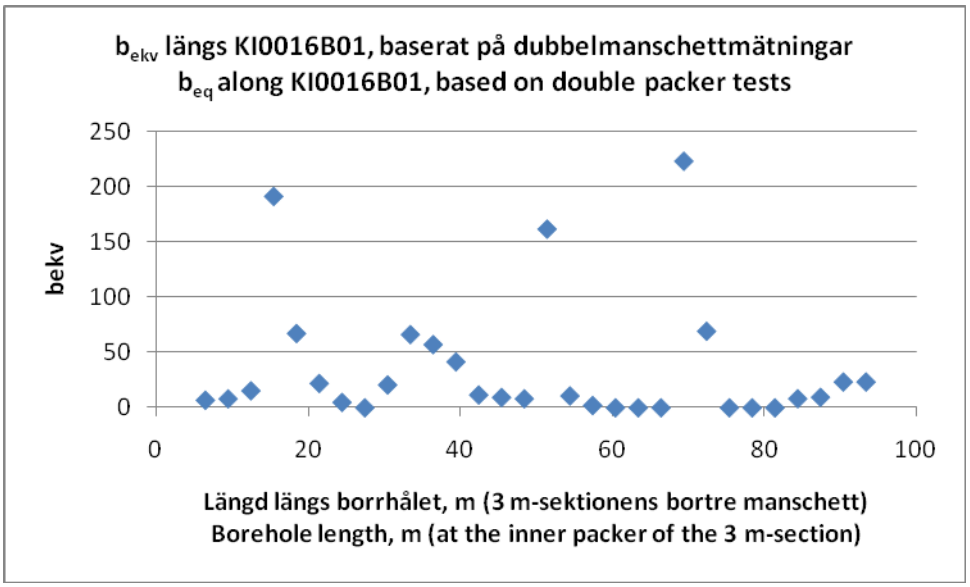

Appendix 6G

Borehole: KI0016B01

Borehole length (m) Bhlängd (m)		T (Moyes) [m^2/s]	b_{eq} [µm]
Upper Övre	Lower Nedre		
90,5	93,5	8,1E-09	23,46
87,5	90,5	8,1E-09	23,41
84,5	87,5	5,5E-10	9,56
81,5	84,5	3,6E-10	8,30
78,5	81,5	0,0E+00	0,00
75,5	78,5	0,0E+00	0,00
72,5	75,5	0,0E+00	0,00
69,5	72,5	2,1E-07	69,50
66,5	69,5	7,0E-06	223,76
63,5	66,5	0,0E+00	0,00
60,5	63,5	0,0E+00	0,00
57,5	60,5	0,0E+00	0,00
54,5	57,5	5,8E-12	2,10
51,5	54,5	8,0E-10	10,84
48,5	51,5	2,7E-06	162,19
45,5	48,5	3,5E-10	8,23
42,5	45,5	5,3E-10	9,44
39,5	42,5	1,0E-09	11,68
36,5	39,5	4,6E-08	41,67
33,5	36,5	1,2E-07	57,38
30,5	33,5	1,8E-07	66,46
27,5	30,5	5,6E-09	20,78
24,5	27,5	0,0E+00	0,00
21,5	24,5	7,4E-11	4,89
18,5	21,5	6,8E-09	22,10
15,5	18,5	1,9E-07	67,48
12,5	15,5	4,4E-06	191,85
9,5	12,5	2,3E-09	15,44
6,5	9,5	3,4E-10	8,14
3,5	6,5	2,0E-10	6,86